University of São Paulo
"Luiz de Queiroz" College of Agriculture

Subcellular dynamics of the endogenous elicitor peptide *At*Pep1 and its receptors in *Arabidopsis*: implications for the plant immunity

Fausto Andres Ortiz-Morea

Thesis presented to obtain the degree of Doctor in Science. Area: Genetics and Plant Breeding

Piracicaba
2015

Fausto Andres Ortiz-Morea
Agroecologist Engineer

Subcellular dynamics of the endogenous elicitor peptide *At*Pep1 and its receptors in *Arabidopsis*: implications for the plant immunity

versão revisada de acordo com a resolução CoPGr 6018 de 2011

Promoter:
Prof. Dr. **DANIEL SCHERER DE MOURA**
Prof Dr**. EUGENIA RUSSINOVA**

Thesis presented to obtain the degree of Doctor in Science. Area: Genetics and Plant Breeding

Piracicaba
2015

Dados Internacionais de Catalogação na Publicação
DIVISÃO DE BIBLIOTECA - DIBD/ESALQ/USP

Ortiz-Morea, Fausto Andres
Subcellular dynamics of the endogenous elicitor peptide *At*Pep1 and its receptors in *Arabidopsis*: implications for the plant immunity / Fausto Andres Ortiz-Morea. - - versão revisada de acordo com a resolução CoPGr 6018 de 2011. - - Piracicaba, 2015.
178 p. : il.

Tese (Doutorado) - - Escola Superior de Agricultura "Luiz de Queiroz".

1. Peptídeos de sinalização 2. Receptores reconhecedores de padrões 3. PTI 4. *At*Pep1 – PEPR 5. Endocitose I. Título

CDD 581.19256
O77s

Ghent University

Faculty of Sciences

Department of Plant Biotechnology and Bioinformatics

VIB department of Plant Systems Biology

Subcellular dynamics of the endogenous elicitor peptide *At*Pep1 and its receptors in *Arabidopsis*: implications for the plant immunity

Fausto Andres Ortiz-Morea

Promoter:

Prof. Dr. Eugenia Russinova

Prof. Dr. Daniel Scherer de Moura

This thesis was submitted as fulfillment of the requirements to obtain the degree of Doctor (PhD) in sciences: Biochemistry and Biotechnology

Academic year 2014-2015

This thesis was carried out at the University of São Paulo, University of Ghent and Flemish Institute for Biotechnology (VIB) department of Plant Systems Biology (PSB). The research was funded by the PEC-PG program of the Coordenação de Aperfeiçoamento de Pessoal de Nível Superior CAPES Brazil, Flemish Government and VIB

Examination committee

Promoter University of São Paulo

Prof. Dr. Daniel Scherer de Moura

"Luiz de Queiroz" College of Agriculture
University of São Paulo

Promoter Ghent University

Prof. Dr. Eugenia Russinova

Department of Plant Systems Biology. VIB,
Ghent University

Reading committee:

Prof. Dr. Victor Alexandre Vitorello

Center of Nuclear Energy in Agriculture
University of São Paulo

Prof. Dr. Maria Helena de Souza Goldman

Faculty of Philosophy, Science and Literature of *Ribeirão PretoUniversity of São Paulo*

Dr. Daniel Van Damme

Department of Plant Systems Biology. VIB,
Ghent University

To my lovely wife Adriana Marcela and my beautiful daughter Gabriela,

My source of motivation and inspiration.

To my family for its understanding, support and encouragement.

“You never know what is around the corner. It could be everything. Or it could be nothing. You keep putting one foot in front of the other, and then one day you look back and you have climbed a mountain”

Tom Hiddleston

ACKNOWLEDGMENT

To God for the wisdom and perseverance that he has bestowed upon me during this phase of my life.

To my family for their unconditional support throughout my degree. Thanks for all the sacrifices that you have made on my behalf. To my eternal love Adriana Marcela, who taught me that who loves knows to wait, that real friends exist and that dreams can become true. Thanks for the patience, the understanding and the motivation every day.

To my promoters Professor Dr. Daniel Scherer de Moura and Professor Dr. Jenny Russinova for encouraging my research, for your support and for allowing me to grow as a research scientist, I really learned a lot and enjoyed being part of your team.

To the graduate program in Plant genetics and Plant breeding of the Universidade de Sao Paulo, and to the graduate program in Biochemistry and Biotechnology of the Gent University for allowing me to be one of its PhD students.

To the BOF Special Research founding of the Flemish Government for a Joint Doctorate fellowship at Ghent University and to the PEC-PG program of the Coordenação de Aperfeiçoamento de Pessoal de Nível Superior CAPES,-Brazil for the Doctorate fellowship at Universidade of São Paulo.

To all members of the Protein Biochemistry Laboratory at ESALQ/USP and all members of the Brassinosteroids group at VIB/Plants Systems Biology Department for a great working atmosphere, the daily exchange of ideas, and the friendship inside and outside the lab.

To my dears friends whom I met along the way of my graduate studies but who occupy an important space in my heart: Paulo, Juanchito, Keini, Geraldo, Ghilherme, Amaral, Bianca, Wilson, Anaxi, Diva, Kiril, Wim, Evelien, Gustavo and Rahul.

And to all the people who directly or indirectly made this possible.

CONTENTS

RESUMO

Dinâmica subcelular do peptídeo endógeno *At*Pep1 e seus receptores em *Arabidopsis*: implicações na imunidade de plantas

Neste trabalho, foi investigada a dinâmica subcelular do peptídeo elicitor de planta *At*Pep1 e suas implicações nas respostas de defesa. Primeiramente, é fornecida uma introdução do sistema imune inato de plantas com ênfase na imunidade ativada por moléculas elicitoras derivadas de organismos invasores ou da mesma planta, após seu reconhecimento por receptores localizados na membrana plasmática (PTI responses). Peptídeos endógenos que têm sido reportados em *Arabidopsis* como ativadores de PTI são descritos, dando especial destaque para o peptídeo *At*Pep1 e seus receptores PEPRs. O tráfego de endomembranas em plantas é introduzido, abrangendo as vias de internalização, endocitose mediada por proteínas clathrinas (CME) e endocitose mediada por receptor (RME). No capítulo seguinte, foram avaliadas estratégias para o estudo *in vivo* da dinâmica subcelular do *At*Pep1. Para isso a proteína precursora do *At*Pep1 (PROPEP1) foi fusionada a GFP e sua localização visualizada, encontrando que PROPEP1 é associado com o tonoplasto e acumula dentro do vacúolo, fato que sugere uma função de armazenamento do PROPEP1 para esta organela, desde onde é liberado em caso de uma situação de perigo dando origem ao *At*Pep1. Adicionalmente, foram produzidas versões biologicamente ativas do *At*Pep1 marcado com fluróforos. No capítulo três foram combinados genética clássica e genética química com visualizações *in vivo* para estudar o comportamento de um *At*Pep1 bioativo e marcado fluorescentemente na células meristemática da ponta da raiz de *Arabidopsis*, sendo encontrado que *At*Pep1 se liga rapidamente na membrana plasmática numa forma dependente de receptor. Em seguida, o complexo *At*Pep1-PEPR foi internalizado via CME e transportado para o vacúolo, passando através do endossomo primário e secundário. Quando o funcionamento da CME foi comprometido, as respostas ao *At*Pep1 também foram afetadas. Estes resultados fornecem a primeira visualização *in vivo* de um peptídeo de sinalização em plantas, mostrando sua dinâmica e destino intracelular. O papel regulatório durante as respostas induzidas pelo *At*Pep1 do co-receptor BRI1-associated kinase 1 (BAK1) foram investigadas (Capítulo quatro). Nossos resultados confirmaram que BAK1 interage com PEPRs numa forma dependente do ligante e indicam que BAK1 modula sinalização e endocitose do *At*Pep1, no entanto quando ausente, BAK1 pode ser substituído por seus homólogos SOMATIC EMBRYOGENESIS RECEPTOR-LIKE KINASE os quais poderiam ter funções adicionais durante as repostas induzidas pelo *At*Pep1. Eventos de fosforilação após a formação do complexo PEPR-BAK1 parecem ditar as bases moleculares da internalização e sinalização do *At*Pep1. Finalmente, são discutidos os resultados encontrados nesta pesquisa numa perspectiva geral, destacando a relevância destas descobertas na área de pesquisa em que estão inseridos, o potencial que representa o uso de ligantes marcados fluorescentemente como ferramenta para o estudo de complexos entre ligante-receptor, a disponibilidade do sistema *At*Pep1-PEPRs como modelo de estudo da endocitose em plantas e sua relação com sinalização, e os futuros desafios na área.

Palavras-chave: Peptídeos de sinalização; Receptores reconhecedores de padrões; PTI; *At*Pep1 – PEPR; Endocitose

ABSTRACT

Subcellular dynamics of the endogenous elicitor peptide *At*Pep1 and its receptors in *Arabidopsis*: implications for the plant immunity

This work investigated the subcellular dynamics of the plant elicitor peptide *At*Pep1 and its interplay with plant defense responses. First, an introduction of the plant innate immunity system is provided with emphasis on pattern trigger immunity (PTI), which is based on the recognition of "non-self" and "self" elicitor molecules by surface-localized pattern-recognition receptors (PRRs). Then, the *Arabidopsis* endogenous peptides that act as self-elicitor molecules are presented, with details on *At*Pep1 and its PEPR receptors. Plant endomembrane trafficking is described, encompassing endocytic pathways, clathrin mediated endocytosis (CME) and receptor-mediated endocytosis (RME). In the next chapter, we explored strategies for the *in vivo* study of the subcellular behavior of *At*Pep1; to this end, we fused the precursor protein of *At*Pep1 (PROPEP1) to GFP and assessed its localization. We found that PROPEP1 was associated with the tonoplast and accumulated in the vacuole, suggesting that this organelle could work as the station where PROPEP1 is stored and later released, only in a danger situation, hence initiating *At*Pep1. Moreover, we generated *At*Pep1 versions labeled with fluorescent dyes and demonstrated that this peptide could be fluorescently tagged without loss of its biological activity. In chapter 3, we combined classical and chemical genetics with life imaging to study the behavior of a bioactive fluorescently labeled *At*Pep1 in the *Arabidopsis* root meristem. We discovered that the labeled *At*Pep1 was able to bind the plasma membrane very quickly in a receptor-dependent manner. Subsequently, the PEPR-*At*Pep1complex was internalized via CME and transported to the lytic vacuole, passing through early and late endosomal compartments. Impairment of CME compromised the *At*Pep1 responses. Our findings provide for the first time an *in vivo* visualization of a signaling peptide in plant cells, thus giving insights into its intracellular fate and dynamics. The role of the coregulatory receptor BRI1-associated kinase 1 (BAK1) in *At*Pep1-responses was also investigated (chapter 4). Our results confirmed that BAK1 interacts with PEPRs in a ligand-dependent manner and indicate that BAK1 modulates *At*Pep1 signaling and endocytosis, but that, when absent, it might be replaced by homologous SOMATIC EMBRYOGENESIS RECEPTOR-LIKE KINASE *(*SERK) proteins that could have additional functions during the *At*Pep1 signaling. Furthermore, phosphorylation events after the formation of PEPR-BAK1 complexes seem to dictate the molecular bases of *At*Pep1 internalization and signaling. Finally, we discussed our findings in a more general perspective, highlighting the important findings for the plant endomembrane trafficking field, the potential use of fluorescently labeled ligands as a tool to study ligand-receptors pairs, the availability of *At*Pep1-PEPRs as an excellent model to study endocytosis and its interplay with signaling, and the future challenges in the field.

Keywords: Plant signaling peptides; PTI; Pattern –recognition receptors; *At*Pep1-PEPR; Endocytosis

SAMENVATTING

De Subcellular dynamiek van de endogene elicitor peptide *At*Pep1 and zijn receptor in *Arabidopsis*: implications voor de immuniteit van de plant

Dit werk onderzoekt de subcellulaire dynamica van de "plant elicitor peptide" *At*Pep1 en de wisselwerking met de verdedigingsresponsen van planten. In de inleiding wordt het immuunsysteem van planten beschreven met de nadruk op de patronen die de immuniteit activeren, en die gebaseerd zijn op de herkenning van "niet-eigen" en "eigen" moleculen door de aan de oppervlakte-gelocaliseerde herkenningsreceptoren. De endogene peptiden van *Arabidopsis* worden beschreven die zich als zelf-elicitoren of auto-immuniteitsopwekkers gedragen met een focus op *At*Pept1 en zijn receptoren. Verder wordt het endomembraantransport in planten besproken, waarbij dieper wordt ingegaan op clathrine gemedieerde endocytose (CME). In het volgend hoofdstuk bestuderen wij de strategieën voor het onderzoek naar de *in vivo* subcellulair localisatie van *At*Pep1. Hiervoor maakten wij een fusie tussen zijn precursorproteïne (PROPEP1) en GFP, en bepaalden zijn lokalisatie. We vonden dat PROPEP1 was geassocieerd met de tonoplast en accumuleerde in de vacuole, wat erop wijst dat dit organel zou kunnen fungeren als opslagplaats voor PROPEP1. In het geval van een immuun response wordt het precursor peptide vrijgegeven, en ontstaat *At*Pep1. Verder genereerden we versies van *At*Pep1 die verbonden zijn met fluorescente kleurstoffen, zonder het verlies van zijn biologische activiteit. In hoofdstuk 3 combineerden we klassieke en chemische genetica met "life"-beeldvorming om het gedrag te bestuderen van een bioactieve en fluorescente vorm van *At*Pept1 in het wortelmeristeem van *Arabidopsis*. We ontdekten dat het fluorescente *At*Pep1 in staat was zeer snel de plasmamembraan te binden in een receptor-afhankelijke wijze. Vervolgens werd de receptor (PEPR) in complex met *At*Pep1 geïnternaliseerd via CME en naar de lytische vacuole getransporteerd doorheen de vroege en late endosomale compartimenten. Inhibitie van CME bracht de *At*Pep1 geïnduceerde responsen in het gedrang. Dankzij onze resultaten werd voor de eerste keer een signaalpeptide gevisualiseerd *in vivo* in plantencellen, waardoor inzicht werd verschaft in zijn intracellulair lot en dynamica. De rol van de co-regulatorische receptor BRI1-associated kinase 1 (BAK1) in de responsen van *At*Pep1 werd ook onderzocht (hoofdstuk 4). Onze resultaten bevestigden dat BAK1 interageert met PEPRs in een ligand-afhankelijke wijze; tevens duiden ze aan dat BAK1 AtPep1 geïnduceerde signalisatie en endocytose moduleert. BAK1 kan, bij afwezigheid, vervangen worden door de homologe proteïnen SOMATIC EMBRYOGENESIS RECEPTOR-LIKE KINASE (SERK), die bijkomende functies zouden kunnen hebben tijdens *At*Pep1 geïnduceerde signalisatie. Daarenboven, fosforylatie na de vorming van de complexen PERP-BAK1 kan de moleculaire basis van de internalisering en signalering van *At*Pep1 te dicteren. Tenslotte bespreken wij onze resultaten in een meer algemeen perspectief. We leggen de nadruk op de voorname bevindingen betreffende het endomembraantransport van het PEPR- *At*Pep1 receptor-ligand complex, we wijzen op het potentieel gebruik van fluorescente liganden als middel om receptor-ligand complexen te bestuderen en op de geschiktheid van *At*Pep1 en PEPRs als model om endocytosis in relatie tot immuun signalisatie te onderzoeken. Finaal vermelden we de toekomstige uitdagingen in het veld.

Keywords: Planten signalisatie peptides; Patroonherkenning receptor; PTI; *At*Pep1-PEPR; Endocytose

LIST OF ABBREVIATIONS

***At*Pep1**	*Arabidopsis thaliana* Plant elicitor peptide1
AFCS	Alexa Fluor 647–castasterone
ARF-GEF	ADP-ribosylation factor–GTP exchange factor
BAK1	BRI1-associated kinase 1
BFA	Brefeldin A
BIK1	Botrytis-induced kinase 1
BIR2	BAK1-interacting receptor2
BR	Brassinosteroid
BRI1	BRASSINOSTEROID INSENSITIVE 1
CCV	Clathrin coated vesicles
CHCs	Clathrin heavy chain
CHX	Cycloheximide
CIE	Clathrin-independent endocytosis
CLCs	Clathrin light chain ~~proteins~~
CME	Clathrin-mediated endocytosis
ConcA	Concanamycin A
Cy5	Cyanine 5
DAMPS	Damage-associated molecular patterns
DMSO	Dimethyl sulfoxide
EFR	EF-Tu receptor
ETI	Effector-triggered immunity
flg	flagellin
FLS2	FLAGELLIN SENSING2
FM4-64	N-(3-triethylammoniumpropyl)-4-(4-diethylaminophenylhexatrienyl) pyridinium dibromide
GFP	Green fluorescent protein
GUS	β-glucuronidase
HPLC	High-performance liquid chromatography
LRR	Leucine-rich repeats
LRRRK	Leucine-reach repeat–receptor kinase
MAMPs	Microbe-associated molecular patterns
MAPKs	Mitogen-activated protein kinases

MS	Murashige and Skoog
MVB	Multivesicular body
PAMPs	Pathogen-associated molecular patterns
PDF1	Plant DEFENSIN 1
PEPR	Peptides Peps receptor
PRR	Pattern-recognition receptors
PTI	Pattern-triggered immunity
RD	Arginine-aspartic acid motif
RLP	Receptor-like protein
RLCKs	Receptor-like cytoplasmic kinases
RME	Receptor-mediated endocytosis
ROS	Reactive oxygen species
SERKs	Somatic embryogenesis-related kinases
TAMRA	5-Carboxytetramethylrhodamine
TGN/EE	*Trans*-Golgi network/early endosome
VHA-a1	Vacuolar H+-ATPase subunit a1

1 INTRODUCTION

1.1 Plant defense

Plants have the ability to use sunlight energy to transform CO_2, water and other elements, into organic molecules that become the primary food source of many organisms. These organisms can be beneficial to plant growth, but many of them have detrimental effects on plant development and long-term survival (JONES; DANGL, 2006). Moreover, because of their sessile life style, plants cannot avoid danger organisms by simply running away and have, therefore, evolved stunning defense strategies to stop invading organisms, thus allowing plants to successfully colonize different environments on earth. The first obstacle that an organism must overcome before it succeeds in invading the plants is the presence of structural, enzymatic or chemical preformed barriers, such as waxy cuticles, lignified cell walls, thorns, trichomes, antimicrobial enzymes and secondary metabolites (BOYAJYAN et al., 2014; THORDAL-CHRISTENSEN, 2003). Once these barriers are breached, the invaders are confronted with a refined plant immune system designed to perceive elicitor molecules derived from the invading organisms and from the already attacked plant cells (BOLLER; FELIX, 2009; MACHO; ZIPFEL, 2014).

1.1.1 The plant immune system

Plants, unlike mammals, lack a somatic adaptive immune system and mobile defender cells that access most part of the organism. Instead, plants rely on the innate immunity of each cell and on systemic signals emanating from infection sites (JONES; DANGL, 2006). The plant innate immunity is based on the recognition of potentially invading organisms and subsequent induction of protective responses, comprising a two-tier perception system (DODDS; RATHJEN, 2010). The first layer is mediated by the recognition of specific microbe- or pathogen-associated molecular patterns (MAMPs or PAMPs) by surface-localized pattern-recognition receptors (PRRs) that induce basal responses termed PRR-triggered immunity (PTI) (BOYAJYAN et al., 2014; MACHO; ZIPFEL, 2014). As exogenous elicitors are conserved and widely distributed within pathogens and non-pathogens from invading organisms (MEDZHITOV; JANEWAY, 1997), we chose to use the term MAMPs to refer to elicitors from invading organisms throughout this thesis. Additionally, PTI can be activated by endogenous host-derived elicitor molecules (damage-associated molecular patterns [DAMPs]) that are released upon pathogen perception or pathogen-induced cell damage, and recognized as danger/alarm signals (BOLLER; FELIX, 2009;

MACHO; ZIPFEL, 2014). As most of the MAMPS are essential for the life style of the pathogens, they cannot easily be amended to evade recognition; however, the existence of PTI has instigated the necessity for plant pathogens to evolve a suite of diverse effector molecules that are secreted into host cells to interfere with specific steps of pathogen detection or subsequent downstream signaling responses (PUMPLIN; VOINNET, 2013). In most cases, these effectors are virulence factors because they promote microbial growth and disease (BOLLER; FELIX, 2009; DODDS; RATHJEN, 2010; PUMPLIN; VOINNET, 2013). As a counter defense to the action of virulence effectors, the second layer of plant immunity appears, based on a large family of mostly intracellular plant receptors of the nucleotide-binding leucine-rich repeat domain class (R proteins) that recognize virulence effectors directly or by monitoring the integrity of their endogenous targets; as a consequence, responses, called effector-triggered immunity (ETI) that is stronger than PTI, are induced and lead, in many cases, to hypersensitive responses characterized by rapid apoptotic cell death and local necrosis (BOLLER; FELIX, 2009; BOYAJYAN et al., 2014; DODDS; RATHJEN, 2010; MACHO; ZIPFEL, 2014; PUMPLIN; VOINNET, 2013).

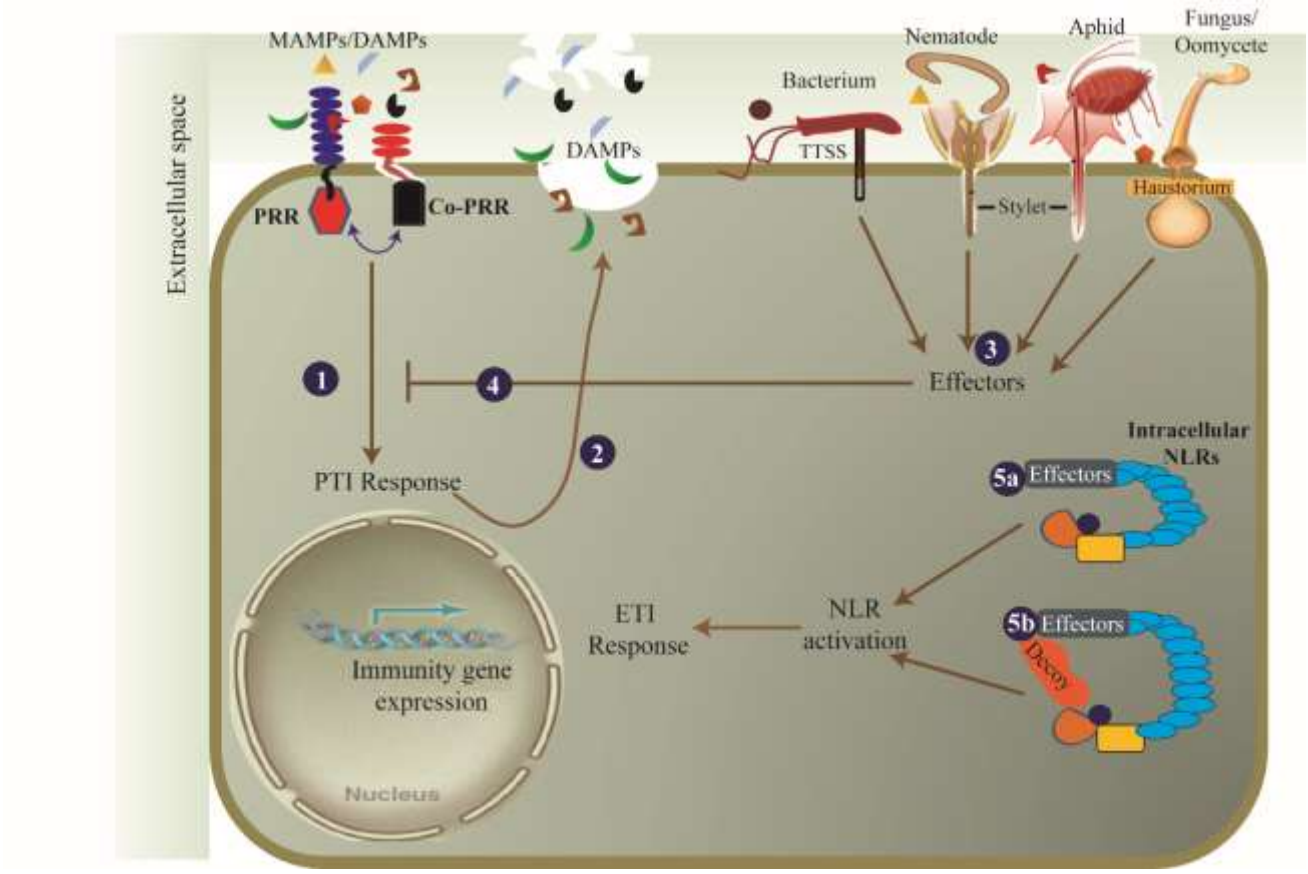

Figure 1 – Schematic of the plant immune system. Pathogens of different life styles release MAMPs (Shapes are color coded to the pathogens) into the extracellular space as they colonize plants. (1) MAMPs are recognized by the extracellular domain of PRR and initiate PTI. Many PRRs interact with coregulatory receptors to initiate PTI signaling pathway. (2) Host-derived elicitor molecules DAMPs are released upon pathogen perception or pathogen-induced cell damage, and they are recognized by PRRs to amplify PTI. (3) Pathogens deliver a suite of effector proteins into host cells through specialized structures. (4) These effector are addressed to specific subcellular locations where they can interfere with PTI and facilitate virulence. (5) However, intracellular nucleotide-binding (NB)-LRR receptors NLRs can recognize virulence effectors directly (5a) or by monitoring the integrity of their endogenous targets (5b), triggering ETI. (TTSS) type III secretion system. Modified from Dangl et al. (2013). Decoy represent an alteration of a host virulence target, like the cytosolic domain of a PRR.

1.1.2 Pattern recognition receptors

Pattern recognition receptors are localized in the plasma membrane and perceive MAMPs or DAMPs of “non-self” and “self” origin, respectively. They are either receptor kinases (RKs) that have a ligand-binding ectodomain, a single-pass transmembrane domain, and an intracellular kinase domain, or receptor-like proteins (RLPs), which share the same overall structure but lack an intracellular kinase domain (ZIPFEL, 2014). As RLPs do not possess an intracellular signaling domain, they are believed to rely on the interaction with one

or several RKs to propagate the signal induced by the receptor-ligand binding (TOR; LOTZE; HOLTON, 2009; ZIPFEL, 2014)

As evidence of their biological relevance, the *Arabidopsis thaliana* genome is predicted to encode more than 600 RKs and 56 RLPs and the rice (*Oryza sativa*) genome encodes more than 1000 RKs and 90 RLPs (DARDICK et al., 2007; FRITZ-LAYLIN et al., 2005; SHIU; BLEECKER, 2003), although not all RKs and RLPs are PRRs, some of which being related to different physiological processes (SHIU; BLEECKER, 2003). According to their sequence analysis, RKs can be classified into 21 structural classes depending on the structure of their extracellular domain, with the leucine-rich repeats (LRR) RKs, being the largest family with at least 233 members divided into 16 subfamilies (LEHTI-SHIU et al., 2009; SHIU; BLEECKER, 2001; SHIU et al., 2004). Furthermore, RKs can also be grouped into RD and non-RD kinases, according to the presence or absence of the so-called RD motif, which refers to a conserved arginine (R) located in front of an aspartate (D) in the catalytic loop that facilitates phosphotransfer (DARDICK; SCHWESSINGER; RONALD, 2012; SHIU; BLEECKER, 2003). Currently, all characterized plant RKs that carry the non-RD kinase motif are involved in the recognition of MAMPs, suggesting that it might be a hallmark of PRRs, but this characteristic cannot be extended to all PRRs because RKPRRs that recognize DAMPs belong to the RD kinases (BOLLER; FELIX, 2009; DARDICK; SCHWESSINGER; RONALD, 2012; SCHWESSINGER; RONALD, 2012).

Presently, in spite of the large number of genes predicted to encode RKs and RLPs, only a minority of PRRs has been characterized and few ligands have been identified. The first successfully characterized ligand-PRR pair was the bacterial flagellin (or the derived peptide flg22) recognized by the LRRRK FLAGELLING SENSIN2 (FLS2) (GOMEZ-GOMEZ; BOLLER, 2000). Initially, FLS2 was identified in the model plant *Arabidopsis*, but functional orthologs have already been found in a wild relative of tobacco (*Nicotiana benthamiana*), rice, tomato (*Solanum lycopersicum*), and grapevine (*Vitis vinifera*) (HANN; RATHJEN, 2007; ROBATZEK et al., 2007; TAKAI et al., 2008; TRDA et al., 2014). Another well-characterized PRR, is the EF-Tu RECEPTOR (EFR) that recognizes the conserved N-acetylated epitope elf18 of the first 18 amino acids of the bacterial elongation factor Tu (ZIPFEL et al., 2006). Nevertheless, whereas flg22 seems to be recognized by most higher plants, the ability to perceive elf18 seems restricted to the plant family *Brassicaceae* (BOLLER; FELIX, 2009).

Table 1 – *Arabidopsis* PRRs and their respective ligands

Receptor	**Receptor type**	**Extracellular domain**	**ligand**	**Ligand Type**	**References**
PEPR1/2	RK	LRR	*At*Peps	DAMPS	(HUFFAKER; PEARCE; RYAN, 2006; YAMAGUCHI et al., 2010)
RLK7	RK	LRR	*At*PIPs		(HOU et al., 2014)
WAK1	RK	EGF	OGs		(BRUTUS et al., 2010)
DORN1/ LecRK-I.9	RK	Lec	eATP		(CHOI et al., 2014)
FLS2	RK	LRR	flg22	MAMPs	(CHINCHILLA et al., 2006; GOMEZ-GOMEZ ; BOLLER, 2000)
EFR	RK	LRR	elf18		(ZIPFEL et al., 2006)
CERK1	RK	LysM	Chitin		(MIYA et al., 2007)
LYK4/5	RK	LysM	Chitin		(PETUTSCHNIG et al., 2010; WAN et al., 2012)
LYM1/3	RLP	LysM	PGN		(WILLMANN et al., 2011)
LYM2	RLP	LysM	Chitin		(FAULKNER et al., 2013; PETUTSCHNIG et al., 2010)
ReMAX	RLP	LRR	eMAX		(JEHLE et al., 2013)
RBGP1	RLP	LRR	PGs		(ZHANG et al., 2014)

RK, receptor kinase; RLP, receptor-like protein; LRR, leucine-rich repeats domain; EGF, epidermal growth factor (EGF)-like domain; Lec, lectin-domain; LysM, lysine motif domain; *At*Peps, *Arabidopsis* elicitor peptides; *At*PIPs, *Arabidopsis* PIP peptides; OGs, oligogalacturonides; eATP, extracellular ATP; flg22, bacterial flagellin peptide; elf18, epitope of the bacterial elongation factor Tu; PGN, Peptidoglycans; eMAX, enigmatic bacterial PAMP partially purified from *Xanthomonas axonopodis pv. citri;* PGs endopolygalacturonases

As an example of RLPPRRs, in *Arabidopsis*, there are two RLPs with lysine motif (LysM)-containing ectodomains, *At*LYM1 and *At*LYM3, that specifically bind peptidoglycans (PGNs) that are the major components of the cell walls of both Gram-positive and Gram-negative bacteria (ERBS; NEWMAN, 2012; WILLMANN et al., 2011). Interestingly, the PGN-induced responses are impaired in the absence of the LysMRK CERK1 that does not bind PGN itself (WILLMANN et al., 2011), implying that PGN perception in *Arabidopsis* employs a multimeric receptor system, comprising PGN-binding LysMRLPs and signaling-transducing LysMRKs, such as CERK1 (ZIPFEL, 2014). Moreover, CERK1 has also been

shown to be required for chitin perception, the major constituent of fungal cell walls. However, in contrast to PGNs, the extracellular domains of CERK1 specifically bind chitin oligomers that act as bivalent ligands, leading to the homodimerization of CERK1 and generation of chitin-induced signaling (LIU et al., 2012; MIYA et al., 2007).

As stated above, PRRs can also sense DAMPs that are self-molecules available for recognition only after cell/tissue damage or pathogen recognition (ZIPFEL, 2014). To date, in *Arabidopsis*, the best-characterized DAMP-PRR pairs correspond to the *At*Pep peptides and the LRRRKs PEPR1 and PEPR2 (BARTELS; BOLLER, 2015) that will be presented further in detail. Recently, the PIP1 and PIP2 peptides have been shown also to bind the receptor-like kinase 7 (RLK7) (HOU et al., 2014). Besides peptides, in *Arabidopsis*, DAMPs can also be lytic plant cell wall fragments, such as oligogalacturonides (OGs) that are perceived by the epidermal growth factor (EGF) motif-containing the RK wall-associated kinase 1 (WAK1) (BRUTUS et al., 2010), and extracellular adenosine 5'-triphosphate (eATP) that is recognized by the receptor DORN1/LecRK-I.9 (CHOI et al., 2014).

1.1.3 Coregulatory receptor kinases

RKs also can act as regulatory proteins that do not necessarily interact with a ligand, but are important facilitators or suppressors of signaling activation and allow signaling cross-talk at the plasma membrane, coordinating the different signals perceived in the apoplast to ensure the proper downstream signaling (SCHWESSINGER; RONALD, 2012). For instance, members of the SERK family have been shown to redundantly hetero-oligomerize with other RKs, albeit with different affinities, and to regulate multiple physiological programs (AAN DEN TOORN; ALBRECHT; DE VRIES, 2015; POSTEL et al., 2010; ROUX et al., 2011). In *Arabidopsis*, the SERK family consists of five close homologs (SERK1 to SERK5) that have arisen through gene duplications, are all characterized by a small extracellular domain consisting of 4.5-5 LRRs and by the presence of a typical serine and proline-rich motif after a truncated extracellular LRR domain, and belong to the LRRRK subclass II (AAN DEN TOORN; ALBRECHT; DE VRIES, 2015; HECHT et al., 2001).

Among the SERK members, SERK3/BAK1 (hereafter referred as BAK1) is the most extensively studied and, because it has been shown to be required for the proper functionality of numerous RKs, it has been proposed as a multifunctional adaptor molecule implicated in plant development, cell death control, and innate immunity (HE et al., 2007; POSTEL et al., 2010; ROUX et al., 2011; SCHWESSINGER et al., 2011). BAK1 was originally discovered to dimerize with the main brassinosteroid (BR) receptor BRASSINOSTEROID-INSENSITIVE1 (BRI1) (LI et al., 2002;

WANG et al., 2001). Later on, its rapid ligand-dependent interaction with PRRs (FLS2 and EFR) and PEPRs has been documented as well (CHINCHILLA et al., 2007; POSTEL et al., 2010; SCHULZE et al., 2010; SCHWESSINGER et al., 2011). This interaction appears to be functionally important because null mutants of BAK1 displayed impaired defense responses upon perception of a plethora of fungal, bacterial, and oomycete-derived conserved microbial signatures, indicating that it is a positive regulator of PRRs. However, this impairing differs between MAMPs and residual responses might still be found (CHINCHILLA et al., 2009; CHINCHILLA et al., 2007; RANF et al., 2011; SCHWESSINGER et al., 2011), possibly due to the BAK1 substitution in the receptor complex by other members of the SERK family (BOLLER; FELIX, 2009). Indeed, the closest BAK1 homolog, SERK4/BKK1 (hereafter referred as BKK1), plays a partially redundant role during PTI signaling and forms ligand-dependent complexes with EFR and FLS2 (ROUX et al., 2011). Partially redundant roles among other SERK family members have been observed with BRI1 that interacts with four out of five members of the SERK family (SERK1 to SERK4) (GOU et al., 2012; HE et al., 2007; LI et al., 2002). Recently, the identification of a novel mutant allele, *bak1-5*, which is specifically impaired in PTI signaling without displaying any other pleiotropic defects in BR signaling or cell death control, confirmed that BAK1 contributes significantly to disease resistance against biotrophic and hemibiotrophyc pathogens (ROUX et al., 2011; SCHWESSINGER; RONALD, 2012; SCHWESSINGER et al., 2011).

The specificity of *bak1-5* to affect immunity responses is determined by a single amino acid substitution (Cys to Tyr at position 408) in the kinase domain that reduces the phosphorylation status, probably by affecting the recruitment or activation of downstream signaling components (SCHWESSINGER et al., 2011). Phosphorylation events are the earliest responses after formation of ligand-induced complexes and they have been proposed to modulate the downstream responses of BAK1 and its interacting partners (SCHULZE et al., 2010; SCHWESSINGER et al., 2011). In supporting of this hypothesis, the recently mapped phosphorylation patterns of BAK1 associated with different RK partners (BRI1, FLS2, and EFR) revealed that differential phosphorylation patterns of RKs resulted from the altered BAK1 phosphorylation status, suggesting that these phosphorylation events could be the molecular basis for selective regulation of multiple BAK1-dependent pathways (WANG et al., 2014).

Additionally, BAK1 can also associate with members of the BAK1-interacting receptor (BIR) of the RK family, predicted to be very similar in structure as BAK1 (GAO et al., 2009; HALTER, et al., 2014b). Interaction between BIR2 and BAK1 has recently been found to occur in the absence of MAMP perception, preventing interaction with the ligand-binding FLS2; however, perception of MAMPs leads to BIR2 release from the BAK1 complex and

enables the recruitment of BAK1 into the FLS2 complex. These findings imply that BIR2 act as a negative regulator of PTI by limiting the BAK1-receptor complex formation in the absence of ligands (HALTER, et al., 2014a; HALTER, et al., 2014b).

1.1.4 Receptor-like cytoplasmic kinases as direct substrates of PRR complexes

In addition to coregulatory receptor kinases, cytoplasmic partners are also required to link the PRR activation with the downstream intracellular signaling. In recent years, receptor-like cytoplasmic kinases (RLCKs) have emerged as direct substrates of PRR complexes and key positive regulators of PTI signaling (MACHO; ZIPFEL, 2014). Currently, the RLCK *Botrytis*-induced kinase 1 (BIK1) that is part of the large multigenic RLCKVII subfamily, has been shown to be an important regulator of the activation of PRR complexes that mediate the innate immunity in *Arabidopsis* and interact constitutively with FLS2, EFR, CERK, PEPRs and BAK1 (LIU et al., 2013; LU et al., 2010; ZHANG et al., 2010). The ligand-binding activation of PRR complexes results in a rapid BIK1 phosphorylation that dissociates from the receptors to trigger the downstream signaling (LU et al., 2010; ZHANG et al., 2010). BIK1 and its closely related proteins (PBLs) seem to have partially redundant functions during PTI, but specific roles have been suggested because PBL1, PBL2 and PBL5 can also regulate flg22-induced responses, whereas only PBL1 additionally interacted with PEPR1 (LIU et al., 2013; ZHANG et al., 2010). The requirement of different RLCKs for specific PTI responses suggests that the choice of specific RLCKs as PRR substrates constitutes another layer in the signaling branching regulation from PRR complexes (MACHO; ZIPFEL, 2014).

1.1.5 Pattern-triggered immunity responses

Most of the known PRRs heteromerize with coregulatory receptor kinases (BAK1 or other RK) almost instantaneously after ligand perception, followed by phosphorylation and activation of the intracellular kinase domain of both receptors and subsequent activation of a sequential set of early and long-term responses as well as downstream signaling cascades to adapt to the imminent attack (BOLLER; FELIX, 2009; MACHO; ZIPFEL, 2014; SCHULZE et al., 2010; SCHWESSINGER et al., 2011). Some of these responses are routinely used as read-outs to study PRRs and their ligands.

In the first minutes after MAMPs/DAMPS perception, changes in the ion fluxes can be detected, including H^+ and Ca^{2+}, leading to membrane depolarization (MITHÖFER; EBEL; FELLE, 2005). The effects on H^+ fluxes can be clearly observed in suspensions of cultured cells in which they lead to alkalinization of the liquid growth medium (BOLLER, 1995). Recently, calcium-dependent protein kinases (CDPKs), acting as Ca^{2+} sensor protein kinases,

have been reported to be major mediators of the early PTI immune signaling (BOUDSOCQ et al., 2010). Another very early response is the production of reactive oxygen species (ROS) that acts as antibiotic agents directly and as secondary signals to induce intracellular and systemic signaling events (APEL; HIRT, 2004). The initial downstream signaling of PTI includes also the activation of so-called mitogen-activated protein (MAP) kinases (MAPKs), considered key regulatory elements in the early transduction of MAMPs/PAMPs-PRRs signaling (HETTENHAUSEN; SCHUMAN; WU, 2014). In *Arabidopsis*, triggered PRRs induce activation of MPK3 and MPK6, starting with a lag phase of approximately 1–2 min and peaking after 5–10 min (RANF et al., 2011). MAPK activation leads to induction of some early defense-related genes, such as some members of the WRKY transcription factor family (ASAI et al., 2002). Interestingly, MAPKs and Ca^{2+}-dependent protein kinases seem to function independently and the transcriptional reprogramming that results from the MAPK activity differs from the modulations achieved through the CDPK activity (BOUDSOCQ et al., 2010).

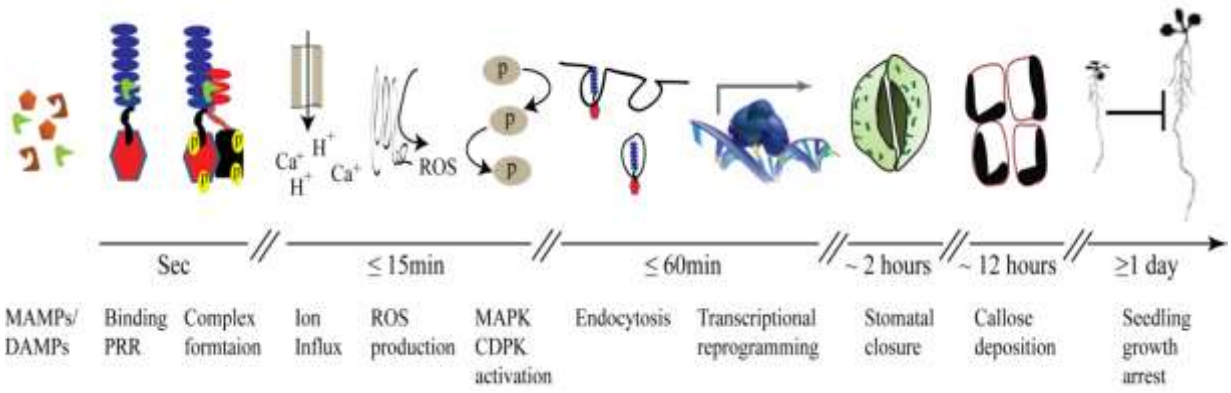

Figure 2 - Proposed model of pattern trigger immunity responses based on studies of known ligand-PRRs pairs. MAMPs/DAMPs are recognized by the respective PRR and almost instantaneously the activated PRR interact with a coregulatory receptor kinase followed by phosphorylation and activation of the intracellular kinase domain of both receptors. Then, a set of very early responses including increased of intracellular calcium, extracellular alkalinization, ROS production, and MAPK and CDPK activation by phosphorylation occur. Subsequently, the activated receptors are removed from the plasma membrane by endocytosis and a massive transcriptional reprogramming is detected. Finally, late responses are found hours or days after the MAMP/DAMP stimuli, including stomata closure, callose deposition and seedling growth inhibition

Following the initial responses, pattern recognition results in a massive transcriptional reprogramming. Transcriptomic studies in *Arabidopsis* indicated that as early as 30 min after flg22 treatment, almost 1000 genes were up-regulated and approximately 200 genes were down-regulated (ZIPFEL et al., 2004). Additional studies also revealed a similar pattern of gene regulation upon elf26 and chitin application, suggesting a stereotypical response to MAMPs and DAMPs (NAVARRO et al., 2004; RAMONELL et al., 2002; ZIPFEL et al., 2006). Most up-regulated genes encode enzymes involved in the synthesis of antimicrobial compounds and proteins involved in signal perception and transduction, including RKs, transcription-regulatory factors and phosphatases (NAVARRO et al., 2004; RAMONELL et al., 2002; ZIPFEL et al., 2006). The fact that several RKs are present implies that the early gene induction plays a role as positive feedback to increase the PRR perception capabilities (BOLLER; FELIX, 2009). Although transcriptomic studies have shown an overlap in genes induced by different MAMPs and DAMPs, assessment of transcriptional changes in long-term patterns resulting from exposure to flg22 and oligosaccharides (OGs) derived from the plant cell walls over an extended time course revealed that the transcriptional regulation can differ not only in timing and amplitude, but also in gene activation during flg22 elicitation and not during OG responses (DENOUX et al., 2008). Thus, although different elicitor molecules may trigger conserved transcriptional responses, specific aspects depend on the sensed elicitor.

Another interesting aspect of PTI is the endocytosis of the PRRs that has been first demonstrated by using GFP-labeled FLS2 that, after flg22 stimulation (30-60 min) is translocated from the plasma membrane via vesicle-mediated endocytosis and targeted to endosomal sorting (BECK et al., 2012; ROBATZEK; CHINCHILLA; BOLLER, 2006). Similar observations have also been documented for the LeEIX2 receptor in tobacco after stimulation with the fungal protein elicitor ethylene-inducing xylanase (EIX) (BAR; AVNI, 2009; SHARFMAN et al., 2011), suggesting that this process could be a hallmark of triggered PRR activation. Although an increasing amount of data indicates that endocytosis is part of the PRR response, its role during PTI signaling, trafficking machinery and subcellular dynamics of the process is still poorly understood.

Subsequently to early PTI events, late responses are detected hours or days after the MAMP/DAMP stimuli, including stomata closure, callose deposition and seedling growth inhibition (BOLLER; FELIX, 2009; MELOTTO et al., 2006). Stomata are considered a constitutively natural access for a significant number of microbes; therefore, plants can restrict pathogen entry by closing stomata or by inhibiting stomata opening (MELOTTO et

al., 2006). Callose deposition is also a hallmark of PTI responses of which the biological relevance is not clear, but that can be detected approximately 16 h after MAMP treatment (GOMEZ-GOMEZ; FELIX; BOLLER, 1999). If MAMP/DAMP perception continues for days, a seedling growth inhibition in a concentration-dependent manner can be detected, suggesting a switch of resource allocation from growth to a defense program; nevertheless, the physiological role and molecular details of this response is under debate (BOLLER; FELIX, 2009; KROL et al., 2010; LOZANO-DURAN; ZIPFEL, 2015). Downstream of PTI, plant hormones can be involved, mainly salicylic acid (SA), ethylene and jasmonic acid (JA), that further finely modulate immune responses, spreading the message of imminent danger to yet unaffected tissues (PIETERSE et al., 2012).

1.2 Endogenous plant elicitor peptides

As indicated above, in addition to elicitor molecules derived from invading organisms, plants also recognize host-derived molecules, referred as DAMPs, to activate PTI. Known DAMPs are, for instance, cell wall fragments, such as OGs and cellulose fragments, cutin monomers, eATP and peptides (CHOI et al., 2014; FERRARI et al., 2013; KAUSS et al., 1999; YAMAGUCHI; HUFFAKER, 2011). Significant progress has been achieved in identifying new endogenous peptide elicitors among the different classes of DAMPs and in delineating their downstream signaling mechanism (YAMAGUCHI; HUFFAKER, 2011). Generally, these small (5-100 amino acids in length) peptides are categorized as plant signaling peptides; within this category, the endogenous plant peptides are grouped that coordinate multiple and very diverse biological and physiological plant responses (GHORBANI et al., 2014). Because of the aims of this thesis, I will present only the signaling peptides related to plant immunity.

Plant elicitor peptides are released from large precursor proteins and have been classified with respect to their precursor protein structure in three major groups: (i) peptides derived from precursor proteins without an N-terminal secretion signal, (ii) peptides derived from precursor with an N-terminal secretion signal, and (iii) peptides derived from proteins with distinct primary functions (ALBERT, 2013; YAMAGUCHI; HUFFAKER, 2011).

1.2.1 Peptides derived from precursor proteins without an N-terminal secretion signal

This category includes the 18-amino-acid peptide systemin that was the first isolated peptide with a hormone characteristic and that had been shown to be involved in systemic responses to wounding in tomato (PEARCE et al., 1991). Systemin derives from the C-

terminus of a 200-amino-acid precursor protein, prosystemin, that mainly accumulates in the cytosol of vascular phloem parenchyma cells (MCGURL et al., 1992) via a still unknown cleavage mechanism. Systemin induces JA biosynthesis in the neighboring cells, leading to induction of proteinase inhibitors, anti-nutritive proteins, and plant volatiles to deter plant herbivores (DEGENHARDT et al., 2010; OROZCO-CARDENAS; MCGURL; RYAN, 1993). Systemin homologs have only been found in the *Solanoideae* subfamily of the *Solanaceae* family (CONSTABEL; YIP; RYAN, 1998) and so far the systemin receptor has not been identified.

In *Arabidopsis*, the first isolated DAMP peptide was the plant elicitor peptide1 (Pep1) that binds two RK PRRs with high affinity PEPRs (YAMAGUCHI et al., 2010). *At*Pep1 that is a representative member of a protein family composed by eight members derives from the C-terminus of a 92-amino-acid precursor protein *At*PROPEP1 (BARTELS et al., 2013; HUFFAKER; PEARCE; RYAN, 2006). The *At*Pep-PEPR system will be presented in detail (see below).

Another peptide that could fit within this category is the recently identified 25-amino-acid peptide Kiss of death (KOD) that has been proposed as an early regulator of programmed cell death (PCD) (BLANVILLAIN et al., 2011). Although no direct link with plant immunity has been demonstrated yet, the *KOD* gene is induced upon biotic and abiotic stresses, suggesting that this peptide could also act as a potential DAMP, but further clarifying studies are needed (ALBERT, 2013; BLANVILLAIN et al., 2011). Interestingly, in contrast to systemin and *At*Pep1, KOD seems to be directly translated as the active form, because the corresponding gene only encodes the active 25-amino-acid sequence, avoiding the cleaving-off from a precursor protein (BLANVILLAIN et al., 2011).

1.2.2 Peptides derived from precursor with an N-terminal secretion signal

This group comprises the secreted peptides, including the hydroxyproline-rich systemin (HypSys) peptides that are derived from a precursor protein with an N-terminal secretion signal for the cell wall matrix localization (PEARCE et al., 2001). Two distinct 18-amino-acid HypSys were first isolated from tobacco leaves (*Nt*HypSysI and *Nt*HypSysII), derived from one single precursor protein encoded by one single gene (PEARCE et al., 2001). Orthologs of *Nt*HypSys have only been isolated in *Solanaceae* and *Convolvulaceae* (NARVÁEZ-VÁSQUEZ; OROZCO-CÁRDENAS; RYAN, 2007). The amino acid sequence of HypSys resembles that of systemin, but, due to their passage through the secretory system, the polyprolines are hydroxylated and then glycosylated with pentose sugar chains (PEARCE

et al., 2001). HypSys peptides have been described as important plant immunity amplifiers and triggers, especially during herbivore attack, but also during interaction with other plant pathogens (BHATTACHARYA et al., 2013). The HypSys receptor still remains to be identified.

Recently, in *Arabidopsis*, members of a new peptide family, termed PAMP-induced peptides (*At*PIP) have been shown to activate immune responses and to enhance resistance against *Pseudomonas syringae* and *Fusarium oxysporum* (HOU et al., 2014). These peptides are derived from the C-terminus of precursor proteins (prePIPs) with an N-terminal signal peptide, localized in the pericellular apoplastic space, of which the transcripts are up-regulated in plants exposed to MAMPs (HOU et al., 2014). Interestingly, transgenic plants expressing the GFP gene under control of the *prePIP1* promoter exhibited fluorescent tissues corresponding either with potential entry points or proliferation routes for invading organisms (HOU et al., 2014). Genetic and biochemical evidence suggested that Receptor Kinase 7 (RLK7) functions as PIP1 receptor (HOU et al., 2014).

1.2.3 Peptides derived from proteins with distinct primary functions

The first peptide that had been discovered to regulate immunity in plants derives from a protein with other primary functions and belongs to the family of inceptin peptides. These acidic 11-13-amino-acid peptides originate from the chloroplastic ATP synthase that is broken down in the gut of fall armyworm larvae (SCHMELZ et al., 2006, 2007). Inceptin treatments of cowpea (*Vigna unguiculata*) leaves was shown to trigger plant defense responses, such as production of SA, JA, and metabolites with defensive roles that together reduce fall armyworm growth (SCHMELZ et al., 2006, 2007). The elicitor activity of inceptins seems to be specific for *Phaseolus* and *Vigna genera* (SCHMELZ et al., 2007).

The *Glycine max* (soybean) subtilase peptide (*Gm*SubPep) is another member of this peptide category. *Gm*SubPep is a 12-amino-acid-long peptide that was discovered embedded in the protein-associated domain of a putative extracellular subtilase and, like other DAMPs, is able to trigger extracellular alkalinization and to induce the expression of defense- and stress-related genes (PEARCE et al., 2010). The mechanism of the *Gm*SubPep release from the subtilase and its receptor has not yet been identified.

1.3 The system of plant elicitor peptides (Peps) and PEPRs

1.3.1 Plant elicitor peptides (Peps)

The Peps are a family of defense–inducible peptides. The first member has been isolated in *Arabidopsis* (*At*Pep1) from an extract of wounded leaves by means of an elicitor-induced alkalinization activity assay with *Arabidopsis* suspension–cultured cells (HUFFAKER; PEARCE; RYAN, 2006). *At*Pep1 is a 23-amino-acid-long peptide derived from the C-terminus of a 92-amino-acid precursor protein PROPEP1 that lacks a secretion N-terminal signal (HUFFAKER; PEARCE; RYAN, 2006). Originally, the PROPEP family in *Arabidopsis* has been described as consisting of seven members, but an additional PROPEP has recently been identified by more sensitive bioinformatic tools (BARTELS et al., 2013; HUFFAKER; PEARCE; RYAN, 2006). Based on sequence homology of the SSGR/KxGxxN motif, all eight PROPEPs are predicted to contain a putative *At*Pep (*At*Pep1 to *At*Pep8) of 23 to 29 amino acids in length at the C-terminus (BARTELS et al., 2013). Although only *At*Pep1 and *At*Pep5 have been biochemically isolated from *Arabidopsis* leaves, the other peptides have been synthetized and their activity confirmed (BARTELS et al., 2013; HUFFAKER; PEARCE; RYAN, 2006). The presence of PROPEPs has been expected in numerous species, including important crops (HUFFAKER; PEARCE; RYAN, 2006), and has been functionally validated in maize (*Zea mays*). The participation of *Zm*Pep1 and *Zm*Pep3 has been demonstrated during maize immunity responses, suggesting that the PROPEP family is largely conserved across the plant kingdom and that such Peps might probably play a role as general defense mediators (HUFFAKER; DAFOE; SCHMELZ, 2011; HUFFAKER et al., 2013).

Exogenous applications of *At*Peps induce a set of similar responses, hinting at functional redundancy (BARTELS et al., 2013; YAMAGUCHI et al., 2010). However, bioinformatic analysis and expression localization assessment revealed that the expression pattern of PROPEPs differs temporally and spatially under normal conditions and in response to various stresses (BARTELS et al., 2013), thus implying differential physiological roles within the *At*Pep members (BARTELS; BOLLER, 2015; BARTELS et al., 2013).

1.3.2 Perception of Peps by PEPRs

The perception of *At*Peps is mediated by binding to the extracellular LRR domain of two RKsPRR, designated PEPRs. PEPR1 is able to detect all eight *At*Peps, whereas PEPR2 can only detect *At*Pep1 and *At*Pep2 (BARTELS et al., 2013). PEPR1 was identified by photoaffinity labeling and further purification from *Arabidopsis* extracts. As the T-DNA

mutants of *pepr1* were only partially compromised in *At*Pep1-induced responses (YAMAGUCHI; PEARCE; RYAN, 2006), additional receptors were looked for. PEPR2 was subsequently identified by phylogenetic analysis, and its role as *At*Pep1 receptor was experimentally demonstrated (KROL et al., 2010; YAMAGUCHI et al., 2010). The double *pepr1 pepr2* mutant completely abolished the *At*Peps immune responses, indicating that they are the only receptors able to perceive this family of peptides (KROL et al., 2010; YAMAGUCHI et al., 2010). PEPRs belong to the XI subgroup of LRRRKs and are classified as kinases with an arginine-aspartic acid (RD) motif in the catalytic site that are different from FLS2 and EFR that are non-RD kinases (YAMAGUCHI et al., 2010). Non-RD kinases generally show weak autophosphorylation activity, and there is a significant correlation between the absence of this motif and a role in the early events of innate immune signaling (DARDICK; SCHWESSINGER; RONALD, 2012).

Recently, the crystal structure of the extracellular LRR domain of PEPR1 (PEPR1LRR) in complex with *At*Pep1 has been revealed, demonstrating that the conserved C-terminal portion of *At*Pep1 dominates the *At*Pep1 binding to PEPR1LRR; moreover, the non-conserved N-terminal sides of *At*Peps might possibly contribute to the preferential recognition of *At*Pep1 and *At*Pep2 by PEPR2 over the other *At*Peps (TANG et al., 2015).

1.3.3 Signaling mediated by Peps-PEPRs

After recognition of *At*Peps by PEPRs, different signaling responses are activated that are greatly similar to those triggered by the receptors FLS2 and EFR, when the bacterial MAMPs flg22 and elf18 are perceived, respectively (BARTELS; BOLLER, 2015). Upon ligand binding, PEPRs interact with the coreceptor BAK1 followed by phosphorylation of both BAK1 and PEPRs (SCHULZE et al., 2010; TANG et al., 2015). Additionally, the RLCK BIK1 that constitutively interacts with PEPR1 and probably with PEPR2 also gets phosphorylated (LIU et al., 2013). Then, induction of ion fluxes across the plasma membrane, ROS and ethylene production, and MPK3 and MPK4 activation are quickly triggered (KROL et al., 2010; RANF et al., 2011; YAMAGUCHI; PEARCE; RYAN, 2006). *At*Peps also lead to a transcriptional reprogramming, inducing expression of pathogen defense genes, such as *PDF1.2*, *MPK3*, *PR-1* and *WRKY* (HUFFAKER; RYAN, 2007; YAMAGUCHI et al., 2010). Interestingly, exogenous *At*Peps also induce the expression of their own precursor genes (except *At*Pep6) and their receptors, potentially indicating a positive feedback loop in the signaling of *At*Peps-PEPRs (HUFFAKER; RYAN, 2007; YAMAGUCHI et al., 2010). Callose deposition and seedling growth inhibition occur when seedlings are maintained in the

presence of *At*Peps (KROL et al., 2010; LIU et al., 2013; RANF et al., 2011). Curiously, in contrast to flg22 that affects the whole seedling, the inhibitory effect of *At*Pep perception impairs mainly root growth (KROL et al., 2010; RANF et al., 2011).

1.3.3 Peps as amplifiers of innate immunity

*At*Peps have proposed to act mainly as amplifiers of innate immunity. This role is proposed because they mediate immunity responses, and the expression of their precursor proteins and receptors are induced upon biotic stresses, such as microbial infection, bacterial elicitors, wounding and JA and ethylene application (BARTELS; BOLLER, 2015; YAMAGUCHI; HUFFAKER, 2011). However, additional role in different physiological processes have been considered as well (BARTELS et al., 2013; GULLY et al., 2015).

As amplifiers, in a danger situation, *At*Peps are believed to be released from their precursor proteins (PROPEPs) into the extracellular spaces, where they subsequently bind their receptors located at the plasma membrane of neighboring cells, thus triggering defense responses and, hence, spreading the message **(**BARTELS; BOLLER, 2015; YAMAGUCHI; HUFFAKER, 2011). However, this assumption is based mostly on data generated from genetic and biochemistry experiments. The subcellular dynamics of the *At*Pep1-PEPR complex remains largely unknown.

1.4 Plant endomembrane system and trafficking

Plant cells possess a sophisticated endomembrane system that physically and functionally interconnects membranous compartments, allowing exchange of materials, such as proteins, polysaccharides, and lipids to their suitable cell locations (MORITA; SHIMADA, 2014). This system needs to be well-coordinated to maintain cellular homeostasis and to generate accurate responses toward different environmental stimuli such as challenges by microorganisms (INADA; UEDA, 2014). The plant endomembrane system includes the plasma membrane, the *trans*-Golgi network/early endosome (TGN/EE), multivesicular body/prevacuolar compartment (MVB/PVC), vacuoles, the Golgi apparatus and the endoplasmic reticulum (PIZARRO; NORAMBUENA, 2014). Material is transported within the plant endomembrane system through sequential steps including budding, movement and vesicle fusion (BONIFACINO; GLICK, 2004). Recently, the plant membrane trafficking pathways have been proposed to be classified into several major categories: (i) the secretory pathway that transports newly synthesized proteins from the endoplasmic reticulum to the plasma membrane and/or the extracellular space; (ii) the vacuolar transport pathway that

delivers newly synthesized or internalized proteins to the vacuole; (iii) the endocytic pathway that transports proteins localized at the plasma membrane or extracellular cargos to an intracellular compartment, and (iv) the recycling pathway when proteins are sorted back to the plasma membrane (INADA; UEDA, 2014). Nevertheless, in view of the aims of this thesis, I will describe in detail the endocytic pathway only.

1.4.1 Plant endocytosis

Endocytosis can be defined as a dynamic process by which cells take up extracellular material and cell surface proteins via vesicle compartments and that is controlled by a network of regulatory proteins (FAN et al., 2015). In the last decade, endocytosis in plant cells has received considerable attention, demonstrating its pivotal role in a plethora of cellular processes, including nutrient uptake, hormonal regulation, signaling transduction, and pathogen defense (DU et al., 2013; IRANI et al., 2012; LUSCHNIG; VERT, 2014; ROBATZEK; CHINCHILLA; BOLLER, 2006; TAKANO et al., 2005). Endocytosis has been more extensively studied in animals than in plants. Endocytosis in animals occurs through multiple mechanisms that fall into two main groups: phagocytosis that is related with the uptake of large particles and pinocytosis that is associated with the uptake of fluids and solutes. Pinocytosis can be further divided into macropinocytosis, clathrin-mediated endocytosis (CME), and clathrin-independent endocytosis (CIE) (CONNER; SCHMID, 2003). In plants, CME is accepted as the predominant endocytosis route and has been well characterized (BAISA; MAYERS; BEDNAREK, 2013; GADEYNE et al., 2014), whereas other mechanisms have only been suggested (BANDMANN; HOMANN, 2012; BARAL et al., 2015; LI et al., 2012).

1.4.2 Clathrin-mediated endocytosis

Presently, CME has been proposed to require a series of sequential and highly coordinated steps, including (i) nucleation that defines the sites on the plasma membrane where clathrin will be recruited and vesicles will bud, (ii) cargo recognition/selection, when cargo-specific adaptor proteins are mobilized, (iii) vesicle coat assembly, where clathrin triskelia are recruited from the cytosol to the adaptor proteins to help organize the formation of clathrin-coated pits (CCPs), (iv) scission, when CCPs maturate and are separated from the plasma membrane to form clathrin-coated vesicles (CCVs), and finally (v) uncoating, when the coat falls off from the CCVs, the uncoated vesicles fuse with an intracellular compartment for further processing and the clathrin machinery goes back into the cytoplasm to be reused in another round of CCV formation (BAISA; MAYERS; BEDNAREK, 2013; CHEN; IRANI;

FRIML, 2011; FAN et al., 2015; MCMAHON; BOUCROT, 2011). These steps have been considered mainly based on research carried out in animals and yeast, but the CME machinery in plants is still poorly defined, despite the recent discoveries toward understanding CME in plants. However, CME seems to be evolutionarily conserved, because of the presence of several homologous CME effectors in plants, animals and yeast, but important kingdom-specific modifications have been evidenced (GADEYNE et al., 2014).

Clathrin consists of three heavy chain subunits and three light chain molecules that interact to self-assemble into a triskelion structure (FAN et al., 2015). The *Arabidopsis* genome encodes two functionally redundant clathrin heavy chain (CHC1 and CHC2) and three clathrin light chain (CLC1 to CLC3). Genetic studies of all five subunits support the conserved mechanism of CME in plants and its importance for growth and development (CHEN; IRANI; FRIML, 2011; KITAKURA et al., 2011; WANG et al., 2013). The c*hc2* single mutants and dominant-negative CHC transgenic lines have been shown to be defective in bulk endocytosis and in internalization of plasma membrane proteins (KITAKURA et al., 2011).

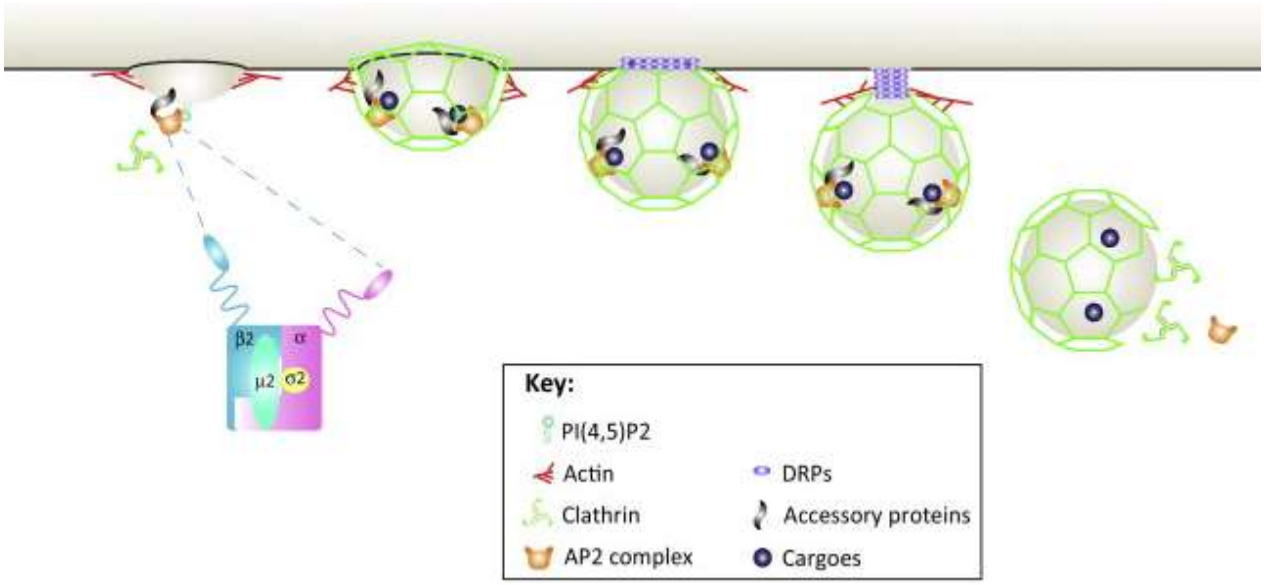

Figure 3 - Proposed model of clathrin-mediated endocytosis (CME) in plants (FAN et al., 2015). CME can be divided into five steps. (1) Clathrin-coated endocytic vesicle formation starts with the association of adaptor protein complex-2 (AP2)) with the plasma membrane (PM) via binding to phosphatidylinositol-4,5-bisphosphate [PI(4,5)P2]. (2) The membrane-associated AP-2 recruits clathrin and the unidentified accessory proteins. After initiation, AP-2 binds to various cargo proteins through its σ2 and μ2 subunits. With the aid of accessory proteins, AP-2 continues to recruit clathrin, which polymerizes and forms a clathrin coat around the newly formed membrane invagination. (3) When the clathrin-coated vesicles (CCVs) mature, the GTPase dynamin-related protein (DRP) is recruited at the neck of the vesicle and (4) is responsible for the detachment of the vesicle from the PM. (5) Once the vesicles have been pinched off, the coated components are disassembled and release the cargo-containing endocytic vesicles into the cytoplasm. In plants, the cortical actin cytoskeleton has been implicated in the regulation of clathrin-coated pit (CCP) dynamics at the PM

Besides clathrin, other components of the CME machinery have been reported, including components of the adaptor protein complex 2 (AP2) that represents the core complex during the cargo recognition/selection of the CME in animals (COCUCCI et al., 2012). The AP2 complex of *Arabidopsis* that has been shown to be similar to its mammalian counterpart consists of four subunits (DI RUBBO et al., 2013) and the *ap-2* mutants of *Arabidopsis* have been found to be defective in BR responses and reproductive organ development (DI RUBBO et al., 2013; YAMAOKA et al., 2013). In support of the idea that CME presents evolutionary modifications in plants, a unique multisubunit protein complex, designated the TPLATE complex (TPC), has been reported to be mobilized early on to endocytic plant foci during CME, without clear yeast and animal homologs (GADEYNE et

al., 2014). The dynamin-related proteins DRP2A and DRP2B have also been described in *Arabidopsis* as players during the scission of CCPs (TAYLOR, 2011).

1.4.3 Intracellular destination of endocytic cargos

Following internalization from the plasma membrane, endocytosed material is delivered to the EEs. In plants, the TGN has been suggested to possess the EE function and to be the first site for endocytic cargo delivery (DETTMER et al., 2006; VIOTTI et al., 2010). From the TGN/EE the cargo may be recycled back to the plasma membrane or continues along the endocytic pathway for possible degradation (VIOTTI et al., 2010). Currently, the best characterized recycling pathway is that of the ADP-ribosylation factor guanine-nucleotide exchange factor (ARF-GEF) that is involved in the constitutive recycling of PIN-FORMED (PIN) proteins and BR receptor BRI1 (GELDNER et al., 2001; GELDNER et al., 2007; TEH; MOORE, 2007). In *Arabidopsis* the sorting functions of the TGN/EEs are associated with the V-ATPase activity (DETTMER et al., 2006) that can modulate the pH homeostasis within this organelle (LUO et al., 2015). Recently, it was shown that inhibition of V-ATPase activity causes substantial alkalinisation of the TGN/EE that in turn negatively affects recycling, providing evidence that acidification of this organelle is indispensable for this process in plants (LUO et al., 2015).

Whether the cargo is directed to be degraded instead of recycling, it is transported to the MVBs/late endosome with intraluminal vesicles that finally fuse to the vacuole (SINGH et al., 2014). In *Arabidopsis*, the endosomal maturation from the TGN/EE to MVB has been proposed to originate in a subdomain of the TGN/EE that recruits Rab5-like ARA7 and subsequently matures into an MVB (SCHEURING et al., 2011; SINGH et al., 2014). The intraluminal vesicles at the MVBs are responsible for the isolation of cargos from the cytosol and they are formed through the endosomal sorting complex required for transport (ESCRT) machinery (HENNE; BUCHKOVICH; EMR, 2011). Posttranslational modifications have been shown to regulate sorting of endocytic cargos. Ubiquitination is considered a targeting signal that directs membrane proteins for degradation (SCHEURING et al., 2012) and phosphorylation has also been reported as an important cue to regulate endocytosis; for instance, plasma membrane and constitutive endocytosis of PIN auxin transporters are misregulated when their phosphorylation state is altered (MICHNIEWICZ et al., 2007; ZHANG, JING et al., 2010).

1.4.4 Receptor-Mediated Endocytosis

Receptor-mediated endocytosis (RME) is the uptake of soluble ligands from the extracellular space, after binding to specific plasma membrane-localized receptors (DI RUBBO; RUSSINOVA, 2012). The first indications of RME in plants were obtained from the study of a ^{125}I-labeled elicitor that was able to bind the cell surface and to internalize in a temperature- and energy-dependent process into a soybean cell suspension, but neither the identity of the receptor nor the nature of the elicitor molecule were known (HORN; HEINSTEIN; LOW, 1989). Subsequently, studies of the plasma membrane receptors have demonstrated the involvement of RME in different physiological processes, including plant development and plant immunity, mainly through research on the BR receptor BRI1 (IRANI et al., 2012) and flg22 receptor FLS2 (BECK et al., 2012; ROBATZEK; CHINCHILLA; BOLLER, 2006).

The internalization of receptors can either be constitutive or ligand induced. BRI1 and FLS2 can constitutively recycle in the absence of their respective ligands, BR and flg22 (BECK et al., 2012; GELDNER et al., 2007). Moreover, after treatments with the ligands, both receptors undergo ligand-induced endocytosis (BECK et al., 2012; IRANI et al., 2012). However, differences in the temporal dynamics of the ligand-induced endocytosis of BRI1 (~ 2 min after ligand application) and FLS2 (~ 30 min after ligand application) are evidenced (BECK et al., 2012; CHOI et al., 2013; IRANI et al., 2012), suggesting that the RME pathways are regulated by distinct mechanisms in plant cells, probably related to the ligand nature.

Usually, after the ligand-binding of the receptors, various signaling events are triggered, leading to specific cell responses (GELDNER; ROBATZEK, 2008; HAN; SUN; CHAI, 2014).Therefore, RME functions as a spatial and temporal modulator of the signaling outputs by (i) attenuating the signaling strength or duration by moving the activated receptor to lytic compartments or (ii) re-localizing active receptor to signaling endosomes from where signaling is sustained or initiated *de novo* (DI RUBBO; RUSSINOVA, 2012; GELDNER; ROBATZEK, 2008; SORKIN; VON ZASTROW, 2009). Both functions have been well-documented in animals, but the interplay between RME and signaling in plants is still a matter of debate. Recently, in *Arabidopsis* has been found that blocking endocytosis of active BRI1-ligand complexes at the plasma membrane enhanced BR signaling, whereas retaining BRI1-ligand complexes at the TGN/EE did not affect signaling (IRANI et al., 2012). Thus, indicating that the majority of BR signaling is initiated from the plasma membrane pool of BRI1 and that its endocytosis is not essential for the downstream signaling activity. Different from BRI1 seems to be the case of *Le*Eix2 receptor in tobacco, as ligand-induced signaling

triggered by EIX is impaired when endocytosis of *Le*Eix2 is blocked (BAR; AVNI, 2009; 2014). Similar observations have been reported for the FLS2 endocytosis that, when blocked with wortmannin (an inhibitor of phosphoinositide 3-kinase and phosphoinositide 4-kinase) or by mutations in its phosphorylation sites, leads to defective pathogen responses due to impaired flg22 signaling (ROBATZEK; CHINCHILLA; BOLLER, 2006; SALOMON; ROBATZEK, 2006). Furthermore, recent work suggests that FLS2 trafficking might be associated differentially with the immunity responses triggered by flg22 (SMITH et al., 2014a, 2014b). These findings imply that appropriate RME trafficking may be required for specific signaling responses that could also take place in endosomal compartments; however, this remains to be clarified.

As the plant genomes encode hundreds of plasma membrane receptors (SHIU; BLEECKER, 2003; SHIU et al., 2004), it is tempting to argue that RME is a mechanism that is amply used to modulate physiological responses. However, future studies are needed to clarify the modulation of endocytic pathways, the machinery involved, and the biological role of endocytosis during signal transduction cascades. So far, RME has been mainly studied through live imaging of genetically engineered fluorescent protein-tagged receptors (GELDNER; ROBATZEK, 2006), but RME can also be visualized with fluorescently labeled ligands (DI RUBBO; RUSSINOVA, 2012). This approach would allow faster assays, because different plant genotypes could be assessed when treated with labeled ligands, avoiding plant transformation or crossing steps that are needed when fluorescent protein-tagged receptors are used. Nevertheless, labeling molecules is a challenging task, because addition of an extra molecule can easily abolish or modify the biological activity. Recently, a BR analog labeled with a small fluorophore, Alexa Fluor 647, allowed the specific tracking of the endocytosis of the BRI1-ligand complexes in *Arabidopsis* meristem root tip cells, hence showing the potential of this approach (IRANI et al., 2012). Therefore, for further understanding of plant endocytosis, the identification of *bona fide* endocytosed ligand cargos that can be labeled with molecular probes without compromising their biological activity is required.

1.5 Aims of this thesis

The main focus of my Ph.D. research has been to understand the subcellular dynamics of plant signaling peptides and their interplay with signaling that have not been reported yet. To this end, I chose as a model the well-characterized plant immunity-related peptide *At*Pep1, because information about its signaling responses and components are available, including the identification of its plasma membrane-localized receptors. Moreover, *At*Pep1 is able to trigger quick, but transient immunity responses, thus providing an excellent scenario to study trafficking and signaling in general. Therefore, the aims of this thesis were the following:

- Develop a fluorescent tool to study the subcellular dynamics of *At*Pep1
- Investigate whether *At*Pep1 and its receptor undergo internalization
- Elucidate the trafficking pathway, mechanism and machinery of the *At*Pep1 internalization
- Examine the role of endocytosis during the *At*Pep1 signaling
- Clarify the role of BAK1, the coreceptor of *At*Pep1 receptors, in the internalization and signaling of *At*Pep1

References

AAN DEN TOORN, M.; ALBRECHT, C.; DE VRIES, S. On the origin of SERKs: bioinformatics analysis of the somatic embryogenesis receptor kinases. **Molecular Plant**, Saint Paul , v.8, n. 5, p.762-782, 2015.

ALBERT, M. Peptides as triggers of plant defence. **Journal of Experimental Botany** , Oxford, v. 64, n. 17, p. 5269-5279, 2013.

APEL, K.; HIRT, H. Reactive oxygen species: metabolism, oxidative stress, and signal transduction. **Annual Review of Plan Biology**, Palo Alto, v. 55, p. 373-399, 2004.

ASAI, T.; TENA, G.; PLOTNIKOVA, J.; WILLMANN, M.R.; CHIU, W.-L.; GOMEZ-GOMEZ, L.; BOLLER, T.; AUSUBEL, F.M.; SHEEN, J. MAP kinase signalling cascade in Arabidopsis innate immunity. **Nature**, London, v. 415, n. 6875, p. 977-983, 2002.

BAISA, G.A.; MAYERS, J.R.; BEDNAREK, S.Y. Budding and braking news about clathrin-mediated endocytosis. **Current Opinion in Plant Biology,** London, v. 16, n. 6, p. 718-725, 2013.

BANDMANN, V.; HOMANN, U. Clathrin-independent endocytosis contributes to uptake of glucose into BY-2 protoplasts. **The Plant Journal,** Oxford, v. 70, n. 4, p. 578-584, 2012.

BAR, M.; AVNI, A. EHD2 inhibits ligand-induced endocytosis and signaling of the leucine-rich repeat receptor-like protein LeEix2. **The Plant Journal: for Cell and Molecular Biology,** Oxford, v. 59, n. 4, p. 600-11, 2009.

BAR, M.; AVNI, A. Endosomal trafficking and signaling in plant defense responses **Current Opinion in Plant Biology,** London, v. 22, p. 86-92, 2014.

BARAL, A.; IRANI, N.G.; FUJIMOTO, M.; NAKANO, A.; MAYOR, S.; MATHEW, M.K. Salt-induced remodeling of spatially restricted clathrin-independent endocytic pathways in arabidopsis root. **The Plant Cell**, Rockville, v. 27, n. 4,p. 1297-1315, 2015.

BARTELS, S.; BOLLER, T. Quo vadis, Pep? Plant elicitor peptides at the crossroads of immunity, stress and development. **Journal of Experimental Botany**, Oxford, v. 66, n. 17, p. 5183-5193, 2015.

BARTELS, S.; LORI, M.; MBENGUE, M.; VAN VERK, M.; KLAUSER, D.; HANDER, T.; BONI, R.; ROBATZEK, S.; BOLLER, T. The family of Peps and their precursors in Arabidopsis: differential expression and localization but similar induction of pattern-triggered immune responses. **Journal of Experimental Botany,** Oxford, v. 64, n. 17, p. 5309-5321, 2013.

BECK, M.; ZHOU, J.; FAULKNER, C.; MACLEAN, D.; ROBATZEK, S. Spatio-temporal cellular dynamics of the Arabidopsis flagellin receptor reveal activation status-dependent endosomal sorting. **The Plant Cell,** Rockville, v. 24, n. 10, p. 4205-4219, 2012.

BHATTACHARYA, R.; KRISHNA KORAMUTLA, M.; NEGI, M.; PEARCE, G.; RYAN, C.A. Hydroxyproline-rich glycopeptide signals in potato elicit signalling associated with defense against insects and pathogens. **Plant Science**, Amsterdam, v. 207, p. 88-97, 2013.

BLANVILLAIN, R.; YOUNG, B.; CAI, Y.M.; HECHT, V.; VAROQUAUX, F.; DELORME, V.; LANCELIN, J.M.; DELSENY, M.; GALLOIS, P. The Arabidopsis peptide kiss of death is an inducer of programmed cell death. **The EMBO Journal,** Oxford, v. 30, n. 6, p. 1173-1183, 2011.

BOLLER, T. Chemoperception of microbial signals in plant cells. **Annual Review of Plant Biology,** Palo Alto, v. 46, n. 1, p. 189-214, 1995.

BOLLER, T.; FELIX, G. A renaissance of elicitors: perception of microbe-associated molecular patterns and danger signals by pattern-recognition receptors. **Annual Review of Plant Biology,** Palo Alto, v. 60, p. 379-406, 2009.

BONIFACINO, J.S.; GLICK, B.S. The mechanisms of vesicle budding and fusion. **Cell**, Cambridge, v. 116, n. 2, p. 153-166, 2004.

BOUDSOCQ, M.; WILLMANN, M.R.; MCCORMACK, M.; LEE, H.; SHAN, L.; HE, P.; BUSH, J.; CHENG, S.-H.; SHEEN, J. Differential innate immune signalling via Ca2+ sensor protein kinases. **Nature,** London, v. 464, n. 7287, p. 418-422, 2010.

BOYAJYAN, A.; DEVEJYAN, H.; HAYKAZYAN, V.; AVETISYAN, G.; KHANOYAN, D. Molecular mechanisms and mediators of the immune response in plants. **Journal of Plant Sciences,** Chicago, v. 2, n. 1, p. 23-30, 2014.

BRUTUS, A.; SICILIA, F.; MACONE, A.; CERVONE, F.; DE LORENZO, G. A domain swap approach reveals a role of the plant wall-associated kinase 1 (WAK1) as a receptor of oligogalacturonides. **Proceedings of the National Academy of Sciences of the United States of America,** Washington, v. 107, n. 20, p. 9452-9457, 2010.

CHEN, X.; IRANI, N. G.; FRIML, J. Clathrin-mediated endocytosis: the gateway into plant cells. **Current Opinion in Plant Biology,** London**,** v. 14, n. 6, p. 674-682, 2011.

CHINCHILLA, D.; BAUER, Z.; REGENASS, M.; BOLLER, T.; FELIX, G. The Arabidopsis receptor kinase FLS2 binds flg22 and determines the specificity of flagellin perception. **The Plant Cell,** Rockville, v. 18, n. 2, p. 465-476, 2006.

CHINCHILLA, D.; SHAN, L.; HE, P.; DE VRIES, S.; KEMMERLING, B. One for all: the receptor-associated kinase BAK1. **Trends in plant science,** Oxford, v. 14, n. 10, p. 535-541, 2009.

CHINCHILLA, D.; ZIPFEL, C.; ROBATZEK, S.; KEMMERLING, B.; NURNBERGER, T.; JONES, J. D.; FELIX, G.; BOLLER, T. A flagellin-induced complex of the receptor FLS2 and BAK1 initiates plant defence. **Nature,** London, v. 448, n. 7152, p. 497-500, 2007.

CHOI, J.; TANAKA, K.; CAO, Y.; QI, Y.; QIU, J.; LIANG, Y.; LEE, S.Y.; STACEY, G. Identification of a plant receptor for extracellular ATP. **Science,** New York, v. 343, n. 6168, p. 290-294, 2014.
CHOI, S.W.; TAMAKI, T.; EBINE, K.; UEMURA, T.; UEDA, T.; NAKANO, A. RABA members act in distinct steps of subcellular trafficking of the flagellin sensing2 receptor. **The Plant Cell,** Rockville, v. 25, n. 3, p. 1174-1187, 2013.

COCUCCI, E.; AGUET, F.; BOULANT, S.; KIRCHHAUSEN, T. The first five seconds in the life of a clathrin-coated pit. **Cell**, Cambridge, v. 150, n. 3, p. 495-507, 2012.

CONNER, S.D.; SCHMID, S.L. Regulated portals of entry into the cell. **Nature,** London, v. 422, n. 6927, p. 37-44, 2003.

CONSTABEL, C.P.; YIP, L.; RYAN, C.A. Prosystemin from potato, black nightshade, and bell pepper: primary structure and biological activity of predicted systemin polypeptides. **Plant Molecular Biology,** Dordrecht, v. 36, n. 1, p. 55-62, 1998.

DANGL, J.L.; HORVATH, D.M.; STASKAWICZ, B.J. Pivoting the plant immune system from dissection to deployment. **Science,** New York, v. 341, n. 6147, p. 746-751, 2013.

DARDICK, C.; SCHWESSINGER, B.; RONALD, P. Non-arginine-aspartate (non-RD) kinases are associated with innate immune receptors that recognize conserved microbial signatures. **Current Opinion in Plant Biology,** London, v. 15, n. 4, p. 358-366, 2012.

DARDICK, C.; CHEN, J.; RICHTER, T.; OUYANG, S.; RONALD, P. The rice kinase database: a phylogenomic database for the rice kinome. **Plant Physiology,** Lancaster, v. 143, n. 2, p. 579-586, 2007.

DEGENHARDT, D.C.; REFI-HIND, S.; STRATMANN, J.W.; LINCOLN, D.E. Systemin and jasmonic acid regulate constitutive and herbivore-induced systemic volatile emissions in tomato, *Solanum lycopersicum*. **Phytochemistry,** Amsterdam, v. 71, n. 17, p. 2024-2037, 2010.

DENOUX, C.; GALLETTI, R.; MAMMARELLA, N.; GOPALAN, S.; WERCK, D.; DE LORENZO, G.; FERRARI, S.; AUSUBEL, F.M.; DEWDNEY, J. Activation of defense response pathways by OGs and Flg22 elicitors in Arabidopsis seedlings. **Molecular plant,** Saint Paul, v. 1, n. 3, p. 423-445, 2008.

DETTMER, J.; HONG-HERMESDORF, A.; STIERHOF, Y.D.; SCHUMACHER, K. Vacuolar H+-ATPase activity is required for endocytic and secretory trafficking in Arabidopsis. **The Plant Cell,** Rockville, v. 18, n. 3, p. 715-730, 2006.

DI RUBBO, S.; IRANI, N.G.; KIM, S.Y.; XU, Z.Y.; GADEYNE, A.; DEJONGHE, W.; VANHOUTTE, I.; PERSIAU, G.; EECKHOUT, D.; SIMON, S.; SONG, K.; KLEINE-VEHN, J.; FRIML, J.; DE JAEGER, G.; VAN DAMME, D.; HWANG, I.; RUSSINOVA, E. The clathrin adaptor complex AP-2 mediates endocytosis of brassinosteroid insensitive1 in Arabidopsis. **Plant Cell,** Rockville, v. 25, n. 8, p. 2986-2997, 2013.

DI RUBBO, S.; RUSSINOVA, E. Receptor-mediated endocytosis in plants. In: **Endocytosis in plants.** Berlin Heidelberg: Springer, 2012. p. 151-164.

DODDS, P.N.; RATHJEN, J.P. Plant immunity: towards an integrated view of plant-pathogen interactions. **Nature Reviews. Genetics,** London, v. 11, n. 8, p. 539-548, 2010.
DU, Y.; TEJOS, R.; BECK, M.; HIMSCHOOT, E.; LI, H.; ROBATZEK, S.; VANNESTE, S.; FRIML, J. Salicylic acid interferes with clathrin-mediated endocytic protein trafficking. **Proceedings of the National Academy of Sciences of the United States of America,** Washington, v. 110, n. 19, p. 7946-7951, 2013.

ERBS, G.; NEWMAN, M.A. The role of lipopolysaccharide and peptidoglycan, two glycosylated bacterial microbe-associated molecular patterns (MAMPs), in plant innate immunity **Molecular Plant Pathology,** Oxford, v. 13, n. 1, p. 95-104, 2012.

FAN, L.; LI, R.; PAN, J.; DING, Z.; LIN, J. Endocytosis and its regulation in plants. **Trends in Plant Science**, Oxford, v. 20, n. 6, p. 388-397, 2015.

FAULKNER, C.; PETUTSCHNIG, E.; BENITEZ-ALFONSO, Y.; BECK, M.; ROBATZEK, S.; LIPKA, V.; MAULE, A.J. LYM2-dependent chitin perception limits molecular flux via plasmodesmata. **Proceedings of the National Academy of Sciences of the United States of America,** Washington, v. 110, n. 22, p. 9166-9170, 2013.

FERRARI, S.; SAVATIN, D. V.; SICILIA, F.; GRAMEGNA, G.; CERVONE, F.; DE LORENZO, G. Oligogalacturonides: plant damage-associated molecular patterns and regulators of growth and development. **Frontiers in Plant Science,** Lausanne, v. 4, n 49, p. 1-9, 2013.

FRITZ-LAYLIN, L.K.; KRISHNAMURTHY, N.; TOR, M.; SJOLANDER, K.V.; JONES, J.D. Phylogenomic analysis of the receptor-like proteins of rice and Arabidopsis. **Plant Physiology,** Lancaster, v. 138, n. 2, p. 611-623, 2005.

GADEYNE, A.; SANCHEZ-RODRIGUEZ, C.; VANNESTE, S.; DI RUBBO, S.; ZAUBER, H.; VANNESTE, K.; VAN LEENE, J.; DE WINNE, N.; EECKHOUT, D.; PERSIAU, G.; VAN DE SLIJKE, E.; CANNOOT, B.; VERCRUYSSE, L.; MAYERS, J. R.; ADAMOWSKI, M.; KANIA, U.; EHRLICH, M.; SCHWEIGHOFER, A.; KETELAAR, T.; MAERE, S.; BEDNAREK, S. Y.; FRIML, J.; GEVAERT, K.; WITTERS, E.; RUSSINOVA, E.; PERSSON, S.; DE JAEGER, G.; VAN DAMME, D. The TPLATE adaptor complex drives clathrin-mediated endocytosis in plants. **Cell**, Cambridge**,** v. 156, n. 4, p. 691-704, 2014.

GAO, M.; WANG, X.; WANG, D.; XU, F.; DING, X.; ZHANG, Z.; BI, D.; CHENG, Y.T.; CHEN, S.; LI, X.; ZHANG, Y. Regulation of cell death and innate immunity by two receptor-like kinases in Arabidopsis. . **Cell Host & Microbe,** Cambridge, v. 6, n. 1, p. 34-44, 2009.

GHORBANI, S.; FERNANDEZ SALINA, A.; HILSON, P.; BEECKMAN, T. Signaling peptides in plants. **Cell & Developmental Biology,** Oxford, v. 3, n. 2, p. 1-11, 2014.

GELDNER, N.; FRIML, J.; STIERHOF, Y. D.; JURGENS, G.; PALME, K. Auxin transport inhibitors block PIN1 cycling and vesicle trafficking. **Nature**, London, v. 413, n. 6854, p. 425-428, 2001.

GELDNER, N.; HYMAN, D.L.; WANG, X.; SCHUMACHER, K.; CHORY, J. Endosomal signaling of plant steroid receptor kinase BRI1. **Genes & Development,** New York, v. 21, n. 13, p. 1598-1602, 2007.

GELDNER, N.; ROBATZEK, S. Plant receptors go endosomal: a moving view on signal transduction. **Plant Physiology,** Washington, v. 147, n. 4, p. 1565-1574, 2008.

GOMEZ-GOMEZ, L.; BOLLER, T. FLS2: an LRR receptor-like kinase involved in the perception of the bacterial elicitor flagellin in Arabidopsis. **Molecular cell**, Cambridge, v. 5, n. 6, p. 1003-1011, 2000.

GOMEZ-GOMEZ, L.; FELIX, G.; BOLLER, T. A single locus determines sensitivity to bacterial flagellin in *Arabidopsis thaliana*. **The Plant Journal : for Cell and Molecular Biology,** Oxford, v. 18, n. 3, p. 277-284, 1999.

GOU, X.; YIN, H.; HE, K.; DU, J.; YI, J.; XU, S.; LIN, H.; CLOUSE, S.D.; LI, J. Genetic evidence for an indispensable role of somatic embryogenesis receptor kinases in brassinosteroid signaling. **PLoS Genet,** San Francisco, v. 8, n. 1, p. e1002452, 2012.

GULLY, K.; HANDER, T.; BOLLER, T.; BARTELS, S. Perception of Arabidopsis AtPep peptides, but not bacterial elicitors, accelerates starvation-induced senescence. **Frontiers in Plant Science,** Lausanne, v. 6, p. 14, 2015.

HALTER, T.; IMKAMPE, J.; BLAUM, B.S.; STEHLE, T.; KEMMERLING, B. BIR2 affects complex formation of BAK1 with ligand binding receptors in plant defense. **Plant Signaling & Behavior**, Georgetown, v.9, n. 6, p. 134-143, 2014.

HALTER, T.; IMKAMPE, J.; MAZZOTTA, S.; WIERZBA, M.; POSTEL, S.; BUCHERL, C.; KIEFER, C.; STAHL, M.; CHINCHILLA, D.; WANG, X.; NURNBERGER, T.; ZIPFEL, C.; CLOUSE, S.; BORST, J.W.; BOEREN, S.; DE VRIES, S.C.; TAX, F.; KEMMERLING, B. The leucine-rich repeat receptor kinase BIR2 is a negative regulator of BAK1 in plant immunity. . **Current Biology,** London, v. 24, n. 2, p. 134-143, 2014.

HAN, Z.; SUN, Y.; CHAI, J. Structural insight into the activation of plant receptor kinases. **Current Opinion in Plant Biology,** London, v. 20, p. 55-63, 2014.

HANN, D.R.; RATHJEN, J.P. Early events in the pathogenicity of Pseudomonas syringae on *Nicotiana benthamiana*. **The Plant Journal: for Cell and Molecular Biology,** Oxford, v. 49, n. 4, p. 607-618, 2007.

HE, K.; GOU, X.; YUAN, T.; LIN, H.; ASAMI, T.; YOSHIDA, S.; RUSSELL, S.D.; LI, J. BAK1 and BKK1 regulate brassinosteroid-dependent growth and brassinosteroid-independent cell-death pathways. **Current Biology,** London, v. 17, n. 13, p. 1109-1115, 2007.

HECHT, V.; VIELLE-CALZADA, J.P.; HARTOG, M.V.; SCHMIDT, E.D.; BOUTILIER, K.; GROSSNIKLAUS, U.; DE VRIES, S.C. The Arabidopsis somatic embryogenesis receptor kinase 1 gene is expressed in developing ovules and embryos and enhances embryogenic competence in culture. **Plant Physiology,** Lancaster, v. 127, n. 3, p. 803-816, 2001.

HENNE, W.M.; BUCHKOVICH, N.J.; EMR, S.D. The ESCRT pathway. **Developmental Cell,** Cambridge, v. 21, n. 1, p. 77-91, 2011.

HETTENHAUSEN, C.; SCHUMAN, M.C.; WU, J. MAPK signaling: a key element in plant defense response to insects. **Insect Science**, Elmsford, v. 22, n. 2, p 157-164. 2014.

HORN, M.A.; HEINSTEIN, P.F.; LOW, P.S. Receptor-mediated endocytosis in plant cells. **The Plant Cell,** Rockville, v. 1, n. 10, p. 1003-1009, 1989.

HOU, S.; WANG, X.; CHEN, D.; YANG, X.; WANG, M.; TURRA, D.; DI PIETRO, A.; ZHANG, W. The secreted peptide PIP1 amplifies immunity through receptor-like kinase 7. **PLoS Pathogens,** San Francisco, v. 10, n. 9, p. e1004331, 2014.

HUFFAKER, A.; DAFOE, N. J.; SCHMELZ, E.A. ZmPep1, an ortholog of Arabidopsis elicitor peptide 1, regulates maize innate immunity and enhances disease resistance. **Plant Physiology,** Lancaster, v. 155, n. 3, p. 1325-1338, 2011.

HUFFAKER, A.; PEARCE, G.; RYAN, C.A. An endogenous peptide signal in Arabidopsis activates components of the innate immune response. **Proceedings of the National Academy of Sciences of the United States of America,** Washington, v. 103, n. 26, p. 10098-10103, 2006.

HUFFAKER, A.; PEARCE, G.; VEYRAT, N.; ERB, M.; TURLINGS, T.C.; SARTOR, R.; SHEN, Z.; BRIGGS, S.P.; VAUGHAN, M.M.; ALBORN, H.T. Plant elicitor peptides are conserved signals regulating direct and indirect antiherbivore defense. **Proceedings of the National Academy of Sciences,** Washington, v. 110, n. 14, p. 5707-5712, 2013.

HUFFAKER, A.; RYAN, C.A. Endogenous peptide defense signals in Arabidopsis differentially amplify signaling for the innate immune response. **Proceedings of the National Academy of Sciences of the United States of America,** Washingtonn, v. 104, n. 25, p. 10732-10736, 2007.

INADA, N.; UEDA, T. Membrane trafficking pathways and their roles in plant–microbe interactions. **Plant and Cell Physiology,** Kyoto, v. 55, n. 4, p. 672-686, 2014.

IRANI, N.G.; DI RUBBO, S.; MYLLE, E.; VAN DEN BEGIN, J.; SCHNEIDER-PIZON, J.; HNILIKOVA, J.; SISA, M.; BUYST, D.; VILARRASA-BLASI, J.; SZATMARI, A.M.; VAN DAMME, D.; MISHEV, K.; CODREANU, M. C.; KOHOUT, L.; STRNAD, M.; CANO-DELGADO, A. I.; FRIML, J.; MADDER, A.; RUSSINOVA, E. Fluorescent castasterone reveals BRI1 signaling from the plasma membrane. **Nature Chemical Biology,** New York, v. 8, n. 6, p. 583-589, 2012.

JEHLE, A.K.; LIPSCHIS, M.; ALBERT, M.; FALLAHZADEH-MAMAGHANI, V.; FÜRST, U.; MUELLER, K.; FELIX, G. The receptor-like protein ReMAX of Arabidopsis detects the microbe-associated molecular pattern eMax from Xanthomonas. **The Plant Cell,** Rockville, v. 25, n. 6, p. 2330-2340, 2013.

JONES, J.D.; DANGL, J.L. The plant immune system. **Nature,** London, v. 444, n. 7117, p. 323-329, 2006.

KAUSS, H.; FAUTH, M.; MERTEN, A.; JEBLICK, W. Cucumber hypocotyls respond to cutin monomers via both an inducible and a constitutive H2O2-generating system. **Plant Physiology,** Lancaster, v. 120, n. 4, p. 1175-1182, 1999.

KITAKURA, S.; VANNESTE, S.; ROBERT, S.; LOFKE, C.; TEICHMANN, T.; TANAKA, H.; FRIML, J. Clathrin mediates endocytosis and polar distribution of PIN auxin transporters in Arabidopsis. **The Plant Cell,** Rockville, v. 23, n. 5, p. 1920-1931, 2011.

KROL, E.; MENTZEL, T.; CHINCHILLA, D.; BOLLER, T.; FELIX, G.; KEMMERLING, B.; POSTEL, S.; ARENTS, M.; JEWORUTZKI, E.; AL-RASHEID, K.A.; BECKER, D.; HEDRICH, R. Perception of the Arabidopsis danger signal peptide 1 involves the pattern recognition receptor AtPEPR1 and its close homologue AtPEPR2. **The Journal of Biological Chemistry,** Baltimore, v. 285, n. 18, p. 13471-13479, 2010.

LEHTI-SHIU, M.D.; ZOU, C.; HANADA, K.; SHIU, S.H. Evolutionary history and stress regulation of plant receptor-like kinase/pelle genes **Plant Physiology,** Lancaster, v. 150, n. 1, p. 12-26, 2009.
LI, J.; WEN, J.; LEASE, K.A.; DOKE, J.T.; TAX, F.E.; WALKER, J.C. BAK1, an Arabidopsis LRR receptor-like protein kinase, interacts with BRI1 and modulates brassinosteroid signaling. **Cell,** Cambridge, v. 110, n. 2, p. 213-222, 2002.

LI, R.; LIU, P.; WAN, Y.; CHEN, T.; WANG, Q.; METTBACH, U.; BALUSKA, F.; SAMAJ, J.; FANG, X.; LUCAS, W.J.; LIN, J. A membrane microdomain-associated protein, Arabidopsis Flot1, is involved in a clathrin-independent endocytic pathway and is required for seedling development **The Plant Cell,** Rockville, 24, n. 5, p. 2105-2122, 2012.

LIU, T.; LIU, Z.; SONG, C.; HU, Y.; HAN, Z.; SHE, J.; FAN, F.; WANG, J.; JIN, C.; CHANG, J.; ZHOU, J.M.; CHAI, J. Chitin-induced dimerization activates a plant immune receptor. **Science,** New York, v. 336, n. 6085, p. 1160-1164, 2012.

LIU, Z.; WU, Y.; YANG, F.; ZHANG, Y.; CHEN, S.; XIE, Q.; TIAN, X.; ZHOU, J. M. BIK1 interacts with PEPRs to mediate ethylene-induced immunity. **Proceedings of the National Academy of Sciences of the United States of America,** Washington, v. 110, n. 15, p. 6205-6210, 2013.

LOZANO-DURAN, R.; ZIPFEL, C. Trade-off between growth and immunity: role of brassinosteroids. **Trends in plant science,** Oxford, v. 20, n. 1, p. 12-9, 2015.

LU, D.; WU, S.; GAO, X.; ZHANG, Y.; SHAN, L.; HE, P. A receptor-like cytoplasmic kinase, BIK1, associates with a flagellin receptor complex to initiate plant innate immunity. **Proceedings of the National Academy of Sciences of the United States of America,** Washington, v. 107, n. 1, p. 496-501, 2010.

LUO, Y.; SCHOLL, S.; DOERING, A.; ZHANG, Y.; IRANI, N. G.; DI RUBBO, S.; NEUMETZLER, L.; KRISHNAMOORTHY, P.; VAN HOUTTE, I.; MYLLER, E. BISCHOFF, V.; VERNHETTES, S.; WINNE, J.; FRIML, J.; STIERHOF, Y.; SCHUMACHER, K.; PERSSON, S.; RUSSINOVA, E. V-ATPase activity in the TGN/EE is required for exocytosis and recycling in Arabidopsis. **Nature Plants**, London, v. 1, n.7, p. 1-10, 2015

LUSCHNIG, C.; VERT, G. The dynamics of plant plasma membrane proteins: PINs and beyond. **Development,** Cambridge, v. 141, n. 15, p. 2924-2938, 2014.

MACHO, A.P.; ZIPFEL, C. Plant PRRs and the activation of innate immune signaling. **Molecular Cell,** Cambridge, v. 54, n. 2, p. 263-272, 2014.

MCGURL, B.; PEARCE, G.; OROZCO-CARDENAS, M.; RYAN, C.A. Structure, expression, and antisense inhibition of the systemin precursor gene. **Science,** New York, v. 255, n. 5051, p. 1570-1573, 1992.

MCMAHON, H.T.; BOUCROT, E. Molecular mechanism and physiological functions of clathrin-mediated endocytosis. **Nature Reviews Molecular cell biology,** London, v. 12, n. 8, p. 517-533, 2011.

MEDZHITOV, R.; JANEWAY, C.A. JR. Innate immunity: the virtues of a nonclonal system of recognition. **Cell,** Cambridge, v. 91, n. 3, p. 295-298, 1997.

MELOTTO, M.; UNDERWOOD, W.; KOCZAN, J.; NOMURA, K.; HE, S.Y. Plant stomata function in innate immunity against bacterial invasion. **Cell,** Cambridge, v. 126, n. 5, p. 969-980, 2006.

MICHNIEWICZ, M.; ZAGO, M.K.; ABAS, L.; WEIJERS, D.; SCHWEIGHOFER, A.; MESKIENE, I.; HEISLER, M.G.; OHNO, C.; ZHANG, J.; HUANG, F. Antagonistic regulation of PIN phosphorylation by PP2A and PINOID directs auxin flux. **Cell,** Cambridge, v. 130, n. 6, p. 1044-1056, 2007.

MITHÖFER, A.; EBEL, J.; FELLE, H.H. Cation fluxes cause plasma membrane depolarization involved in β-glucan elicitor-signaling in soybean roots. **Molecular plant-microbe interactions,** Saint Paul, v. 18, n. 9, p. 983-990, 2005.

MIYA, A.; ALBERT, P.; SHINYA, T.; DESAKI, Y.; ICHIMURA, K.; SHIRASU, K.; NARUSAKA, Y.; KAWAKAMI, N.; KAKU, H.; SHIBUYA, N. CERK1, a LysM receptor kinase, is essential for chitin elicitor signaling in Arabidopsis **Proceedings of the National Academy of Sciences of the United States of America**, Washington, 104, n. 49, p. 19613-19618, 2007.

MORITA, M.T.; SHIMADA, T. The plant endomembrane system: a complex network supporting plant development and physiology. **Plant and Cell Physiology,** Kyoto, v. 55, n. 4, p. 667-671, 2014.

NARVÁEZ-VÁSQUEZ, J.; OROZCO-CÁRDENAS, M.L.; RYAN, C.A. Systemic wound signaling in tomato leaves is cooperatively regulated by systemin and hydroxyproline-rich glycopeptide signals. **Plant Molecular Biology,** Dordrecht, v. 65, n. 6, p. 711-718, 2007.

NAVARRO, L.; ZIPFEL, C.; ROWLAND, O.; KELLER, I.; ROBATZEK, S.; BOLLER, T.; JONES, J.D. The transcriptional innate immune response to flg22. Interplay and overlap with Avr gene-dependent defense responses and bacterial pathogenesis. **Plant Physiology,** Lancaster, v. 135, n. 2, p. 1113-1128, 2004.

OROZCO-CARDENAS, M.; MCGURL, B.; RYAN, C.A. Expression of an antisense prosystemin gene in tomato plants reduces resistance toward Manduca sexta larvae. **Proceedings of the National Academy of Sciences of the United States of America,** Washington, v. 90, n. 17, p. 8273-8276, 1993.

PEARCE, G.; MOURA, D.S.; STRATMANN, J.; RYAN, C.A. Production of multiple plant hormones from a single polyprotein precursor. **Nature,** London, v. 411, n. 6839, p. 817-820, 2001.

PEARCE, G.; STRYDOM, D.; JOHNSON, S.; RYAN, C.A. A polypeptide from tomato leaves induces wound-inducible proteinase inhibitor proteins. **Science,** New York, v. 253, n. 5022, p. 895-897, 1991.

PEARCE, G.; YAMAGUCHI, Y.; BARONA, G.; RYAN, C.A. A subtilisin-like protein from soybean contains an embedded, cryptic signal that activates defense-related genes. **Proceedings of the National Academy of Sciences of the United States of America,** Washington, v. 107, n. 33, p. 14921-14925, 2010.

PETUTSCHNIG, E.K.; JONES, A.M.; SERAZETDINOVA, L.; LIPKA, U.; LIPKA, V. The lysin motif receptor-like kinase (LysM-RLK) CERK1 is a major chitin-binding protein in Arabidopsis thaliana and subject to chitin-induced phosphorylation. **Journal of Biological Chemistry,** Rockville, v. 285, n. 37, p. 28902-28911, 2010.

PIETERSE, C.M.; VAN DER DOES, D.; ZAMIOUDIS, C.; LEON-REYES, A.; VAN WEES, S.C. Hormonal modulation of plant immunity. **Annual Review of Cell and Developmental Biology,** Palo Alto, v. 28, p. 489-521, 2012.

PIZARRO, L.; NORAMBUENA, L. Regulation of protein trafficking: posttranslational mechanisms and the unexplored transcriptional control. **Plant Science,** Limerick , v. 225, p. 24-33, 2014.

POSTEL, S.; KUFNER, I.; BEUTER, C.; MAZZOTTA, S.; SCHWEDT, A.; BORLOTTI, A.; HALTER, T.; KEMMERLING, B.; NURNBERGER, T. The multifunctional leucine-rich repeat receptor kinase BAK1 is implicated in Arabidopsis development and immunity. **European Journal of Cell Biology,** Stuttgart, v. 89, n. 2/3, p. 169-174, 2010.

PUMPLIN, N.; VOINNET, O. RNA silencing suppression by plant pathogens: defence, counter-defence and counter-counter-defence. **Nature reviews: Microbiology,** London, v. 11, n. 11, p. 745-760, 2013.

RAMONELL, K.M.; ZHANG, B.; EWING, R.M.; CHEN, Y.; XU, D.; STACEY, G.; SOMERVILLE, S. Microarray analysis of chitin elicitation in Arabidopsis thaliana. **Molecular Plant Pathology,** London, v. 3, n. 5, p. 301-311, 2002.

RANF, S.; ESCHEN-LIPPOLD, L.; PECHER, P.; LEE, J.; SCHEEL, D. Interplay between calcium signalling and early signalling elements during defence responses to microbe- or damage-associated molecular patterns. **The Plant Journal : for Cell and Molecular Biology**, London, v. 68, n. 1, p. 100-113, 2011.

ROBATZEK, S.; CHINCHILLA, D.; BOLLER, T. Ligand-induced endocytosis of the pattern recognition receptor FLS2 in Arabidopsis **Genes & Development,** Cold Spring Harbor, v. 20, n. 5, p. 537-542, 2006.

ROBATZEK, S.; BITTEL, P.; CHINCHILLA, D.; KOCHNER, P.; FELIX, G.; SHIU, S.H.; BOLLER, T. Molecular identification and characterization of the tomato flagellin receptor LeFLS2, an orthologue of Arabidopsis FLS2 exhibiting characteristically different perception specificities. **Plant Molecular Biology,** Dordrecht, v. 64, n. 5, p. 539-547, 2007.

ROUX, M.; SCHWESSINGER, B.; ALBRECHT, C.; CHINCHILLA, D.; JONES, A.; HOLTON, N.; MALINOVSKY, F.G.; TOR, M.; DE VRIES, S.; ZIPFEL, C. The Arabidopsis leucine-rich repeat receptor-like kinases BAK1/SERK3 and BKK1/SERK4 are required for innate immunity to hemibiotrophic and biotrophic pathogens. **The Plant Cell,** Rockville, v. 23, n. 6, p. 2440-24455, 2011.

SALOMON, S.; ROBATZEK, S. Induced endocytosis of the receptor kinase FLS2. **Plant Signaling & Behavior,** Georgetown, v. 1, n. 6, p. 293-295, 2006.

SCHEURING, D.; KÜNZL, F.; VIOTTI, C.; YAN, M.S.W.; JIANG, L.; SCHELLMANN, S.; ROBINSON, D.G.; PIMPL, P. Ubiquitin initiates sorting of Golgi and plasma membrane proteins into the vacuolar degradation pathway. **BMC Plant Biology,** London, v. 12, n. 1, p. 164, 2012.

SCHEURING, D.; VIOTTI, C.; KRUGER, F.; KUNZL, F.; STURM, S.; BUBECK, J.; HILLMER, S.; FRIGERIO, L.; ROBINSON, D. G.; PIMPL, P.; SCHUMACHER, K. Multivesicular bodies mature from the trans-golgi network/early endosome in arabidopsis. **The Plant Cell,** Rockville, v. 23, n. 9, p. 3463-3481, 2011.

SCHMELZ, E.A.; CARROLL, M.J.; LECLERE, S.; PHIPPS, S.M.; MEREDITH, J.; CHOUREY, P.S.; ALBORN, H.T.; TEAL, P.E. Fragments of ATP synthase mediate plant perception of insect attack. **Proceedings of the National Academy of Sciences of the United States of America,** Washington, v. 103, n. 23, p. 8894-8899, 2006.

SCHMELZ, E.A.; LECLERE, S.; CARROLL, M.J.; ALBORN, H.T.; TEAL, P.E. Cowpea chloroplastic ATP synthase is the source of multiple plant defense elicitors during insect herbivory. **Plant Physiology,** Lancaster, v. 144, n. 2, p. 793-805, 2007.

SCHULZE, B.; MENTZEL, T.; JEHLE, A.K.; MUELLER, K.; BEELER, S.; BOLLER, T.; FELIX, G.; CHINCHILLA, D. Rapid heteromerization and phosphorylation of ligand-activated plant transmembrane receptors and their associated kinase BAK1. **The Journal of Biological Chemistry,** Baltimore, v. 285, n. 13, p. 9444-9451, 2010.

SCHWESSINGER, B.; RONALD, P. C. Plant innate immunity: perception of conserved microbial signatures. **Annual Review of Plant Biology,** Palo Alto, v. 63, p. 451-482, 2012.

SCHWESSINGER, B.; ROUX, M.; KADOTA, Y.; NTOUKAKIS, V.; SKLENAR, J.; JONES, A.; ZIPFEL, C. Phosphorylation-dependent differential regulation of plant growth, cell death, and innate immunity by the regulatory receptor-like kinase BAK1. **PLoS Genetics,** San Francisco, v. 7, n. 4, p. e1002046, 2011.

SHARFMAN, M.; BAR, M.; EHRLICH, M.; SCHUSTER, S.; MELECH-BONFIL, S.; EZER, R.; SESSA, G.; AVNI, A. Endosomal signaling of the tomato leucine-rich repeat receptor-like protein LeEix2. **Plant Journal,** Oxford, v. 68, n. 3, p. 413-423, 2011.

SHIU, S.H.; BLEECKER, A.B. Expansion of the receptor-like kinase/Pelle gene family and receptor-like proteins in Arabidopsis. . **Plant physiology,** Lancaster, v. 132, n. 2, p. 530-543, 2003.

SHIU, S.H.; BLEECKER, A.B. Plant receptor-like kinase gene family: diversity, function, and signaling. **Science Signaling,** Washington, v. 2001, n. 113, p. re22, 2001.

SHIU, S.H.; KARLOWSKI, W.M.; PAN, R.; TZENG, Y.H.; MAYER, K.F.; LI, W.H. Comparative analysis of the receptor-like kinase family in Arabidopsis and rice. **The Plant Cell,** Rockville, v. 16, n. 5, p. 1220-1234, 2004.

SINGH, M.K.; KRUGER, F.; BECKMANN, H.; BRUMM, S.; VERMEER, J.E.; MUNNIK, T.; MAYER, U.; STIERHOF, Y.D.; GREFEN, C.; SCHUMACHER, K.; JURGENS, G. Protein delivery to vacuole requires SAND protein-dependent Rab GTPase conversion for MVB-vacuole fusion. **Current Biology,** London, v. 24, n. 12, p. 1383-1389, 2014.

SMITH, J.M.; SALAMANGO, D.J.; LESLIE, M.E.; COLLINS, C.A.; HEESE, A. Sensitivity to Flg22 is modulated by ligand-induced degradation and de novo synthesis of the endogenous flagellin-receptor flagellin-sensing2. **Plant Physiology,** Lancaster, v. 164, n. 1, p. 440-454, 2014.

SMITH, J.M.; LESLIE, M.E.; ROBINSON, S.J.; KORASICK, D.A.; ZHANG, T.; BACKUES, S.K.; CORNISH, P.V.; KOO, A.J.; BEDNAREK, S.Y.; HEESE, A. Loss of *Arabidopsis thaliana* dynamin-related protein 2b reveals separation of innate immune signaling pathways. **PLoS Pathogens,** San Francisco, v. 10, n. 12, p. e1004578, 2014.

SORKIN, A.; VON ZASTROW, M. Endocytosis and signalling: intertwining molecular networks. **Nature Reviews Molecular cell biology,** London, v. 10, n. 9, p. 609-622, 2009.

TAKAI, R.; ISOGAI, A.; TAKAYAMA, S.; CHE, F.S. Analysis of flagellin perception mediated by flg22 receptor OsFLS2 in rice **Molecular Plant-Microbe Interactions,** Saint Paul, v. 21, n. 12, p. 1635-1642, 2008.

TAKANO, J.; MIWA, K.; YUAN, L.; VON WIREN, N.; FUJIWARA, T. Endocytosis and degradation of BOR1, a boron transporter of Arabidopsis thaliana, regulated by boron availability. **Proceedings of the National Academy of Sciences of the United States of America,** Washington, v. 102, n. 34, p. 12276-12281, 2005.

TANG, J.; HAN, Z.; SUN, Y.; ZHANG, H.; GONG, X.; CHAI, J. Structural basis for recognition of an endogenous peptide by the plant receptor kinase PEPR1. **Cell Research,** New York, v. 25, n. 1, p. 110-120, 2015.

TAYLOR, N.G. A role for Arabidopsis dynamin related proteins DRP2A/B in endocytosis; DRP2 function is essential for plant growth. **Plant Molecular Biology,** Dordrecht, v. 76, n. 1/2, p. 117-129, 2011.

TEH, O.-K.; MOORE, I. An ARF-GEF acting at the Golgi and in selective endocytosis in polarized plant cells. **Nature,** New York, v. 448, n. 7152, p. 493-496, 2007.

THORDAL-CHRISTENSEN, H. Fresh insights into processes of nonhost resistance. **Current Opinion in Plant Biology,** London, v. 6, n. 4, p. 351-357, 2003.

TOR, M.; LOTZE, M.T.; HOLTON, N. Receptor-mediated signalling in plants: molecular patterns and programmes. **Journal of Experimental Botany,** Oxford, v. 60, n. 13, p. 3645-3654, 2009.

TRDA, L.; FERNANDEZ, O.; BOUTROT, F.; HELOIR, M.C.; KELLONIEMI, J.; DAIRE, X.; ADRIAN, M.; CLEMENT, C.; ZIPFEL, C.; DOREY, S.; POINSSOT, B. The grapevine flagellin receptor VvFLS2 differentially recognizes flagellin-derived epitopes from the endophytic growth-promoting bacterium Burkholderia phytofirmans and plant pathogenic bacteria. **The New Phytologist,** London, v. 201, n. 4, p. 1371-1384, 2014.

VIOTTI, C.; BUBECK, J.; STIERHOF, Y.D.; KREBS, M.; LANGHANS, M.; VAN DEN BERG, W.; VAN DONGEN, W.; RICHTER, S.; GELDNER, N.; TAKANO, J.; JURGENS, G.; DE VRIES, S.C.; ROBINSON, D.G.; SCHUMACHER, K. Endocytic and secretory traffic in *Arabidopsis merge* in the trans-golgi network/early endosome, an independent and highly dynamic organelle. **The Plant Cell,** Rockville, v. 22, n. 4, p. 1344-1357, 2010.

WAN, J.; TANAKA, K.; ZHANG, X.-C.; SON, G.H.; BRECHENMACHER, L.; NGUYEN, T.H.N.; STACEY, G. LYK4, a lysin motif receptor-like kinase, is important for chitin signaling and plant innate immunity in Arabidopsis. **Plant Physiology,** Lancaster, v. 160, n. 1, p. 396-406, 2012.

WANG, C.; YAN, X.; CHEN, Q.; JIANG, N.; FU, W.; MA, B.; LIU, J.; LI, C.; BEDNAREK, S.Y.; PAN, J. Clathrin light chains regulate clathrin-mediated trafficking, auxin signaling, and development in Arabidopsis. **The Plant Cell** , Rockville, v. 25, n. 2, p. 499-516, 2013.

WANG, Y.; LI, Z.; LIU, D.; XU, J.; WEI, X.; YAN, L.; YANG, C.; LOU, Z.; SHUI, W. Assessment of BAK1 activity in different plant receptor-like kinase complexes by quantitative profiling of phosphorylation patterns. **Journal of Proteomics,** Amsterdam, v. 108, p. 484-493, 2014.

WANG, Z.Y.; SETO, H.; FUJIOKA, S.; YOSHIDA, S.; CHORY, J. BRI1 is a critical component of a plasma-membrane receptor for plant steroids. **Nature,** New York, v. 411, n. 6834, p. 219-219, 2001.

WILLMANN, R.; LAJUNEN, H.M.; ERBS, G.; NEWMAN, M.A.; KOLB, D.; TSUDA, K.; KATAGIRI, F.; FLIEGMANN, J.; BONO, J.J.; CULLIMORE, J.V.; JEHLE, A.K.; GOTZ, F.; KULIK, A.; MOLINARO, A.; LIPKA, V.; GUST, A.A.; NURNBERGER, T. Arabidopsis lysin-motif proteins LYM1 LYM3 CERK1 mediate bacterial peptidoglycan sensing and immunity to bacterial infection. **Proceedings of the National Academy of Sciences of the United States of America,** Washington, v. 108, n. 49, p. 19824-19829, 2011.

YAMAGUCHI, Y.; HUFFAKER, A. Endogenous peptide elicitors in higher plants. **Proceedings of the National Academy of Sciences of the United States of America,** Washington, v. 14, n. 4, p. 351-357, 2011.

YAMAGUCHI, Y.; HUFFAKER, A.; BRYAN, A.C.; TAX, F.E.; RYAN, C.A. PEPR2 is a second receptor for the Pep1 and Pep2 peptides and contributes to defense responses in Arabidopsis **The Plant Cell,** Rockville, v. 22, n. 2, p. 508-522, 2010.

YAMAGUCHI, Y.; PEARCE, G.; RYAN, C.A. The cell surface leucine-rich repeat receptor for AtPep1, an endogenous peptide elicitor in Arabidopsis, is functional in transgenic tobacco cells. . **Proceedings of the National Academy of Sciences of the United States of America,** Washington, v. 103, n. 26, p. 10104-10109, 2006.

YAMAOKA, S.; SHIMONO, Y.; SHIRAKAWA, M.; FUKAO, Y.; KAWASE, T.; HATSUGAI, N.; TAMURA, K.; SHIMADA, T.; HARA-NISHIMURA, I. Identification and dynamics of Arabidopsis adaptor protein-2 complex and its involvement in floral organ development. **The Plant Cell,** Rockville**,** v. 25, n. 8, p. 2958-2969, 2013.

ZHANG, J.; NODZYŃSKI, T.; PĚNČÍK, A.; ROLČÍK, J.; FRIML, J. PIN phosphorylation is sufficient to mediate PIN polarity and direct auxin transport. **Proceedings of the National Academy of Sciences of the United States of America,** Washington, v. 107, n. 2, p. 918-922, 2010.

ZHANG, J.; LI, W.; XIANG, T.; LIU, Z.; LALUK, K.; DING, X.; ZOU, Y.; GAO, M.; ZHANG, X.; CHEN, S.; MENGISTE, T.; ZHANG, Y.; ZHOU, J.M. Receptor-like cytoplasmic kinases integrate signaling from multiple plant immune receptors and are targeted by a *Pseudomonas syringae* effector. **Cell Host & Microbe,** Cambridge, v. 7, n. 4, p. 290-301, 2010.

ZHANG, L.; KARS, I.; ESSENSTAM, B.; LIEBRAND, T.W.; WAGEMAKERS, L.; ELBERSE, J.; TAGKALAKI, P.; TJOITANG, D.; VAN DEN ACKERVEKEN, G.; VAN KAN, J. A. Fungal endopolygalacturonases are recognized as microbe-associated molecular patterns by the arabidopsis receptor-like protein responsiveness to Botrytis polygalacturonases1. **Plant Physiology,** Lancaster, v. 164, n. 1, p. 352-364, 2014.

ZIPFEL, C. Plant pattern-recognition receptors. **Trends in Immunology,** London, v. 35, n. 7, p. 345-351, 2014.

ZIPFEL, C.; KUNZE, G.; CHINCHILLA, D.; CANIARD, A.; JONES, J.D.; BOLLER, T.; FELIX, G. Perception of the bacterial PAMP EF-Tu by the receptor EFR restricts Agrobacterium-mediated transformation. **Cell**, Cambridge, v. 125, n. 4, p. 749-760, 2006.

ZIPFEL, C.; ROBATZEK, S.; NAVARRO, L.; OAKELEY, E.J.; JONES, J.D.; FELIX, G.; BOLLER, T. Bacterial disease resistance in Arabidopsis through flagellin perception. **Nature,** New York**,** v. 428, n. 6984, p. 764-767, 2004.

2 DEVELOPMENT OF FLUORESCENT TOOLS TO STUDY THE SUBCELLULAR DYNAMICS OF *At*Pep1

Fausto Andres Ortiz-Morea[1], Paulo HO Ceciliato[1], Keini Dressano[1], Daniel Scherer de Moura[1]

[1]Laboratório de Bioquímica de Proteínas, Departamento de Ciências Biológicas, Escola Superior de Agricultura Luiz de Queiroz, Universidade de São Paulo USP, Piracicaba, SP 13418-900, Brazil.

Abstract

Plant signaling peptides are now recognized as important regulators in cell-to-cell communication, of which some well-studied have generated robust information about their signaling mechanisms and responses. However, the subcellular dynamics of plant signaling peptides remains to be investigated. In the present study, we explored two strategies for the *in vivo* study of the subcellular behavior of the *Arabidopsis thaliana* plant elicitor peptide1 (*At*Pep1), known to derive from the C-terminus of a 92-amino-acid precursor protein PROPEP1 and to induce innate immune responses in a receptor-dependent manner. First, we fused the PROPEP1 to GFP and assessed its localization via confocal microscopy. We found that PROPEP1 was associated with the tonoplast and accumulated in the vacuole, suggesting that this organelle could work as the station where PROPEP1 is stored and later released, only in a danger situation, hence originating *At*Pep1. Next, we generated *At*Pep1 versions labeled with fluorescent dyes and demonstrated that this peptide could be fluorescently tagged without loss of its biological activity, thus providing a powerful tool for cell biology studies aiming to understand the *At*Pep1 subcellular dynamics and its interplay with signaling. This approach could be extended for other plants signaling peptides.

Keywords: Signaling peptides; *At*Pep1; PROPEP1; PTI; Fluorescent labeling

2.1 Introduction

Signaling peptides have emerged as an important class of regulators in cell-to-cell communication networks in eukaryotes. Over the last decade, they have been shown to mediate a variety of developmental processes and physiological responses in plants, including innate immunity (YAMAGUCHI AND HUFFAKER, 2011; GHORBANI et al., 2014). Most plant signaling peptides identified to date are recognized by membrane-localized receptor kinases (Endo et al., 2014). This peptide-receptor interaction has been shown to be essential for initiating intracellular signaling cascades. Although the signaling mechanisms and responses of some plant signaling peptides are well studied, their subcellular dynamics is yet poorly understood, mainly due to the absence of tools that allow the monitoring of the behavior of these molecules *in vivo.*

*At*Pep1 is a well-characterized signaling peptide of 23 amino-acids that belongs to a family of eight members and is derived from the C-terminus of a 92-amino-acid precursor protein PROPEP1 (Figure 1) that lacks a classical signal sequence to enter the secretory pathway, but has been predicted to be secreted by an unconventional pathway (BARTELS et al., 2013; HUFFAKER; PEARCE; RYAN, 2006). *At*Pep1 has been shown to mediate plant immunity responses in association with its receptors PEPR1 and PEPR2 (KROL et al., 2010; YAMAGUCHI; PEARCE; RYAN, 2006) and its application to trigger responses reminiscent of pattern-triggered immunity (PTI), including extracellular alkalinization, intracellular Ca^{2+} elevation, induction of defense-related gene expression, and root growth inhibition (HUFFAKER; RYAN, 2007; KROL et al., 2010; RANF et al., 2011). Recently, the crystal structure of the leucine-rich repeat (LRR) domain of PEPR1 and structure-activity studies of *At*Pep1 have revealed that the C-terminus portion of the peptide is vital for binding of its receptors and for its biological activity (PEARCE et al., 2008; TANG et al., 2015).

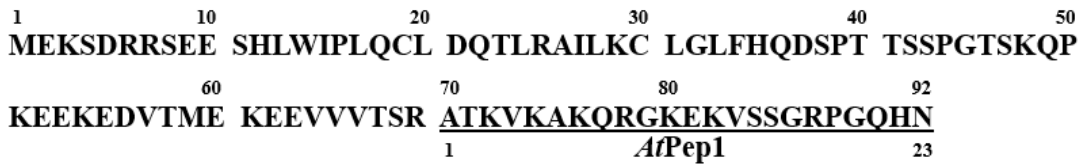

Figure 1 – Amino acid sequence of the precursor protein of *At*Pep1, PROPEP1. The *At*Pep1 sequence is located at the C-terminus of PROPEP1

*At*Pep1 has been proposed to act as an amplifier molecule during plant immunity responses and in a danger situation to be released from its precursor protein into the extracellular space, where it subsequently binds its receptors located at the plasma membrane of neighboring cells, triggering defense responses and, hence, spreading the message

(BARTELS; BOLLER, 2015; YAMAGUCHI; HUFFAKER, 2011). This inducible and transient behavior of *At*Pep1 makes it an excellent candidate to initiate subcellular dynamics studies of plant signaling peptides.

In the last decades, advanced microscopy tools have appeared that permit the study of organic molecules at the cellular level, but require that molecule of interest is labeled with a tag to allow its detection. Labeling molecules is a challenging task, because the addition of an extra molecule can easily abolish or modify the biological activity. For instance, when the multifunctional leucine-rich repeat receptor kinase BAK1 is fused with C-terminal tags, such as the green fluorescent protein (GFP), it is not fully functional in PTI (NTOUKAKIS et al., 2011). Classical labeling methods of plant peptides made use of radiolabeling with ^{125}I, ^{35}S, or ^{3}H, and, more recently, labeling with acridinium esters has also been documented (BUTENKO et al., 2014; YAMAGUCHI; PEARCE; RYAN, 2006); however, these probes are used mainly for biochemical assays and their usage for studies involving life imaging is limited.

Currently, companies manufacture a wide variety of fluorescent dyes that can link covalently organic molecules, thus allowing molecular study through approaches involving fluorescent detection similar to that of confocal microscopy (GOLDYS, 2009). Although labeling of plant signaling peptides has not been reported, other kinds of plant ligands have been successfully tagged with fluorescent dyes, for instance, the brassinosteroid (BR) hormone analog castasterone labeled with the fluorescent probe Alexa Fluor 647, which is used routinely to study subcellular dynamics of BR and its receptor in *Arabidopsis thaliana* cells (DI RUBBO et al., 2013; IRANI et al., 2012). Two of the extensively used fluorescent dyes in imaging are Cyanine and Rhodamine that comprise different members or derivatives with multiple absorption and fluorescence emission spectral profiles. These dyes are usually amine-reactive probes that reacting with aliphatic amines of the target protein, thus forming a carboxamide bond (LYTTLE et al., 2000; SPENCE; JOHNSON, 2010; WESSENDORF; BRELJE, 1992).

Here, we explored two approaches to generate tools that could be used to study the subcellular dynamics of *At*Pep1 via confocal microscopy. Initially, the precursor protein of *At*Pep1 was fused to GFP and its localization assessed. As previously reported, the PROPEP1 was associated to the tonoplast (BARTELS et al., 2013), but, additionally, accumulated into the vacuole, suggesting that this organelle could work as the place where PROPEP1 is stored and released later only in a danger situation, to give rise *At*Pep1 that fulfills its proposed role as amplifier of innate immunity responses. However, we were unsuccessful in proving this

assumption and need further experiments for clarification. Next, we showed that *At*Pep1 can be labeled with fluorescent dyes without loss of its biological activity, providing a valuable tool for cell biology studies aiming at understanding the *At*Pep1 subcellular dynamics and its interplay with signaling. This labeling approach could be extended for other signaling peptides and could be used as tool for ligand-receptor studies in plants.

2.2 Results

2.2.1 PROPEP1-GFP is associated with the tonoplast and stored in the vacuole

*At*Pep1 is believed to need to reach the extracellular medium and to be released via a still unknown cleavage mechanism from its precursor protein to bind the extracellular domain of its plasma membrane receptors PEPR1 and PEPR2 (HUFFAKER et al., 2006; YAMAGUCHI et al., 2010). As the subcellular dynamics of this process is not well understood, we aimed at developing a tool to study the subcellular behavior of *At*Pep1. To this end, we generated a transgenic *Arabidopsis* line constitutively expressing its precursor protein PROPEP1 fused at the C-terminus to the fluorescent protein GFP under the promoter 35S. When the subcellular localization of this protein was assessed in epidermal cells of cotyledons and root tips of five-day-old transgenic seedlings, the GFP signal was detected associated mainly to the tonoplast (Figure 2) as previously reported for PROPEP1-YFP (BARTELS et al., 2013). Aggregations into the vacuole were also observed in both cotyledons and meristem root tips cells tissues.

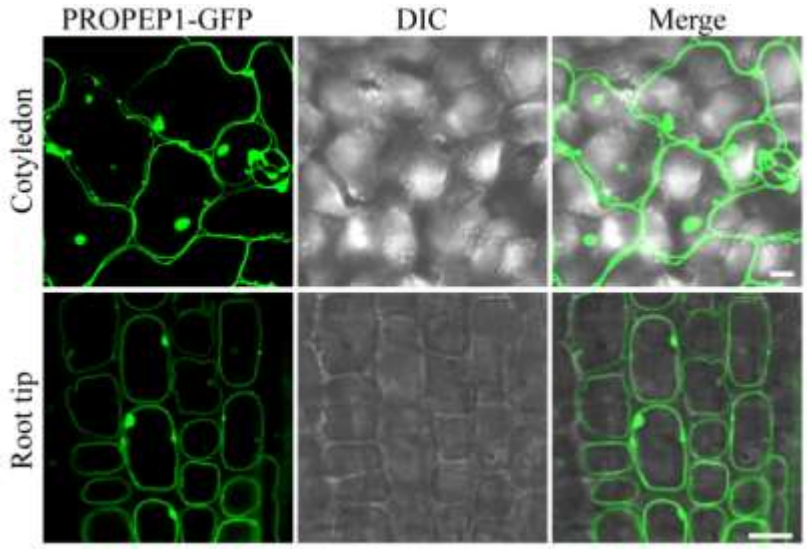

Figure 2 - Association of the PROPEP1-GFP protein with the tonoplast in different tissues. Confocal images of cotyledon and meristem root tip cells of five-day-old *Arabidopsis* transgenic lines, expressing PROPEP1-GFP under the control of the cauliflower mosaic virus 35S promoter. Similar results were obtained in three independent transgenic lines. Scale bars, 10 μm. DIC, differential interference contrast

As the fluorescent properties of GFP are negatively affected at low pH (KNEEN at al., 1998), we thought that information of PROPEP1-GFP localization in subcellular compartments with acidic pH , such as the vacuole and the apoplast (SHEN et al., 2013) could have been missed. In attempt to improve the GFP signal and overcome the issue imposed by the low pH, we employed a strategy to raise the cellular pH of transgenic plants expressing PROPEP1-GFP. For that, five-day-old seedlings were incubated for 24 h before imaging in the dark in half-strength Murashige and Skoog (½MS) or in the dark in MES-buffered solid medium at pH 7.2 (Figure 3) (KNEEN et al., 1998; ZHENG et al., 2004; HURTH et al., 2005). Moreover, to label the plasma membrane, FM4-64 staining (2 µM, 20 min) was used (BOLTE at al., 2004). We found that in addition to labeling of the tonoplast, the GFP fluorescence was accumulated into the vacuole when seedlings were kept in the dark in ½MS (Figure 3A) or in the dark in alkaline medium (Figure 3B). These observations suggest that PROPEP1 is not just associated to the tonoplast as reported (Bartels et al., 2013), but might also be stored into the vacuole.

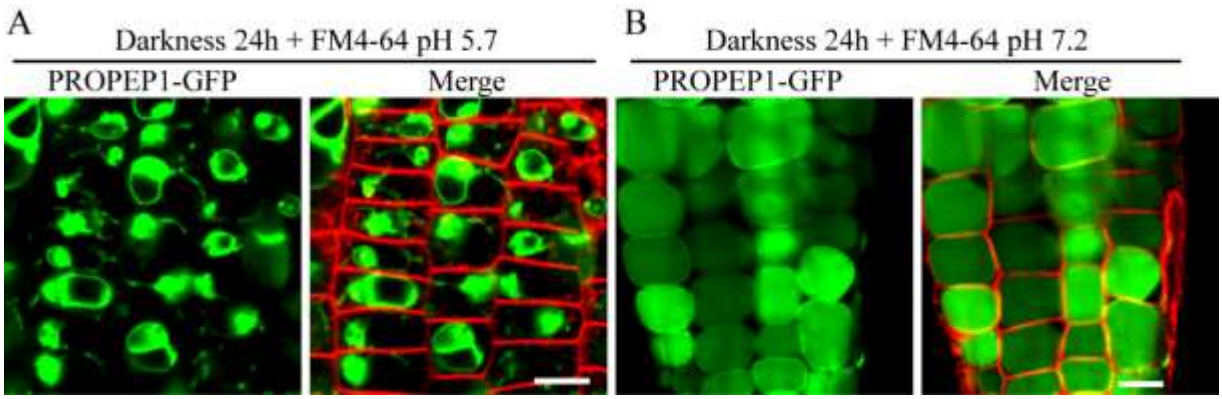

Figure 3 – Storage of the PROPEP1-GFP protein into the vacuole. Confocal images of the root meristem epidermal cells of five-day-old *Arabidopsis* transgenic lines expressing PROPEP1-GFP kept 24 h in the dark in ½MS (A) or in the dark and in a solid alkaline medium (B) before imaging. Co-staining with FM4-64 (2 µM, 20 min, red channel) highlights the plasma membrane. Similar results were obtained in three independent transgenic lines. Scale bars, 10 µm

The association of GFP signal with the tonoplast and its accumulation into the vacuole together with the proposed role of *At*Pep1 as amplifier of immune responses (Huffaker and Ryan, 2007; Yamaguchi and Huffaker, 2011), led us to hypothesize that the pro-peptide might be stored on the tonoplast and/or in the vacuole under normal conditions; however, upon biotic stresses the PROPEP1 is delivered to the extracellular medium, where the active

peptide *At*Pep1 is released and binds its receptors to initiate responses. To test this hypothesis, we evaluated the PROPEP1-GFP localization in the root meristem epidermal cells of five-day-old seedlings after exposition for 1 h to an elicitor cocktail solution, containing 1µM of *At*Pep1 and 1 µM of flg22 that resembled biotic stresses, in the presence or not of the fungal inhibitor brefeldin A (BFA 50 µM) (Figure 4) that has been described as a secretion inhibitor forming typical structures, designated BFA bodies (NEBENFUHR et al., 2002; ROBINSON et al., 2008). GFP signal was neither detected outside of cells delimited by FM4-64 (Figure 4A and 4B) nor into BFA bodies stained with FM4-64 (Figure 4B). Together these findings suggest that PROPEP1-GFP was not released through a BFA-dependent pathway upon *At*Pep1 and flg22 treatment.

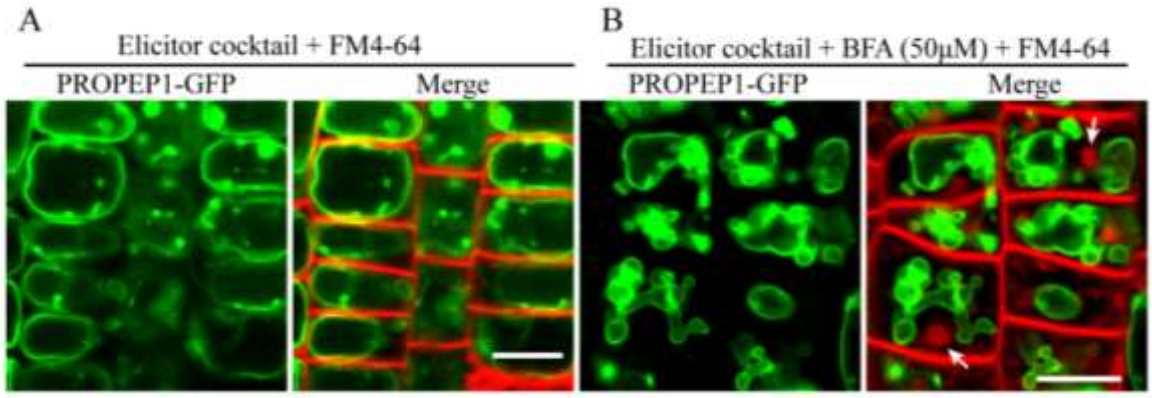

Figure 4 – Unmodified subcellular localization of PROPEP1-GFP upon *At*Pep1 and flg22 elicitation. (A) Confocal images of root meristem epidermal cells of *Arabidopsis* transgenic lines expressing PROPEP1-GFP, treated for 1h with an elicitor cocktail solution (1 µM AtPep1 and 1 µM flg22) or (B) pretreated with BFA (30 min, 50 µM) and treated for 1 h with the elicitor cocktail solution in the presence of BFA. Co-staining with FM4-64 (2 µM, 20 min red channel) highlights the plasma membrane. Similar results were obtained in three independent transgenic lines. Scale bars, 10 µm

2.2.2 PROPEP1-GFP does not induce expression of *At*Pep1-responsive genes

Transgenic lines expressing pro*35S:PROPEP1* have been reported to express the *At*Pep1-responsive gene *PDF1.2* at higher levels than those found in wild-type plants (HUFFAKER; RYAN, 2007). Therefore, we examined by RT-PCR analysis whether the expression of this gene also increased in the transgenic pro*35S:PROPEP1*-expressing lines. Besides *PDF1.2*, we also evaluated the expression of the gene coding for the *At*Pep1 receptor *PEPR1* that had been shown to be induced upon *At*Pep1 elicitation (YAMAGUCHI et al., 2010). In any of three independent transgenic lines evaluated were found increased expression levels of *PDF1.2* or *PEPR1* (Figure 5), suggesting that the activity of PROPEP1 may be affected by the addition of GFP at the C-terminus.

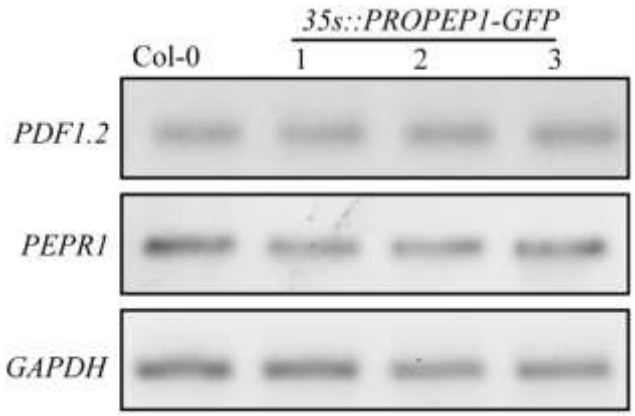

Figure 5 – Gene expression analysis of *At*Pep1-responsive genes by *PROPEP1-GFP* overexpression. RT-PCR analysis of the *PDF1.2* and *PEPR1* genes in Six-day-old seedlings of three independent transgenic lines expressing pro*35S:PROPEP1-GFP*. *G*lyceraldehyde-3-phosphate dehydrogenase (*GAPDH,* At1g13440) was used as a loading control. Similar results were obtained in three independent experiments

2.2.3 *At*Pep1 can be labeled with the Cy5 dye

As an alternative strategy to study subcellular dynamics, we covalently linked a synthetic *At*Pep1 with the fluorescent probe Cy5 that produces a signal in the far-red of the spectrum. This tool would allow us to monitor the *At*Pep1 behavior through assays based on fluorescent detection. *At*Pep1 was labeled with Cy5 in a single reaction with purifications steps, including acidic dialysis followed by HPLC purification. When the reaction product was passed through HPLC, two additional peaks occurred in the HPLC chromatogram that were not detected in the HPLC chromatogram of pure *At*Pep1 (Figures 6 and Figure Supplemental 1). The first peak was eluted after 3 min and corresponded to the unconjugated dye, whereas the second one eluted approximately after 13 min and contained the *At*Pep1 successfully labeled with Cy5. Because most of the *At*Pep1 remained unlabeled, as indicated by the large peak observed between 10 and 11 min that matched the peak in the chromatogram of the pure *At*Pep1 (Figure Supplemental 1), probably the labeling reaction did not have a good performance.

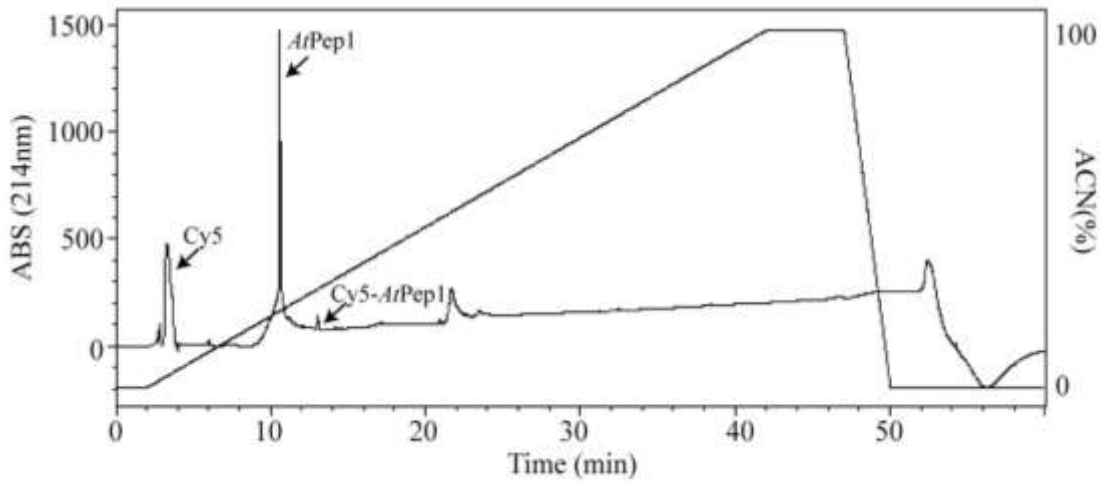

Figure 6 – Cy5 labeling of *At*Pep1. The HPLC chromatogram of the binding solution *At*Pep1 and Cy5 is shown with the corresponding retention times. Arrows point to the peaks of the indicated molecule. Graph line represents concentration of acetonitrile (ACN) during the separation. ABS, absorbance

The *At*Pep1 fraction labeled with Cy5 (Cy5-*At*Pep1) was collected and quantified by measuring the integration of the corresponding HPLC peak by means of as reference curve previously defined. This fraction was used to evaluate the biological activity of the labeled peptide by assessing the alkalinization of the extracellular medium in the cell culture and the gene expression of the *At*Pep1 receptor *PEPR1* in seedlings (Figure 7). Cy5-*At*Pep1 was able to alkalinize the extracellular medium, but its half-maximal activity (2.5 nM) was lower than that of the unlabeled *At*Pep1 (0.25 nM) (Figure 7A). RT-PCR analysis revealed that Cy5-*At*Pep1 was able to induce the expression of *PEPR1* in six-day-old *Arabidopsis* seedlings, although the induction level seemed higher for unlabeled *At*Pep1, as indicated by the intensity of the amplified band upon Cy5-*At*Pep1 treatment that was weaker than that of the band amplified upon treatment with the unlabeled peptide (Figure 7B). These results showed that *At*Pep1 was successfully labeled with the molecular probe Cy5 and that the labeled peptide was active.

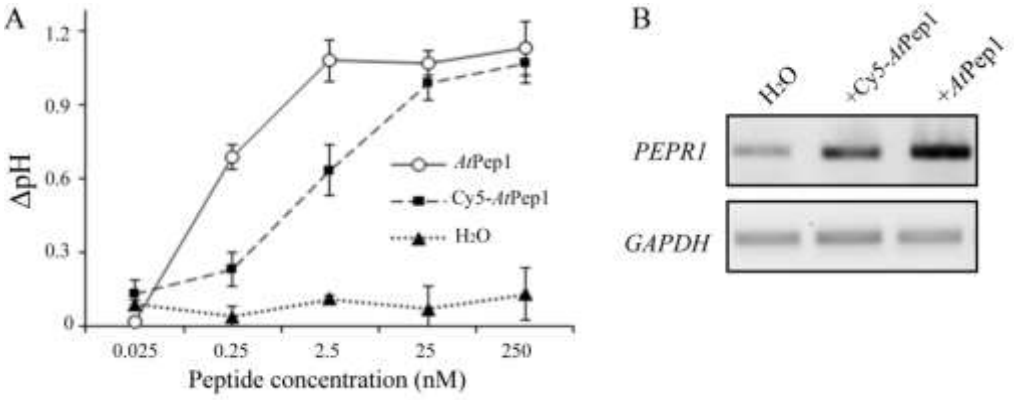

Figure 7 – Biological activity of *At*Pep1 and Cy5-*At*Pep1. (**A**) pH of the extracellular medium of *Arabidopsis* cell suspension measured after 20 min of exposure to different concentrations of *At*Pep1 or Cy5-*At*Pep1. Error bars indicate S.D. (n=9 wells). (**B**) RT-PCR analysis of *PEPR1* gene expression in *Arabidopsis* seedlings treated with 100 nM of *At*Pep1 or Cy5-*At*Pep1 for 60 min. Glyceraldehyde-3-phosphate dehydrogenase (*GAPDH*, At1g13440), was used as loading control and water as control. These experiments were done three times with similar results

2.2.4 Cy5-*At*Pep1 labels the plasma membrane of *Arabidopsis* root meristem epidermal cells

As Cy5-*At*Pep1 was biologically active, we examined whether the fluorescence of this molecular probe could be detected *in vivo* through confocal microscopy. To this end, 5-day-old Col-0 seedlings were incubated for 10 min with different concentrations of Cy5-*At*Pep1 and the root meristem epidermal cells were visualized after washing off the excess peptide. When the Cy5-*At*Pep1 concentration was lower than 1 µM, no fluorescence signal could be detected (data not showed), but at higher concentrations (10 µM), a fluorescence signal outside of the cell was observed (Figure 8). These results showed the potential of this fluorescent probe to be used to study the subcellular dynamics of *At*Pep1.

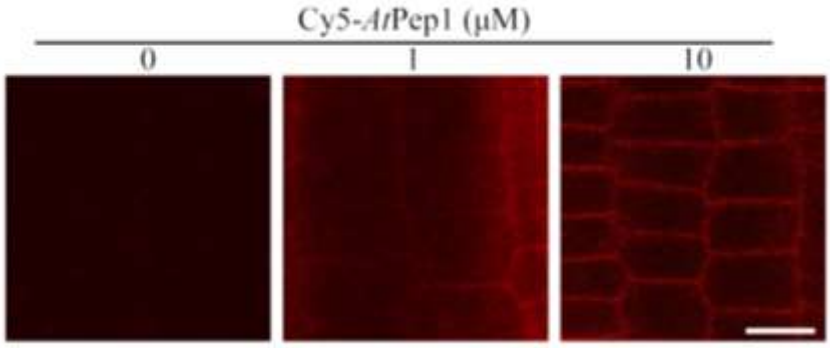

Figure 8 – Binding of Cy5-*At*pep1 in the plasma membrane of *Arabidopsis* root cells. Five-day-old *Arabidopsis* seedlings were treated with different concentrations of Cy5-*At*Pep1 for 10 min, washed, and epidermal root meristem epidermal cells visualized under a confocal microscope. Scale bar, 10 µm

2.2.5 TAMRA-*At*Pep1 is a bioactive fluorescently labeled *At*Pep1

Alternatively to Cy5 labeling, we synthesized an *At*Pep1 labeled with the 5-TAMRA dye at the N-terminus (TAMRA-*At*Pep1). TAMRA is smaller in size (430 Da) than Cy5 (792 Da) (MUJUMDAR et al., 1993; LYTTLE et al., 2000) and is detected at the red end of the spectrum (Figure Supplemental 2). TAMRA-*At*Pep1 was purchased from Life Technologies that synthetizes peptides with the FMOC solid-phase technology (ALBERICIO, 2000). We evaluated if TAMRA-*At*Pep1 is biologically active by assessing four different known *At*Pep1 responses (Figure 9) (HUFFAKER et al., 2006; KROL et al., 2010; YAMAGUCHI et al., 2010). First, we monitored the alkalinization activity in *Arabidopsis* cell suspension after 20 min of exposure to different concentrations of TAMRA-*At*Pep1 and found that TAMRA-*At*Pep1 displayed a dose-response activity in a manner similar to that of the unlabeled *At*Pep1 (Figure 9A). Then, we investigated the cytosolic calcium mobilization *in vivo* upon treatment with the labeled and unlabeled peptide (10 nM) with transgenic *Arabidopsis* plants expressing the cytosol-localized Ca^{2+} sensor protein aquorin (HARUTA et al., 2008); both peptides had similar total luminescence counts over a period of 360 sec (Figure 9B). When the root length of seedlings growing on medium containing 50 nM TAMRA-*At*Pep1 or *At*Pep1 was examined, an inhibitory effect of the root growth was observed in both cases, but the outcome of the unlabeled *At*Pep1 was stronger (Figure 9C) and higher concentrations of TAMRA-*At*Pep1 were needed to obtain an inhibitory effect similar to that of *At*Pep1. Finally, we evaluated through RT-PCR analysis whether the *PEPR1* expression was induced by TAMRA-*At*Pep1 in six-day-old *Arabidopsis* seedlings. As expected, the expression of this gene was clearly induced upon treatment with the labeled peptide as seen for *At*Pep1 (Figure 9D). Furthermore, the TAMRA-*At*Pep1 fluorescence was monitored *in vivo* via confocal microscopy that is quickly detected at the plasma membrane of epidermal *Arabidopsis* root meristem cells at nanomolar concentrations. These results are presented in the Chapter 3 of this thesis.

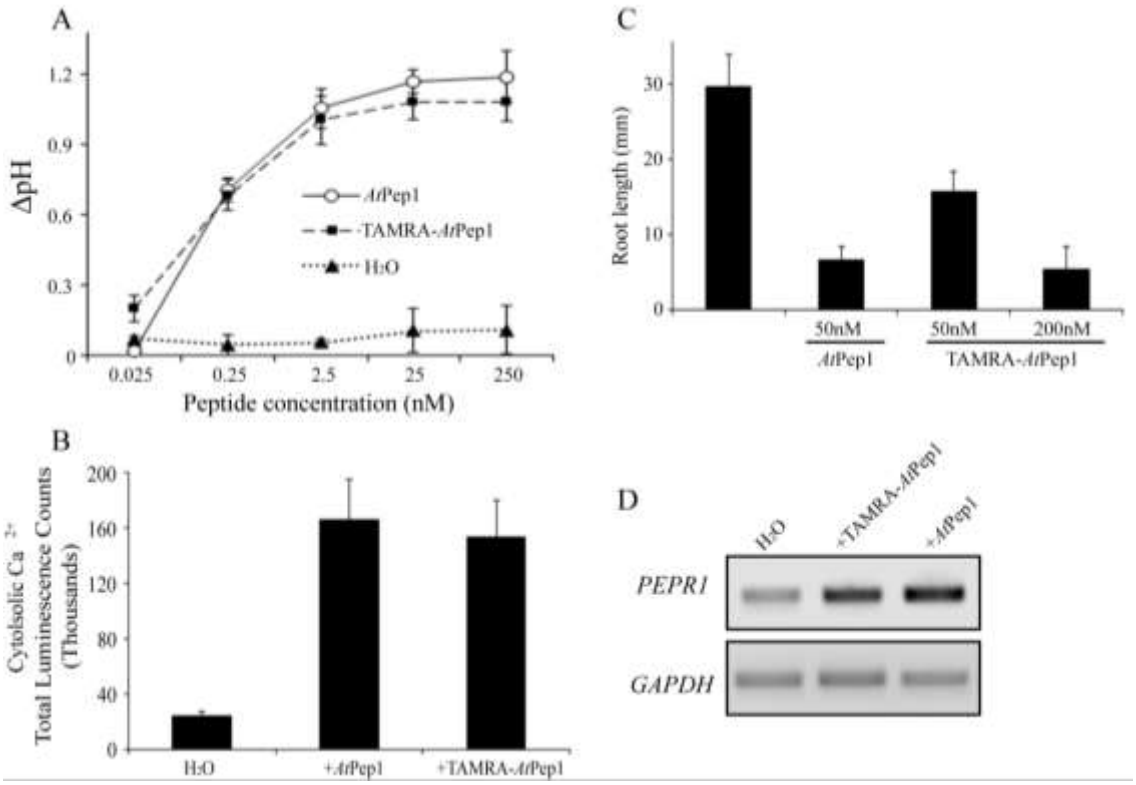

Figure 9 – Biological activity of *At*Pep1 labeled with the TAMRA dye. (A) Measurement of the pH of *Arabidopsis* cell suspensions after 20 min of exposure to different concentrations of *At*Pep1 or TAMRA-*At*Pep1. Error bars indicate standard deviation (n=9 wells). (**B**) Total luminescence of aequorin-expressing *Arabidopsis* plants subjected to the aquorin Ca^{2+} assay and treated with 10 nM *At*Pep1 or TAMRA-*At*Pep1. Error bars indicate S.D. (n=9 seedlings). (**C**) Root growth inhibition of Col-0 in the presence of *At*Pep1 or TAMRA-*At*Pep1. Error bars indicate standard deviation (n=10 seedlings). (**D**) RT-PCR analysis of *PEPR1*genes in six-day-old *Arabidopsis* seedlings treated for 60 min with 100 nM *At*Pep1 or TAMRA-*At*Pep1. Glyceraldehyde-3-phosphate dehydrogenase (*GAPDH,* At1g13440) was used as a loading control and water as control. These experiments were repeated at least twice with similar results

2.3 Discussion

Here, we examined two different approaches to generate tools that can be used for cell biology studies of *At*pep1. First, we produced plants expressing constitutively the *At*Pep1 precursor protein PROPEP1 fused to GFP. Interestingly, the PROPEP1-GFP signal was associated to the tonoplast in epidermal cells of cotyledons as well as of root epidermal cells. The same observation has recently been reported in transgenic plants expressing PROPEP1-YFP, but not *At*Pep1-YFP that is localized in the cytoplasm (BARTELS et al., 2013),

confirming that PROPEP1-YFP and PROPEP1-GFP fusions are associated with the tonoplast and indicating that an unknown localization signal or interaction domain forwarding it to the tonoplast is present at the N-terminus. An exciting future study would be to investigate how the different N-terminus domains of PROPEP1 affect this protein localization. As PROPEP1 lacks a transmembrane domain, it is also an open question how this protein is attached to the tonoplast. An explanation might be the existence of a PROPEP1 receptor protein localized at the tonoplast (BARTELS et al., 2013), but this issue remains to be clarified.

By assessing the PROPEP1-GFP signal under conditions that improve the GFP signal, besides the signal present at the tonoplast, we detected a strong accumulation of GFP fluorescence in the vacuoles; in contrast, we were not able to identify any fluorescence signal at the apoplast, suggesting that PROPEP1-GFP is not mainly exported to the extracellular medium under normal conditions. These observations together with the fact that *At*Pep1 is expected to bind its receptors outside of the plasma membrane (YAMAGUCHI; HUFFAKER, 2011), led us to wonder whether vacuoles work as organelles where PROPEP1 is stored and later released only in a danger situation, thus fulfilling its proposed role as amplifier of innate immunity responses. However, it cannot be discarded that the GFP fluorescence inside the vacuole belongs to free GFP that was released from the PROPEP1-GFP, hence is needed further experiments to check the nature of this GFP signal.

In attempt to test our assumption that the tonoplast or vacuoles serves as a storage organelle for PROPEP1, we treated transgenic PROPEP1-GFP-expressing *Arabidopsis* seedlings with an elicitor cocktail composed of *At*Pep1 and the biotic stress-stimulating MAMP flg22. However, we were unable to detect any change in the subcellular localization of PROPEP1-GFP under our experimental conditions. This finding suggests that biotic stress induced by DAMPs and/or MAMPs cannot induce the release of PROPEP1-GFP from the vacuole, however additional experiments are needed to confirm it. Currently, the molecular circumstances that enable and promote the release of *At*Pep1 into the extracellular space are a matter of debate. Furthermore, besides its amplifier role during plant immunity responses after detection of danger signals, such as MAMPs (e.g. flg22), a model in which *At*Pep1 is released upon loss of cellular integrity due to damage has also been proposed (BARTELS; BOLLER, 2015). The damage model is based on the involvement of *At*pep1 with JA and ethylene signaling that is required for the integration of responses against herbivores and necrotrophic pathogens (HUFFAKER et al., 2006; HUFFAKER; RYAN, 2007; BARTELS; BOLLER, 2015). These pathogens could lead to an impaired cellular integrity that allows the

release of PROPEP1 or *At*Pep1 to the extracellular environment (BARTELS; BOLLER, 2015). Future experiments are needed to clarify how *At*Pep1 reaches the apoplast.

As PROPEP1 lacks a known secretion or subcellular localization signal and PROPEP1-GFP fusion proteins do not localize to the secretory pathway as illustrated by our experiments with BFA that is a drug capable of blocking the default secretory machinery into BFA bodies (DETTMER et al., 2006; ROBINSON et al., 2008), PROPEP1 is probably released from the vacuole through an unconventional protein secretion mechanism. The release of leaderless secretory proteins to the cell exterior via unconventional routes has been amply studied in animals and yeast, reporting cases that involve fusion of lysosome with the plasma membrane (DING et al., 2012). However, leaderless secretion pathway has just begun to be understood in plants. PROPEP1 appears to be a good candidate to investigate this process in plants.

Plants stably expressing pro*35S:PROPEP1-GFP* did not show induced expression levels of *At*Pep1-responsive genes as reported for plants expressing pro*35S:PROPEP1* (HUFFAKER; RYAN, 2007), implying that addition of a GFP tag (27 kDa) at the C-terminus of *At*Pep1 can compromise the ability of the peptide to bind its receptors and to induce immunity responses. This assumption is supported by recent studies that demonstrate that the C-terminus portion of *At*Pep1 dominates the binding of this peptide to it receptors and that deletion of the last residue of *At*pep1 significantly compromised the *At*Pep1-PEPR1 interaction and responses (PEARCE et al., 2008; TANG et al., 2015). Future approaches must consider addition of a fluorescent protein between the C-terminus of PROPEP1 that contains the active peptide and the N-terminus with the precursor protein, thus allowing an eventual cleavage of the C-terminus given the origin of GFP-*At*Pep1.

The second approach examined in this work was related to the *At*Pep1 labeling with a dye aiming at developing a molecular probe that can be used to study the subcellular dynamics of *At*Pep1 when applied exogenously. Presently, companies offer different dyes to tag peptides and successful examples exist in the animal field (BECKER et al., 2001; JIN et al., 2006). In plants, was reported that a fluorescent labeled version of the peptide CLE19 that is involved in the regulation of *Arabidopsis* root meristem, is located predominantly in the intercellular spaces of the root meristem cells. However, biological assays showing the activity of this fluorescent-tagged CLE19 were not presented (FIERS et al., 2005).

Initially, we used the Cy5 dye to label a synthetic *At*Pep1 that belongs to the group of cyanine reagents known to be intensely fluorescent and highly water soluble and, thus, provides significant advantages over other existing fluorophores (WESSENDORF; BRELJE,

1992). Cy5 used to label the peptide contains a chemical NHS ester that is predicted to react with primary amines to yield stable amide bonds (HERMANSON, 2013). Therefore, we expected efficient labeling because *At*Pep1 has six sites that might potentially link with Cy5, including the N-terminus of the chain and five lysines that present a primary amine group in their side-chain. However, after purification through HPLC of the product of the linking reaction, only a minor portion of the peptide was labeled. To improve the yield of the *At*Pep1 labeling with Cy5 in future attempts, we could alter the protein concentrations and mainly the pH, because the amine groups of the peptide can be protonated in function of the pH, disturbing the acylation reaction with the NHS-ester group (MUJUMDAR et al., 1993).

Interestingly, both the Cy5-*At*Pep1 and the TAMRA-*At*Pep1 were able to induce *At*Pep1-responses, thus indicating that a fluorescent tag at the N-terminus does not abolish the AtPep1 activity. Moreover, when fluorescent probes were evaluated by confocal microscope, both Cy5-*At*Pep1 and TAMRA-*At*Pep1were able to bind the plasma membrane of epidermal cells of the *Arabidopsis* root tip meristem. However, TAMRA-*At*Pep1 showed activity and plasma membrane binding in lower concentrations than Cy5-*At*Pep1. This could be related with the nature of the dye that would differentially affect the activity of the peptide. Another possibility is that the amount of Cy5-*At*Pep1 was underestimated, as the quantification was based on a reference curve defined for unlabeled *At*Pep1 and not for a labeled peptide. As all *At*Pep1 responses are triggered at nanomolar concentrations, the use of a molecular probe biologically active at lower concentrations would certainly provide more accurate results when the subcellular dynamics of *At*Pep1 are investigated. In general, our results showed that signaling peptides can be labeled with fluorescent dyes, becoming a powerful tool for ligand-receptor studies in plants.

Author contribution

Ortiz-Morea F. A. and Moura D. S. conceived the study and designed the experiments. Ortiz-Morea F. A. performed all imaging, root length inhibition, alkalinization and RT-PCRs assays. Ortiz-Morea F.A., Dressano, K. generated material. Ortiz-Morea F.A. and Dressano, K. performed Ca^{2+} Mobilization Assay. Ortiz-Morea F.A. and Ceciliato P.H.O labeled the Cy5-AtPep1. Ortiz-Morea F. A. and Moura D. S. wrote the manuscript.

Acknowledgements

We thank Martine De Cock (VIB/Ghent University, Belgium) for help in preparing the manuscript. Ortiz-Morea F. A. is indebted to the PEC-PG program of the Coordenação de Aperfeiçoamento de Pessoal de Nível Superior CAPES Brazil for the Doctorate fellowship.

2.4 Materials and Methods

2.4.1 Plant material and growth conditions

Arabidopsis thaliana (L.) Heyhn., accession Columbia (Col-0), was used for all the experiments. Seeds were sterilized, maintained for 2 days at 4°C in the dark, and germinated on vertical half-strength Murashige and Skoog (½MS) medium (1% [w/v] sucrose) agar plates, pH 5.8 at 22°C in a 16-h/8-h light/dark cycle for 5 days. Transgenic plants overexpressing *PROPEP1-GFP* under the control of the constitutive promoter 35S (*pro35S:PROPEP1-GFP*) were obtained by amplifying using specific primers (Supplemental table 1) and cloning the 276-bp fragment containing the *AtPROPEP1* cDNA into the binary vector pK7FWG2 (KARIMI; INZE; DEPICKER, 2002). *Arabidopsi*s was transformed with *Agrobacterium tumefaciens* by means of the floral dip method (CLOUGH; BENT, 1998). Primary transformants were selected on kanamycin (50 mg/L) ½MS medium. T3 homozygous lines were used for microscopic analyses.

2.4.2 Imaging

Arabidopsis seedlings were imaged on a FluoView 1000 inverted confocal microscope (Olympus) equipped with a water-corrected 60× objective (NA1.2). The excitation wavelength was 488 nm for GFP, 555 for FM4-64, and 635 for Cy5. Emission was detected between 500–530 nm for GFP, 570–670 nm for FM4-64, and 640–680 nm for Cy5.

For the detection assay of the Cy5-*At*Pep1 fluorescent signal, 5-day-old seedlings were dipped into 500 µL at the indicated concentrations of Cy5-*At*Pep1 dissolved in ½MS medium, pulsed for 10 min, washed with ½MS liquid medium three times, and transferred to coverslips for visualization of the meristem epidermal cells.

2.4.3 Treatments to improve GFP signals

Five-day-old seedlings were transferred to darkness at 22°C on vertical ½MS medium (1% [w/v] sucrose) agar plates, pH 5.8 or 7.2 for 24 h before imaging. The alkaline pH was stabilized by addition of 20 mM of 2-(*N*-morpholino) ethanesulfonic acid (MES) buffer (Sigma-Aldrich).

2.4.4 Peptides and Chemicals

The *At*Pep1 (ATKVKAKQRGKEKVSSGRPGQHN) peptide with a HPLC purity of 95.16% and molecular weight of 2491.78 and *At*Pep1 labeled with 5'-carboxytetramethylrhodamine at the N-terminal (TAMRA-*At*Pep1) with a HPLC purity of 97.07% and molecular weight of 2905.75 were purchased from Life Technologies. The flg22

(QRLSTGSRINSAKDDAAGLQIA) peptide with a HPLC purity of 95% and a molecular weight of 2272.50 was acquired from Genscript (catalog No. RP19986). The peptides were dissolved in water to obtain peptide stocks of 100 µM. Further dilutions were done with ½MS medium. The inhibitors BFA (50 mM DMSO stock) were purchased from Sigma-Aldrich. FM4-64 was acquired from Molecular Probes (2 mM water stock). All chemicals were diluted in ½MS medium to prepare solution at the final concentrations.

2.4.5 Elicitor cocktail treatment

Five-day-old seedlings were incubated for 1 h into 1 mL of liquid ½MS medium containing the elicitor cocktail solution composed of 1 µM *At*Pep1 and 1 µM flg22 and then imaged. For cotreatment with BFA, seedlings were pretreated with 1 mL liquid ½MS medium containing 50 µM BFA, then added to cocktail solution, kept in the presence of BFA, and imaged after 60 min**.** Treatments were performed in combination with the endosomal marker FM4-64 at room temperature. For FM4-64 staining, seedlings were incubated for 5 min in 1 mL ½MS liquid medium containing 4 µM of the dye plus the respective treatment. Control treatments were done with equal amounts of DMSO. All washed steps and imaging were carried out in the presence of the respective treatment.

2.4.6 *At*Pep1 Labeling

The synthetic *At*Pep1 peptide was fluorescently labeled with Fluorolink^{TM} Cy5-reactive (GE Healthcare). The peptide was dissolved at 1 mg/mL in sodium carbonate-sodium bicarbonate buffer (SOUTHWICK et al., 1990), added to the dye vial (1 mL), and mixed thoroughly. The reaction was incubated for 2 h and mixed every 10 min. For separation of the labeled *At*Pep1 from the free dye and the unlabeled *At*Pep1, the linking solution was first dialyzed with a 1 kDa (GE-Healthcare) membrane against 1 L of TFA buffer (0.2%) for 48 h at 4^{o}C. The TFA buffer was replaced every 24 h. Then, the solution was passed through high-performance liquid chromatography (*HPLC*) with a HPLC C18 column, previously equilibrated with 0.1% formic acid (v/v). A 20 min gradient from 0 to 50% acetonitrile (v/v) with 0.1% (v/v) formic acid was applied after injection of the linking solution. To determine the collected time points of the fractions, the chromatographs of the linking reaction run was compared with a run of the, previously injected, unlabeled peptide. Finally, the amount of fully labeled *At*Pep1 was estimated by calculating the integration of the corresponding peak, using as reference a previously defined concentration curve of *At*Pep1.

2.4.7 Alkalinization Assay

The alkalinization assay has been described previously (YAMAGUCHI; PEARCE; RYAN, 2006). Briefly, 1mL cell suspension (5 days after subculture) was transferred into each well of a 24-well plate (Corning) and allowed to equilibrate on an orbital shaker at 120 rpm for 1 h. The pH of the medium was measured at the time points at the indicated peptide concentrations with a EA940 pH meter (Orion) with a semi-micro pH electrode (Orion).

2.4.8 RT-PCR

Six-day-old seedlings were used for all gene expression experiments. Total RNA was extracted with Trizol reagent (Life Technologies), according to the manufacturer's instructions, followed by DNAse I treatment (Life Technologies) to remove any residue of genomic DNA, and quantified with a Nanodrop spectrophotometer (Thermo Scientific). cDNa was synthesized from 1µg total RNA with Improm-II Reverse Transcriptase (Promega).
The *At*Pep1-induced genes *PEPR1* and *PDF1.2* were analyzed. The *GAPDH* gene was used as a control. The primers used are described in Supplementary Table 1. For the PCR reactions, 1 µL cDNA was used. The reactions were placed in the thermocycler under the following conditions: 94°C for 2 min and appropriate cycle numbers of 94°C for 20 sec, 60°C for 30sec, and 72°C for 45 sec. These experiments were repeated at least three times.

2.4.9 Ca^{2+} Mobilization Assay

The cytoplasmic Ca^{2+} assay in *Arabidopsis* seedlings has been described previously (HARUTA et al., 2008; MORATO DO CANTO et al., 2014). The induced Ca^{2+} signaling was evaluated by monitoring the level of cytosolic Ca^{2+} in *Arabidopsis* seedlings. Seedlings were studied of the *Arabidopsis* line homozygous for a single insertion of a transgene encoding a cytoplasmically expressed aequorin driven by the cauliflower mosaic virus 35S promoter. Seeds were sterilized as described before and plated on ½MS medium without vitamins. The plates were kept under constant light at 24°C [150 µE $m^{-2}.s^{-1}$ (E, Einstein; 1 E, 1 mol of photons)] for 4 days. A single seedling was transferred into each well of a 96-well white microplate (Thermo Labsystems) containing 200 mL of ½ MS medium supplemented with 2.5 mM coelenterazine cp (Biotium) and incubated in the dark at 24°C for 16 h. In each plate well containing a single seedling, TAMRA-*At*Pep1 or *At*Pep1 was added at a final concentration of 10 nM. The resulting luminescence emission was monitored with a microplate reader (Biotec ELx 800) for 24 time points during approximately 360 sec after addition of the respective peptide. Water was used as control.

2.4.10 Root growth assay

Seeds were sown on ½MS solid medium, stratified for 2 days at 4°C in the dark, and placed vertically in the light. Ten days after germination, seedlings were transferred to square transparent Petri dishes with solid ½MS medium supplemented with or without the indicated amount of *At*Pep1 and incubated for 4 more days; then, the plates were scanned and the root growth measured. For measurements, scanned images were processed and evaluated with the ImageJ software.

Supplemental information

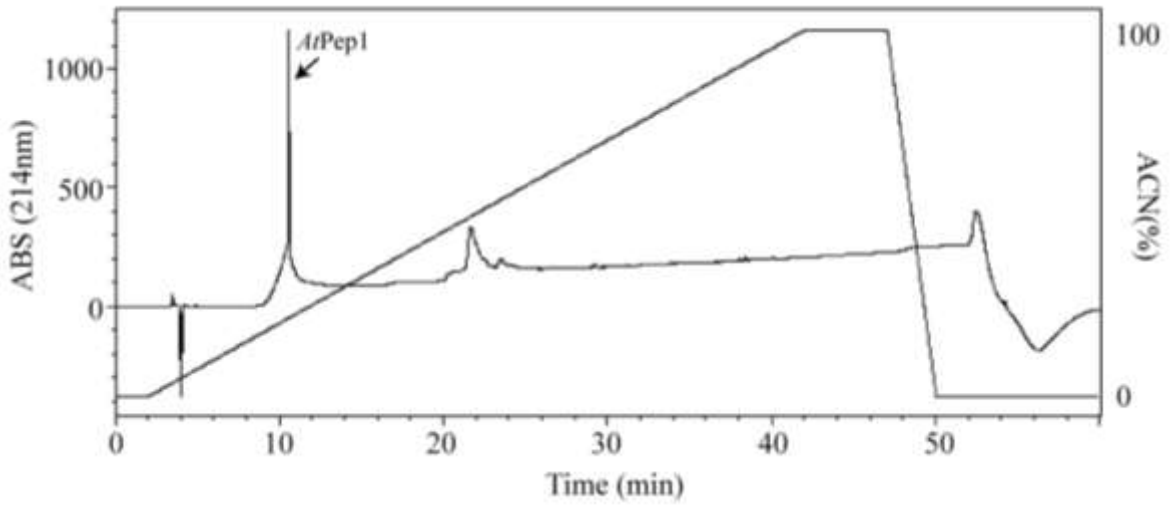

Supplemental Figure 1 – HPLC chromatogram of the *At*Pep1 with its corresponding retention time. Arrows point the peaks of *At*Pep1. Graph line represents concentration of acetonitrile (ACN) during the running. ABS, absorbance

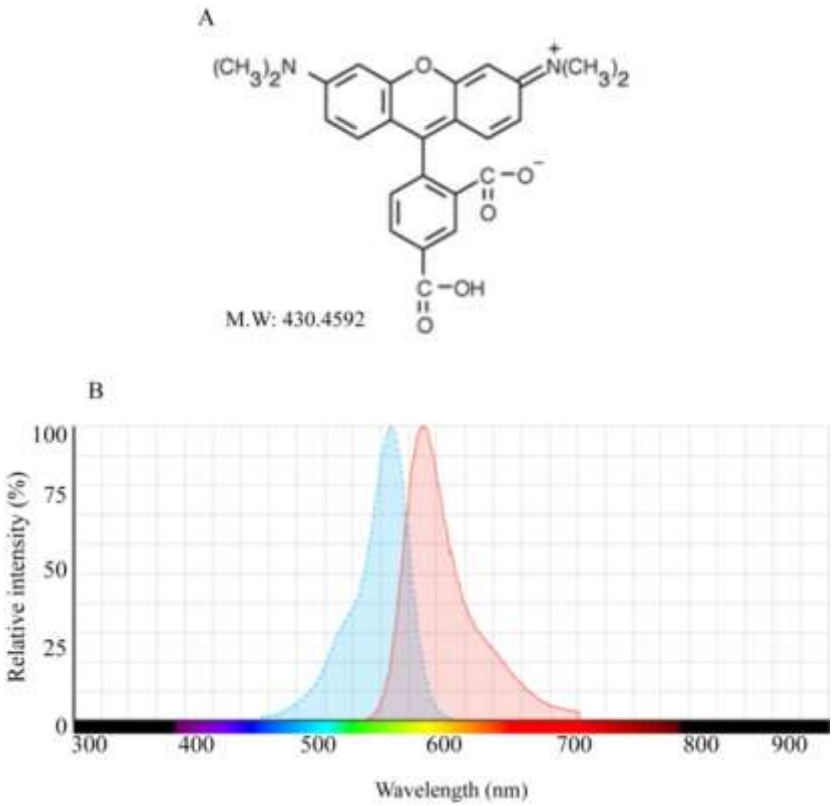

Supplemental Figure 2 – Chemical structure (A), and fluorescent spectra (B) of 5-TAMRA. Colored areas represent the excitation (blue) and emission (red) wave lengths. M.W: molecular weight

Source: http://www.lifetechnologies.com/be/en/home/life-science/cell-analysis/labeling-chemistry/fluorescence-spectraviewer.html

Supplemental Table 1 – Primer used for cloning and RT-PCR analysis

Gene	**Primer**	**Sequence 5' – 3'**
Cloning		
PROPEP1	Forward	CACCGATAACACAAAAGTTTCGGTTGA
	Reverse	CTGAGTTTAAAGATCGAGAAACATGCA
RT-PCR		
GAPDH	Forward	TTGGTGACAACAGGTCAAGCA
	Reverse	AAACTTGTCGCTCAATGCAA
PEPR1	Forward	GTTTTGGCTGAGGAAAGACG
	Reverse	ACATTGTACCGTGCAGACCA
PDF1.2	Forward	AACCTTGAAGGAGCCAAACA
	Reverse	CACACGATTTAGCACCAAAGA

References

ALBERICIO, F. **Solid-phase synthesis:** a practical guide. New York: CRC Press, 2000. 819 p.

BARTELS, S.; BOLLER, T. Quo vadis, Pep? Plant elicitor peptides at the crossroads of immunity, stress and development. **Journal of Experimental Botany**, Oxford, v. 66, n. 17, p. 5183-5193, 2015.

BARTELS, S.; LORI, M.; MBENGUE, M.; VAN VERK, M.; KLAUSER, D.; HANDER, T.; BONI, R.; ROBATZEK, S.; BOLLER, T. The family of Peps and their precursors in Arabidopsis: differential expression and localization but similar induction of pattern-triggered immune responses. **Journal of Experimental Botany,** Oxford, v. 64, n. 17, p. 5309-5321, 2013.

BECKER, A.; HESSENIUS, C.; LICHA, K.; EBERT, B.; SUKOWSKI, U.; SEMMLER, W.; WIEDENMANN, B.; GROTZINGER, C. Receptor-targeted optical imaging of tumors with near-infrared fluorescent ligands. **Nature Biotechnology,** New York, v. 19, n. 4, p. 327-331, 2001.

BOLTE, S.; TALBOT, C.; BOUTTE, Y.; CATRICE, O.; READ, N.D.; SATIAT-JEUNEMAITRE, B. FM-dyes as experimental probes for dissecting vesicle trafficking in living plant cells. **Journal of Microscopy**, Hoboken, v. 214, n. 2, p. 159-173, 2004.

BUTENKO, M.A.; WILDHAGEN, M.; ALBERT, M.; JEHLE, A.; KALBACHER, H.; AALEN, R.B.; FELIX, G. Tools and strategies to match peptide-ligand receptor pairs. **The Plant Cell** ,Rockville, v. 26, n. 5, p. 1838-1847, 2014.

CLOUGH, S.J.; BENT, A.F. Floral dip: a simplified method for Agrobacterium-mediated transformation of *Arabidopsis thaliana*. **The Plant Journal : for Cell and Molecular Biology,** Oxford, v. 16, n. 6, p. 735-743, 1998.

DETTMER, J.; HONG-HERMESDORF, A.; STIERHOF, Y.D.; SCHUMACHER, K. Vacuolar H+-ATPase activity is required for endocytic and secretory trafficking in Arabidopsis. **The Plant Cell,** Rockville, v. 18, n. 3, p. 715-730, 2006.

DI RUBBO, S.; IRANI, N.G.; KIM, S.Y.; XU, Z.Y.; GADEYNE, A.; DEJONGHE, W.; VANHOUTTE, I.; PERSIAU, G.; EECKHOUT, D.; SIMON, S.; SONG, K.; KLEINE-VEHN, J.; FRIML, J.; DE JAEGER, G.; VAN DAMME, D.; HWANG, I.; RUSSINOVA, E. The clathrin adaptor complex AP-2 mediates endocytosis of brassinosteroid insensitive1 in Arabidopsis. **The Plant Cell,** Rockville, v. 25, n. 8, p. 2986-2997, 2013.

DING, Y.; WANG, J.; WANG, J.; STIERHOF, Y.D.; ROBINSON, D.G.; JIANG, L. Unconventional protein secretion. **Trends in Plant Science,** Oxford, v. 17, n. 10, p. 606-615, 2012.

ENDO, S.; BETSUYAKU, S.; FUKUDA, H. Endogenous peptide ligand-receptor systems for diverse signaling networks in plants. **Current Opinion in Plant Biology,** London, v. 21, p. 140-146, 2014.

GHORBANI, S.; FERNANDEZ SALINA, A.; HILSON, P.; BEECKMAN, T. Signaling peptides in plants. **Cell & Developmental Biology,** Oxford, v. 3, n. 2 p. 1-11, 2014.

GOLDYS, E.M. **Fluorescence applications in biotechnology and life sciences**. Hoboken: John Wiley, 2009. 314 p.

HARUTA, M.; MONSHAUSEN, G.; GILROY, S.; SUSSMAN, M.R. A cytoplasmic Ca2+ functional assay for identifying and purifying endogenous cell signaling peptides in Arabidopsis seedlings: identification of AtRALF1 peptide. **Biochemistry,** Washington, v. 47, n. 24, p. 6311-6321, 2008.

HERMANSON, G.T. **Bioconjugate techniques.** Amsterdam: Academic Press, 2013.1095 p.

HUFFAKER, A.; RYAN, C.A. Endogenous peptide defense signals in Arabidopsis differentially amplify signaling for the innate immune response. **Proceedings of the National Academy of Sciences of the United States of America,** Washington, v. 104, n. 25, p. 10732-10736, 2007.

HUFFAKER, A.; PEARCE, G.; RYAN, C.A. An endogenous peptide signal in Arabidopsis activates components of the innate immune response **Proceedings of the National Academy of Sciences of the United States of America,** Washington,v. 103, n. 26, p. 10098-10103, 2006.

HURTH, M.A.; SUH, S.J.; KRETZSCHMAR, T.; GEIS, T.; BREGANTE, M.; GAMBALE, F.; MARTINOIA, E.; NEUHAUS, H.E. Impaired pH homeostasis in Arabidopsis lacking the vacuolar dicarboxylate transporter and analysis of carboxylic acid transport across the tonoplast. **Plant Physiology,** Lancaster, v. 137, n. 3, p. 901-910, 2005.

IRANI, N.G.; DI RUBBO, S.; MYLLE, E.; VAN DEN BEGIN, J.; SCHNEIDER-PIZON, J.; HNILIKOVA, J.; SISA, M.; BUYST, D.; VILARRASA-BLASI, J.; SZATMARI, A.M.; VAN DAMME, D.; MISHEV, K.; CODREANU, M.C.; KOHOUT, L.; STRNAD, M.; CANO-DELGADO, A.I.; FRIML, J.; MADDER, A.; RUSSINOVA, E. Fluorescent castasterone reveals BRI1 signaling from the plasma membrane. **Nature Chemical Biology,** New York, v. 8, n. 6, p. 583-589, 2012.

FIERS, M.; GOLEMIEC, E.; XU, J.; VAN DER GEEST, L.; HEIDSTRA, R.; STIEKEMA, W.; LIU, C.-M. The 14–Amino Acid CLV3, CLE19, and CLE40 Peptides Trigger Consumption of the Root Meristem in Arabidopsis through a CLAVATA2-Dependent Pathway. **The Plant Cell,** Rockville, v. 17, n. 9, p. 2542-2553, 2005.

JIN, Z.H.; JOSSERAND, V.; RAZKIN, J.; GARANGER, E.; BOTURYN, D.; FAVROT, M.C.; DUMY, P.; COLL, J.L. Noninvasive optical imaging of ovarian metastases using Cy5-labeled RAFT-c(-RGDfK-)4. **Molecular Imaging,** Cambridge, v. 5, n. 3, p. 188-197, 2006.

KARIMI, M.; INZE, D.; DEPICKER, A. Gateway vectors for Agrobacterium-mediated plant transformation. **Trends in Plant Science,** Oxford, v. 7, n. 5, p. 193-195, 2002.

KNEEN, M.; FARINAS, J.; LI, Y.; VERKMAN, A.S. Green fluorescent protein as a noninvasive intracellular pH indicator. **Biophysical Journal,** New York, v. 74, n. 3, p. 1591-1599, 1998.

KROL, E.; MENTZEL, T.; CHINCHILLA, D.; BOLLER, T.; FELIX, G.; KEMMERLING, B.; POSTEL, S.; ARENTS, M.; JEWORUTZKI, E.; AL-RASHEID, K.A.; BECKER, D.; HEDRICH, R. Perception of the Arabidopsis danger signal peptide 1 involves the pattern recognition receptor AtPEPR1 and its close homologue AtPEPR2. **The Journal of Biological Chemistry,** Baltimore, v. 285, n. 18, p. 13471-13479, 2010.

LYTTLE, M.H.; CARTER, T.G.; DICK, D.J.; COOK, R.M. A tetramethyl rhodamine (Tamra) phosphoramidite facilitates solid-phase-supported synthesis of 5'-Tamra DNA. **The Journal of Organic Chemistry,** Washington, v. 65, n. 26, p. 9033-9038, 2000.

MORATO DO CANTO, A.; CECILIATO, P.H.; RIBEIRO, B.; ORTIZ MOREA, F.A.; FRANCO GARCIA, A.A.; SILVA-FILHO, M.C.; MOURA, D.S. Biological activity of nine recombinant AtRALF peptides: implications for their perception and function in Arabidopsis. **Plant Physiology and Biochemistry,** Paris, v. 75, p. 45-54, 2014.

MUJUMDAR, R.B.; ERNST, L.A.; MUJUMDAR, S.R.; LEWIS, C.J.; WAGGONER, A.S. Cyanine dye labeling reagents: sulfoindocyanine succinimidyl esters. **Bioconjugate Techniques,** Amsterdam, v. 4, n. 2, p. 105-111, 1993.

NEBENFUHR, A.; RITZENTHALER, C.; ROBINSON, D.G. Brefeldin A: deciphering an enigmatic inhibitor of secretion. **Plant Physiology,** Lancaster, v. 130, n. 3, p. 1102-1108, 2002.

NTOUKAKIS, V.; SCHWESSINGER, B.; SEGONZAC, C.; ZIPFEL, C. Cautionary notes on the use of C-terminal BAK1 fusion proteins for functional studies. **The Plant Cell,** Rockville, v. 23, n. 11, p. 3871-3878, 2011.

PEARCE, G.; YAMAGUCHI, Y.; MUNSKE, G.; RYAN, C.A. Structure-activity studies of AtPep1, a plant peptide signal involved in the innate immune response. **Peptides,** New York, v. 29, n. 12, p. 2083-2089, 2008.

RANF, S.; ESCHEN-LIPPOLD, L.; PECHER, P.; LEE, J.; SCHEEL, D. Interplay between calcium signalling and early signalling elements during defence responses to microbe- or damage-associated molecular patterns. **The Plant Journal : for Cell and Molecular Biology,** Oxford, v. 68, n. 1, p. 100-113, 2011.

ROBINSON, D.G.; JIANG, L.; SCHUMACHER, K. The endosomal system of plants: charting new and familiar territories. **Plant Physiology,** Lancaster,v. 147, n. 4, p. 1482-1492, 2008.

SHEN, J.; ZENG, Y.; ZHUANG, X.; SUN, L.; YAO, X.; PIMPL, P.; JIANG, L. Organelle pH in the Arabidopsis endomembrane system. **Molecular Plant,** Saint Paul, v. 6, n. 5, p. 1419-1437, 2013.

SOUTHWICK, P.L.; ERNST, L.A.; TAURIELLO, E.W.; PARKER, S.R.; MUJUMDAR, R.B.; MUJUMDAR, S.R.; CLEVER, H.A.; WAGGONER, A.S. Cyanine dye labeling reagents—carboxymethylindocyanine succinimidyl esters. **Cytometry,** New York, v. 11, n. 3, p. 418-430, 1990.

SPENCE, M.T.; JOHNSON, I.D. **The molecular probes handbook:** a guide to fluorescent probes and labeling technologies. Life Technologies Corporation, 2010.

TANG, J.; HAN, Z.; SUN, Y.; ZHANG, H.; GONG, X.; CHAI, J. Structural basis for recognition of an endogenous peptide by the plant receptor kinase PEPR1 **Cell Research,** New York, v. 25, n. 1, p. 110-120, 2015.

WESSENDORF, M.; BRELJE, T. Which fluorophore is brightest? A comparison of the staining obtained using fluorescein, tetramethylrhodamine, lissamine rhodamine, Texas red, and cyanine 3.18. **Histochemistry,** New York, v. 98, n. 2, p. 81-85, 1992.

YAMAGUCHI, Y.; HUFFAKER, A. Endogenous peptide elicitors in higher plants. **Current Opinion in Plant Biology,** London, v. 14, n. 4, p. 351-357, 2011.

YAMAGUCHI, Y.; PEARCE, G.; RYAN, C.A. The cell surface leucine-rich repeat receptor for AtPep1, an endogenous peptide elicitor in Arabidopsis, is functional in transgenic tobacco cells. **Proceedings of the National Academy of Sciences of the United States of America,** Washington,v. 103, n. 26, p. 10104-10109, 2006.

YAMAGUCHI, Y.; HUFFAKER, A.; BRYAN, A.C.; TAX, F.E.; RYAN, C.A. PEPR2 is a second receptor for the Pep1 and Pep2 peptides and contributes to defense responses in Arabidopsis. **The Plant Cell,** Rockville, v. 22, n. 2, p. 508-522, 2010.

ZHENG, H.; KUNST, L.; HAWES, C.; MOORE, I. A GFP-based assay reveals a role for RHD3 in transport between the endoplasmic reticulum and Golgi apparatus. **The Plant Journal: for Cell and Molecular Biology,** Oxford, v. 37, n. 3, p. 398-414, 2004.

3 INTERNALIZATION AND INTRACELLULAR TRAFFICKING OF THE ENDOGENOUS PEPTIDE *At*Pep1 AND ITS RECEPTORS IN *ARABIDOPSIS*

Fausto Andres Ortiz-Morea[1,2,3], Yu Luo[1,2], Wim Dejonghe[1,2], Maciej Adamowski[4], Jiří Friml[4], Daniel Scherer de Moura[3] and Eugenia Russinova[1,2]

[1]Department of Plant Systems Biology, VIB, Technologiepark 927, 9052 Ghent, Belgium
[2]Department of Plant Biotechnology and Bioinformatics, Ghent University, Technologiepark 927, 9052 Gent, Belgium
[3]Laboratório de Bioquímica de Proteínas, Departamento de Ciências Biológicas, Escola Superior de Agricultura Luiz de Queiroz, Universidade de São Paulo USP, Piracicaba, SP 13418-900, Brazil.
[4]Institute of Science and Technology Austria (IST Austria), Am Campus 1, 3400 Klosterneuburg, Austria

Abstract

Recently, a growing number of small signaling peptides has been found to play important roles in a variety of biological and physiological responses in plants. Among them, the plant elicitor peptide1 (Pep1) has been shown to induce innate immune responses and to be expressed upon biotic stresses. In *Arabidopsis thaliana*, the *At*Pep1 binds the plasma membrane receptors PEPR1 and PEPR2 with high affinity. Although a large amount of information about the PEPR-mediated signaling components and responses is available, the subcellular dynamics of the *At*Pep1-PEPRs remains largely unknown. In the present study, we combined classical and chemical genetics with life imaging to study the behavior of a bioactive fluorescently labeled *At*Pep1 in the *Arabidopsis* root meristem. We discovered that *At*Pep1 was able to label the plasma membrane very quickly in a receptor-dependent manner. Subsequently, the PEPR-*At*Pep1 complex was internalized via clathrin-mediated endocytosis (CME) and transported to the lytic vacuole, passing through early and late endosomal compartments. Impairment of CME compromised the *At*Pep1 responses. Our findings provide an *in vivo* visualization of a signaling peptide in plant cells, thus giving insights into its intracellular fate and dynamics and serving as an excellent model to study the implications of endocytosis in plant immunity.

Keywords: Endocytosis; *At*Pep1; PEPR; Clathrin-mediated endocytosis; Plant immunity

3.1 Introduction

Plants are sessile organisms exposed throughout their life time to changing environments to which they need to adapt constantly. Therefore, accurate communication networks are needed to respond efficiently and to ensure survival. Several molecules have been described as essential players during plant responses, among which plant signaling peptides are highlighted for their role in cell-to-cell communication that works as molecular message between cells and tissues (GHORBANI et al., 2014). Recently, a growing number of small signaling peptides have been discovered to play an active role in a variety of biological and physiological responses in plants (GHORBANI et al., 2014; YAMAGUCHI; HUFFAKER, 2011). Signaling peptides are secreted into the apoplast where they are recognized by the extracellular domains of the plasma membrane-localized receptors in order to trigger intracellular signaling (ENDO; BETSUYAKU; FUKUDA, 2014). Although the *Arabidopsis thaliana* genome is predicted to encode more than 600 receptors and more than 1,000 potential peptide ligands (CZYZEWICZ et al., 2013), currently, only a few peptide-receptor pairs have been identified.

One well-characterized peptide-receptor pair is the plant elicitor peptide1 (*At*Pep1) and its receptors PEPR1 and PEPR2 (KROL et al., 2010; TANG et al., 2015; YAMAGUCHI et al., 2010). *At*Pep1 is a 23-amino-acid peptide that belongs to a family of eight members and is derived from the C-terminus of a 92-amino-acid precursor protein *At*PROPEP1 (BARTELS et al., 2013; HUFFAKER; PEARCE; RYAN, 2006). *At*Pep1 has been shown to mediate defense signaling in a receptor-dependent manner, triggering responses reminiscent of pattern-triggered immunity (PTI), including intracellular Ca^{2+} elevation, extracellular alkalinization, reactive oxygen species production, mitogen-activated protein (MAP) kinase activation, induction of defense-related gene expression, root growth inhibition, and interaction with defense-related phytohormones (HUFFAKER; PEARCE; RYAN, 2006; KROL et al., 2010; RANF et al., 2011; ROSS et al., 2014).

Although information about the *At*Pep1 signaling responses is available, the subcellular localization and dynamics of *At*Pep1 are totally unknown. Internalization of signaling peptides via endocytosis has long been known in animal cells, where it plays a key role in the regulation of intracellular signaling (CLAGUE, 1998). Interestingly and despite the ever-growing number of plant signaling peptides, internalization has not been reported in plants thus far. *At*Pep1 receptors are structurally similar to the plasma membrane-localized receptor kinases FLAGELLING SENSIN2 (FLS2) and BRASSINOSTEROID

INSENSITIVE1 (BRI1) that undergo endocytosis both independently and dependently of their ligands, the bacterial peptide flagellin 22 (flg22) and the brassinosteroid (BR) hormone, respectively (BECK et al., 2012; IRANI et al., 2012; RUSSINOVA et al., 2004). Endocytosis in animals cells is clathrin-mediated (CME) or clathrin-independent (CIE) according to the protein machinery involved in the formation of vesicles (WIEFFER; MARITZEN; HAUCKE, 2009). In plants, CME is well characterized (BAISA; MAYERS; BEDNAREK, 2013; GADEYNE et al., 2014; LI et al., 2012), whereas CIE has only been suggested (BARAL et al., 2015; LI et al., 2012). During CME, clathrin-coated vesicles (CCV) are created through polymerization of clathrin that form triskelions of three clathrin heavy chain (CHC) and three clathrin light chain (CLC) proteins. The triskelions build a cage that coats vesicles that bud off from the plasma membrane (KIRCHHAUSEN, 2009). Genetic studies of two *CHC* and three *CLC* genes encoded in *Arabidopsis* support the conserved mechanism of CME in plants and its importance for growth and development (CHEN; IRANI; FRIML, 2011; KITAKURA et al., 2011; WANG et al., 2013). Recently, CHC2 has also been found to modulate plant defense responses (WU et al., 2015), although, in general, the role of CME in plant immunity has not been addressed completely. Once internalized, the receptor-ligand complexes in plants enter the endocytic trafficking route, first reaching the *trans*-Golgi network/early endosome (TGN/EE) compartments where the cargo is further sorted, either for recycling back to the plasma membrane or for degradation into the vacuole via the multivesicular body (MVB)/late endosome (LE) compartments (BAR; AVNI, 2014; IRANI; RUSSINOVA, 2009; VIOTTI et al., 2010). Thus, endocytosis can control the outcome of receptor-mediated signaling by regulating the amount of the respective receptors and ligands at the plasma membrane. In animals, besides signaling initiated from the plasma membrane, endosomes have also been shown to be signaling platforms in various signaling pathways (MURPHY et al., 2009; RAJAGOPALAN, 2010). Although there are no reasons for the absence of endosomal signaling in plants, its role is still not well understood.

Over the past few years, significant progress has been made on the characterization of CME in plants, but its machinery, regulation, and role during signaling are still poorly defined when compared to the counterpart systems in animals (BAISA; MAYERS; BEDNAREK, 2013). To gain insights into CME in plants, *bona fide* endocytosed ligand cargos have to be identified that can be tagged with fluorescent probes allowing their study via life imaging. However, this task is challenging because the addition of an extra molecule to a ligand can easily abolish its activity. Labeled plant endocytic cargos and the trace of their trafficking

routes from the plasma membrane into the cell would provide bases to better understand the role of endocytosis during signaling in plants.

Here, taking advantage of the bioactive fluorescently labeled signaling peptide TAMRA-*At*Pep1 in combination with genetics, chemicals, and confocal live-cell imaging tools, we studied the subcellular dynamics of this plant signaling peptide and its receptor, as well as the interplay between trafficking and signaling of this ligand-receptor pair. We found that TAMRA-*At*Pep1 was able to label the plasma membrane very quickly in a receptor-dependent manner. Subsequently, the receptor-ligand complex was internalized via CME and transported to the lytic vacuole, passing through TGN/EE and MVB. We also detected that CME impairment compromised the *At*Pep1 responses, suggesting a role during signaling. Our findings provide the *in vivo* visualization of a signaling peptide in plant cells, thus giving insights into its intracellular fate and dynamics, and serving as an excellent model to study the implications of endocytosis in plant immunity.

3.2 Results

3.2.1 *At*Pep1 labeled the plasma membrane in a receptor-dependent manner

Although recent crystal structure analyses have revealed the mechanism of the *At*Pep1-induced activation of the receptor PEPR1 (TANG et al., 2015), the intracellular fate of the active PEPR remains as yet unknown. To simultaneously monitor the localization of the *At*Pep1-bound and presumably active PEPRs in living cells, we synthesized a fluorescently labeled *At*Pep1, designated TAMRA-*At*Pep1. TAMRA-*At*Pep1 was bioactive at nanomolar concentrations, but slightly less than the nonlabeled *At*Pep1 (Chapter 2, this thesis). The intracellular localization of TAMRA-*At*Pep1 was studied in wild type *Arabidopsis* root meristem epidermal cells. Five-day-old seedlings were incubated for 1, 10, 60 and 600 sec with 100 nM of the TAMRA-*At*Pep1 fluorescent probe and visualized immediately after washing off the excess peptide. A plasma membrane labeling of TAMRA-*At*Pep1 in the root epidermal cells was observed as fast as after 1 sec of incubation (Supplemental Figure 1). As *At*Pep1 binds two plasma membrane receptor, PEPR1 and PEPR2 with high affinity (KROL et al., 2010; TANG et al., 2015; YAMAGUCHI; PEARCE; RYAN, 2006), we tested the ability of TAMRA-*At*Pep1 to label the plasma membrane in root cells of the double homozygous mutant *pepr1pepr2* (KROL et al., 2010). In contrast to the wild type, incubation of *pepr1pepr2* mutant seedlings with TAMRA-*At*Pep1 (100 nM, 60 sec) did not result in a plasma membrane labeling as the wild type treated with the TAMRA fluorophore alone for the same time (Figure 1A). These results demonstrate that the TAMRA-

*At*Pep1 binding to the plasma membrane in the root meristem cells depends on the presence of the PEPR1 and PEPR2. The specificity of theTAMRA-*At*Pep1 binding to the plasma membrane was evaluated by a competition assay in which unlabeled *At*Pep1 was tested for its ability to compete with TAMRA-*At*Pep1. When seedlings were pretreated with a 10-fold excess of unlabeled *At*Pep1 for 5 min, TAMRA-*At*Pep1 was no longer found in the plasma membrane, but pretreatment with flg22, known to bind and activate the FLS2 receptor (BAUER et al., 2001; ZIPFEL et al., 2004) did not affect the TAMRA-*At*Pep1 labeling (Figure 1B and 1C).

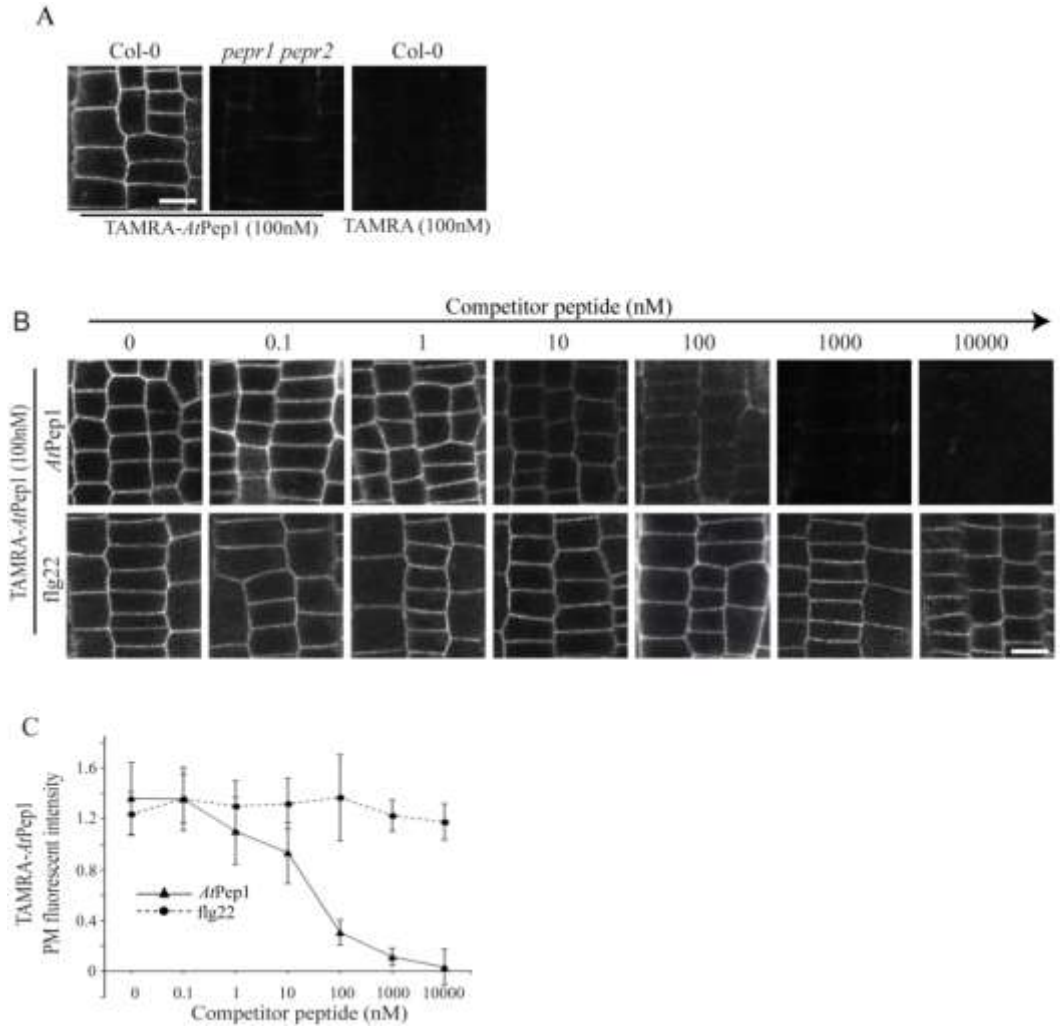

Figure 1 – TAMRA-*At*Pep1 labeled the plasma membrane in a receptor-dependent manner. (A) Root meristem epidermal cells of Col-0 and *pepr1pepr2* seedlings treated with TAMRA-*At*Pep1 (100 nM, 60 sec), and Col-0 seedlings treated with the TAMRA fluorophore alone (100 nM, 60 sec). (B) Seedlings were incubated with varying doses of *At*Pep1 or flg22 for 5 min, then treated with TAMRA-*At*Pep1 for 10sec, washed and imaged. (**C**) Quantification of the plasma membrane intensity in (B). Error bars indicate S.D. (n=48 cells). Scale bars, 1 µm

3.2.2 PEPR1 and PEPR2 are expressed in the *Arabidopsis* root meristem

As we used *Arabidopsis* root meristem epidermal cells as our *in vivo* imaging model system and the TAMRA-*At*Pep1 binding was receptor-dependent, we investigated whether the plasma membrane binding of the labeled *At*Pep1 correlates with the expression pattern of its receptors in the root meristem cells. TAMRA-*At*Pep1 was found to label the plasma membrane of the different cell types in the root depending on the incubation time with the fluorescent probe and 60 sec of incubation were sufficient to label all cells in the root meristem (Figure 2A). However, previous promoter-β-glucoronidase (GUS) reporter studies of the *PEPR1* and *PEPR2* genes have revealed that the two receptors are expressed in *Arabidopsis* leaves and in differentiated root cells, but not in the root tip (BARTELS et al., 2013; MA et al., 2014). In agreement, the *PEPR1* promoter fused to the nuclear localization signal (*NLS*)-green fluorescent protein (*GFP*) was expressed in the mature root tissues, but not in the root meristem, whereas the *PEPR2* promoter activity was mostly restricted to the vascular tissue in the whole root (Supplemental Figure 2A). Because the TAMRA-*At*Pep1 efficiently labeled the plasma membrane of root meristem cells, we wanted to clarify this discrepancy in localization pattern. To this end, the genomic sequences of *PEPR1* and *PEPR2* fused to GFP under their native promoters were expressed into the double *pepr1pepr2* mutant and, subsequently, their expression pattern and subcellular localization in the root meristem were evaluated. The two chimeric proteins, PEPR1-GFP and PEPR2-GFP were functional and complemented the double *pepr1pepr2* mutant as assessed by growth of the transgenic lines on medium containing 100 nM *At*Pep1 and estimation of root growth inhibition (Supplemental Figure 2B). In all transgenic plants, root growth was significantly inhibited as seen for the wild type and opposite to the *pepr1pepr2* mutant that was completely insensitive to the *At*Pep1 application (KROL et al., 2010; MA et al., 2014). Whereas the expression pattern of the PEPR2-GFP protein was similar to that of the *proPEPR2:NLS-GFP* fusion, the PEPR1-GFP signal was detected in root cells in the differentiation zone but also in the root meristem, in correlation with the TAMRA-*At*Pep1 localization (Figure 2B; Supplemental Figure 2C). Altogether, our results suggest that PEPR1 is the main receptor for *At*Pep1 in the root meristem.

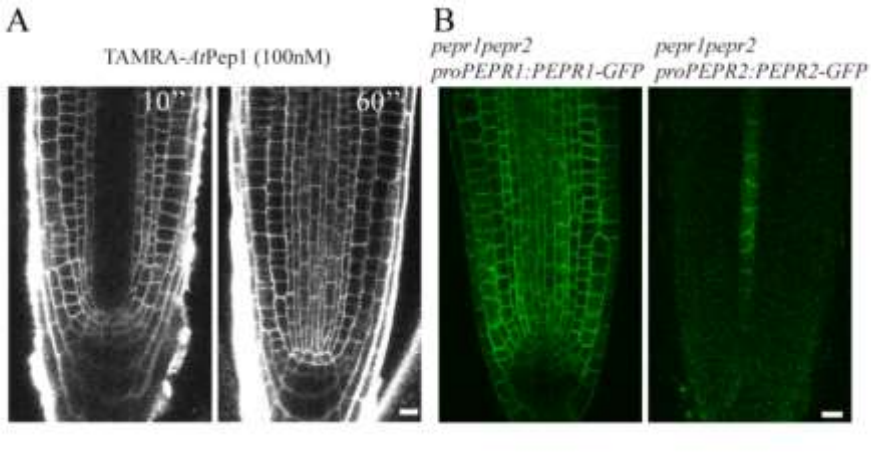

Figure 2 – Correlation of *PEPR1* expression with TAMRA-*At*Pep1 localization. (A) TAMRA-*At*Pep1 labeled the plasma membrane of all cellular layers in the root tip after 60 sec of incubation. (**B**) Root tip localization of PEPR1-GFP and PEPR2-GFP expressed under their endogenous promoters in the *pepr1pepr2* double mutant. Five-day-old seedlings were visualized. Scale bars, 10 µm

3.2.3 *At*Pep1 undergoes receptor-mediated endocytosis

To monitor the behavior of the bioactive fluorescently labeled *At*Pep1 over time when applied to live cells, *Arabidopsis* seedlings were pulsed with 100 nM of TAMRA-*At*Pep1 for 10 sec, washed three times with liquid medium to remove the excess peptide, and imaged at different time points (the time after the wash hereafter is referred as a chase) (Figure 3A). After a 10-min chase, most of the TAMRA fluorescence was associated with the plasma membrane. Some vesicle-like structures were visible inside the cell after a 20-min chase and became more evident after 40 min. Later (90 min), the fluorescent signal was concentrated into structures that resembled vacuoles. The TAMRA-*At*Pep1 internalization was temperature dependent, because seedlings treated with TAMRA-*At*Pep1 at 4^{o}C did not show fluorescence accumulation inside the cells, although labeling of the plasma membrane was observed (Supplemental Figure 3).

Next, we investigated whether the PEPR1 and PEPR2 also undergo internalization after stimulation with their ligand, *At*Pep1. Therefore, we used *pepr1pepr2* double mutant *Arabidopsis* plants complemented by the stable expression of *PEPR1-GFP* or *PEPR2-GFP* with the *RPS5A* promoter to allow robust expression of both receptors in the root meristem cells (WEIJERS et al., 2001) (Supplemental Figure 2B). As TAMRA-*At*Pep1 (100 nM) internalized clearly in vesicle-like compartments after a chase of 40 min (Figure 3A), the subcellular localization of PEPR1-GFP was evaluated in similar time points (after a chase of 5 and 40 min) following treatments with different *At*Pep1 concentrations (10-sec pulse, three washouts) (Supplemental Figure 4A). Although some vesicle-like structures labeled with PEPR1-GFP were detected even without *At*Pep1 treatment, their presence was induced by

*At*Pep1 in a time- and dose-dependent manner. Especially, the vesicles were more abundant after a chase of 40 min when the seedlings were treated with the nonlabeled peptide at a concentration of 100 nM.

To determine if the PEPR1 internalization followed a similar to TAMRA-*At*Pep1 dynamics, *pepr1pepr2/proRPS5A:PEPR1-GFP* seedlings were pulsed with *At*Pep1 (100 nM, 10 sec, three washouts) and imaged over time. Comparable to TAMRA-*At*Pep1, the PEPR1-GFP signal was first associated with the plasma membrane (10-min chase), later (20-min chase) vesicles-like structures began to appear and became more abundant after a 40-min chase. At later time points (90-min chase), PEPR1-GFP accumulated in the vacuole (Figure 3B). In contrast, PEPR1-GFP remained localized in the plasma membrane after treatment with flg22 (Figure 3B), suggesting that the PEPR1 internalization is specifically induced by its ligand. Differences in the temporal dynamics of PEPR1-GFP internalization were not detected when *At*Pep1 was applied as a continuous pulse (Supplemental Figure 4B).

Next, we studied the subcellular dynamics of *At*Pep1-PEPRs, ligand-receptor complexes in root meristem epidermal cells of *pepr1pepr2/proRPS5A:PEPR1-GFP* and *pepr1pepr2/proRPS5A:PEPR2-GFP* plants (Supplemental Figure 5). Seedling were pulsed with TAMRA-*At*Pep1 (100 nM, 10 sec) and imaged after washout. TAMRA-*At*Pep1 and PEPR1-GFP underwent endocytosis as a complex and followed the same temporal dynamics as previously shown individually for TAMRA-*At*Pep1 and PEPR1-GFP (Supplemental Figure 5A). High values of Pearson's correlation coefficient were obtained when TAMRA-*At*Pep1 colocalized with either PEPR1-GFP or PEPR2-GFP (Supplemental Figures 5A and 5B). Thus, our observations are consistent with the view that *At*Pep1 is internalized by receptor-mediated endocytosis.

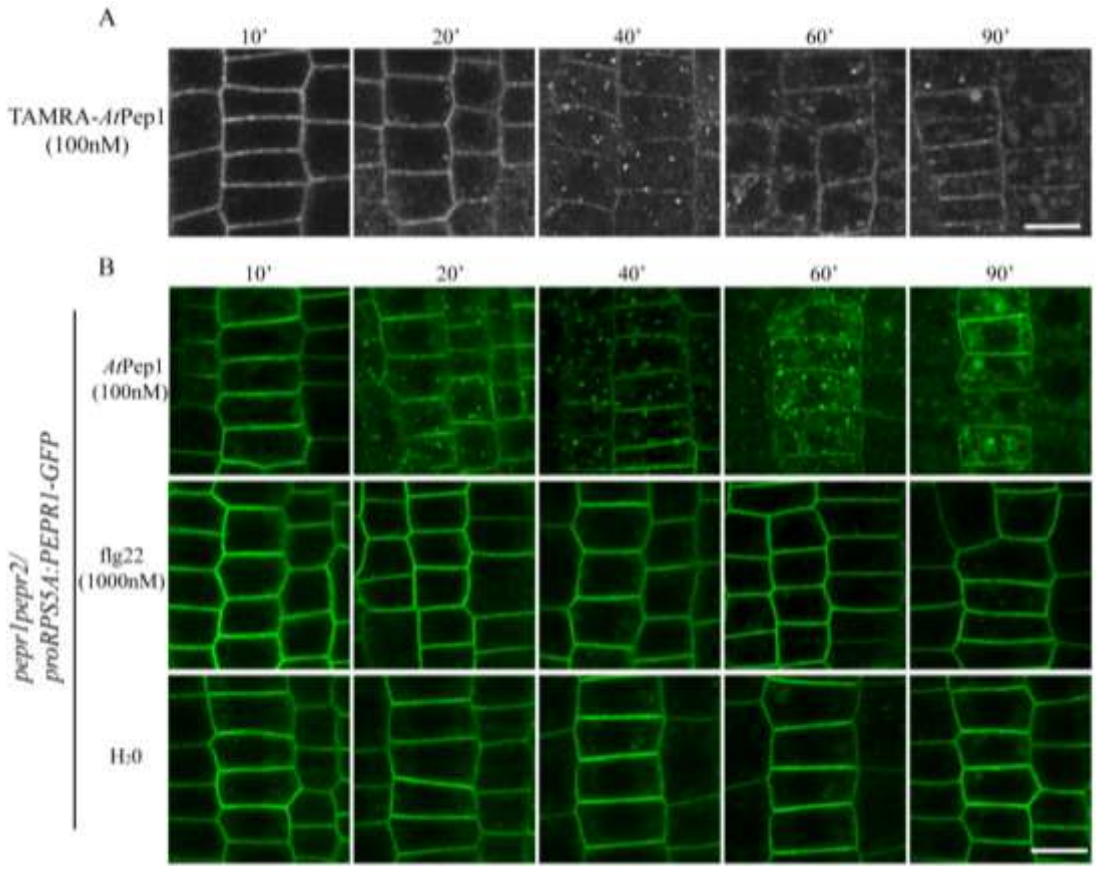

Figure 3 - Internalization of TAMRA-*At*Pep1 and PEPR1-GFP. (A) Internalization of TAMRA-*At*Pep1. Five-day-old seedlings were treated with TAMRA-*At*Pep1 (100 nM, 10 sec), washed with liquid medium and root tip epidermal cells were imaged after the indicated time points. (**B**) Internalization of PEPR1-GFP after treatment with *At*Pep1. Application of flg22 and mock (water) did not change the PEPR1-GFP localization. Five-day-old *pepr1pepr2* seedlings complemented with PEPR1-GFP expressed under the *RPS5A* promoter were treated with the respective elicitors for 10 sec and washed. Root tip epidermal cells were imaged after the indicated time. Scale bars, 10 µm

3.2.4 *At*Pep1-PEPR complexes traffic to the vacuole via TGN/EE and MVB compartments

Until now, live-cell microscopy studies of PEPRs have not been carried out. To better understand the endocytic route of PEPRs in the context of their ligand, we incubated various fluorescence-tagged endomembrane makers with TAMRA-*At*Pep1 (100 nM, 10-sec pulse, three washouts) and assessed their colocalization after a 40-min chase by counting manually the amount of colabeled vesicles that were considered positive when the colocalization value calculated by the Pearson's correlation coefficient was higher than 0.5. TAMRA-*At*Pep1 colabeled partially with compartments that were marked by known TGN/EE markers, 18% with VHA-a1-GFP (DETTMER et al., 2006) (Figure 4A), 28% with SYP61-CFP (ROBERT et al., 2008), and 37% with GFP-SYP42-GFP (UEMURA et al., 2012) (Supplemental Figures

6A and 6B). Further, TAMRA-*At*Pep1 colabeled the MVBs marked by the *Arabidopsis* Rab5 GTPase homologs YFP-ARA7 (GELDNER et al., 2009) (84%) (Figure 4B) and ARA6-GFP (GOH et al., 2007) (76%), and by the R-SNARE GFP-VAMP727 (EBINE et al., 2008) (65%). (Supplemental Figures 6B and 6C). As expected, the receptor-ligand complexes only partially overlapped with the Golgi compartments (5%) marked by the SNARE YFP-MEMB12 (GELDNER et al., 2009) (Figure 4C). TAMRA-*At*Pep1 finally accumulated in the vacuole delimited by GFP-VAMP727 that, besides the MVBs also marked the tonoplast (EBINE et al., 2008) (Figure 4D). Thus, our live-cell imaging analyses show that TAMRA-*At*Pep1 and, presumably, its bound receptors follow an endocytic trafficking route from the plasma membrane to the vacuole, passing through the TGN/EEs and MVBs.

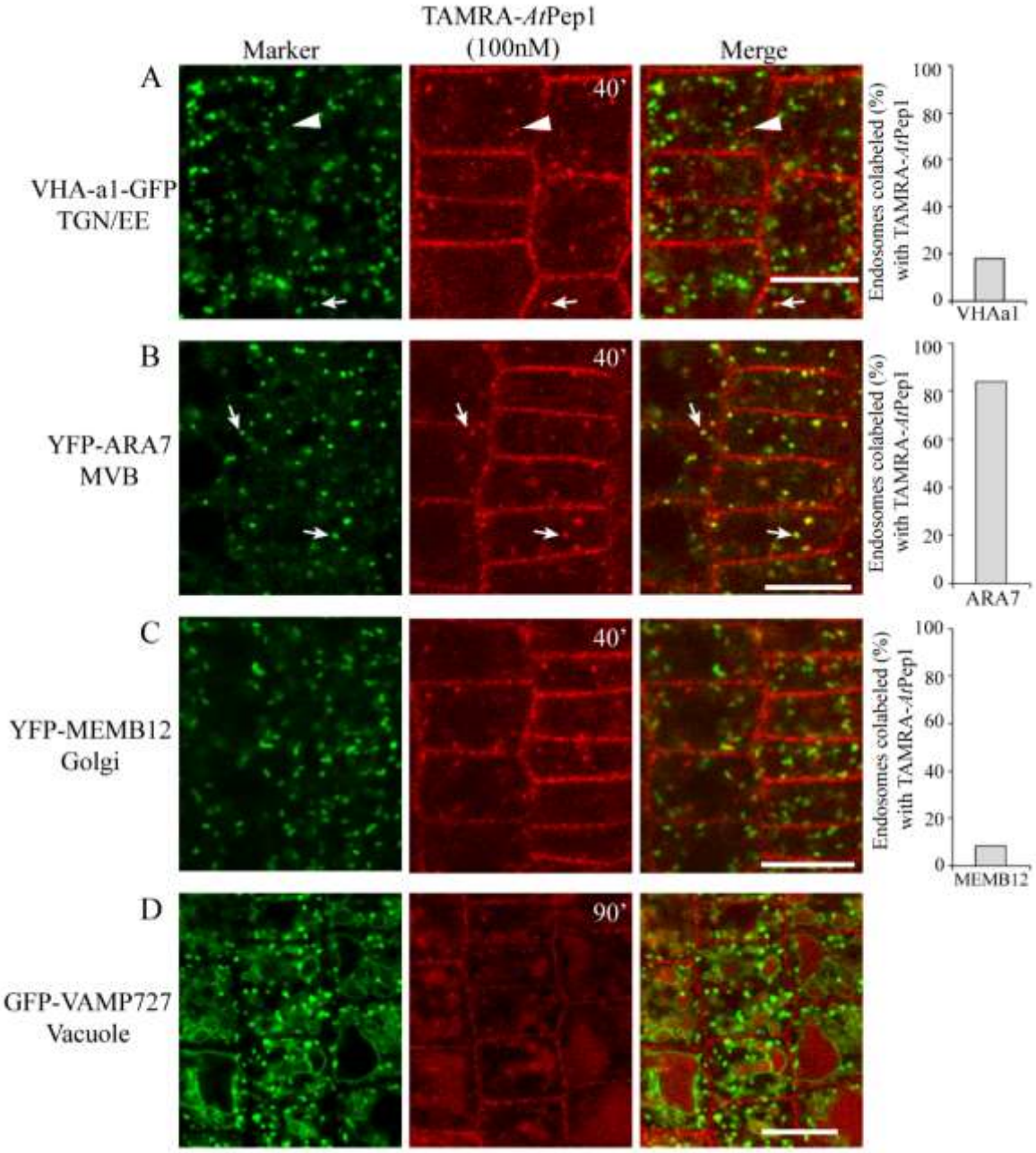

Figure 4 – Endocytic route of TAMRA-*At*Pep1 in *Arabidopsis* root epidermal meristem cells. (A)TAMRA-*At*Pep1-labeled vesicles colocalized partially with the TGN/EE marker VHA-a1-GFP. Arrows and arrowheads marked colocalized and not colocalized vesicles. Graph indicates the percentage of TAMRA-*At*Pep1-positive vesicles labeled by VHA-a1-GFP. n=318. (B) Majority of TAMRA-*At*Pep1-vesicles labeled the MVB marker YFP-ARA7 (arrows). Graph indicates the percentage of TAMRA-*At*Pep1-positive vesicles labeled by YFP-ARA7. n=345. (C) TAMRA-*At*Pep1-vesicles did not colocalize with the Golgi compartments marked by YFP-MEMB12. Graph indicates the percentage of TAMRA-*At*Pep1-positive vesicles labeled by YFP-MEMB12. n=312. (D) TAMRA-*At*Pep1 fluorescence accumulated into the vacuoles, delimited by the tonoplast marker GFP-VAMP727, after a chase of 90 min. Five-day-old seedlings were treated with TAMRA-*At*Pep1 (100 nM, 10 sec), washed with liquid medium and root tip epidermal cells were imaged after 40-min chase (A, B and C) or 90 min (D). Only the TAMRA-*At*Pep1-positive vesicles presenting a colocalization value over 0.5 calculated by the Person's correlation coefficient were considered as colocalized. n=TAMRA-*At*Pep1-positive vesicles. Scale bars, 10 µm

3.2.5 *At*Pep1-PEPRs trafficking is largely independent of the V-ATPase activity at the TGN/EE

Our previous studies revealed that when internalized the brassinosteroid receptor, BRI1-ligand pair colabeled more than 80% of the TGN/EE compartments marked by the VHA-a1-RFP (IRANI et al., 2012), a number significantly higher than that observed in the case of TAMRA-*At*Pep1 (Figure 4A). Thus, we investigated whether the trafficking route of the *At*Pep1-PEPR complexes required the function of the vacuolar H^+-ATPase (V-ATPase) in the TGN/EE. To this end, we took advantage of a specific TGN/EE inhibitor acting on the V-ATPase, namely ConcanamycinA (ConcA) (DETTMER et al., 2006). Initially, we examined the subcellular dynamics and localization of TAMRA-*At*Pep1 (100 nM, 10-sec pulse, three washouts, 40, 60, and 90-min chase) when applied to transgenic lines that expressed the TGN/EE fluorescent marker, VHA-a1-GFP in the presence of ConcA (Figure 5A). Surprisingly, after a chase of 40 min the fluorescent probe did not accumulate in typical ConcA bodies, as seen for the VHA-a1-GFP, although some colocalization between the TAMRA-*At*Pep1-positive vesicles and VHA-a1-GFP-positive ConcA bodies was observed. The same phenotype was found when TAMRA-*At*Pep1 was internalized in seedlings expressing -SYP61-CFP and GFP-SYP42 in the presence of ConcA (Supplemental Figure 7). Furthermore, TAMRA-*At*Pep1 internalization was not blocked in the presence of ConcA, although the trafficking might be delayed because after a 60-min chase a high amount of vesicles were still visualized in the presence of ConcA, in contrast to the control in which a reduced amount of vesicles was observed and the fluorescence started to accumulate into the vacuole (Figure 5A). After a 90-min chase, the TAMRA-*At*Pep1 signal was clearly concentrated into vacuoles in the DMSO control, but in the presence of ConcA, a small population of TAMRA-*At*Pep1-positive vesicles was still visible, in addition to the signal into vacuoles. Similar effects in the subcellular dynamics of this fluorescent probe were observed in the *deetiolated3* (*det3*) mutant that is defective in the V-ATPase activity (Figure 5B) (SCHUMACHER et al., 1999).

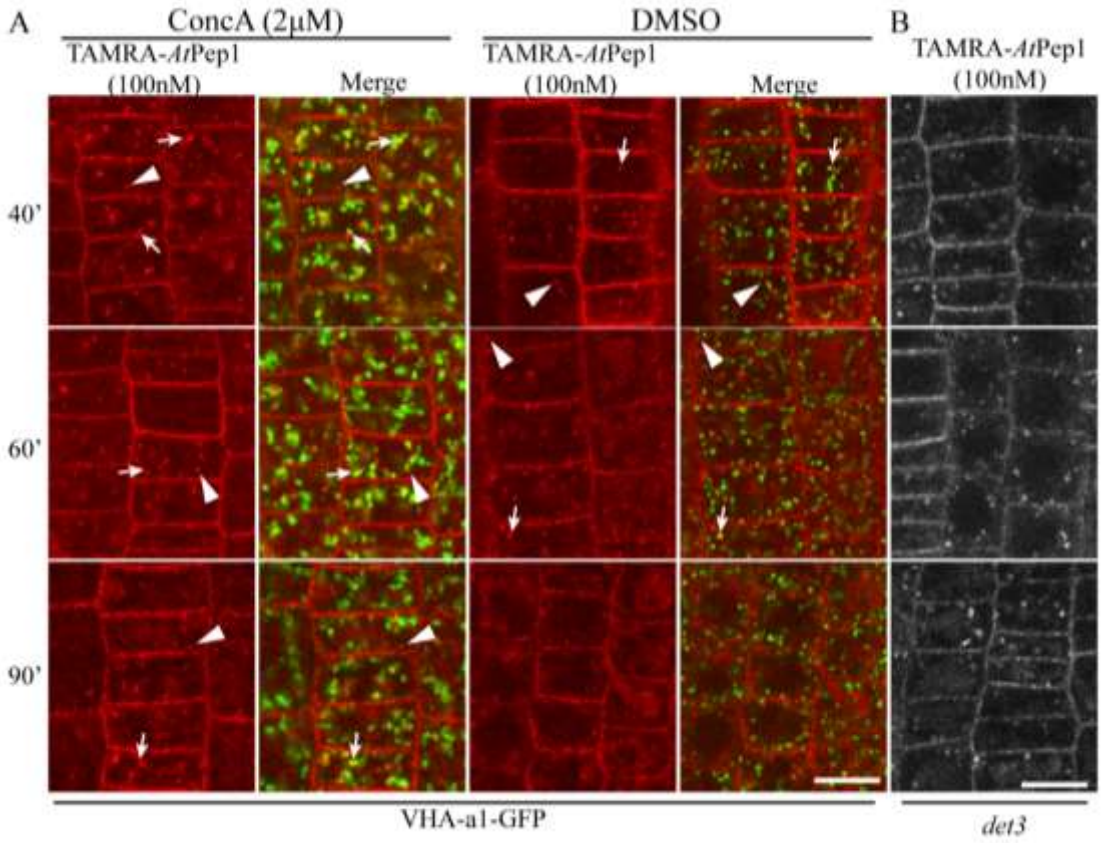

Figure 5 – Impaired activity of the vacuolar H^+-ATPase did not block the trafficking of TAMRA-*At*Pep1 to the vacuole. (A) TAMRA-*At*Pep1 subcellular localization in *Arabidopsis* root epidermal meristem cells of transgenic seedlings expressing the TGN/EE marker VHA-a1-GFP in the presence of ConcanamycinA (ConcA) and DMSO (mock control) over time. Five-day-old seedlings were pretreated with ConcA (2 μM, 30 min), subsequently treated with TAMRA-*At*Pep1 (100 nM, 10-sec pulse, three washouts), in the presence of ConcA (2 μM) for 40, 60, and 90 min before imaging. Arrows and arrowheads marked colocalized and not colocalized vesicles of TAMRA-*At*Pep1 with VHA-a1-GFP ConcA bodies, respectively. (**B**) Internalization of TAMRA-*At*Pep1 (100 nM, 10-sec pulse, three washouts) in five-day-old *deetiolated3 (det3)* mutant seedlings and imaged after 40, 60 and 90-min chase. Scale bars, 10 μm

Our findings were further supported by monitoring the subcellular dynamics of PEPR1-GFP in the presence of ConcA and in combination with the endosomal tracer FM4-64, that previously was shown to accumulate into the TGN/EE-positive ConcA bodies but whose trafficking to the tonoplast was blocked by the V-ATPase inhibitor (DETTMER et al., 2006). For this experiment we pretreated five-day-old *pepr1pepr2/proRPS5A:PEPR1-GFP* seedlings with ConcA (30 min, 2 μM), then pulsed or not with *At*Pep1 (100 nM, 10 sec, three

washouts), in the presence of FM4-64 (4 µM, 5 min, 3 washouts) and kept all the time in the presence of ConcA (2 µM) until imaging for the indicated time. Seedlings stained with FM4-64 pretreated and treated with DMSO were used as control (Figure 6A-C). Without *At*Pep1 elicitation, the localization of PEPR1-GFP was not significantly affected in the presence of ConcA, although at later points some GFP-positive compartments were seen in either the proximity of or colocalizing with the FM4-64-positive ConcA bodies (Figure 6B). After pretreatment with ConcA and *At*Pep1 application in the presence of the inhibitor, a considerable portion of PEPR1-GFP vesicles clearly colocalized with FM4-64 into the ConcA bodies, still better visualized after 40- and 60-min chases (Figure 6C). However, as seen for TAMRA-*At*Pep1 (Figure 5), the trafficking of PEPR1-GFP to the vacuoles was not blocked. Though, more control experiments are required to evaluate if the trafficking of PEPR1-GFP in the presence of ConcA is delayed. However, this might be the case as in the absence of ConcA, after a 60-min *At*Pep1 elicitation, most of the PEPR1-GFP fluorescence accumulated into the vacuoles (Figure 3B), whereas in the presence of ConcA this pattern was observed after 90 min (Figure 6C). Based on these results, we can conclude that the trafficking of the *At*Pep1-PEPR complexes to the vacuole was not largely compromised by the impaired V-ATPase activity in the TGN/EE.

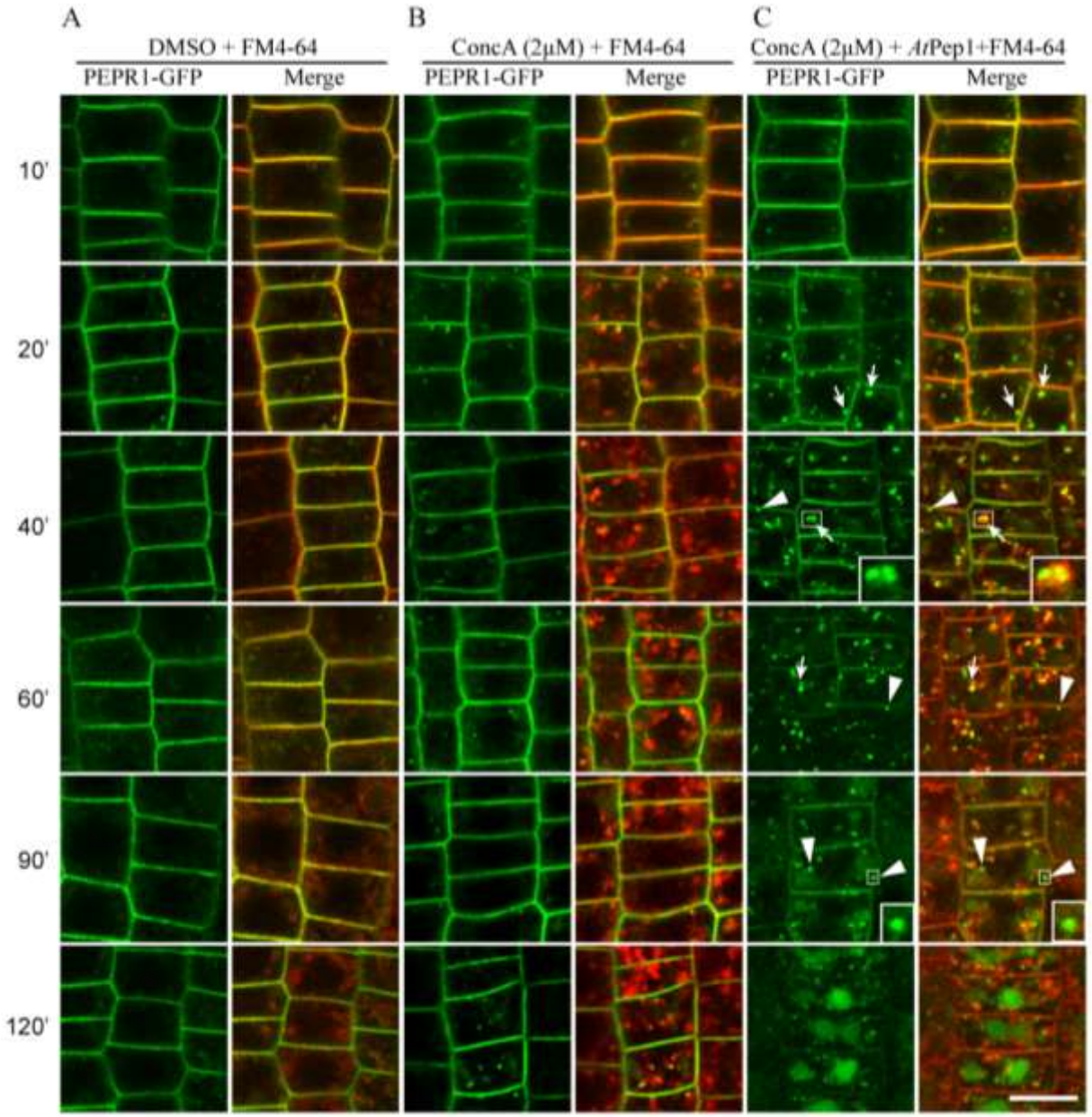

Figure 6 – The endocytosis of *At*Pep1-PEPR1 complexes was not blocked by the TGN/EE inhibitor ConcanamycinA (ConcA). Subcellular localization of PEPR1-GFP in *Arabidopsis* root epidermal meristem cells in the presence of mock control (DMSO) (**A**), ConcA (2 µM) (**B**), ConcA (2 µM) and *At*Pep1 (100 nM for 10 sec) (**C**) over time. Five-day-old *pepr1pepr2* seedlings complemented with *PEPR1-GFP* expressed under the *RPS5A* promoter were pretreated with ConcA (30 min, 2 µM), then exposed or not to *At*Pep1, stained with FM4-64 (4 µM, 5 min, three washouts) and kept all the time in the presence of ConcA (2 µM) until imaging for the indicated time. Arrows and arrowheads indicate PEPR1-GFP colocalized and not colocalized vesicles with FM4-64 ConcA bodies, respectively. Insets, 3× magnification showing details of the PEPR1-GFP vesicles. Scale bar, 10 µm

3.2.6 Inactive PEPR is not recycled and its secretion but not its endocytosis is ARF-GEF-dependent

Previously, most of the plant plasma membrane proteins, including receptors, have been shown to constitutively cycle between plasma membrane and endosomal compartments, which is a mechanism to modulate their abundance and activity (BECK et al., 2012; GELDNER et al., 2001; GELDNER et al., 2007). Therefore, we investigated whether PEPR1 also undergoes recycling. For this purpose, we applied the fungal inhibitor brefeldin A (BFA) that is commonly used to block recycling in plants (ROBINSON; JIANG; SCHUMACHER, 2008). Upon treatment with BFA (50 µM, 60 min), PEPR1-GFP fluorescence accumulated clearly in BFA bodies as revealed by co-staining with FM4-64 (4 µM, 5 min, three washouts) (Figures 7A and 7B), which is sensitive to BFA treatment (BOLTE et al., 2004). To clarify the origin of these BFA bodies (PEPR1-GFP secretion or recycling), 50 µM of the protein synthesis inhibitor cycloheximide (CHX) (PESTOVA; HELLEN, 2003) was added 60 min before and during BFA treatment (Figure 7C). In this case no BFA bodies were detected, suggesting that most PEPR1 fluorescence signals visualized into BFA bodies without CHX belonged to newly synthetized, but not recycled, PEPR1 proteins.

Next, the PEPR1-GFP fluorescence was visualized after 40- and 60-min chases of *At*Pep1 elicitation (100 nM, 10 sec, three washouts) in the presence of BFA (50 µM) (Figure 7D). After a 40-min chase, the PEPR1-GFP fluorescence accumulated into BFA bodies (probably derived from secretion), together with a population of vesicles similar to that shown previously without BFA (Figure 3B). Interestingly, most of these vesicles were arranged around the BFA bodies and some of them seemed to colocalize with the BFA bodies (Figure 7D inset). After a 60-min chase, the PEPR1-GFP fluorescent signal was also visualized in the vacuole, indicating that the ligand-induced internalization of PEPR1 was not blocked. To confirm this observation, we evaluated the internalization of TAMRA-*At*Pep1 (100 nM, 10-sec pulse, three washouts) in the presence of BFA (50 µM) (Figures 7E). The treatment was carried out on transgenic plants expressing the endosomal marker VHA-a1-GFP that had been previously detected in the core of BFA bodies (DETTMER et al., 2006; ROBINSON; JIANG; SCHUMACHER, 2008). As expected, the localization pattern for TAMRA-*At*Pep1 in the presence of BFA was similar to that seen for PEPR1-GFP, with vesicles surrounding the BFA bodies and some of them apparently localized into the BFA bodies after a 40-min chase, and vacuolar accumulation of TAMRA-*At*Pep1 fluorescence after a 60-min chase (Figure 7E). These observations suggest that the endocytic trafficking of *At*Pep1-PEPR complexes is not compromised in the presence of BFA.

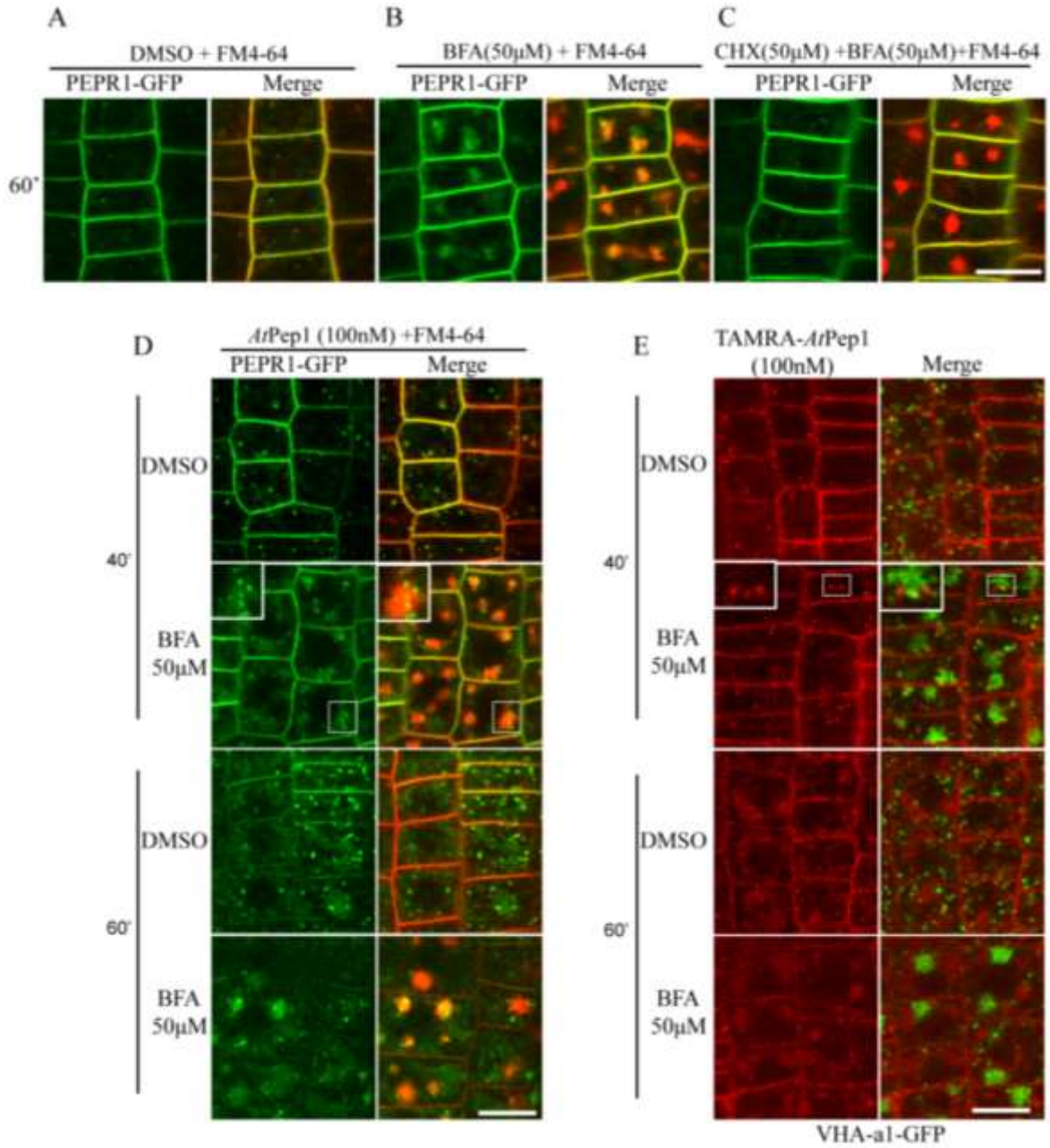

Figure 7 – Inactive PEPR is not recycled and its secretion but not its endocytosis is ARF-GEF-dependent. (**A**-**C**) Subcellular localization of PEPR1-GFP in the presence of mock control (DMSO) (**A**), BFA (50 μM) (**B**), and CHX+BFA (50 μM) (**C**). Plants were pretreated with CHX (50 μM) for 1 h (**C**). (**D**) Subcellular localization of PEPR1-GFP after 40 and 60 min of *At*Pep1 elicitation (10-sec pulse) in the presence or not of BFA (50 μM). For these experiments (**A** –**D)** five-day-old *pepr1pepr2* seedlings complemented with *PEPR1-GFP* expressed under the *RPS5A* promoter were used, and stained with FM4-64 (4 μM, 5 min, and three washouts). (**E**) Subcellular localization of TAMRA-*At*Pep1 in the presence or not of BFA. Seedlings expressing VHA-a1-GFP were treated with TAMRA-*At*Pep1 for 10 sec, washed, kept in the presence or absence of BFA (50 μM), and imaged after 40 and 60 min. Insets show details of BFA bodies at 2.5× magnification. Scale bars, 10 μm

3.2.7 *At*Pep1-PEPR1 complexes undergo clathrin-mediated endocytosis

CME is the major known route for internalization of plant plasma membrane-localized receptors in plants (CHEN; IRANI; FRIML, 2011; DI RUBBO et al., 2013; GADEYNE et

al., 2014). To gain further insight into the internalization mechanism of *At*Pep1-PEPR complexes, we used genetic and chemical approaches to study the role of CME during this process. First, we characterized the internalization of TAMRA-*At*Pep1 in the single *CHC2* knockout mutants (*chc2-1* and *chc2-2*) that are defective in FM4-64 endocytosis (KITAKURA et al., 2011), and in the double mutant of the CLC genes, *CLC2* and *CLC3* (*clc2-1/clc3-1*) (WANG et al., 2013). In both *chc2* mutant alleles, the intracellular accumulation of TAMRA-*At*Pep1 (100nM, 10-sec pulse, 2-3 min of washout, 40-min chase) was reduced when compared with the wild type, implying that the endocytosis was impaired. In contrast, defects in the TAMRA-*At*Pep1 uptake were not detected in the double *clc2-1/clc3-1* mutant (Figures 8A and 8B). To corroborate these observations, we took advantage of the β-estradiol-inducible line, named XVE:AX2, expressing the clathrin-interacting protein AUXILIN2 (AUX2), of which the overexpression has been reported to block CME in plants (ADAMOWSKI, M., FRIML, J. UNPUBLISHED).

When seedlings were incubated for 24 h on solid medium supplemented with 5 µM β-estradiol, the TAMRA-*At*Pep1 internalization (100 nM, 10-sec pulse, three- washout, 40-min chase) as well as the FM4-64 uptake (4 µM, 5 min, three washouts, 30-min chase) were totally blocked at the plasma membrane (Figure 8C). β-estradiol induction of auxilin expression was confirmed phenotypically by the plant growth arrest (Supplemental Figure 8). Finally, we used the ES9-17 compound that has been proposed as a tool to dissect CME in plants because of its specific CHC-binding ability (DEJONGHE, 2015). When *Arabidopsis* seedlings were exposed to ES9-17 (10 µM) in the presence of TAMRA-*At*Pep1, the TAMRA-*At*Pep1 internalization was inhibited (Figure 8D). Altogether these findings indicate that *At*Pep1-PEPR complexes are internalized via CME.

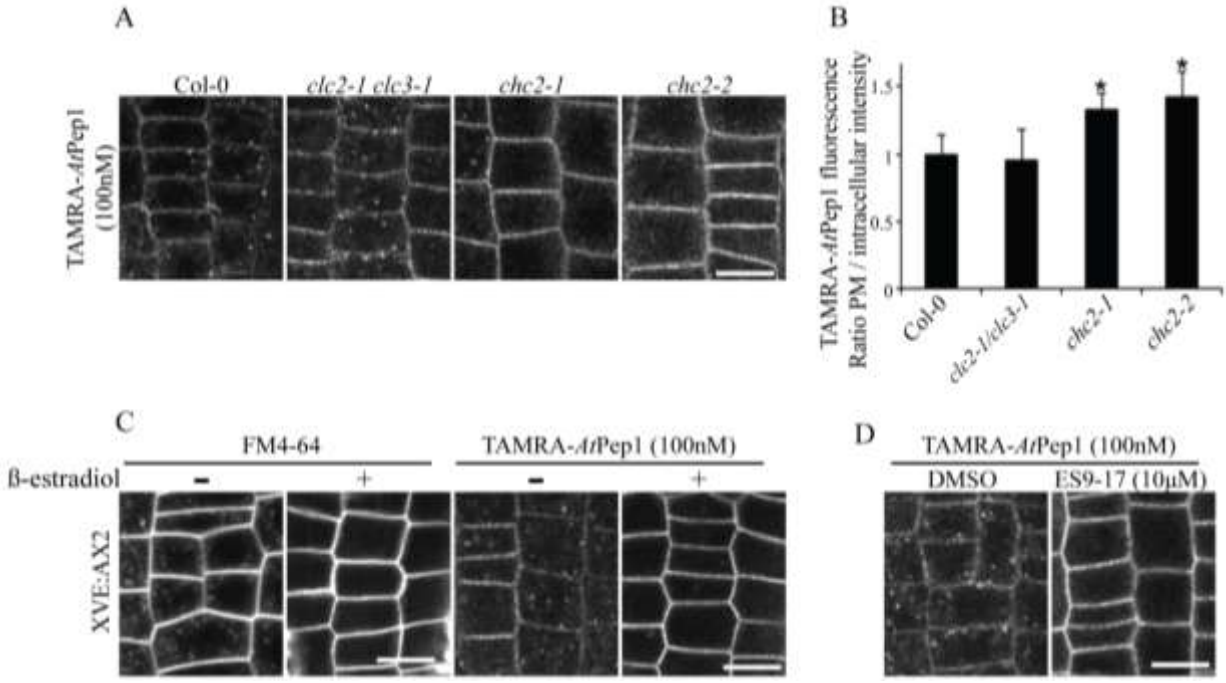

clc2-1clc3-1, chc2-1 and *chc2-2* mutants were treated with TAMRA-*At*Pep1 for 10 sec, washed, imaged after 40-min chase. (**B**) Graph illustrating the ratio between the plasma membrane signal intensity divided by the intracellular signal intensity of images in (**A**) (n=45 – 51cells). Error bars indicate S. D. *P* values (Student's *t* test): * < 0.01 relative to Col-0. (**C**) The internalization of FM4-64 (left) (4µM, 5 min, three washouts, 30-min chase) and TAMRA-*At*Pep1 (right) (100 nM, 10-sec pulse, three washouts, 40-min chase) was blocked after induction of *AUXILIN2* expression in 5-day-old XVE:AX2 seedlings with 5 µM β-estradiol for 24 h. (**D**) The internalization of TAMRA-*At*Pep1 was blocked in the presence of the ES9-17 compound. Five-day-old Col-0 seedlings were pretreated for 20 min with the ES9-17 and kept in its presence after TAMRA-*At*Pep1 treatment (100 nM, 10-sec pulse, three washouts, 40-min chase). For all experiments root epidermal meristem cells were imaged. Scale bars, 10 µm

3.2.8 *At*Pep1 signaling responses are compromised when CME is impaired

We next address the question if impairment of CME will affect *At*Pep1-responses by monitoring over time the phosphorylation of the MAP kinases MPK6 and MPK3 (RANF et al., 2011). When XVE:AX2 seedlings incubated for 24 h on solid medium supplemented with 5 µM β-estradiol to block endocytosis by inducing AUX2 were treated with *At*Pep1 (20 nM), at all assessed time points activation of MPK3 and MPK6 was strongly reduced (Figure 9A). To clarify that this negative effect in MAPK activation is caused by the induction of AUX2 and not by β-estradiol, we evaluated the *At*Pep1-induced MAPK phosphorylation in Col-0 seedlings incubated for 24 h on solid medium supplemented with 5 µM β-estradiol, but not differences with the control treatment were detected (Supplemental Figure 9).

In addition, we evaluated the root growth inhibition of the *chc2-1* and *chc2-2* mutants in the presence of 50 nM and 100 nM of *At*Pep1. Both alleles displayed a significant root growth inhibition, but they were less sensitive than Col-0 in the presence of 50 nM of *At*Pep1 (Figure 9B). These results suggest that CME is required to trigger *At*Pep1 responses.

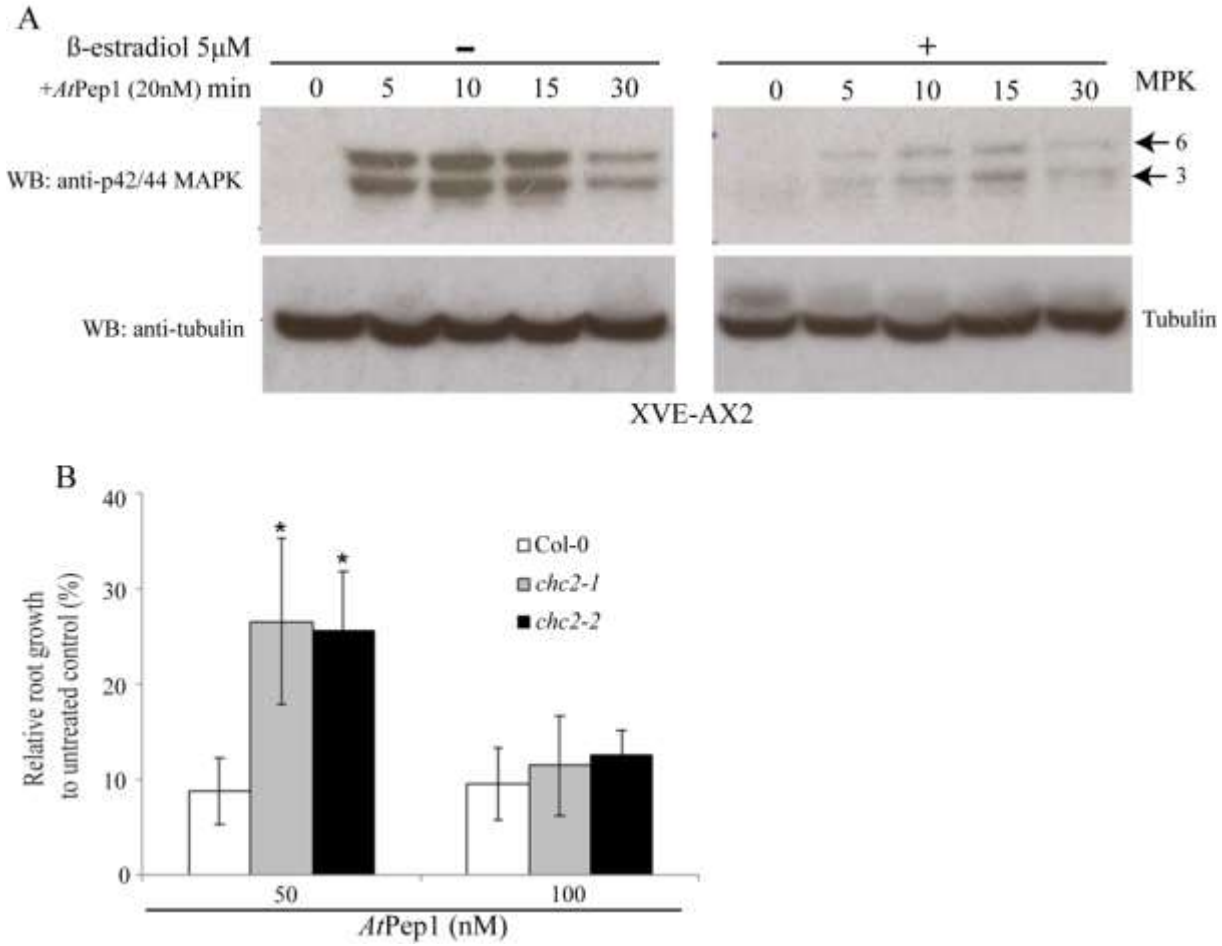

Figure 9 – *At*Pep1 responses were compromised by impaired CME. (A) Reduced *At*Pep1-induced (20 nM) MAPK activation after induction of *AUXILIN2* expression in the XVE:AX2 genotype with 5 µM β-estradiol for 24 h. MAPK phosphorylation was detected by immunoblotting with anti-phospho-p44/p42-MPK antibody detecting the pTE-pY motif of MPK6 and MPK3. The immunoblot was reprobed with anti-tubulin to show protein loading. Individual MPKs were identified by molecular mass and indicated by arrows. (**B**) Root growth inhibition of Col-0, *chc2-1* and *chc2-2* in the presence of 50 nM and 100 nM *At*Pep1 (n=12 plants). Root growth is presented relative to untreated control. Error bars indicate standard deviation. *P* values (Student's *t* test): ** < 0.01 relative to Col-0. These experiments were repeated at least twice with similar results

3.3 Discussion

3.3.1 *At*Pep1, PEPR1 and PEPR2are coexpressed and colocalized in the *Arabidopsis* root meristem and are internalized together

Because of the absence of cell mobility and the presence of rigid cell walls, well-coordinated cell-to-cell communication networks play an essential role in plant responses to the environment that need to happen quickly to adapt soon to the new surroundings. The crucial relevance of signaling peptides into these communication networks is becoming more evident, but the knowledge about their subcellular dynamics and their relationship with the signaling responses is poorly characterized, mainly due to the lack of cell biology tools that allow plant signaling peptides to be studied *in vivo*. A well-characterized signaling peptide is *At*Pep1 that is associated with plant immune responses (HUFFAKER; PEARCE; RYAN, 2006; YAMAGUCHI; HUFFAKER, 2011). In our work, we used a bioactive fluorescently labeled *At*Pep1, TAMRA-*At*Pep1, to address the issue exposed above.

Kinetics study of TAMRA-*At*Pep1 showed that the fluorescently labeled probe was able to label very quickly to the plasma membrane of root meristem cells in a receptor-dependent manner. Our findings are in agreement with previous work that revealed with biochemistry methods that receptor-ligands complexes are formed within seconds (CHINCHILLA et al., 2007; SCHULZE et al., 2010; YAMAGUCHI; PEARCE; RYAN, 2006), but our data provided the visualization of the ligand binding in living cells.

Previously, the *At*Pep1 receptors have been found not expressed in the root tips (BARTELS et al., 2013), but our cell biology system showed that TAMRA-*At*Pep1 labeled the plasma membrane of the cells in this tissue in a receptor-dependent manner. Therefore, we reinvestigated the expression patterns of both receptors in *Arabidopsis* roots by means of transgenic lines expressing the genomic fragments of PEPR1 and PEPR2 fused to GFP under their endogenous promoters. Interestingly, the expression patterns differed from the one reported for the transcriptional fusion of the PEPR1 receptor (BARTELS et al., 2013). The PEPR1-GFP protein was detected in most root meristem cells, supporting the observed TAMRA-*At*Pep1 localization. The differences in expression between the PEPR1 transcriptional and translational GFP fusions can be explained by either the presence of intronic transcriptional regulatory sequences or by less likely protein movement. Indeed, several studies have shown that the transcriptional enhancer can also be located in the 3’ of the transcription initiation site, in exons, introns, or even on the transcribed RNA itself (JEONG et al., 2006; KOOIKER et al., 2005; OGBOURNE; ANTALIS, 1998).

After plasma membrane labeling, the TAMRA-*At*Pep1 was internalized in a temperature-dependent manner. The same spatiotemporal dynamics were found for PEPR1-GFP when treated with *At*Pep1, but not with flg22, hinting at this process specificity. In addition, TAMRA-*At*Pep1 and PEPR-GFP fusions were internalized as complexes from the plasma membrane to the vacuole, similarly as described previously for the BRI1 receptor and the fluorescent BR analog AFCS (IRANI et al., 2012).

In plants, the receptor-mediated endocytosis has been shown to be involved in different physiological processes, including development and plant immunity, mainly by the study of the BR receptor BRI1 (IRANI et al., 2012) and flg22 receptor FLS2 (BECK et al., 2012; ROBATZEK; CHINCHILLA; BOLLER, 2006). Because PEPRs, BRI1, FLS2 as well as most of the receptors of other signaling peptides described so far are structurally similar (ENDO; BETSUYAKU; FUKUDA, 2014), internalization of the ligand-receptor pairs can be a common mechanism executed by plant cells in order to remove them from the plasma membrane.

We found that *At*Pep1-PEPR complexes transited in early and late endosomal compartments and finally accumulated into the vacuole, a common fate for ligands and receptors once internalized, where they are degraded, thus allowing desensitization of the signal (BENYA et al., 1994; IRANI et al., 2012; MURPHY et al., 2005). Therefore, the vacuolar targeting of *At*Pep1-PEPR complexes can be interpreted as a mechanism to desensitize cells of the *At*Pep1 stimulus, but a signal relay inside the cells cannot be discarded. Interestingly, the temporal dynamics of the *At*Pep1-PEPR complexes differed from those of BRI1 and its ligand that internalized more quickly (2 min after ligand application) (IRANI et al., 2012), but were more similar to those of the FLS2 receptor, in which endosomes were visualized in leaves 30 min after flg22 application (BECK et al., 2012). Hence, the endocytosis pathways are coordinated in different ways in plant cells, probably related to the signaling responses.

3.3.2 The importance of the TGN/EE for *At*Pep1-PEPR complexes trafficking

Taking advantage of TAMRA-*At*Pep1 in combination with transgenic plants expressing different fluorescent endosomal markers, we mapped the endocytic route of *At*Pep1-PEPR complexes. As TGN/EE is the first compartment in which most of the early endocytosed cargos are localized (DETTMER et al., 2006; VIOTTI et al., 2010), we expected a higher colabeling of this compartment with TAMRA-*At*Pe1, as previously observed for the AFCS-BRI1 complex (IRANI et al., 2012). Surprisingly, TAMRA-*At*Pe1 showed a low

colocalization with different TGN/EE markers with the lowest colocalization values observed for VHA-a1 and somewhat higher values for SYP61 and SYP42, in contrast to the ARA7 and ARA6 late endosomal markers for which high colocalization values were obtained. These results can be explained by two scenarios, first, most of the *At*Pep1-PEPR complexes are internalized directly to MVBs without passing through the TGN/EE and, second, the *At*Pep1-PEPR complexes are transported via a VHA-a1-negative part of the TGN/EE that rapidly matures into ARA7/ARA6-positive compartments. Previously, based on visualizations of the activated FLS2 endocytosis in *Nicotiana benthamiana*, it has been reported that the flg22-activated FLS2 traffics via only the ARA7- and ARA6-positive endosomes (BECK et al., 2012). In addition, the existence of a transient compartment with intermediate properties between TGN/EE and late endosomes has been proposed to mediate the FLS2 internalization. The hybrid identity of these compartments was defined by the colocalization between ARA7 with the TGN/EE marker SYP61, but not with the TGN/EE marker VHA-a1 (CHOI et al., 2013). FLS2 and PEPRs are receptors related to plant defense and share signaling mechanisms, therefore they probably present similar trafficking routes, in which ligand-pair complexes are associated with transient TGN/EE populations or subdomains excluded from VHA-a1, but marked with SYP42/SYP61. This specific SYP42/SYP61-positve TGN/EE population or subdomains could later precede the ARA7-dependent TGN/EE maturation into MVBs. This assumption is in agreement with recent studies showing that ARA7 is also found at the TGN/EE and that the endosomal maturation in *Arabidopsis* appears to originate in a TGN/EE subdomain that recruits ARA7 (SCHEURING et al., 2011; SINGH et al., 2014; STIERHOF; EL KASMI, 2010). Regardless, further studies are needed to assess the possible TGN/EE partitioning during the *At*Pep1-PEPR internalization. It would be essential to evaluate the subcellular dynamics of different TGN/EE markers in combination with ARA7 after elicitation with *At*Pep1.

The differential regulatory role of the TGN/EE during the *At*Pep1-PEPR internalization is also supported by our experiments with the V-ATPase inhibitors ConcA and genetically with the *det3* mutant. ConcA inhibits the V-ATPase activity that causes loss of the TGN/EE identity, impairs the MVB maturation, and blocks vacuolar transport (DETTMER et al., 2006; SCHEURING et al., 2011; VIOTTI et al., 2010). Intriguingly, the transport of TAMRA-*At*Pep1 and PEPR1-GFP complexes to the vacuole was not blocked by ConcA, although some colocalization between TAMRA-*At*Pep1 and VHA-a1-positive ConcA bodies occurred. These observations imply that the *At*Pep1-PEPR complexes are trafficking either through compartments accumulated into the ConcA bodies or in their close proximity, but,

nonetheless, the physiological effect of this drug does not block their trafficking to the vacuole, same effect was previously reported for the boron transporter BOR1 at high boron concentration (TAKANO et al., 2005). Recently, the plant TGN/EE has been shown to be acidic (pH 6.0) and to be probably a V-ATPase-dependent process, because pharmacological interference of the V-ATPase activity with ConcA caused drastic alkalinization and disturbed its behavior (HUSS et al., 2002; MARTINIERE et al., 2013; SHEN et al., 2013). Thus, is tempting to assume that the pH of the TGN/EE can modulate its function, as seen in animal and yeast cells along endocytic and secretory pathways (HUANG; CHANG, 2011; KANE, 2006). Following this line or reasoning it is possible to argue that there is a pH-dependent cargo sorting mechanism that operates at the plasma membrane. If this were correct, it will explain why vacuolar transport of some endocytic cargos, such as AFCS and FM4-64, is completely blocked in the presence of ConcA (DETTMER et al., 2006; IRANI et al., 2012), whereas the trafficking of *At*Pep1-PEPR complexes to the vacuole is only slightly delayed. Other important remarks that fit into our assumption is that *At*Pep1 induces extracellular medium and possibly apoplast alkalinization, and that the interaction with its receptors depends on pH (HUFFAKER; PEARCE; RYAN, 2006; TANG et al., 2015), hence it could be that the *At*Pep1-PEPR complexes are transported through endosomal compartments with an alkaline pH, thus ensuring that peptides and receptors reach the end of their intracellular journey. Considering the fast emergence of new tools that allow measurements of pH *in vivo*, an interesting project would be to investigate the effects of different cargos in the pH of subcellular compartments and their relationships with plant trafficking and signaling.

3.3.3 Recycling does not regulate the pool of inactive PEPRs at the plasma membrane

The fungal toxin BFA induced the accumulation of the PEPR1-GFP signal into BFA bodies, but these bodies were not detected in seedlings in which the protein synthesis was inhibited, implying that most signals detected into BFA bodies derived from secreted instead of recycled proteins. It remains to be tested, however, if inhibition of the protein synthesis affects endocytosis of PEPR1. Although we cannot exclude the possibility of a BFA-insensitive recycling pathway or very slow recycling, our results suggest that abundance and activity of the *At*Pep1 receptors are not mainly regulated by recycling as for BRI1, FLS2, BOR1, and PIN proteins (BECK et al., 2012; GELDNER et al., 2007; TAKANO et al., 2005; TANAKA et al., 2013). Absence or low recycling rates of PEPRs could be due to their function. PEPR receptors are proposed to function as innate immunity amplifiers and their

expression to be induced by *At*Peps, indicating a positive feedback loop in the *At*Pep-PEPR signaling (YAMAGUCHI; HUFFAKER, 2011; YAMAGUCHI et al., 2010). In this context, PEPRs are internalized just upon *At*Pep perception and replaced later by newly synthetized PEPR proteins. This hypothesis is supported by the presence of the PEPR1-GFP intracellular vesicles without exogenous *At*Pep1 that was still visualized in the presence of BFA and CHX; these vesicles can represent PEPR1-GFP internalization triggered by endogenous peptides that are maintained at a low rate under normal conditions as a form to regulate the *At*Pep1 receptor pool, in agreement with the ubiquitous *At*Peps and PEPRs expression at low basal levels (BARTELS et al., 2013; HUFFAKER; PEARCE; RYAN, 2006). Confirming that the major effect of BFA is related to secretion and recycling, we did not found any appreciable effect during the *At*Pep1-PEPR1 trafficking, the same was reported for the activated FLS2 receptor and the fluorescent BR analog AFCS (BECK et al., 2012; IRANI et al., 2012).

3.3.4 *At*Pep1-PEPR endocytosis is mediated by clathrin and CME impairment compromises the *At*Pep1 responses

Although direct evidence of CME in plant signaling peptides has been not reported so far, we provided some solid proof that the *At*Pep1-PEPR endocytosis is mediated by clathrin proteins. First, we found a delayed internalization of TAMRA-*At*Pep1 in *chc2-1* and *chc2-2*, as reported for FM4-64 (KITAKURA et al., 2011); curiously, no internalization defects of this molecular probe were detected in the double mutant *clc2-1/clc3-1*, hinting at a minor role of these proteins and/or at a partial redundancy with CLC1 that shares 55% amino acid identity with CLC2 and CLC3 (WANG et al., 2013). Additionally, the TAMRA-*At*Pep1 endocytosis was totally impeded when the clathrin-interacting and CME-blocking protein AUXILIN2 was overproduced (ADAMOWSKI, M., FRIML, J. UNPUBLISHED), and in the presence of the ES9-17 compound that targets CHC proteins inhibiting CME (DEJONGHE, 2015). Collectively, our results showed that internalization of *At*Pep1/PEPRs complexes is clathrin-mediated, highlighting CME as the dominant route for endocytosis in plants.

It is well known that after association between *At*Pep1 and its receptors at the plasma membrane, swift and transient plant immunity signals are transmitted (KROL et al., 2010; YAMAGUCHI; HUFFAKER, 2011; YAMAGUCHI et al., 2010). Therefore, we examined the role of the endocytosis during *At*Pep1 responses. The *chc2-1* and *chc2-2* mutants were less sensitive to *At*Pep1 in the root growth assay when 50 nM of the peptide was used, but at higher concentrations, this effect was not observed, probably because, albeit delayed, the TAMRA-*At*Pe1 endocytosis still operated; hence, high concentrations of *At*Pep1 might mask

the effect in the signaling. Phosphorylation of MPKs was strongly reduced when endocytosis was blocked by the induced overexpression of the clathrin-interacting protein auxilin, although low activation levels were still detected, indicating that MPK signaling can be initiated from the plasma membrane, but for full activation, a functional CME is needed. Although the defects in the *At*Pep1 responses could not be attributed to a specific inhibition of the *At*Pep1-PEPR endocytosis, because the CME is affected in a general manner, these defects could also reflect impairment of the endosomal signaling that would not operate when endocytosis is blocked. Endosomal signaling has been amply documented for animals (MURPHY et al., 2009; RAJAGOPALAN, 2010), but its role in plants is still not well understood. Our biological system provides a suitable model to further clarify the interplay between plant trafficking and signaling.

Author contribution

Ortiz-Morea F. A., Moura D. S., and Russinova E. conceived the study and designed the experiments. Ortiz-Morea F. A. performed all experiments involving imaging, root growth assays and generated the transgenic material. Yu L. did the MAPK assays. Dejonghe W. characterized the ES9-17 compound. Adamowski M. and Friml J. generated the XVE:AX2 line. Ortiz-Morea F. A. and Russinova E. wrote the manuscript.

Acknowledgements

We thank Daniël Van Damme and Evellien Mille (VIB-Ghent University, Belgium) for advice in microscopy and Martine De Cock (VIB-Ghent University, Belgium) for help in preparing the manuscript. Ortiz-Morea F. A. is indebted to the BOF Special Research founding of the Flemish Government for a Joint Doctorate fellowship at Ghent University and to the PEC-PG program of the Coordenação de Aperfeiçoamento de Pessoal de Nível Superior CAPES Brazil for the Doctorate fellowship at Universidade of São Paulo.

3.4 Material and Methods

3.4.1 Plant material and growth conditions

All mutants and transgenic lines used in this study were in the background of the *Arabidopsis thaliana* accession Columbia (Col-0). Seeds were sterilized, maintained for 2 days at 4°C in the dark, and germinated on vertical half-strength Murashige and Skoog (½MS) medium (1% [w/v] sucrose) agar plates, pH 5.8 at 22°C in a 16-h/8-h light–dark cycle for 5 days with a light intensity of 120 $\mu E \cdot m^{-2} \cdot s^{-1}$ (E, Einstein; 1E = 1mol of photons). The following mutant and transgenic *Arabidopsis* lines have been described previously:

pepr1/pepr2 (KROL et al., 2010), *chc2-1* and *chc-2* (KITAKURA et al., 2011), *clc2-1/clc3-1* (WANG et al., 2013), *det3* (SCHUMACHER et al., 1999), GFP-VAMP727 (EBINE et al., 2008), VHA-a1-GFP (DETTMER et al., 2006), SYP61-CFP (ROBERT et al., 2008), GFP-SYP42 (UEMURA et al., 2012), YFP-ARA7 and YFP-MEMB12 (GELDNER et al., 2009), ARA6-GFP (GOH et al., 2007), For induction of β-estradiol-inducible line, XVE:AX2, seedlings were germinated as described before, transferred 4 days after germination for 24 h to ½MS plates containing 5 µM β-estradiol (Sigma-Aldrich) and then used for the respective assays; ethanol instead of β-estradiol was used as control.

3.4.2 Generation of constructs

The PEPR1 and PEPR22 putative promoters and coding sequences were amplified by PCR with KaPaHIFI polymerase (Sopachem) from genomic DNA (accession Col-0) with specific primers (Table 1). The obtained fragments were introduced into pDONR entry vectors (pDONRP4-P1R promoter sequences and pDONR221 coding sequences) by means of the Gateway system-compatible attB sites (Invitrogen).

To create transcriptional reporter vectors of PEPR1 and PEPR2, the entry clones pDONRP4-P1R-proPEPR1/2 were introduced into the destination vector pMK7S*NFm14GW (KARIMI et al., 2007) with the Gateway-based cloning (Invitrogen) to yield pMK7S*NFm14GW-proPEPR1/2:NLS-GFP.

The entry vectors pDONRP4-P1R-proPEPR1/2 and pDONR221-PEPR1/2 were used in a triple LR reaction (MultiSite-Gateway, Invitrogen), combining pDONRP2-P3R-GFP and pB7m34GW (KARIMI; DE MEYER; HILSON, 2005) to yield pB7m34GW-proPEPR1/2:PEPR1/2-GFP that expressed the *At*Pep1 receptors fused in-frame to GFP. To make constructs expressing the *At*Pep1 receptors under the promoter RPS5A, during the triple LR reaction the entry vector pDONRP4-P1R-proPEPR1/2 was replaced by pDONRP4-P1R-proRPS5A (GADEYNE et al., 2014), producing the pB7m34GW-proRPs5A:PEPR1/2-GFP vectors.

3.4.3 Generation of *Arabidopsis* transgenic lines

Plants were transformed with *Agrobacterium tumefaciens* by means of the floral dip method (Clough & Bent, 1998). Plants expressing NLS-GFP under the endogenous promoters of PEPR1 and PEPR2 were transformed into Col-0 background. Primary transformants were selected on ½MS medium containing kanamycin (50 mg/l). The proRPS5A:PEPR1/2-GFP construct was dipped into the *pepr1/pepr2* mutant background and transformants were selected on ½MS medium containing 10 mg/l phosphinothricin.

3.4.4 Peptides

The peptide *At*Pep1 (ATKVKAKQRGKEKVSSGRPGQHN) with a HPLC purity of 95.16% and molecular weight of 2491.78, and the peptide *At*Pep1 labeled with 5'-carboxytetramethylrhodamine at the N-terminal (TAMRA-*At*Pep1) with a HPLC purity of 97.07% and molecular weight of 2905.75 were purchased from Life Technologies. The peptide flg22 (QRLSTGSRINSAKDDAAGLQIA) with a HPLC purity of 95% and a molecular weight of 2272.50 was acquired from Genscript (catalog No. RP19986).The peptides were dissolved in water to obtain peptide stocks of 100 µM. Further dilutions were done with ½MS medium.

3.4.5 Imaging

Arabidopsis seedlings were imaged on a FluoView 1000 inverted confocal microscope (Olympus) equipped with a water-corrected 60× objective (NA1.2) at digital zoom 3; for the evaluation of the TAMRA-*At*Pep1 plasma membrane-binding pattern at the different cell layers of the root meristem and of the root expression pattern of the *At*Pep1 receptors, a digital zoom 1 was used. The excitation wavelength was 488 nm for GFP and YFP, 458 nm for CFP and 559 for TAMRA and FM4-64. Emission was detected between 500 – 530 nm for GFP and YFP, 460 – 500 for CFP and 570 – 670 for TAMRA and FM4-64. For TAMRA-*At*Pep1, the intensity was manipulated with the Olympus software.

3.4.6 TAMRA-*At*Pep1 application and competition assays

For the plasma membrane binding assay, 5-day-old seedlings were dipped into 500 µL of 100 nM TAMRA-*At*Pep1 dissolved in ½MS medium, pulsed for different times as indicated, washed with ½MS liquid medium three times, and transferred to coverslips for visualization of the meristem epidermal cells under the confocal microscope. For the competition assay, seedlings were pretreated with 0, 0.1, 1, 10, 100, 1000, and 10000 nM of *At*Pep1 or flg22 for 5 min and washed with ½MS medium three times before being dipped into TAMRA-*At*Pep1 for 10 sec. For quantification, images were converted to 8-bit images and fixed regions of interest were selected to measure the fluorescent intensity of the plasma membrane and background into the intracellular space with imageJ, then the relative plasma membrane fluorescence was calculated by dividing the plasma membrane intensity by the background intensity. Six epidermal cells from eight plants were quantified.

3.4.7 TAMRA-*At*Pep1 internalization assay

Five-day-old seedlings were dipped into 500 µL of 100 nM TAMRA-*At*Pep1 dissolved in ½MS medium for 10 sec, washed with ½MS liquid medium three times, kept in 500 µL of ½MS medium over a piece of parafilm placed in a Petri plate, and then imaged for the indicated time points. To compare the TAMRA-*At*Pep1 uptake between the clathrin mutants and the Col-0 wild type, images were quantified with imageJ. To this end, images were first converted to 8-bit images; subsequently, the entire plasma membrane and intracellular space were selected with the brush tool size 5 pixels and the polygon selection tool, respectively; then, the average intensity of the top 100 highest pixels for both plasma membrane and intracellular space was used to obtain a ratio between plasma membrane and intracellular fluorescence. Six epidermal cells from eight plants were quantified.

3.4.8 Colocalization analysis

For the colocalization analysis of confocal images acquired by confocal laser microscopy, imageJ was used with the plugin PSC colocalization (FRENCH et al., 2008) that allowed to obtain the Pearson correlation coefficient as colocalization readout, as well as a pixel distribution diagram, called scatter plot, in which the pixels in the green image are used as the Y-coordinate of the scatter plot and the intensity of the corresponding pixels in the red image as the X-coordinate. For colocalization between TAMRA-*At*Pep1 and PEPR1-GFP and PEPR2-GFP, the regions of interest were selected and colocalization analysis was carried out with a threshold of 10. To the determine the percentage of vesicles of TAMRA-AtPep1 colocalized with VHAa1-GFP, GFP-SYP42, SYP61-CFP, ARA7-YFP, ARA6-GFP, VAMP727-GFP and MEMB12-YFP, each individual TAMRA-*At*Pep1 spot was selected as individual region of interest and colocalization was analyzed with a threshold of 10, considering as positively labeled endosomes the spots of which the Person correlation value was over 0.5. A threshold of 10 was used in order to avoid noise and it was calculated measuring the background gray value present at the analyzed images.

3.4.9 Chemical treatments

The inhibitors BFA (50 mM DMSO stock), ConcA (2 mM DMSO stock) and CHX (50 mM DMSO stock) were purchased from Sigma-Aldrich. FM4-64 was acquired from Molecular Probes (2 mM water stock). Compound ES9-17 was provided by Dejonghe. (2015)) (10 mM DMSO stock). All chemicals were diluted in ½MS medium to prepare final concentration solutions.

Five-day-old seedlings were incubated for the indicated times into 1 mL of liquid ½MS medium containing 10 µM ES9-17, 2 µM ConcA, 50 µM BFA, 50 µM CHX or in combination between BFA and CHX. For seedlings expressing the PEPR1-GFP inhibitor, treatments were performed in combination with the endosomal marker FM4-64 at room temperature. For FM4-64 staining, seedlings were incubated for 5 min in 1 mL of ½MS liquid medium containing 4 µM of the dye plus the respective inhibitor treatment. Control treatments were done with equal amounts of DMSO. All washed steps and imaging were carried out in the presence of the respective inhibitors.

3.4.10 MAP kinase assay

Six-day-old seedlings were treated with 2 mL of 20 nM *At*Pep1 dissolved in ½MS medium for 0, 5, 10, 15, and 30 min. Per each time point, 50-60 seedlings were ground to a fine powder in liquid nitrogen and solubilized in better lacus buffer (SCHWESSINGER et al., 2011): 50 mM Tris-HCl, pH 7.5; 100 mM NaCl; 15 mM EGTA; 10 mM $MgCl_2$; 1 mM NaF; 1 mM $Na_2MoO_4.2H_2O$; 0.5 mM $NaVO_3$; 30 mM b-glycerophosphate; 0.1% IGEPAL CA 630; 100 nM calyculin A (CST); 0.5 mM PMSF; and 1% protease inhibitor cocktail (Sigma-Aldrich, P9599)]. The extracts were vortexed, kept on ice for 15 min, vortexed for 1 min, centrifuged at 12,700 rpm (4°C, 25 min), and then supplemented with 5×SDS loading buffer. An aliquot of the supernatant was brought over to a new tube before addition of the SDS loading buffer, to be used for protein quantification the through Bradford assay (Bio-Rad). Total protein (20 mg) was separated by SDS-PAGE with 10% precast polyacrylamide gels (Bio-Rad) and blotted onto PVDF membranes (Bio-Rad). Immunoblots were blocked with bovine serum albumin (BSA) 5% (w/v) (Sigma-Aldrich) in 1× Tris-buffered saline Tween 0.1% (TBS-T) for 2 h. Subsequently, the protein was washed 3× with TBS-T and incubated overnight at 4°C with anti-p42/44 MAPK primary antibodies (1:2000; Cell Signaling Technology) diluted in 1× TBS-T supplemented with 5% BSA. After three washing steps with TBS-T, the membrane was incubated for 2 h with anti-rabbit-HRP (horseradish peroxidase) conjugated secondary antibody (1:20,000 GE-Healthcare). Membranes were developed with the Western Lightning® Plus–ECL [enhanced chemiluminescence substrate (Perkin-Helmer) and Amersham Hyperfilm ECL (GE-Healthcare). Finally, the immunoblot was reprobed with the anti-tubulin antibody (1:50000 sigma) to determine equal loading.

3.4.11 Root growth assay

Seeds were sown on ½MS solid medium, stratified for 2 days at 4°C in the dark, and place in the light vertically. Four days after germination, seedlings were transferred to square

transparent Petri dishes with solid ½MS medium supplemented with or without the indicated amount of *At*Pep1 and incubated for 4 further days; then, the plates were scanned and the root growth measured. For measurements, scanned images were processed and evaluated with Rootreader2D software (http://www.plantmineralnutrition.net/rr2d.php) and plotted relative to untreated control.

3.4.12 Statistical analysis

P values were calculated with a two-tailed Student's *t*-test using the Excel software.

Supplemental Information

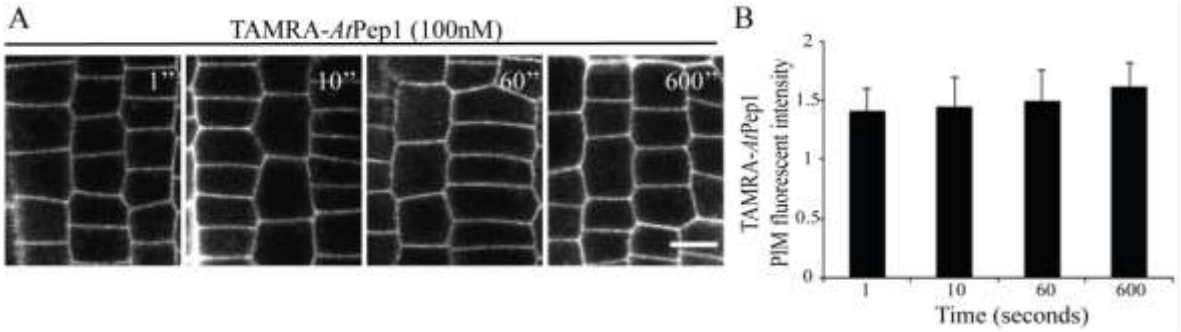

Supplemental Figure 1 – Kinetics of TAMRA-*At*Pep1 plasma membrane labeling in *Arabidopsis* root epidermal meristem cells. (A) TAMRA-*At*Pep1 labeled the plasma membrane within seconds after application. Seedlings were treated with TAMRA-*At*Pep1 (100 nM) for different time points, washed, and visualized under a confocal microscope. (**B**) Quantification of the plasma membrane fluorescence in (A) (n= 48 cells). Error bars indicate S.D

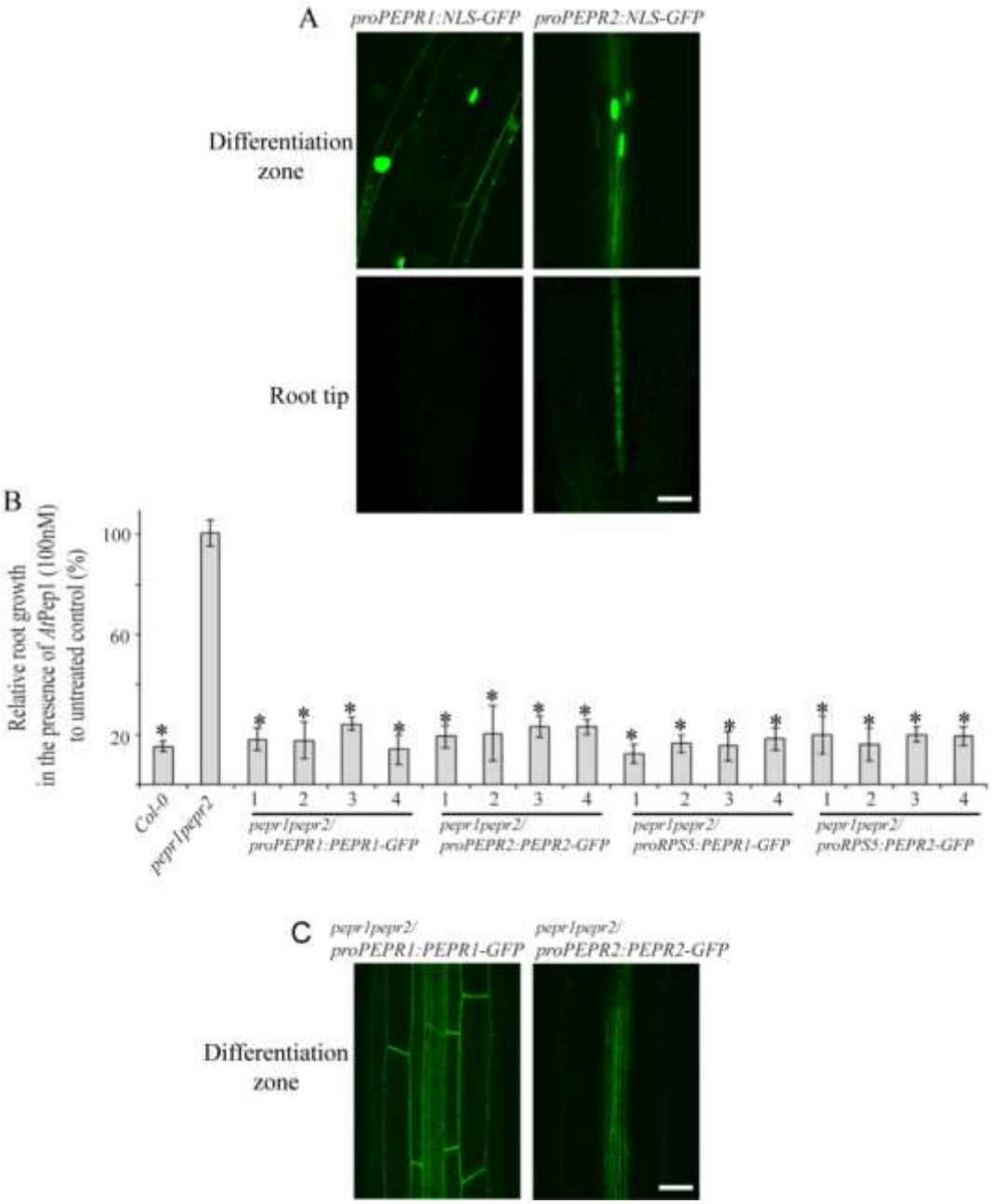

Supplemental Figure 2 – Expression pattern of the receptors PEPR1 and PEPR2 and subcellular localization of *At*Pep1 in the *Arabidopsis* root. (**A**) Expression pattern of *proPEPR1*::*NLS-GFP* and *proPEPR2*::*NLS-GFP* in the differentiation zone (top) and meristem (bottom) of the *Arabidopsis* root of five-day-old seedlings. (**B**) Mutant complementation. *PEPR1* and *PEPR2* fused to GFP and expressed under their endogenous promoters or under *RPS5A* promoter complemented the *pepr1pepr2* double mutant. Root growth inhibition analysis of *Arabidopsis* Col-0, *pepr1pepr2, pepr1pepr2/proPEPR1:PEPR1-GFP*, p*epr1pepr2/proPEPR2:PEPR2-GFP*, *pepr1pepr2/proRPs5A:PEPR1-GFP*, *pepr1pepr2/proRPS5A:PEPR2-GFP* seedlings (n=10). Seedlings were germinated on ½ MS medium and then transferred for 4 days to ½ MS medium supplemented with *At*Pep1 (100 nM). Root growth is presented relative to untreated control. Error bars indicate S.D. *P* values (Student's *t* test): * < 0.001 relative to untreated control. Four independent transgenic lines were analyzed for each construct. (**C**) Localization of *PEPR1-GFP* and *PEPR2-GFP* expressed under their endogenous promoter in the *pepr1pepr2* mutant in the differentiation zone of the roots of root of five day old seedlings. Scale bars, 30 µm

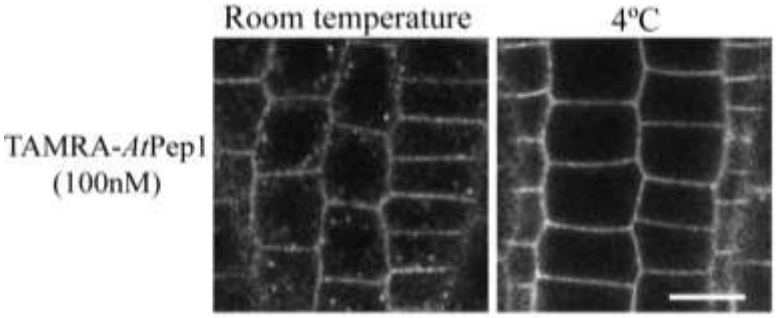

Supplemental Figure 3 – The internalization of TAMRA-AtPep1 is temperature dependent. Five-day-old *Arabidopsis* Col-0 seedlings were incubated at 4°C for 2 h before treatment with TAMRA-*At*Pep1 (100 nM, 10 min) washed and left for another 40 min at 4°C before imaging. The same TAMRA-*At*Pep1treatment was carried out for seedlings at room temperature. Scale bar, 10 µM

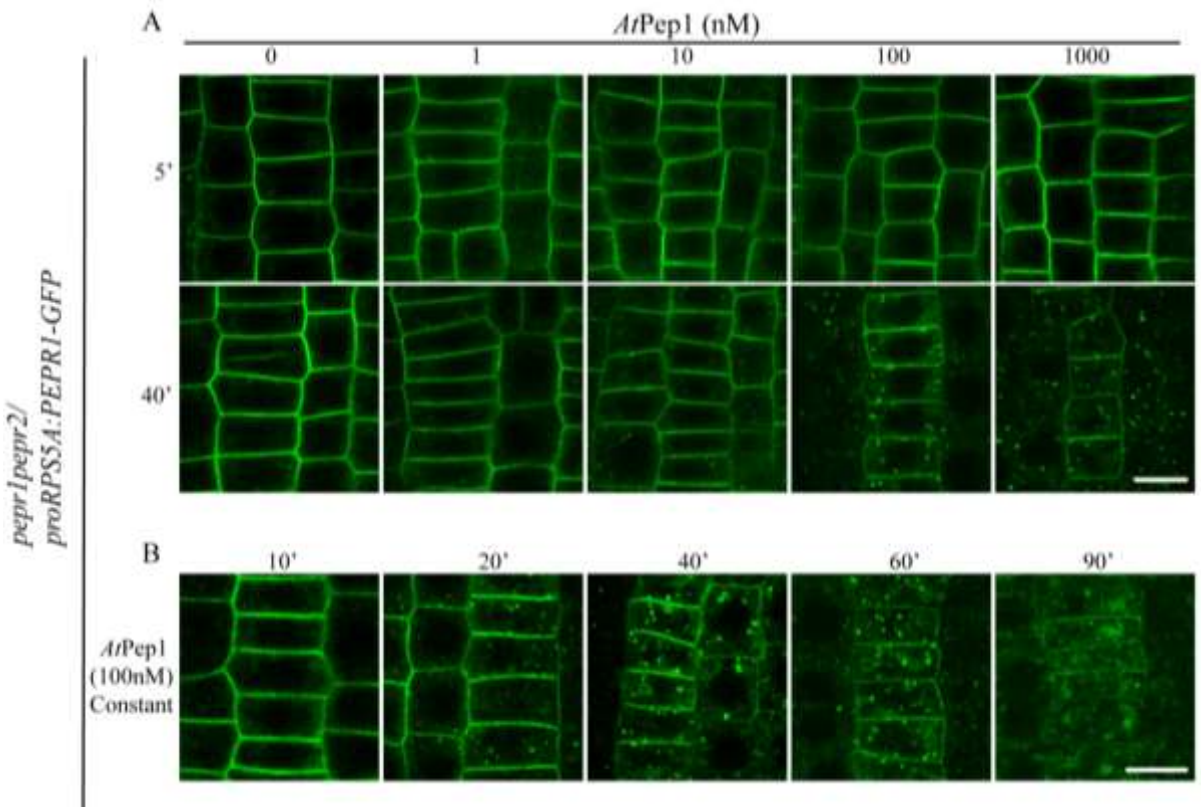

Supplemental Figure 4 – PEPR1-GFP internalization upon *At*Pep1 elicitation. (A) PEPR1-GFP internalization was triggered by *At*Pep1 in a dose-response manner. Seedlings were treated with different concentrations of *At*Pep1 for 10 sec, washed with liquid medium, and imaged after a chase of 5 and 40 min. (**B**) PEPR1-GFP internalization upon constant elicitation with *At*Pep1. For these experiments, five-day-old *pepr1pepr2* seedlings complemented with PEPR1-GFP expressed under the *RPS5A* promoter were used . Scale bars, 10 µm

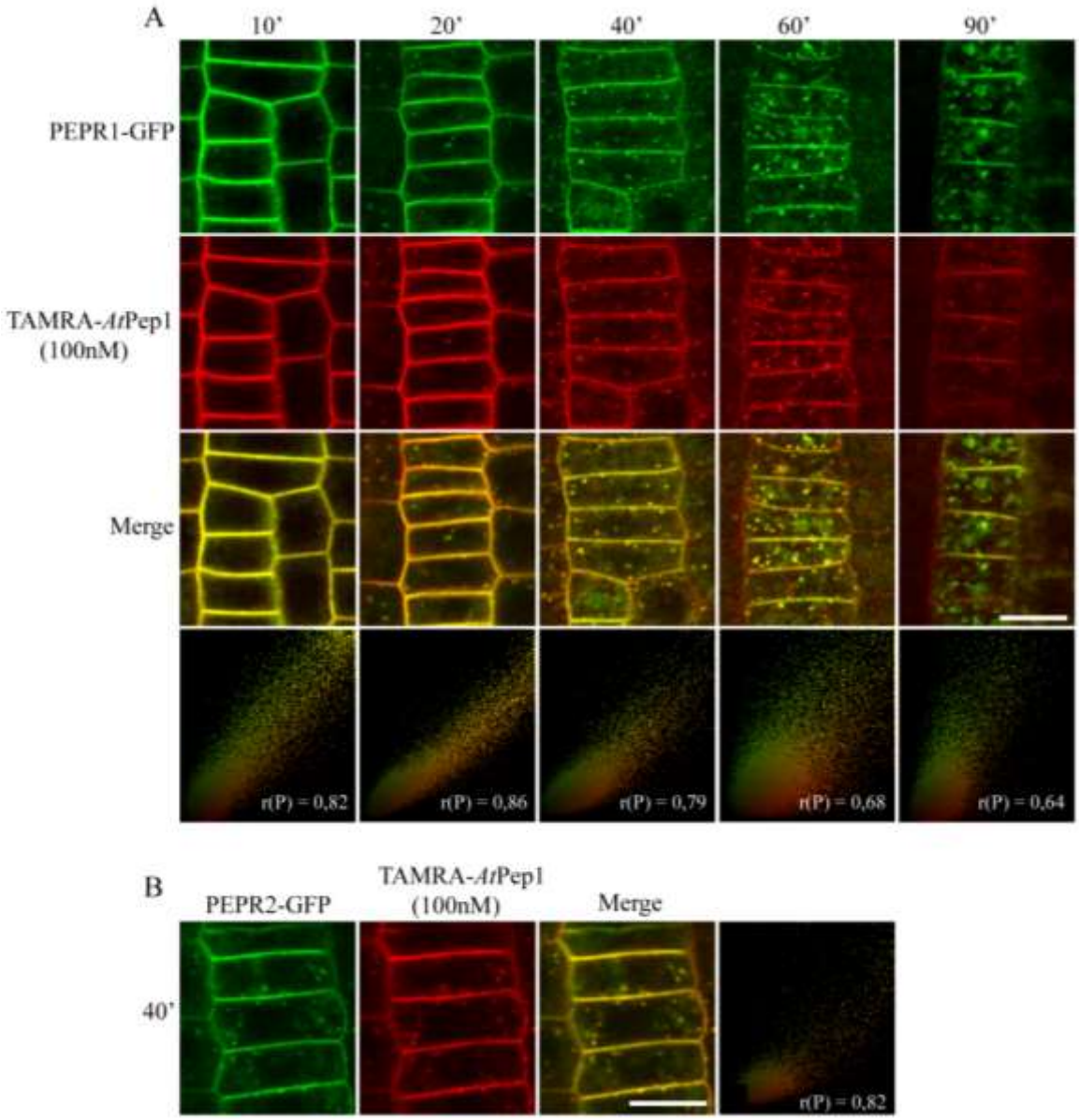

Supplemental Figure 5 - *At*Pep1 and its receptors internalized as a complex. Internalization of TAMRA-*At*Pep1/PEPR1-GFP complexes in (A) and TAMRA-*At*Pep1/PEPR2-GFP complexes in (B). Five-day-old *pepr1pepr2* seedlings complemented with PEPR1-GFP or PEPR2-GFP expressed under the *RPS5A* promoter were treated with TAMRA-*At*Pep1 for 10 sec, washed with liquid medium, and imaged at the indicated times. As colocalization indicator, the Pearson correlation r(P) was calculated for images in (A) and (B). Scale bars, 10 µm

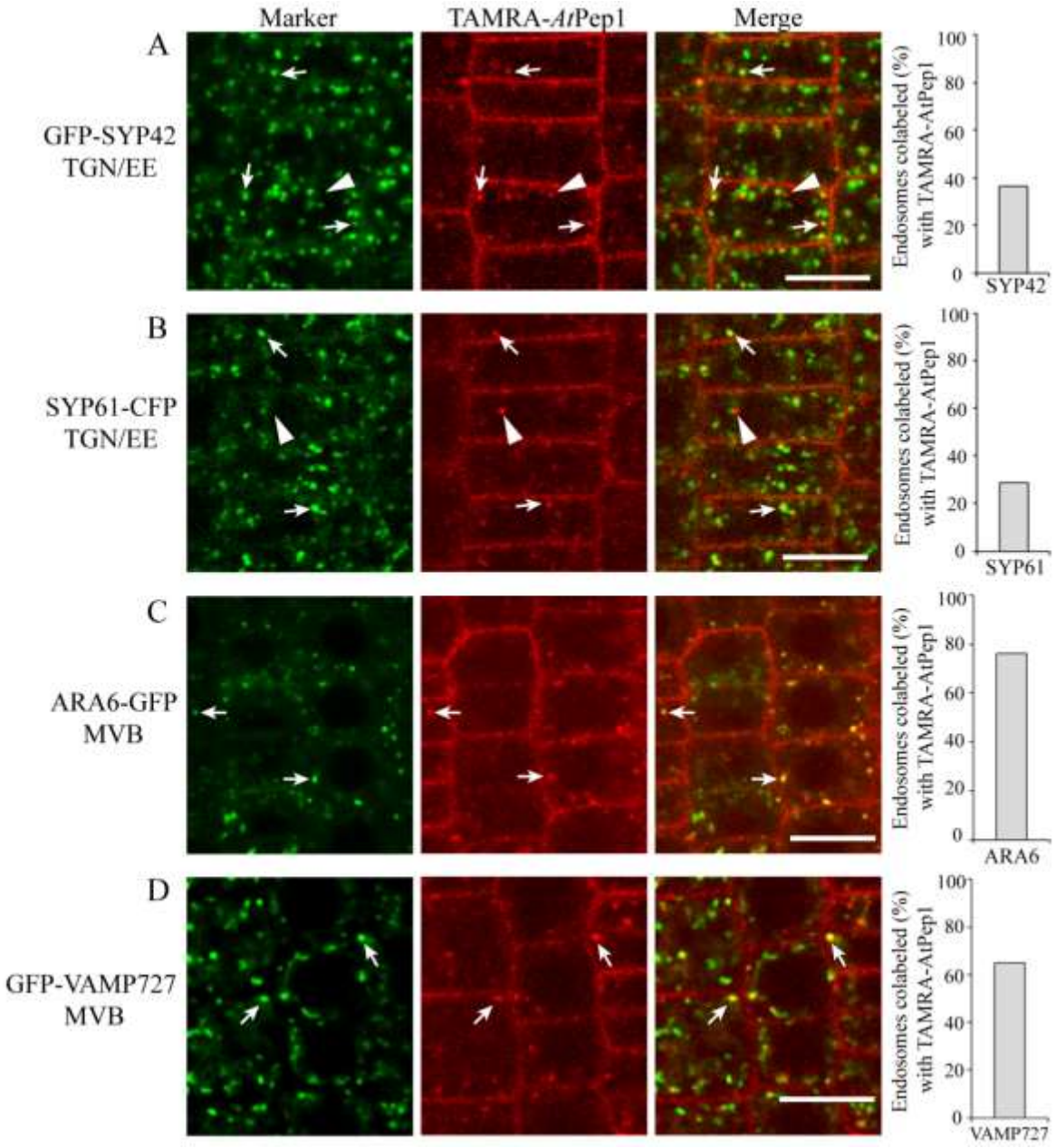

Supplemental Figure 6 – Colocalization of TAMRA-A*t*Pep1with different endosomal markers. TAMRA-*At*Pep1 marked vesicles colocalized with the TGN/EE markers GFP-SYP42 (**A**) and CFP-SYP61 (**B**), and the LE/MVB markers ARA6-GFP (**C**) and GFP-VAMP727 (**D**). Five-day-old seedlings were treated with TAMRA-*At*Pep1 (100 nM, 10 sec), washed with liquid medium and root meristem epidermal cells were imaged after 40-min chase. Graphs present the percentage of the marker line and the positively labeled TAMRA-*At*Pep1-vesicles (n=307 – 336). Only the TAMRA-*At*Pep1-positive vesicles presenting a colocalization value over 0.5 calculated by the Person's correlation coefficient were considered as colocalized. n = TAMRA-*At*Pep1-positive vesicles. Scale bars, 10 µm

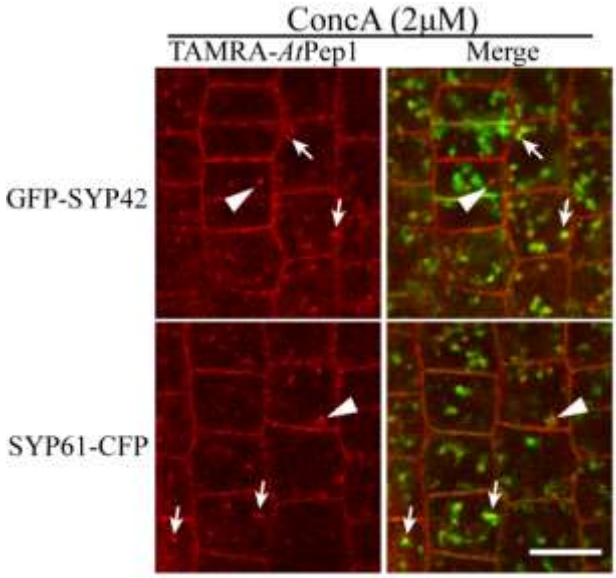

Supplemental Figure 7 – Partial colocalization of the TAMRA-*At*Pep1 vesicles with the TGN/EE markers GFP-SYP42 and CFP-SYP61 in the presence of ConcanamycinA (ConcA). Seedlings were pretreated with ConcA (2 µM, 30 min), subsequently treated with TAMRA-*At*Pep1 for 10sec, washed, and kept in the presence of ConcA for 40 min before imaging. Arrows and arrowhead indicate colocalized and not colocalized structures, respectively. Scale bar, 10 µm

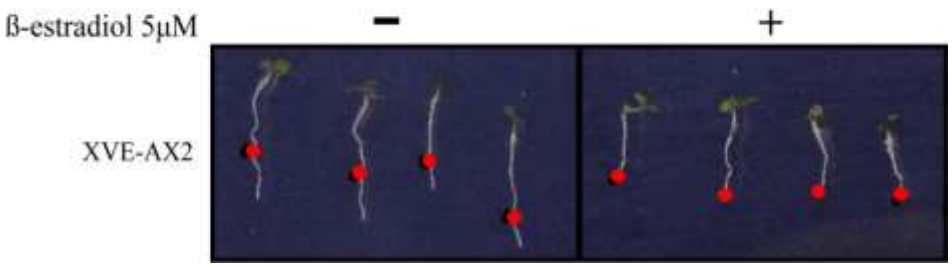

Supplemental Figure 8 – Induction of *AUXILIN2* expression inhibits the root growth. 5-day-old XVE:AX2 seedlings transferred for 24 h to ½ MS medium not supplemented (-) or supplemented (+) with 5 µM β-estradiol to induce *AUXILIN2* expression. Red circles marked the length of the root when transferred to the correspondent medium

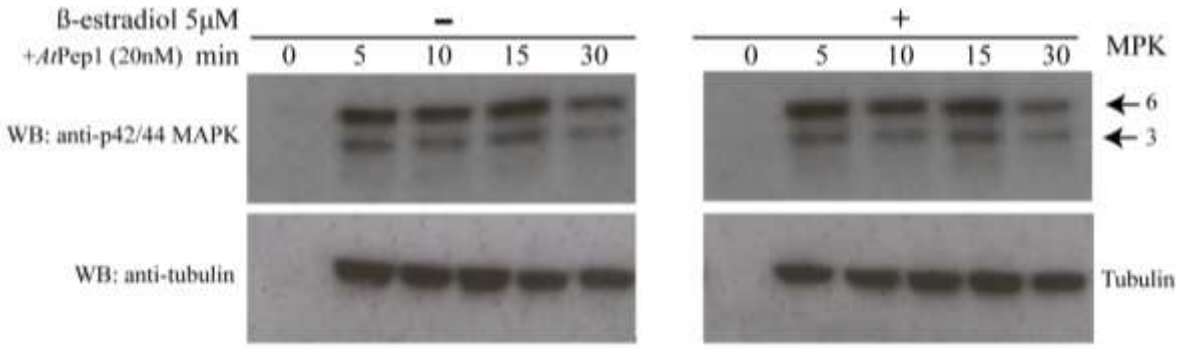

Supplemental Figure 9 – *At*Pep1-induced MAPK activation is not affected by β-estradiol in wild type *Arabidopsis* plants. MAPK activation in 5-day-old Col-0 seedlings transferred for 24 h to ½ MS medium not supplemented (-) or supplemented (+) with 5 µM β-estradiol, and subsequently treated with *At*Pep1 (20 nM) for the indicated times. MAPK phosphorylation was detected by immunoblotting with anti-phospho-p44/p42-MPK antibody detecting the pTE-pY motif of MPK6 and MPK3. The immunoblot was reprobed with anti-tubulin to show protein loading. Individual MPKs were identified by molecular mass and indicated by arrows

Supplemental Table 1 – Primers used for cloning

DNA region	**Primer**	**Sequence 5' – 3'**
Coding PEPR1	Forward	GGGGACAAGTTTGTACAAAAAAGCAGGCTCAATGAAGAATCTTGGGGGGTTGTTC
	Reverse	GGGGACCACTTTGTACAAGAAAGCTGGGTACCGAACTGAATCAGAGGAGCA
Coding PEPR2	Forward	GGGGACAAGTTTGTACAAAAAAGCAGGCTCAATGAGGAATCTTGGGTTACTCG
	Reverse	GGGGACCACTTTGTACAAGAAAGCTGGGTAGTGAACTGAACCCGAAGTGCTTCT
Promoter PEPR1	Forward	GGGGACAACTTTGTATAGAAAAGTTGCTTCACTGATCTGTTTGTTGCAAAC
	Reverse	GGGGACTGCTTTTTTGTACAAACTTGCCTGAGTTTAAAGATCGAGAAACATG
PromoterPEPR2	Forward	GGGGACAACTTTGTATAGAAAAGTTGCTATTAGGGTGGTCTATCGGTCAG
	Reverse	GGGGACTGCTTTTTTGTACAAACTTGCATTAGAGCTCAAGAGACTGAAATATG

References

BAISA, G.A.; MAYERS, J.R.; BEDNAREK, S.Y. Budding and braking news about clathrin-mediated endocytosis **Current Opinion in Plant Biology**, London, v. 16, n. 6, p. 718-725, 2013.

BAR, M.; AVNI, A. Endosomal trafficking and signaling in plant defense responses. **Current Opinion in Plant Biology,** London, v. 22, p. 86-92, 2014.

BARAL, A.; IRANI, N.G.; FUJIMOTO, M.; NAKANO, A.; MAYOR, S.; MATHEW, M.K. Salt-induced remodeling of spatially restricted clathrin-independent endocytic pathways in Arabidopsis root. **The Plant Cell**, Rockville, v. 27, n.4,p. 1297-1315, 2015.

BARTELS, S.; LORI, M.; MBENGUE, M.; VAN VERK, M.; KLAUSER, D.; HANDER, T.; BONI, R.; ROBATZEK, S.; BOLLER, T. The family of Peps and their precursors in Arabidopsis: differential expression and localization but similar induction of pattern-triggered immune responses. **Journal of Experimental Botany** , Oxford, v. 64, n. 17, p. 5309-5321, 2013.

BECK, M.; ZHOU, J.; FAULKNER, C.; MACLEAN, D.; ROBATZEK, S. Spatio-temporal cellular dynamics of the Arabidopsis flagellin receptor reveal activation status-dependent endosomal sorting. **The Plant Cell**, Rockville, v. 24, n. 10, p. 4205-4219, 2012.

BENYA, R.V.; KUSUI, T.; SHIKADO, F.; BATTEY, J.F.; JENSEN, R.T. Desensitization of neuromedin B receptors (NMB-R) on native and NMB-R-transfected cells involves down-regulation and internalization. **The Journal of Biological Chemistry,** Baltimore, v. 269, n. 16, p. 11721-11728, 1994.

BOLTE, S.; TALBOT, C.; BOUTTE, Y.; CATRICE, O.; READ, N.D.; SATIAT-JEUNEMAITRE, B. FM-dyes as experimental probes for dissecting vesicle trafficking in living plant cells. **Journal of Microscopy**, Hoboken, v. 214, n. 2, p. 159-173, 2004.

CHEN, X.; IRANI, N. G.; FRIML, J. Clathrin-mediated endocytosis: the gateway into plant cells **Current Opinion in Plant Biology**, London, v. 14, n. 6, p. 674-682, 2011.

CHINCHILLA, D.; ZIPFEL, C.; ROBATZEK, S.; KEMMERLING, B.; NURNBERGER, T.; JONES, J.D.; FELIX, G.; BOLLER, T. A flagellin-induced complex of the receptor FLS2 and BAK1 initiates plant defence. **Nature,** London, v. 448, n. 7152, p. 497-500, 2007.

CHOI, S.W.; TAMAKI, T.; EBINE, K.; UEMURA, T.; UEDA, T.; NAKANO, A. RABA members act in distinct steps of subcellular trafficking of the flagellin sensing2 receptor. **The Plant Cell**, Rockville, v. 25, n. 3, p. 1174-1187, 2013.

CLAGUE, M. J. Molecular aspects of the endocytic pathway. **Biochemical Journal,** London, v. 336, p. 271-82, 1998.

CZYZEWICZ, N.; YUE, K.; BEECKMAN, T.; DE SMET, I. Message in a bottle: small signalling peptide outputs during growth and development. **Journal of Experimental Botany**, Oxford, v. 64, n. 17, p. 5281-5296, 2013.

DETTMER, J.; HONG-HERMESDORF, A.; STIERHOF, Y.D.; SCHUMACHER, K. Vacuolar H+-ATPase activity is required for endocytic and secretory trafficking in Arabidopsis. **The Plant Cell**, Rockville, v. 18, n. 3, p. 715-730, 2006.

DI RUBBO, S.; IRANI, N.G.; KIM, S.Y.; XU, Z.Y.; GADEYNE, A.; DEJONGHE, W.; VANHOUTTE, I.; PERSIAU, G.; EECKHOUT, D.; SIMON, S.; SONG, K.; KLEINE-VEHN, J.; FRIML, J.; DE JAEGER, G.; VAN DAMME, D.; HWANG, I.; RUSSINOVA, E. The clathrin adaptor complex AP-2 mediates endocytosis of brassinosteroid insensitive1 in Arabidopsis. **The Plant Cell**, Rockville, v. 25, n. 8, p. 2986-2997, 2013.

DEJONGHE, W. **Endomembrane traffic and brassinosteroid signaling from a small molecule perspective.** 2015. 237p. Thesis (PhD in sciences: Biochemistry and Biotechnology) – VIB Department of Plant Systems Biology, Gent University, Gent, 2015.

EBINE, K.; OKATANI, Y.; UEMURA, T.; GOH, T.; SHODA, K.; NIIHAMA, M.; MORITA, M.T.; SPITZER, C.; OTEGUI, M.S.; NAKANO, A.; UEDA, T. A SNARE complex unique to seed plants is required for protein storage vacuole biogenesis and seed development of Arabidopsis thaliana. **The Plant Cell**, Rockville, v. 20, n. 11, p. 3006-3021, 2008.

ENDO, S.; BETSUYAKU, S.; FUKUDA, H. Endogenous peptide ligand-receptor systems for diverse signaling networks in plants. **Current Opinion in Plant Biology**, London, , v. 21, p. 140-146, 2014.

FRENCH, A.P.; MILLS, S.; SWARUP, R.; BENNETT, M.J.; PRIDMORE, T.P. Colocalization of fluorescent markers in confocal microscope images of plant cells. **Nature Protoc,** London, v. 3, n. 4, p. 619-628, 2008.

GADEYNE, A.; SANCHEZ-RODRIGUEZ, C.; VANNESTE, S.; DI RUBBO, S.; ZAUBER, H.; VANNESTE, K.; VAN LEENE, J.; DE WINNE, N.; EECKHOUT, D.; PERSIAU, G.; VAN DE SLIJKE, E.; CANNOOT, B.; VERCRUYSSE, L.; MAYERS, J.R.; ADAMOWSKI, M.; KANIA, U.; EHRLICH, M.; SCHWEIGHOFER, A.; KETELAAR, T.; MAERE, S.; BEDNAREK, S.Y.; FRIML, J.; GEVAERT, K.; WITTERS, E.; RUSSINOVA, E.; PERSSON, S.; DE JAEGER, G.; VAN DAMME, D. The TPLATE adaptor complex drives clathrin-mediated endocytosis in plants. **Cell**, Cambridge, v. 156, n. 4, p. 691-704, 2014.

GELDNER, N.; FRIML, J.; STIERHOF, Y.D.; JURGENS, G.; PALME, K. Auxin transport inhibitors block PIN1 cycling and vesicle trafficking. **Nature,** London, v. 413, n. 6854, p. 425-428, 2001.

GELDNER, N.; HYMAN, D.L.; WANG, X.; SCHUMACHER, K.; CHORY, J. Endosomal signaling of plant steroid receptor kinase BRI1. **Genes & Development,** New York, v. 21, n. 13, p. 1598-1602, 2007.

GELDNER, N.; DENERVAUD-TENDON, V.; HYMAN, D.L.; MAYER, U.; STIERHOF, Y.D.; CHORY, J. Rapid, combinatorial analysis of membrane compartments in intact plants with a multicolor marker set. **The Plant Journal,** Oxford, v. 59, n. 1, p. 169-178, 2009.

GHORBANI, S.; FERNANDEZ SALINA, A.; HILSON, P.; BEECKMAN, T. Signaling peptides in plants. **Cell & Developmental Biology,** Oxford, v. 3, n. 2, p. 1-11, 2014.

GOH, T.; UCHIDA, W.; ARAKAWA, S.; ITO, E.; DAINOBU, T.; EBINE, K.; TAKEUCHI, M.; SATO, K.; UEDA, T.; NAKANO, A. VPS9a, the common activator for two distinct types of Rab5 GTPases, is essential for the development of Arabidopsis thaliana **The Plant Cell**, Rockville, v. 19, n. 11, p. 3504-3515, 2007.

HUANG, C.; CHANG, A. pH-dependent cargo sorting from the Golgi. **The Journal of Biological Chemistry,** Bethesda, v. 286, n. 12, p. 10058-10065, 2011.

HUFFAKER, A.; PEARCE, G.; RYAN, C.A. An endogenous peptide signal in Arabidopsis activates components of the innate immune response. **Proceedings of the National Academy of Sciences of the United States of America,** Washington, v. 103, n. 26, p. 10098-10103, 2006.

HUSS, M.; INGENHORST, G.; KONIG, S.; GASSEL, M.; DROSE, S.; ZEECK, A.; ALTENDORF, K.; WIECZOREK, H. Concanamycin A, the specific inhibitor of V-ATPases, binds to the V(o) subunit c. **The Journal of Biological Chemistry,** Baltimore, v. 277, n. 43, p. 40544-40548, 2002.

IRANI, N.G.; DI RUBBO, S.; MYLLE, E.; VAN DEN BEGIN, J.; SCHNEIDER-PIZON, J.; HNILIKOVA, J.; SISA, M.; BUYST, D.; VILARRASA-BLASI, J.; SZATMARI, A.M.; VAN DAMME, D.; MISHEV, K.; CODREANU, M.C.; KOHOUT, L.; STRNAD, M.; CANO-DELGADO, A.I.; FRIML, J.; MADDER, A.; RUSSINOVA, E. Fluorescent castasterone reveals BRI1 signaling from the plasma membrane. **Nature Chemical Biology,** London, v. 8, n. 6, p. 583-589, 2012.

IRANI, N.G.; RUSSINOVA, E. Receptor endocytosis and signaling in plants. **Current Opinion in Plant Biology,** London, v. 12, n. 6, p 653-659, 2009.

JEONG, Y.M.; MUN, J.H.; LEE, I.; WOO, J.C.; HONG, C.B.; KIM, S.G. Distinct roles of the first introns on the expression of Arabidopsis profilin gene family members. **Plant Physiology,** Lancaster, v. 140, n. 1, p. 196-209, 2006.

KANE, P.M. The where, when, and how of organelle acidification by the yeast vacuolar H+-ATPase. **Microbiology and Molecular Biology Reviews,** Washington, v. 70, n. 1, p. 177-191, 2006.

KARIMI, M.; DE MEYER, B.; HILSON, P. Modular cloning in plant cells. **Trends in Plant Science**, Oxford, v. 10, n. 3, p. 103-105, 2005.

KARIMI, M.; BLEYS, A.; VANDERHAEGHEN, R.; HILSON, P. Building blocks for plant gene assembly. **Plant Physiology,** Lancaster, v. 145, n. 4, p. 1183-1191, 2007.

KIRCHHAUSEN, T. Imaging endocytic clathrin structures in living cells. **Trends in cell biology,** Cambridge, v. 19, n. 11, p. 596-605, 2009.

KITAKURA, S.; VANNESTE, S.; ROBERT, S.; LOFKE, C.; TEICHMANN, T.; TANAKA, H.; FRIML, J. Clathrin mediates endocytosis and polar distribution of PIN auxin transporters in Arabidopsis. **The Plant Cell**, Rockville, v. 23, n. 5, p. 1920-1931, 2011.

KOOIKER, M.; AIROLDI, C.A.; LOSA, A.; MANZOTTI, P.S.; FINZI, L.; KATER, M.M.; COLOMBO, L. Basic pentacysteine1, a GA binding protein that induces conformational changes in the regulatory region of the homeotic Arabidopsis gene SEEDSTICK. **The Plant Cell**, Rockville, v. 17, n. 3, p. 722-729, 2005.

KROL, E.; MENTZEL, T.; CHINCHILLA, D.; BOLLER, T.; FELIX, G.; KEMMERLING, B.; POSTEL, S.; ARENTS, M.; JEWORUTZKI, E.; AL-RASHEID, K.A.; BECKER, D.; HEDRICH, R. Perception of the Arabidopsis danger signal peptide 1 involves the pattern recognition receptor AtPEPR1 and its close homologue AtPEPR2. **The Journal of Biological Chemistry,** Baltimore, v. 285, n. 18, p. 13471-13479, 2010.

LI, R.; LIU, P.; WAN, Y.; CHEN, T.; WANG, Q.; METTBACH, U.; BALUSKA, F.; SAMAJ, J.; FANG, X.; LUCAS, W.J.; LIN, J. A membrane microdomain-associated protein, Arabidopsis Flot1, is involved in a clathrin-independent endocytic pathway and is required for seedling development. **The Plant Cell**, Rockville, v. 24, n. 5, p. 2105-2122, 2012.

MA, C.; GUO, J.; KANG, Y.; DOMAN, K.; BRYAN, A.C.; TAX, F.E.; YAMAGUCHI, Y.; QI, Z. AtPEPTIDE RECEPTOR2 mediates the AtPEPTIDE1-induced cytosolic Ca(2+) rise, which is required for the suppression of Glutamine Dumper gene expression in Arabidopsis roots. **Journal of Integrative Plant Biology,** Beijing, v. 56, n. 7, p. 684-694, 2014.

MARTINIERE, A.; BASSIL, E.; JUBLANC, E.; ALCON, C.; REGUERA, M.; SENTENAC, H.; BLUMWALD, E.; PARIS, N. In vivo intracellular pH measurements in tobacco and Arabidopsis reveal an unexpected pH gradient in the endomembrane system. **The Plant Cell**, Rockville, v. 25, n. 10, p. 4028-4043, 2013.

MURPHY, A.S.; BANDYOPADHYAY, A.; HOLSTEIN, S.E.; PEER, W.A. Endocytotic cycling of PM proteins. **Annual Review of Plant Biology,** Palo Alto, v. 56, p. 221-251, 2005.

MURPHY, J.E.; PADILLA, B.E.; HASDEMIR, B.; COTTRELL, G.S.; BUNNETT, N.W. Endosomes: a legitimate platform for the signaling train **Proceedings of the National Academy of Sciences of the United States of America,** Washington, v. 106, n. 42, p. 17615-17622, 2009.

OGBOURNE, S.; ANTALIS, T.M. Transcriptional control and the role of silencers in transcriptional regulation in eukaryotes. **Biochemical Journal**, London, v. 331, p. 1-14, 1998.

PESTOVA, T.V.; HELLEN, C.U. Translation elongation after assembly of ribosomes on the Cricket paralysis virus internal ribosomal entry site without initiation factors or initiator tRNA. **Genes & Development,** New York, v. 17, n. 2, p. 181-186, 2003.

RAJAGOPALAN, S. Endosomal signaling and a novel pathway defined by the natural killer receptor KIR2DL4 (CD158d). **Traffic,** Hoboken, v. 11, n. 11, p. 1381-1390, 2010.

RANF, S.; ESCHEN-LIPPOLD, L.; PECHER, P.; LEE, J.; SCHEEL, D. Interplay between calcium signalling and early signalling elements during defence responses to microbe- or damage-associated molecular patterns. **The Plant journal,** Oxford, v. 68, n. 1, p. 100-113, 2011.

ROBATZEK, S.; CHINCHILLA, D.; BOLLER, T. Ligand-induced endocytosis of the pattern recognition receptor FLS2 in Arabidopsis. **Genes & development,** New York, v. 20, n. 5, p. 537-42, 2006.

ROBERT, S.; CHARY, S. N.; DRAKAKAKI, G.; LI, S.; YANG, Z.; RAIKHEL, N.V.; HICKS, G.R. Endosidin1 defines a compartment involved in endocytosis of the brassinosteroid receptor BRI1 and the auxin transporters PIN2 and AUX1 **Proceedings of the National Academy of Sciences of the United States of America,** Washington, v. 105, n. 24, p. 8464-8469, 2008.

ROBINSON, D.G.; JIANG, L.; SCHUMACHER, K. The endosomal system of plants: charting new and familiar territories. **Plant Physiology,** Lancaster, v. 147, n. 4, p. 1482-1492, 2008.

ROSS, A.; YAMADA, K.; HIRUMA, K.; YAMASHITA-YAMADA, M.; LU, X.; TAKANO, Y.; TSUDA, K.; SAIJO, Y. The Arabidopsis PEPR pathway couples local and systemic plant immunity. **The EMBO Journal,** Oxford, v. 33, n. 1, p. 62-75, 2014.

RUSSINOVA, E.; BORST, J.W.; KWAAITAAL, M.; CANO-DELGADO, A.; YIN, Y.; CHORY, J.; DE VRIES, S. C. Heterodimerization and endocytosis of Arabidopsis brassinosteroid receptors BRI1 and AtSERK3 (BAK1). **The Plant Cell**, Rockville, v. 16, n. 12, p. 3216-3229, 2004.

SCHEURING, D.; VIOTTI, C.; KRUGER, F.; KUNZL, F.; STURM, S.; BUBECK, J.; HILLMER, S.; FRIGERIO, L.; ROBINSON, D.G.; PIMPL, P.; SCHUMACHER, K. Multivesicular bodies mature from the trans-golgi network/early endosome in Arabidopsis. **The Plant Cell**, Rockville, v. 23, n. 9, p. 3463-3481, 2011.

SCHULZE, B.; MENTZEL, T.; JEHLE, A.K.; MUELLER, K.; BEELER, S.; BOLLER, T.; FELIX, G.; CHINCHILLA, D. Rapid heteromerization and phosphorylation of ligand-activated plant transmembrane receptors and their associated kinase BAK1. **The Journal of Biological Chemistry,** Baltimore, v. 285, n. 13, p. 9444-94451, 2010.

SCHUMACHER, K.; VAFEADOS, D.; MCCARTHY, M.; SZE, H.; WILKINS, T.; CHORY, J. The Arabidopsis det3 mutant reveals a central role for the vacuolar H(+)-ATPase in plant growth and development. **Genes & Development,** New York, v. 13, n. 24, p. 3259-3270, 1999.

SHEN, J.; ZENG, Y.; ZHUANG, X.; SUN, L.; YAO, X.; PIMPL, P.; JIANG, L. Organelle pH in the Arabidopsis endomembrane system. **Molecular Plant,** Saint Paul, v. 6, n. 5, p. 1419-1437, 2013.

SINGH, M.K.; KRUGER, F.; BECKMANN, H.; BRUMM, S.; VERMEER, J.E.; MUNNIK, T.; MAYER, U.; STIERHOF, Y.D.; GREFEN, C.; SCHUMACHER, K.; JURGENS, G. Protein delivery to vacuole requires SAND protein-dependent Rab GTPase conversion for MVB-vacuole fusion. **Current Biology,** London, v. 24, n. 12, p. 1383-1389, 2014.

STIERHOF, Y.D.; EL KASMI, F. Strategies to improve the antigenicity, ultrastructure preservation and visibility of trafficking compartments in Arabidopsis tissue. **European Journal of Cell Biology,** Stuttgart, v. 89, n. 2/3, p. 285-297, 2010.

TAKANO, J.; MIWA, K.; YUAN, L.; VON WIREN, N.; FUJIWARA, T. Endocytosis and degradation of BOR1, a boron transporter of Arabidopsis thaliana, regulated by boron availability **Proceedings of the National Academy of Sciences of the United States of America,** Washington, v. 102, n. 34, p. 12276-12281, 2005.

TANAKA, H.; KITAKURA, S.; RAKUSOVA, H.; UEMURA, T.; FERARU, M.I.; DE RYCKE, R.; ROBERT, S.; KAKIMOTO, T.; FRIML, J. Cell polarity and patterning by PIN trafficking through early endosomal compartments in Arabidopsis thaliana. **PLoS Genetics,** San Francisco, v. 9, n. 5, p. e1003540, 2013.

TANG, J.; HAN, Z.; SUN, Y.; ZHANG, H.; GONG, X.; CHAI, J. Structural basis for recognition of an endogenous peptide by the plant receptor kinase PEPR1. **Cell Research,** New York, v. 25, n. 1, p. 110-120, 2015.

UEMURA, T.; KIM, H.; SAITO, C.; EBINE, K.; UEDA, T.; SCHULZE-LEFERT, P.; NAKANO, A. Qa-SNAREs localized to the trans-Golgi network regulate multiple transport pathways and extracellular disease resistance in plants. **Proceedings of the National Academy of Sciences of the United States of America,** Washington, v. 109, n. 5, p. 1784-1789, 2012.

VIOTTI, C.; BUBECK, J.; STIERHOF, Y.D.; KREBS, M.; LANGHANS, M.; VAN DEN BERG, W.; VAN DONGEN, W.; RICHTER, S.; GELDNER, N.; TAKANO, J.; JURGENS, G.; DE VRIES, S.C.; ROBINSON, D.G.; SCHUMACHER, K. Endocytic and secretory traffic in *Arabidopsis merge* in the trans-golgi network/early endosome, an independent and highly dynamic organelle. **The Plant Cell**, Rockville, v. 22, n. 4, p. 1344-1357, 2010.

WANG, C.; YAN, X.; CHEN, Q.; JIANG, N.; FU, W.; MA, B.; LIU, J.; LI, C.; BEDNAREK, S.Y.; PAN, J. Clathrin light chains regulate clathrin-mediated trafficking, auxin signaling, and development in Arabidopsis. **The Plant Cell**, Rockville, v. 25, n. 2, p. 499-516, 2013.

WEIJERS, D.; FRANKE-VAN DIJK, M.; VENCKEN, R.J.; QUINT, A.; HOOYKAAS, P.; OFFRINGA, R. An Arabidopsis minute-like phenotype caused by a semi-dominant mutation in a ribosomal protein S5 gene. **Development,** Cambridge, v. 128, n. 21, p. 4289-4299, 2001.

WIEFFER, M.; MARITZEN, T.; HAUCKE, V. SnapShot: endocytic trafficking. **Cell,** Cambridge, v. 137, n. 2, p. 382 e1-3, 2009.

WU, G.; LIU, S.; ZHAO, Y.; WANG, W.; KONG, Z.; TANG, D. Enhanced disease resistance4 associates with clathrin heavy chain2 and modulates plant immunity by regulating relocation of EDR1 in Arabidopsis. **The Plant Cell**, Rockville, v 27, n. 3, p 857-873, 2015.

YAMAGUCHI, Y.; HUFFAKER, A. Endogenous peptide elicitors in higher plants. **Current Opinion in Plant Biology**, London, v. 14, n. 4, p. 351-357, 2011.

YAMAGUCHI, Y.; HUFFAKER, A.; BRYAN, A.C.; TAX, F.E.; RYAN, C.A. PEPR2 is a second receptor for the Pep1 and Pep2 peptides and contributes to defense responses in Arabidopsis. **The Plant Cell**, Rockville, v. 22, n. 2, p. 508-522, 2010.

YAMAGUCHI, Y.; PEARCE, G.; RYAN, C.A. The cell surface leucine-rich repeat receptor for AtPep1, an endogenous peptide elicitor in Arabidopsis, is functional in transgenic tobacco cells **Proceedings of the National Academy of Sciences of the United States of America,** Washington, v. 103, n. 26, p. 10104-10109, 2006.

4 BAK1 MODULATES ENDOCYTOSIS AND SIGNALING OF THE PLANT ELICITOR PEPTIDE *At*Pep1

Fausto Andres Ortiz-Morea[1,2,3], Yu Luo[1,2], Keini Dressano[3], Daniel Scherer de Moura[3] and Eugenia Russinova[1,2]

[1]Department of Plant Systems Biology, VIB, Technologiepark 927, 9052 Ghent, Belgium
[2]Department of Plant Biotechnology and Bioinformatics, Ghent University, Technologiepark 927, 9052 Gent, Belgium
[3]Laboratório de Bioquímica de Proteínas, Departamento de Ciências Biológicas, Escola Superior de Agricultura Luiz de Queiroz, Universidade de São Paulo USP, Piracicaba, SP 13418-900, Brazil.

Abstract

In *Arabidopsis*, the endogenous elicitor peptide *At*Pep1 is known to trigger innate immune responses after having been recognized by the plasma membrane receptor kinases (RKs) PEPR1 and PEPR2. Once the *At*Pep1-PEPRs complexes are formed, they are removed from the plasma membrane by endocytosis. Additionally, the *At*Pep1 receptors are predicted to complex with the regulatory RK BRASSINOSTEROID INSENSITIVE1–ASSOCIATED KINASE1 (BAK1), but the role of this interaction during *At*Pep1 endocytosis remains to be clarified. Here, we first confirmed by co-immunoprecipitation that both PEPRs and BAK1 interact in a ligand-dependent manner *in planta*. Next, we tested the *At*Pep1-induced early and late responses and through life-cell imaging, we monitored the endocytosis of a bioactive fluorescently labeled *At*Pep1 in different BAK1 genotypes. In the null *bak1-4* mutants, both the *At*Pep1 responses and endocytosis were not inhibited, whereas some responses were enhanced. The opposite was observed in the hypoactive kinase *bak1-5*, in which the *At*Pep1 endocytosis and signaling were largely compromised, and in a transgenic BAK1-overexpressing line, in which these responses were abolished. Altogether, our results indicate that BAK1 plays an essential role in *At*Pep1 signaling and endocytosis, but that, when absent, it might be replaced by homologous *SOMATIC EMBRYOGENESIS RECEPTOR-LIKE KINASE* (SERK) proteins that could have additional functions during the *At*Pep1 signaling. Furthermore, phosphorylation events after the formation of PEPR-BAK1 (or other SERK) complexes, seem to dictate the molecular bases of *At*Pep1 internalization and signaling. Finally, we also propose that BAK1 might be required for attenuation of the *At*Pep1 responses.

Keywords: Endocytosis; BAK1; *At*Pep1; PEPRs; Plant immunity; DAMPs

4.1 Introduction

Plants have evolved sophisticated communication networks to monitor environmental changes, including pathogenic attacks, in which plasma membrane receptors are one of the main components of these sensing systems that play a critical role in translation of extracellular signals into appropriate intracellular responses. Activation of plant innate immunity responses is initiated through the perception by plasma membrane-localized receptors, designated pattern recognition receptors (PRRs) of microbe-associated molecular patterns (MAMPs) from invading organisms (ZIPFEL, 2014). The receptor kinase FLAGELLIN SENSING2 (FLS2) and the ELONGATION FACTOR Tu (EF-Tu) receptor (EFR) are PRRs that have been amply studied in *Arabidopsis*, which after recognition of the respective MAMPs, a conserved peptide domain of the bacterial flagellin (flg22) and EF-Tu (elf18), activate PAMP-triggered immunity (PTI) (GOMEZ-GOMEZ; BOLLER, 2000; ZIPFEL et al., 2006). In addition to MAMPs, PTI responses are also induced after specific PRRs that have recognized endogenous host-derived damage-associated molecular patterns (DAMPs), including signaling peptides released upon biotic stress (HOU et al., 2014; HUFFAKER; PEARCE; RYAN, 2006; YAMAGUCHI; HUFFAKER, 2011).

The plant elicitor peptide *At*Pep1 is a well-characterized signaling peptide involved with immunity responses. *At*Pep1 is a 23-amino-acid peptide isolated from *Arabidopsis* leaves by means of an elicitor-induced alkalinization activity assay (HUFFAKER; PEARCE; RYAN, 2006). *At*Pep1 belongs to a small family of eight homologous members that are derived from the C-terminal portion of the precursor proteins PROPEP1 to PROPEP8 (BARTELS et al., 2013; HUFFAKER; PEARCE; RYAN, 2006). PROPEPs are believed to be cleaved releasing the active Peps into the apoplast under biotic stress, which in turn, binds with high affinity a RK PRR at the plasma membrane, PEPR (BARTELS; BOLLER, 2015). In *Arabidopsis* the existence of two PEPR has been reported, and interestingly whereas PEPR1 is able to detect all eight *At*Peps, PEPR2 detects only *At*Pep1 and *At*Pep2 (BARTELS et al., 2013; YAMAGUCHI et al., 2010). Recently, the crystal structure of the leucine-rich repeat (LRR) domain of PEPR1 (PEPR1LRR) has revealed that *At*Pep1 adopts a fully extended conformation and binds to the inner surface of the superhelical PEPR1LRR (TANG et al., 2015). After *At*Pep1 has been recognized by its receptors, downstream early and late PTI responses are initiated. One of the earliest signaling events of PTI is the activation of mitogen-activated protein kinases (MAPKs) that is induced by *At*Pep1 in *Arabidopsis*,

triggering phosphorylation of MPK3 and MPK6 within the first minutes after the *At*Pep1 treatment, thus providing a good read-out for immediate *At*Pep1 responses (RANF et al., 2011). Additionally, *At*Pep1 leads to gene expression reprogramming by increasing the transcript levels of the plant *DEFENSIN* (*PDF1.2*) gene and the WRKY transcription factor genes after *At*Pep1 elicitation (HUFFAKER; PEARCE; RYAN, 2006; YAMAGUCHI et al., 2010). The *At*Pep1-induced root growth arrest is also a mark of the activity related to late responses of this peptide (KROL et al., 2010; MA et al., 2014). By using bioactive fluorescently labeled AtPep1 we characterized the subcellular dynamics of *At*Pep1-PEPRs complexes in living cell (Chapter 3, this thesis). We reported that the *At*Pep1-PEPRs ligand-receptor pairs are internalized via clathrin-mediated endocytosis (CME) and trafficked to the lytic vacuole, passing through early and late endosomal compartments. However, the interplay between *At*Pep1 endocytosis and *At*Pep1-signalings is unclear. It is of great interest to elucidate whether these processes can regulate each other.

PEPRs hetero-oligomerize in a ligand-dependent manner with another RK, BAK1. This is based on an *in vivo* phospholabeling assay in *Arabidopsis* cell culture that showed the formation of a heterocomplex consisting of *de novo* phosphorylated BAK1 and a protein matching the size of PEPRs, triggered by *At*Pep1 treatment (SCHULZE et al., 2010). Recently this interaction was further supported by biochemical assays showing that *At*Pep1 is capable of inducing heterodimerization of extracellular domains of PEPRs and BAK1 (TANG et al., 2015). BAK1 has been implicated in regulating multiple independent signaling pathways including growth, cell death control and innate immunity, by forming ligand-dependent complexes with several plasma membrane receptors (SCHULZE et al., 2010; SCHWESSINGER et al., 2011). BAK1 is also named SOMATIC EMBRYOGENESIS-RELATED KINASE 3 (SERK3) and is a member of the SERK family (HECHT et al., 2001) that contains five members with potentially redundant functions as interaction partners (AAN DEN TOORN; ALBRECHT; DE VRIES, 2015). The brassinosteroid (BR)-receptor BR INSENSITIVE1 (BRI1) has been reported to interact with four out of five members of the SERK family that might play redundant roles in BR signaling (GOU et al., 2012; HE et al., 2007; LI et al., 2002). FLS2 and EFR receptors were also found to interact with different SERKs including the closest BAK1 homolog SERK4/BKK1 (hereafter referred as BKK1) (ROUX et al., 2011) as seemingly also the case for PEPRs, because minor *At*Pep1 signaling defects when assessed intracellular Ca^{2+} elevation, MAPK activation, root growth inhibition and ROS production are reported in the null *bak1-4* mutant (HOU et al., 2014; RANF et al., 2011). Besides *bak1-4* other *bak1* mutants have been used to study the role of this protein.

Interestingly a novel mutant *bak1-5* that harbors a single amino acid substitution (C408Y) in the kinase domain that leads to reduced phosphorylation status, was described as severely impaired for PTI responses, but not impaired in BR responses or cell death control (SCHWESSINGER et al., 2011). Phosphorylation events are the earliest response after ligand-induced complexes formation, and they are proposed to modulate the downstream responses of BAK1 and its interacting partners (SCHULZE et al., 2010; SCHWESSINGER et al., 2011). Strongest negative effect in PTI was found in the double mutant *bak1-5 bkk1-1*, indicating that BKK1 is also required for innate immunity (SCHWESSINGER et al., 2011). Additionally, BAK1 can also associate with member of the BAK1-interacting receptors (BIR)-RKs family, predicted to be very similar in structure to BAK1 (GAO et al., 2009; HALTER, et al., 2014b). Interaction between BIR2 and BAK1 was recently found to occur constitutively in the absence of MAMP perception preventing interaction with the ligand-binding FLS2; however perception of MAMPs leads to BIR2 release from the BAK1 complex and enables the recruitment of BAK1 into FLS2 complex. These findings imply that BIR2 act is a negative regulator of PTI by limiting BAK1-receptor complex formation in the absence of ligands (HALTER, et al., 2014a, 2014b).

In this work, we used co-immunoprecipitation experiments to validate that both PEPR1 and PEPR2 interact with BAK1 in a ligand-dependent manner *in planta*. Next, we explored different BAK1 genotypes to gain further insights into the role of BAK1 in *At*Pep1-PEPR endocytosis and signaling. We demonstrated that in absence of BAK1 endocytosis and signaling are not compromised due to a possibly redundancy of the SERK proteins. In contrast, these processes were largely affected in the *bak1-5* mutant that presents reduced phosphorylation status, implying that phosphorylation events into the PEPRs-BAK1 complex can regulate *At*Pep1 endocytosis and signaling. Finally our findings also suggest a negative effect of BAK1 on *At*Pep1 responses, since first, BAK1 was induced after *At*Pep1 elicitation, second, some *At*Pep1 responses were enhanced in the null bak1-4 mutant, and third, *At*Pep1 endocytosis and signaling was totally inhibited in a transgenic line overexpressing BAK1.

4.2 Results

4.2.1 BAK1 is an active component of the *At*Pep1-mediated signaling

Recently the crystal structure of the extracellular PEPR1LRR in complex with AtPep1 was elucidated, and in combination with biochemical assays was shown that *At*Pep1 is capable of inducing PEPR1LRRBAK1LRR heterodimerization (TANG et al., 2015).The capacity of *At*Pep1 to induce the formation of a heteromeric complexes consisting of *de novo*

phosphorylated BAK1 and a protein matching the size of PEPR1 was previously shown in *Arabidopsis* cell cultures (SCHULZE et al., 2010). To validate this interaction *in planta* we used *pepr1pepr2* mutant plants complemented by the stable expression of *PEPR1-GFP* and *PEPR2-GFP* with the *RPS5A* promoter (Chapter 3, this thesis) to carry on co-immunoprecipitation (co-IP) experiments. Following IP with GFP-trap beads and detection with anti-BAK1 antibodies, we observed that BAK1 was recruited in a complex with PEPR1 only after plants were stimulated with *At*Pep1 (20 nM, 5 min), supporting that the PEPRs interact with BAK1 in a ligand-dependent manner (Figure 1A). Interestingly, the amount of BAK1 present in the PEPR2-GFP complex after the *At*Pep1 treatment seemed lower than that in PEPR1-GFP. Besides forming a ligand-induced complex with PEPRs, *BAK1* transcript accumulation was found to increase when 6-day-old *Arabidopsis* seedlings were treated with *At*Pep1 (20 nM, 60 min) (Figure 1B). Together, these results demonstrated that BAK1 is an active component of the *At*Pep1-mediated signaling.

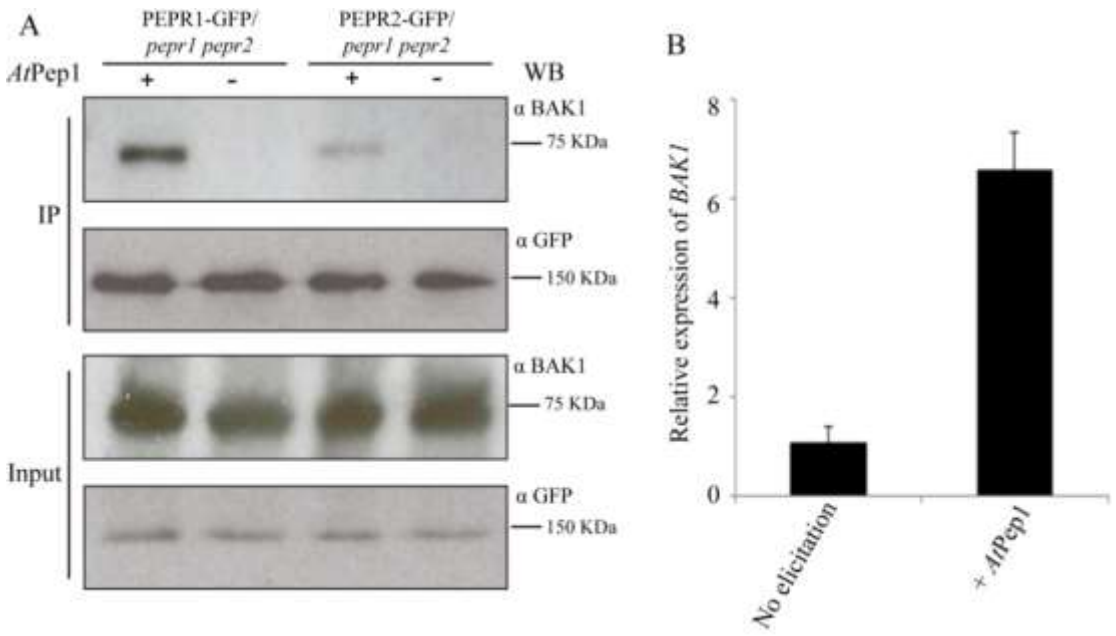

Figure 1 – BAK1 is an active component of *At*Pep1-mediated signaling. (A) **.** (**A**) Co-immunoprecipitation (co-IP) of BAK1 with PEPR1-GFP or PEPR2-GFP complementing *pepr1pepr2* mutant, treated (+) or not (-) with 20 nM of *At*Pep1 for 5 min, respectively. Total protein extracts (input) was immunoprecipitated with anti-GFP immunoaffinity beads followed by immunoblot analysis with anti-BAK1 and anti-GFP antibodies to detect BAK1 and PEPR1-GFP and PEPR2-GFP, respectively. (**B**) *BAK1* gene expression in 6-day-old *Arabidopsis* seedlings (Col-0) 60 min after treatment with *At*Pep1 (20 nM, for 5 min (+) or not (-) followed by a wash). Expression levels were measured by quantitative RT-PCR analysis, normalized to the reference gene glyceraldehyde-3-phosphate

dehydrogenase (*GAPDH,* At1g13440), and plotted relative to expression levels of untreated plants. Results are average of three biological replicates. Error bars indicate S.D.

4.2.2 *At*Pep1 endocytosis and signaling are not largely impaired in the absence of BAK1

Previously, by using a bioactive fluorescently labeled *At*Pep1, designated TAMRA-*At*Pep1, we showed that *At*Pep1 undergoes receptor-mediated endocytosis (Chapter 3, this thesis). Therefore, we investigated whether BAK1 plays a regulatory role during *At*Pep1 endocytosis. For this, we evaluated the uptake of TAMRA-*At*Pep1 in root epidermal meristem cells of the null *bak1-4* mutant. Five-day-old seedlings were pulsed with 100 nM of the fluorescent probe for 10 sec, washed three times with liquid medium to remove the excess peptide (the time after the wash hereafter is referred as a chase), and imaged after 40-min chase. The intracellular accumulation of TAMRA-*At*Pep1 in *bak1-4* was similar to that of the wild type (Figure 2A and 2B). In addition, we also evaluated the TAMRA-*At*Pep1 uptake in the null mutant of BKK1, that has been proposed to act redundantly to BAK1 in PTI responses (ROUX et al., 2011), but no defects in the peptide internalization were detected. (Supplemental Figures 1A and 1B). These results suggest that BAK1 and BKK1 are either not essential for the *At*Pep1 endocytosis or their function is redundant with other SERK homologs. BAK1 and BKK1 are members of the SERK protein family of which the members are often functionally redundant (ALBRECHT et al., 2008; ROUX et al., 2011), possibly the reason for the absence of observable defects during the TAMRA-*At*Pep1 internalization. To overcome the functional redundancy of SERKs genes, we examined the TAMRA-*At*Pep1 internalization in plants lacking altogether BAK1, BKK1, and SERK1. For this assay, we used 10-day-old *serk1-8 bak1-4 bkk1-1* triple mutant plants selected from a segregation population of the described triple SERK mutant *serk1-8 bak1-4 bkk1-1* --/+-/-- (Supplemental Figure 1C) that was heterozygous for *bak1* and homozygous for the two other genes because of the cell death phenotypes (GOU et al., 2012). The uptake of the labeled TAMRA-*At*Pep1 was quantified in *serk1-8 bak1-4 bkk1-1* seedlings after 40-min chase, and found to be slightly but significantly lower than that in the Col-0 wild type (*P* values (*t* -test), * <0.05) (Supplemental Figures 1A and 1B). We also tested the endocytosis of TAMRA-*At*Pep1 in the null mutant of the receptor-like cytoplasmic kinase BIK1 (Botrytis-induced kinase 1), which had been shown to interact with PEPR1 and to modulate *At*Pep1 responses (LIU et al., 2013). Nonetheless, no defects in the internalization were observed (Figure Supplemental 1A and 1B).

To clarify the importance of BAK1 for the *At*Pep1 responses, we evaluated early and late responses triggered by this peptide in *bak1-4* null mutant. First, we examined the early responses by assessing the gene expression of the *PDF1.2* gene and of the *WRKY33* transcription factor that are induced upon *At*Pep1 treatment and the MAPK phosphorylation (HUFFAKER; PEARCE; RYAN, 2006; RANF et al., 2011; YAMAGUCHI et al., 2010). For all analysis 6-day-old *Arabidopsis* seedlings were treated with 20 nM of *At*Pep1 for 5 min, washed with ½ MS medium and maintained in the same medium until samples were collected. These experimental conditions were selected based on observations that *At*Pep1 bound its receptors very fast (Chapter 3 of this thesis), the concentration and time of elicitation were sufficient to trigger full MAPK activation (Supplemental Figure 2) and to avoid undesirable effects of peptide overexposure. Surprisingly, the expression of the *PDF1.2* gene and *WRKY33* transcription factor after *At*Pep1 elicitation was not impaired in *bak1-4* (Figures 2C and 2D), being even slightly higher than that in Col-0 after 60 min for both genes and after 180 min for *PDF1.2* only. By contrast, MAPK activation was faintly reduced in *bak1-4* in time 0 (0 min after *At*Pep1 elicitation [20 nM, 5 min]) (Figure 2E; Supplemental Figure 3), which was consistent with previous observations that reported a reduction of the MAPK activation in *bak1-4* during the first minutes after *At*Pep1 treatment (RANF et al., 2011).

Next, we analyzed the impact of *bak1-4* on the *At*Pep1-induced root growth arrest at different concentrations (Figure 2F; Supplemental Figure 4). Unexpectedly, *At*Pep1 had a stronger effect on the root growth inhibition in *bak1-4* than in Col-0. These findings imply that BAK1 is either not essential for *At*Pep1 responses or its function is redundant with other SERK proteins, similar to its effect on *At*Pep1 endocytosis. Moreover, enhanced expression of *At*Pep1-responsives genes and root growth inhibition indicate a possible role for BAK1 in attenuating *At*Pep1 responses.

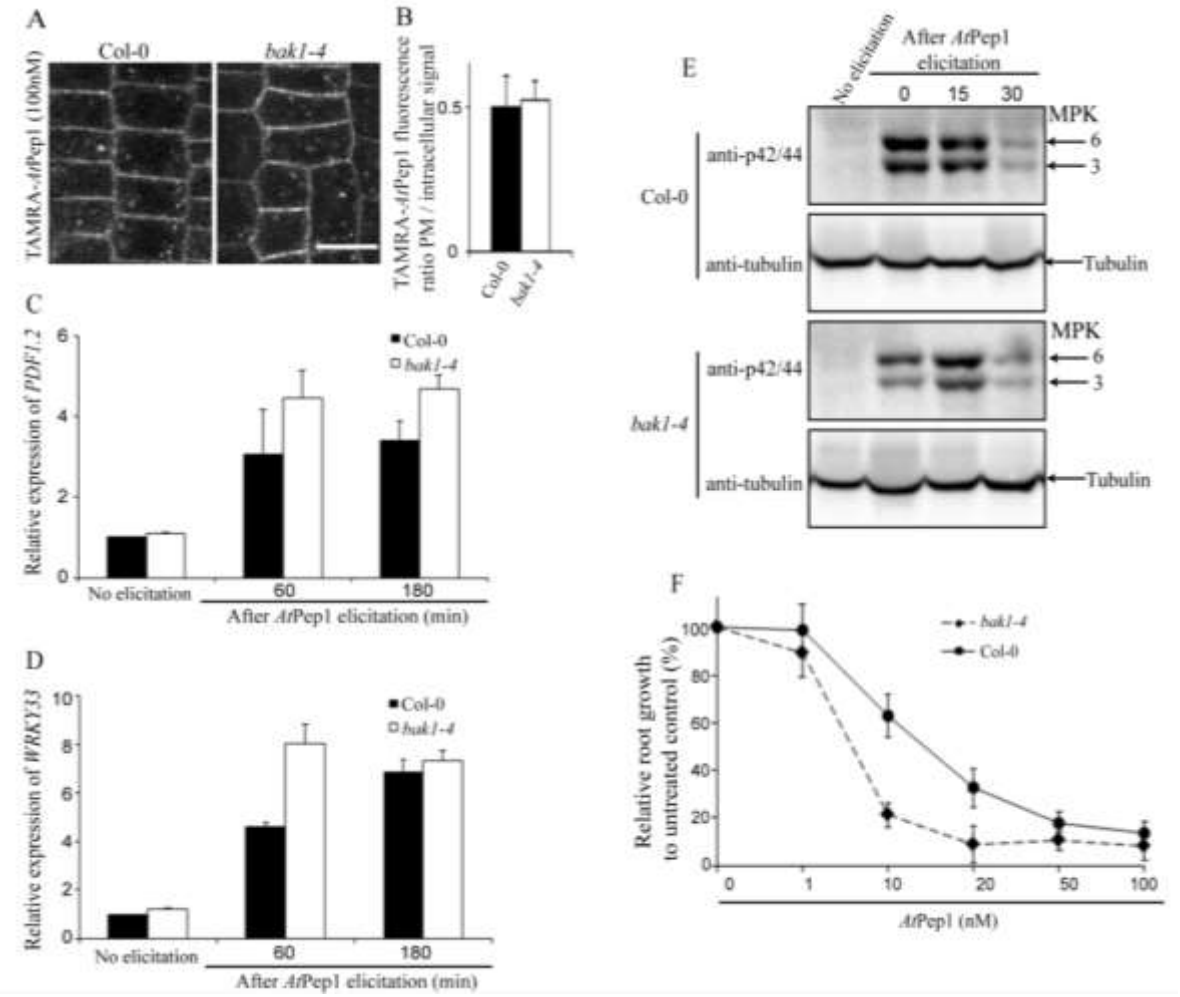

Figure 2 – Endocytosis and signaling of *At*Pep1 are not largely compromised in the null *bak1-4* mutant. (**A**) TAMRA-*At*Pep1 uptake in Col-0 and *bak1-4*. Seedlings were treated with 100 nM of TAMRA-*At*Pep1 for 10 sec and washed. Root epidermal meristem cells were imaged after a chase of 40 min. (**B**) Quantification of TAMRA-*At*Pep1 internalization of images in **A** (n = 44–51 cells). Graph presents the ratio between the plasma membrane signal intensity divided by the intracellular signal intensity. Gene expression studies of *PDF1.2* (**C)** and *WRKY33* (**D**) in Col-0 and *bak1-4* seedlings treated with *At*Pep1 (20 nM, 5 min, followed by a wash and maintained in liquid ½ medium for the indicated time). (**E**) MAPK activation monitored in 6-day-old seedlings of Col-0 (top) and *bak1-4* (bottom) after 0, 15, and 30 min of *At*Pep1 elicitation (20 nM, 5 min). MAPK activation level in plants not elicited is showed as control. MAPK phosphorylation was detected by immunoblotting with anti-phospho-p44/p42-MAPK antibody. The immunoblot with anti-tubulin shows protein loading. Individual MAPKs were identified by molecular mass and indicated by arrows. (**F**) Root growth inhibition of Col-0 and *bak1-4* at different concentrations of *At*Pep1 (n=12 plants). Root growth is presented relative to untreated control. Error bars indicate S.D. (**E – F**) these experiments were repeated at least twice with similar results

4.2.3 Defects in BAK1 phosphorylation and *BAK1* overexpression affect the *At*Pep1 internalization

We showed that the absence of BAK1 did not compromise endocytosis of TAMRA-*At*Pep1, but that the uptake of this fluorescent probe was slightly reduced in the triple *serk1-8 bak1-4 bkk1-1* mutant, suggesting that other members of the SERK family or other RK are functionally redundant with BAK1 thus, making it difficult to study the role of BAK1 alone in the *At*Pep1 internalization. Recently, a novel semi-dominant BAK1mutant, *bak1-5,* has been identified. In *bak1-5* a point mutation results in a hypoactive kinase that strongly impairs plant immune responses, but displays a normal developmental growth and is not impaired in cell death control (SCHWESSINGER et al., 2011). To gain further insights into the role of BAK1 during the *At*Pep1 internalization, we assessed the uptake of TAMRA-*At*Pep1 in *bak1-5* and in the double *bak1-5 bkk1-1* mutant (Figures 3A and 3B). Interestingly, after treatment with TAMRA-*At*Pep1 (100 nM, 10-sec pulse, three washouts, 40 min chase) most of the fluorescent signal remained in the plasma membrane and intracellular vesicles occurred rarely in both mutants. This genotype implies that BAK1 regulates the *At*Pep1 internalization and as *bak1-5* has altered phosphorylation patterns (SCHWESSINGER et al., 2011; WANG et al., 2014) this process depends probably on phosphorylation events occurring after PEPR1-BAK1 heterodimerization upon *At*Pep1 treatment.

Next, we investigated the effect of *BAK1* overexpression on the *At*Pep1 endocytosis. For that we used seedlings of the previously described transgenic *BAK1*-overexpressing line under its native promoter in the *bak1-4* mutant (*bak1-4*/proBAK1:BAK1) (NTOUKAKIS et al., 2011; SCHWESSINGER et al., 2011). The *BAK1* overexpression in this genotype was also confirmed by quantitative PCR analysis (Figure 3C). When *bak1-4*/proBAK1:BAK1 seedlings were treated with TAMRA-*At*Pep1 (100 nM, 10-sec pulse, three washouts) and imaged them after a 40-min chase, surprisingly, endocytosis of TAMRA-*At*Pep1 was blocked similarly as seen in the *bak1-5* and *bak1-5 bkk-1* mutants (Figures 3A and 3B). Hence, we examined whether the negative effect observed in *bak1-5* during the *At*Pep1 internalization was also caused by *BAK1* overexpression. However, the basal *BAK1-5* expression level was similar to that of Col-0 (Figure 3C). To investigate whether the TAMRA-*At*Pep1 endocytosis was blocked in a specific manner in this genotype, we evaluated the uptake of the endocytic tracer FM4-64 in all three backgrounds (Supplemental Figure 5). As expected, FM4-64 endocytosis was not inhibited, confirming that the TAMRA-*At*Pep1 endocytosis was blocked specifically.

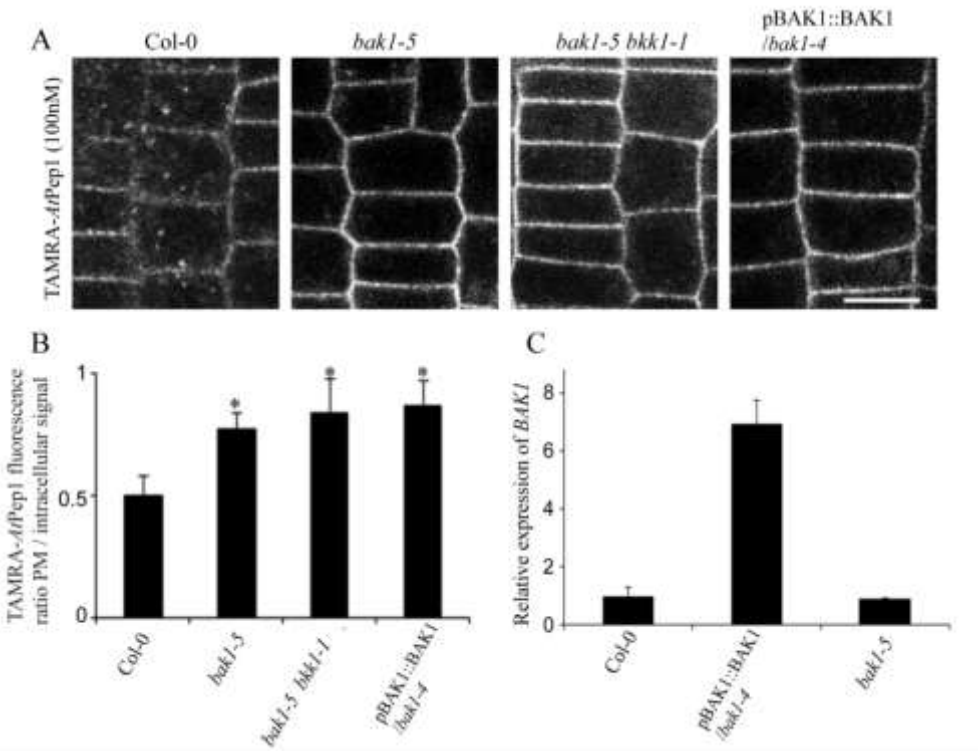

Figure 3 – Endocytosis of TAMRA-*At*Pep1 is impaired in *bak1-5* and *bak1-5 bkk1-1 Arabidopsis* mutants, and in *bak1-4*/proBAK1:BAK1overexpression line. (**A**) TAMRA-*At*Pep1 uptake in *bak1-5, bak1-5 bkk1-1*, and *bak1-4*/proBAK1:BAK1. Five-day-old seedlings were treated with 100 nM of TAMRA-*At*Pep1 for 10 sec and washed. Root epidermal meristem cells imaged after 40 min. Scale bar, 10 µm. (**B**) Quantification of TAMRA-*At*Pep1 internalization of images in (A). Graph represents the ratio between the plasma membrane signal intensity divided by the intracellular signal intensity. (n=45–49 cells). *P* values (*t*-test), *<0.001 relative to Col-0. (**C**) Expression level of *BAK1* in 6-day-old Col-0, *bak1-5*, and *bak1-4*/proBAK1:BAK1*4 Arabidopsis* seedlings. Gene expression was measured by quantitative PCR analysis, normalized to the reference gene glyceraldehyde-3-phosphate dehydrogenase (*GAPDH*, At1g13440), and plotted relative to the Col-0 expression level. Results are average of three biological replicates. Error bars indicate S.D.

4.2.4 The *Arabidopsis bak1-5* mutant and *BAK1* overexpressing plants are strongly impaired in *At*Pep1 signaling

As *bak1-5* mutant and *bak1-4*/proBAK1:BAK1 overexpression were able to block endocytosis of *At*Pep1, we examined whether the *At*Pep1 responses are also compromised in these backgrounds. Previously it has been shown that *At*Pep1-induced reactive oxygen species (ROS) burst and ethylene production are attenuated in *bak1-5* (ROUX et al., 2011). We used qRT-PCR analysis to assess the expression levels of the *At*Pep1-responsive genes *WRKY33* and *BAK1 bak1-5* mutant after *At*Pep1 elicitation (20 nM, 5 min, followed by a wash and incubation in liquid ½ MS medium for the indicated time) in (Figures 4A-4C). For the wild

type, it was already possible to detect induction of both gene expressions at 30 min after *At*Pep1 removal and the expression gradually increased until 180 min but after 240 min the *BAK1* and *WRKY*33 mRNA levels decreased (Figure 4A). In *bak1-5*, a slight induction was observed 30 to 60 min after the *At*Pep1 removal, but the expression levels of *BAK1* and *WRKY33* were not induced at the subsequent time points (Figure 4B), as seen for Col-0 (Figure 4A). For *bak1-4*/proBAK1:BAK1, the transcript levels of both genes did not change at any time point evaluated after the *At*Pep1 removal (Figure 4C). Similarly to the expression levels of the *At*Pep1-responsive genes, MAPK activation was clearly reduced in *bak1-5* and almost abolished in *bak1-4*/proBAK1:BAK1 after *At*Pep1 washout (Figure 4D). Finally, we examined the effect of different *At*Pep1 concentrations on the root growth inhibition, which is a late response ((RANF et al., 2011). *bak1-5* was less sensitive than the wild type and *bak1-4*/proBAK1:BAK1 was totally insensitive to *At*Pep1 in this assay (Figure 4E; Supplemental Figure 4). These finding showed induction of *At*Pep1-responsive genes, MAPK phosphorylation and inhibition of root growth upon *At*Pep1 elicitation are also compromised in *bak1-5* mutant. Furthermore, the increased levels of *BAK1* expression led to completely *At*Pep1 insensitive plants.

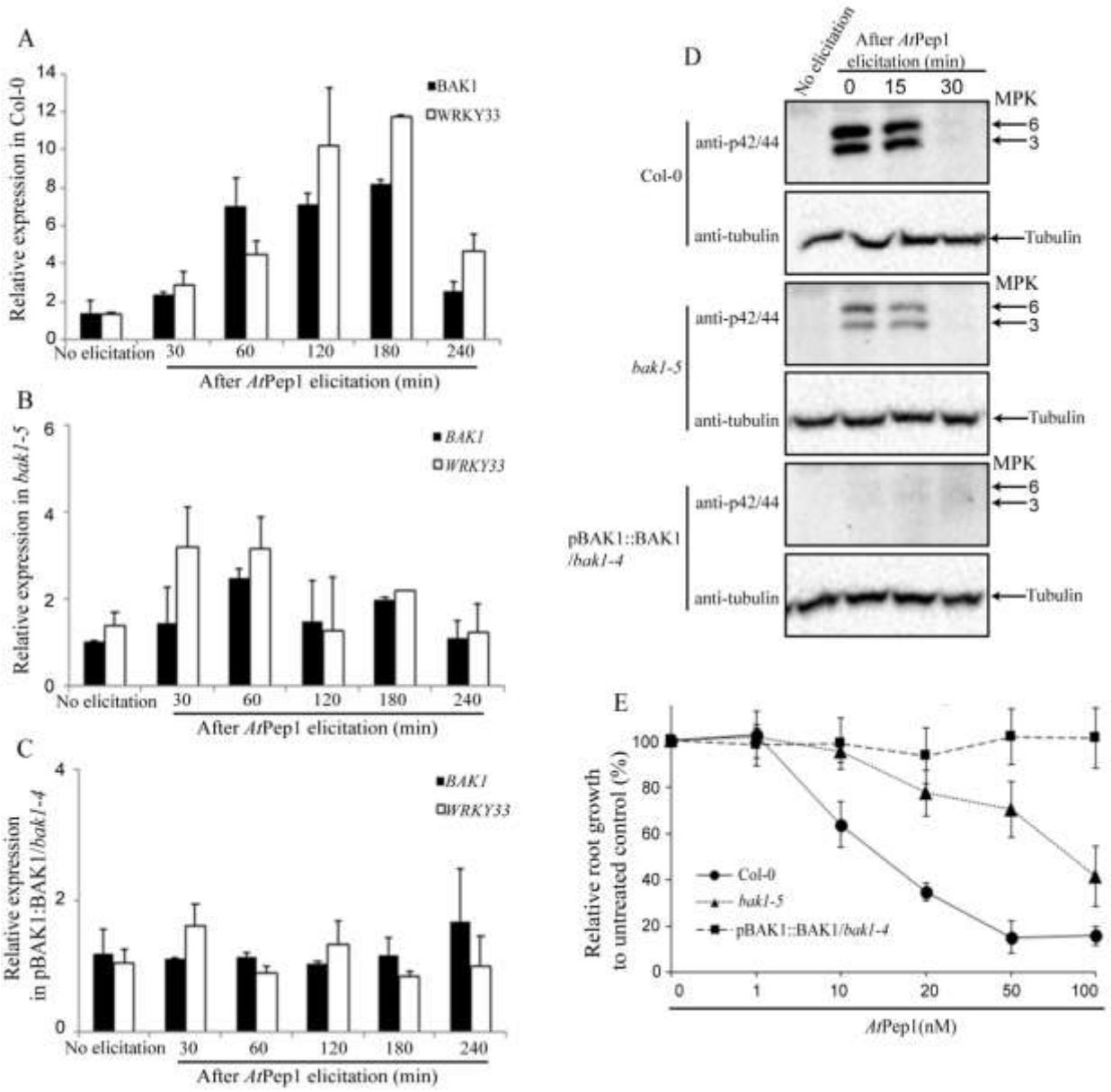

Figure 4 – Arabidopsis *bak1-5* mutant and *bak1-4*/proBAK1:BAK1overexpression line are strongly impaired in *At*Pep1-mediated signaling. *BAK1* and *WRKY33* gene expression in 6-day-old Col-0 (A), *bak1-5* (B), and *bak1-4*/proBAK1:BAK1 (C) *Arabidopsis* seedlings after *At*Pep1 elicitation (20 nM, 5 min, followed by a wash and maintained in liquid ½ medium for the indicated time). Results are average of three biological replicates. (D) MAPK activation monitored in 6-day-old seedlings of Col-0 (top), *bak1-5* (middle), and *bak1-4*/proBAK1:BAK1 (bottom) after 0, 15, and 30 min of *At*Pep1 elicitation. MAPK activation level in plants not elicited is shown as control. MAPK phosphorylation was identified by immunoblotting with anti-phospho-p44/p42-MAPK antibody. The immunoblot with anti-tubulin shows protein loading. Individual MAPKs were identified by molecular mass and indicated by arrows. (D) Root growth inhibition of Col-0, *bak1-5*, and *bak1-4*/proBAK1:BAK1at different concentrations of *At*Pep1 (n=12 plants). Root growth is presented relative to untreated control. Error bars indicate S.D. These experiments were repeated at least twice with similar results

4.2.5 BIR2, a negative regulator of BAK1, does not affect the *At*Pep1 endocytosis

Recently, BIR2 has been reported to negatively control BAK1 in his plant immunity functions by regulating BAK1 receptor complex formation (HALTER et al., 2014a). (BAK1 has been proposed to constitutively interact with BIR2 in the absence of ligands, but in their presence to be released and recruited into ligand-binding receptor complexes, like the one formed by PEPRs in the presence of *At*Pep1 (HALTER, et al., 2014b). This feature and our observation that the *At*Pep1 internalization is blocked when *BAK1* is overexpressed led us to hypothesize that the absence of BIR2 will make more BAK1 available to interact with PEPRs, causing a negative effect during the *At*Pep1 endocytosis similarly to *BAK1* overexpression. Therefore, we evaluated the TAMRA-*At*Pep1 uptake in the *bir2-1* mutant, the amiRNA-BIR2 transgenic line with reduced levels of BIR2 protein and in *BIR2*-overexpressing line (HALTER, et al., 2014a) (Figure 5A). After treatment with TAMRA-*At*Pep1 (100 nM, 10-sec pulse, 1-2 min of washout, 40 min chase) none of the mutants tested showed any defects in the internalization of the fluorescent probe, implying that the negative regulation of BAK1 by BIR2 does not affect the endocytosis of *At*Pep1.

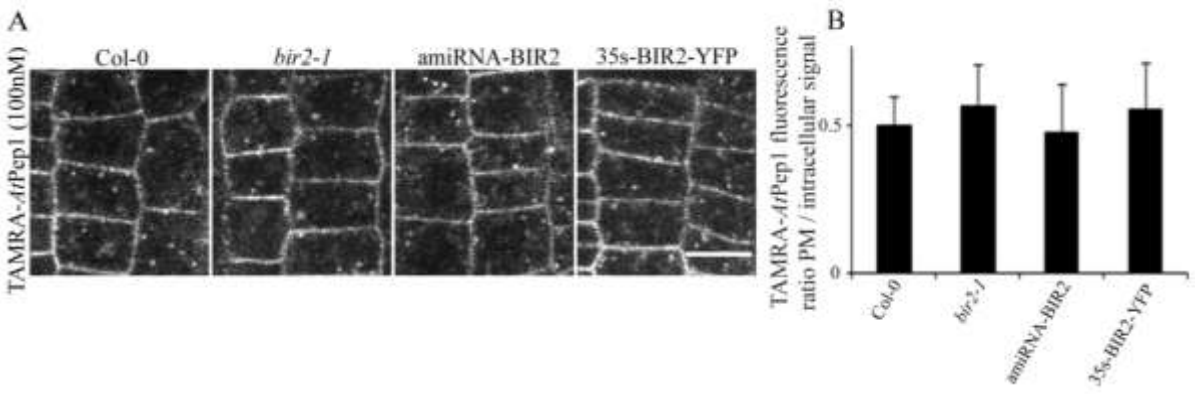

Figure 5 – Endocytosis of TAMRA-*At*Pep1 is not affected in different BIR2 genotypes. **A**) Uptake of TAMRA-*At*Pep1 in *bir2-1*, amiRNA-BIR2, and 35S-BIR2-YFP. Five-day-old seedlings were treated with 100 nM of TAMRA-*At*Pep1 for 10 sec and washed. Root epidermal meristem cells imaged after 40 min. Scale bar, 10 µm. (**B**) Quantification of TAMRA-*At*Pep1 internalization of images in (A). Graph represents the ratio between the plasma membrane signal intensity divided by the intracellular signal intensity (n=43–52 cells). Error bars indicate S.D.

4.3 Discussion

4.3.1 BAK1 interacted in a ligand-dependent manner with both *At*Pep1 receptors

BAK1 is a member of the SERK protein family known to form receptor complexes with several ligand-binding LRR RK in the plasma membrane, including BRI1, FLS2, and EFR that regulate growth responses, innate immunity, and cell death (CHINCHILLA et al., 2006; LI et al., 2002; ROUX et al., 2011). The *At*Pep1 LRR RKs, PEPR1 and PEPR2 that modulate innate immunity responses also interacted with BAK1 in a ligand-dependent manner. Indeed, previous studies have shown that cytoplasmic and extracellular domains of the *At*Pep1 receptors and BAK1 interact (POSTEL et al., 2010; TANG et al., 2015). Furthermore the formation of a heteromeric complexes consisting of *de novo* phosphorylated BAK1 and a protein matching the size of PEPR1 in *Arabidopsis* cell cultures after *At*Pep1 application was also reported (SCHULZE et al., 2010). In this study, by means of co-IP in *Arabidopsis*, we confirmed that both *At*Pep1 receptors associated with BAK1 after *At*Pep1 elicitation *in planta*, similarly to the FLS2-BAK1 and EFR-BAK1 interactions triggered by flg22 and elf18, respectively (ROUX et al., 2011; SCHWESSINGER et al., 2011). Thus, our data supported the proposed role of BAK1 as a multifunctional adaptor molecule required for the proper functionality of numerous RKs. Although the co-IP assay is not quantitative, we observed an enhanced interaction between BAK1 and PEPR1 in a stimulus-dependent manner, suggesting that affinity for BAK1 is higher in PEPR1 than in PEPR2. If this is the case, we can hypothesize that PEPR2 associates with other SERK members. Further studies are needed to clarify the importance of different PEPR1/PPER2- SERK protein complexes for *At*Pep1-induced signaling.

4.3.2 The absence of BAK1 does not affect the *At*Pep1 internalization and does not largely compromise AtPep1 responses

As BAK1 interacted with PEPR1 and PEPR2 in a ligand-dependent manner, we asked whether BAK1 is required for *At*Pep1 internalization. However, by using the null *bak1-4* mutant, we were unable to detect any defects during the internalization of the fluorescently labeled *At*Pep1 suggesting that *At*Pep1 undergoes endocytosis in a BAK1-independent manner. Nevertheless, because BAK1 is one of the five members of the SERK protein family, additional SERKs might associate with PEPRs *in vivo*. In that context, other SERK proteins would replace BAK1 in the interaction with PEPRs to allow the plant to carry out the *At*Pep1-

mediated responses and endocytosis in a proper manner. As support for this assumption we found that internalization of TAMRA-*At*Pep1 is slightly decreased in the triple *serk1-8 bak1-4/bkk1-1* mutant. A possible redundancy between different SERK proteins in the interaction with PEPRs can be responsible for the observed *At*Pep1 responses in *bak1-4*. When this mutant was stimulated with *At*Pep1, the MAPK activation was only slightly lower than that of Col-0, which is in agreement with previous studies in which Ca^{2+} elevation, ROS production, and also MAPK activation were not largely impaired in *bak1-4* (RANF et al., 2011; ROUX et al., 2011; SCHULZE et al., 2010). In contrast to the MAPK activation, the expression of *At*Pep1-responsive genes and root growth inhibition after *At*Pep1 application were enhanced in *bak1-4* as compared with the wild type, implying that BAK1 can also be required for the subsequent attenuation of the *At*Pep1 responses. The enhancement of these *At*Pep1responses could also be due to the incomplete BR perception due to lack of BRI1 co-receptor BAK1. It has been proposed that BR-mediated growth directly antagonizes PTI-responses (ALBRECHT et al., 2012), thus might be that an impaired BR-signaling in *bak1-4* renders this genotype hypersensitive to root growth inhibition and activation of *At*Pep1-responsive genes.

BAK1 has been reported to differentially contribute to responses induced by different MAMPs. The flg22-induced early and late responses are both altered in *bak1-4*, whereas early but not late signaling, responses are compromised by elf18 (CHINCHILLA et al., 2007; RANF et al., 2011; SCHWESSINGER et al., 2011). These dissimilarities between signaling responses induced by different elicitor molecules in the *bak1-4* mutant might reflect different interactions between the ligand-binding LRR RKs and the SERK proteins. Redundancy of SERK proteins has already been reported for BRI1 that, besides forming a ligand-induced complex with BAK1, can also complex with SERK1 and BKK1 (HE et al., 2007; KARLOVA et al., 2006; LI et al., 2002). Similar results have been obtained for the FLS2 and EFR receptors upon elicitation with flg22 and elf18, respectively, revealing that FLS2 preferentially interacts with BAK1 and potentially with SERK2, whereas EFR strongly interacts with SERK1, SERK2, BAK1, and BKK1 (ROUX et al., 2011). In view of these reports and our findings, we propose that BAK1 is not a limiting component of *At*Pep1 signaling and endocytosis and those additional SERK proteins are most likely part of the PEPR1 and PEPR2 complexes.

4.3.3 *At*Pep1 endocytosis and signaling depend on BAK1 activation

Because elucidation of the role of BAK1 during *At*Pep1 endocytosis and signaling is hampered by the SERK redundancy we examined *At*Pep1 internalization and *At*Pep1 responses in the *bak1-5* mutant. The full-length mutant BAK1-5 transcripts accumulated in *bak1-5* at levels similar to those of the wild type, which is in agreement with previous reports (SCHWESSINGER et al., 2011). Thus, we expected that in the *bak1-5* mutant BAK1-5 protein would not be replaced by other SERKs . Furthermore, *bak1-5* is impaired exclusively in plant immune responses, displaying a wild type-like BR signaling capacity and normal developmental growth (SCHWESSINGER et al., 2011). This observation allowed us to obtain more accurate results than those with the triple *serk1-8 bak1-4 bkk1-1* mutant, of which the seedling present lethality phenotypes and misshapen root meristem tip cells approximately 2 weeks after germination (GOU et al., 2012).

Interestingly, in contrast to *bak1-4*, the endocytosis of TAMRA-*At*Pep1 was undoubtedly blocked in *bak1-5* seedlings. As *bak1-5* is a hypoactive kinase with a corresponding C408Y amino acid mutation located just before the catalytic loop of the kinase domain (SCHWESSINGER et al., 2011), this phenotype could be attributed to defects in the PEPR-BAK1 complex activation by phosphorylation. Different studies have revealed that after the LRRRKs-BAK1 complexes formation in a ligand-dependent manner subsequent phosphorylation events occurred, which are important to regulate the multiple signaling pathways where BAK1 is involved (SCHULZE et al., 2010; SCHWESSINGER et al., 2015; WANG et al., 2014). Interestingly, in the animal field phosphorylation has been shown to regulate CME of many plasma membrane cargoes including receptors (DELOM; FESSART, 2011; SLEPNEV et al., 1998). Therefore, it is tempting to speculate that phosphorylation events of PEPR-BAK1 (or other SERK) complexes provide the mechanism to recruit the endocytosis machinery responsible for the internalization of *At*Pep1-PEPRs. Further work would involve the investigation of the effects of different phosphorylation events on BAK1 or PEPRs on *At*Pep1-PEPRs endocytosis.

Another possible explanation for the blocking of the *At*Pep1 endocytosis is the possibility that BAK1-5 mutation is somehow over stabilizing the complex with PEPRs in the plasma membrane even without *At*Pep1 elicitation and preventing the internalization of the *At*Pep1-PEPRs complexes. This assumption is based on a report in which BAK1-5 displayed interaction with FLS2 and EFR in a ligand-independent manner, and that the amount of BAK1-5 in complex with these receptors after flg22 or elf18 treatment was greater than in the case of BAK1 (SCHWESSINGER et al., 2011). However, it remains to be clarified whether

BAK1-5 also constitutively interacts with PEPRs. As the interaction between BRI1 and BAK1-5 is also enhanced both dependent and independent of brassinolide (the most bioactive BR) whereas the BR signaling of *bak1-5* is normal (SCHWESSINGER et al., 2011), it would be interesting to evaluate whether the internalization of the fluorescent BR analog (IRANI et al., 2012) that is mediated by BRI1 is also blocked in *bak1-5*.

As the endocytosis of TAMRA-*At*Pep1 was blocked in *bak1-5*, it was important to test whether the *At*Pep1 responses are also impaired. Indeed, we found that induction of the *At*Pep1-responsive genes, the MAPK activation, and root growth inhibition were strongly impaired in *bak1-5*, in agreement to what had been previously reported in the evaluation of ROS and ethylene production induced by *At*Pep1 (ROUX et al., 2011).

Altogether, these observations indicate that the formation of an *At*Pep1-dependent active PEPR-BAK1 (or other SERK) signaling receptor complexes is required to accomplish *At*Pep1 endocytosis and signaling. Previously, we have revealed that *At*Pep1-PEPRs are internalized as complexes to the lytic vacuole (Chapter 3, this thesis). Hence, it would be interesting to further investigate whether BAK1 is also internalized with *At*Pep1-PEPR complexes.

4.3.4 Overexpression of BAK1 blocks *At*Pep1 endocytosis and abolishes *At*Pep1 signaling

Additionally, we also evaluated the impact of *BAK1* overexpression on *At*Pep1 endocytosis and signaling. Surprisingly, we found that the transgenic line *bak1-4*/proBAK1:BAK1 with increased *BAK1* transcript levels and BAK1 protein respectively (NTOUKAKIS et al., 2011) blocked the endocytosis of TAMRA-*At*Pep1 and inhibited *At*Pep1-induced early and late responses nearly completely. This effect suggests that BAK1 can function as a negative regulator of *At*Pep1-mediated responses when overexpressed. Interestingly, during this study, we also found out that the expression of *BAK1* is induced upon *At*Pep1 stimulation and that *At*Pep1-responsive genes and root growth inhibition are enhanced in the null *bak1-4* mutant. Although merely speculative, these facts allow us to hypothesize that BAK1, in addition to its regulatory role at the early stages of *At*Pep1 endocytosis and signaling, is also required later to attenuate and balance the system after *At*Pep1 elicitation.

In an attempt to test this hypothesis, we assessed the uptake of TAMRA-*At*Pep1 in plants with different levels of BIR2 protein. BIR2 has been previously shown to interact with BAK1 and to act as a negative regulator of BAK1 in plant immunity (HALTER et al., 2014a). We hypothesized that the absence of BIR2 would increase the amounts of the available for

PEPRs interaction BAK1 and it will cause *At*Pep1 endocytosis defects as observed in *BAK1* overexpression. However, we were not able to observe defects in the internalization of TAMRA-*At*Pep1 in *bir2-1* mutants, *amiRNA-BIR2* transgenic line or in plans overexpressing *BIR2*. As in *bir2-1* mutants and amiRNA-BIR2 lines still low BIR2 protein levels are present, it is possible that the effect in BAK1-free levels is not strong enough to cause a phenotype that can be detected in our uptake assay. Thus, further experiments that assess the effect of different *BAK1* expression levels in *At*Pep1 endocytosis and signaling as well as the characterization of the interaction within BAK1 and *At*Pep1 receptors would bring extra information for a better understanding of this phenotype.

Author contribution

F. A. Ortiz-Morea and E. Russinova conceived the study and designed the experiments. F. A Ortiz-Morea performed all imaging, MAP Kinase, root growth assays and generated materials. Y. Luo did the coimunoprecipitation experiments. K. Dressano and F.A. Ortiz-Morea performed qRT-PCR analysis. F.A. Ortiz-Morea and D. S. Moura synthesized the TAMRA-*At*Pep1 probe. F. A. Ortiz-Morea and E. Russinova wrote the manuscript.

Acknowledgements

We thank Cyril Zipfel (The Sainsbury Laboratory, Norwich, UK) for sharing BAK1 antibodies and *bak1-4, bak1-5, bkk1-1, bak1-5 bkk1-1*and *bak1-4*/proBAK1:BAK1 genotypes, Birgit Kemmerling (ZMBP, University Tübingen, Germany) for sharing *bir2-1*, amiRNA-BIR2, and 35S-BIR2-YFP lines, Daniël Van Damme and Evellien Mille (VIB/UGent, Belgium) for advice in microscopy and Martine De Cock (VIB/UGent, Belgium) for help in preparing the manuscript. Ortiz-Morea F. A. is indebted to the BOF Special Research founding of the Flemish Government for a Joint Doctorate fellowship at Ghent University and to the PEC-PG program of the Coordenação de Aperfeiçoamento de Pessoal de Nível Superior CAPES Brazil for the Doctorate fellowship at Universidade de São Paulo.

4.4 Materials and Methods

4.4.1 Plant material and growth conditions

All mutants and transgenic lines of *Arabidopsis thaliana* (L.) Heynh used in this study were in the Columbia (Col-0) background. The *Arabidopsis* seeds were sterilized, maintained for 2 days at 4°C in the dark, and germinated on vertical ½MS medium (1% [w/v] sucrose) agar plates, pH 5.8 at 22°C in a 16 h/8 h light/dark cycle. The mutants and transgenic plants have been described previously: *bak1-4* (CHINCHILLA et al., 2007), *bak1-5* and *bak1-*

4/proBAK1:BAK1 (SCHWESSINGER et al., 2011), *bkk1-1* (HE et al., 2007), *serk1-8 bak1-4 bkk1-1* (GOU et al., 2012), *bik1-1* (LU et al., 2010), and *bir2-1*, *amiRNA-BIR2*, and p35S:BIR2-YFP (HALTER et al., 2014b). proRPS5A::PEPR1-GFP and proRPS5A::PEPR2-GFP were previously described (Chapter 3, this thesis).

4.4.2 Peptides and molecular probes

Peptide AtPep1 (ATKVKAKQRGKEKVSSGRPGQHN) with HPLC purity of 95.16% and molecular weight of 2491.78, and peptide AtPep1 labeled with 5-carboxytetramethylrhodamine at the N-terminus (TAMRA-AtPep1) with HPLC purity of 97.07% and molecular weight of 2905.75 were purchased from Life Technologies. The peptides were dissolved in water to obtain peptides stocks of 100 µM; further dilutions were done with ½MS medium. FM4-64 was acquired from Molecular Probes (2mM water stock).

4.4.2 Co-immunoprecipitation

Seven-day-old seedlings were dipped for 5 min into 2 mL of ½MS medium supplemented or not with 20 nM of *At*Pep1. The material was collected and ground to a fine powder in liquid nitrogen, and per g tissue powder 1 mL extraction buffer [20 mM Tris-HCl, pH 7.5; 100 mM NaCl; 10% glycerol; 1 mM EDTA; 0.2% NP-40; 1% proteinase inhibitor (Sigma-Aldrich; 1 mM PMSF (Sigma-Aldrich)] was added. Samples were centrifuged twice at 12,700 rpm (4°C, 30 min). Protein extracts (1.5 mL) were immunoprecipitated by addition of 20 µL of GFP-Trap coupled to agarose beads (Chromotek) and incubated at 4°C for 2 h. After centrifugation (2 min, 4°C, 500 rpm), beads were washed three times with 500 µL of washing buffer (20 mM Tris-HCl, pH 7.5; 100 mM NaCl; 0.2% NP-40). Immunoprecipitates were eluted with 60 µL elution buffer (20 µL washing buffer + 20 µL 4× Laemmli Sample Buffer [Bio-Rad]) and heated at 70°C for 10 min, followed by centrifugation (2 min, 4°C, 500 rpm).

4.4.3 SDS-PAGE and immunoblotting

Proteins were separated by SDS-PAGE with 10 % precast polyacrylamide gels (Bio-Rad) and blotted onto PVDF membranes (Bio-Rad). Immunoblots were blocked with 1.5% skimmed milk powder (Difco BD) in 1× Tris-buffered saline Tween 0.1% (TBS-T) for 2 h. Subsequently, the membrane washed 3× with TBS-T. Primary antibodies were diluted in blocking solution to the following concentrations and incubated for 1 h: anti-BAK1 (1:500; Eurogentec) and anti-GFP (1:1000; Clontech). Membranes were washed 3× in TBS-T before a 1 h incubation with the secondary antibody anti-rabbit-HRP conjugated for anti-BAK1

detection (1:10,000; GE-Healthcare) or and anti-mouse-HRP conjugated for anti-GFP detection (1:10,000; GE-Healthcare). Signals were visualized with chemiluminescent substrate (lightning plus-ECL; PerkinElmer) before exposure to film (GE-Healthcare).

4.4.4 Real-time quantitative PCR

Six-day-old seedlings were used for all gene expression experiments. Total RNA was extracted with Trizol reagent (Life Technologies) according to the manufacturer's instructions, followed by DNAse I treatment (Life Technologies) to remove any residue of genomic DNA, and quantified with a Nanodrop spectrophotometer (Thermo Scientific). cDNa was synthesized from 1 µg total RNA with Improm-II Reverse Transcriptase (Promega). Real-Time quantitative PCR analysis was done with 10-fold-diluted cDNA, Maxima SyBR Green Rox/qPCR Master Mix (Thermo Scientific), and a StepOne™ Real-Time PCR System (Applied Biosystems). The *At*Pep1-induced genes *BAK1*, *WRKY33*, and *PDF1.2* were analyzed. The *GAPDH* gene was used as a control. The primers used are described in Supplementary Table 1. A template-free reaction was used as a negative control. Three replicates were analyzed for each biological sample and three biological samples were analyzed. The threshold cycle (CT) was determined automatically by the instrument and the equation $2^{-\Delta\Delta CT}$ (Livak and Schmittgen, 2001) was used to calculate the fold change in each gene. An arbitrary value of 1 was attributed to control treatments.

4.4.5 Imaging

Arabidopsis seedlings were imaged on a FluoView 1000 inverted confocal microscope (Olympus) equipped with a water-corrected 60× objective (NA1.2) at digital zoom 3. TAMRA-*At*Pep1 and FM4-64 were excited at 559 nm, and fluorescence emission was captured between 570–670 nm. The signal intensity was manipulated with the Olympus software.

4.4.6 TAMRA-*At*Pep1 internalization

Five-day-old seedlings were dipped into 200 µL of 100 nM of TAMRA-*At*Pep1 dissolved in ½MS medium for 10 sec, washed with ½MS liquid medium three times, and kept in 500 µL ½MS medium over a piece of parafilm placed in a Petri plate. The meristems of epidermal root tip cells were imaged after 40-min chase. In the case of the triple mutant *serk1-8 bak1-4 bkk1-1*, 10-day-old seedlings were used. Images were quantified with imageJ. To this end, the first images were converted to 8-bit images; subsequently, the entire plasma membrane of individual cells were selected with the brush tool size 5 pixels as well as the

intracellular space with the polygon selection tool; then, the average intensity of the top 100 highest pixels for both plasma membrane and intracellular space was used to obtain a ratio between plasma membrane and intracellular fluorescence. Six epidermal cells from eight plants were quantified

4.4.7 FM4-64 uptake

Five-day-old seedlings were dipped for 5 min into 1 mL ½MS liquid medium containing 4 µM of FM4-64, washed with ½ MS liquid medium three times, and kept in 1 mL ½MS medium over a piece of parafilm placed in a Petri plate. The meristems of epidermal root tip cells were imaged after a 30-min chase.

4.4.8 MAP kinase assay

Six-day-old seedlings were dipped into 2 mL of 20 nM *At*Pep1 dissolved in ½MS medium for 5 min, washed with ½MS liquid medium three times, and kept in 2 mL ½MS medium for the indicated time points (0, 15, and 30 min). Seedlings were treated with water for 5 min instead of 20 nM *At*Pep1 as control. Per each time point, 50-60 seedlings were ground to a fine powder in liquid nitrogen and solubilized in better lacus buffer [50 mM Tris-HCl, pH 7.5; 100 mM NaCl; 15 mM EGTA; 10 mM $MgCl_2$; 1 mM NaF; 1 mM $Na_2MoO_4.2H_2O$; 0.5mM $NaVO_3$; 30mM b-glycerophosphate; 0.1% IGEPAL CA 630; 100 nM calyculin A (CST); 0.5 mM PMSF; 1% protease inhibitor cocktail (Sigma-Aldrich)] (SCHWESSINGER et al., 2011). The extracts were vortexed, kept on ice for 15 min, vortexed for 1 min, centrifuged at 12,700 rpm (4°C, 25 min), and supplemented with 5× SDS loading buffer. An aliquot of the supernatant was poured in a new tube before addition of SDS loading buffer to quantify proteins with the Bradford assay (Bio-Rad). Twenty mg of total protein was separated by SDS-PAGE with 10% precast polyacrylamide gels (Bio-Rad) and blotted onto PVDF membranes (Bio-Rad). Immunoblots were blocked with bovine serum albumin (BSA) 5% (w/v) (Sigma-Aldrich) in 1× TBS-T for 2 h. Subsequently, the membrane was washed 3× with TBS-T and incubated overnight at 4°C with anti-p42/44 MAPK primary antibodies (1:2000; Cell Signaling Technology) diluted in 1× TBS-T supplemented with 5% BSA. Membranes were washed 3× with TBS-T before incubation for 2 h with anti-rabbit-HRP conjugated secondary antibody (1:20,000; Sigma-Aldrich). Signals were visualized with chemiluminescent substrates (lightning plus-ECL; PerkinElmer) before exposure to film. Finally, the immunoblot was reprobed with anti-tubulin antibody (1:50,000; Sigma-Aldrich) to determine equal loading.

4.4.9 Root growth assay

Seeds were sown on ½MS solid medium, stratified for 2 days at 4°C in the dark, and grown vertically in the light. Four days after germination, seedlings were transferred to square transparent Petri dishes with solid ½MS medium supplemented with the indicated amounts of *At*Pep1 and incubated for 4 further days; then, the plates were scanned and the root growth measured from the point where the root was transferred to the new medium. For measurements, scanned images were processed and evaluated with the Rootreader2D software (http://www.plantmineralnutrition.net/rr2d.php) and blotted relative to untreated controls.

4.4.10. Statistical analysis

P values were calculated with a two-tailed Student's *t*-test by means of the Excel software.

Supplemental Figures

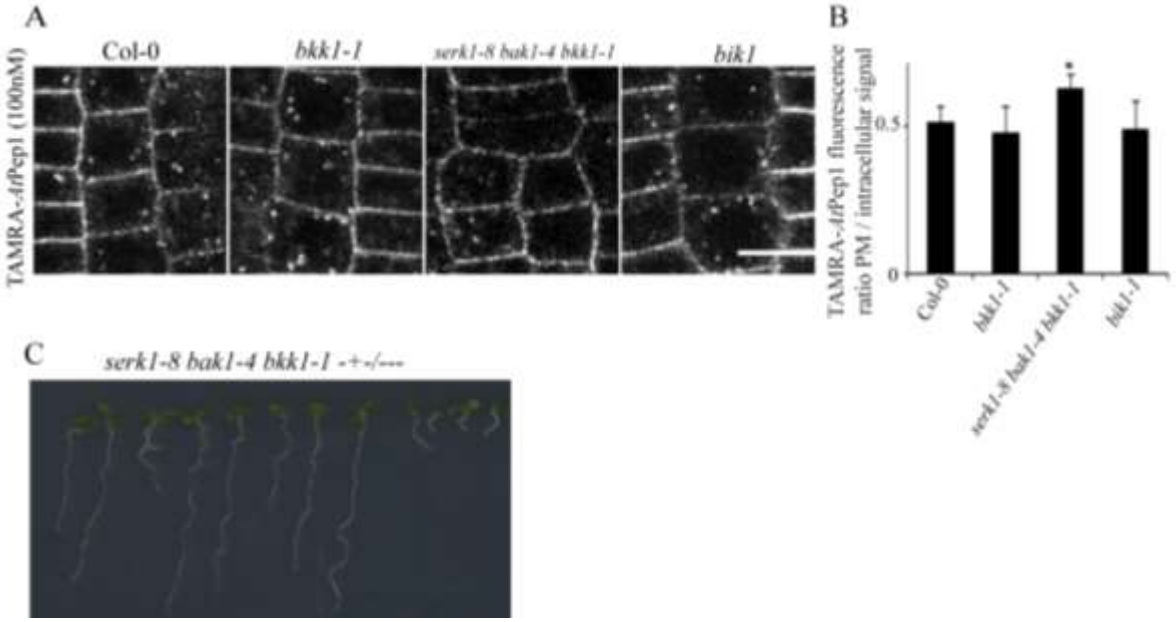

Supplemental Figure 1 – Uptake of TAMRA-*At*Pep1 in different mutants defective in *At*Pep1 responses. (A) Uptake of TAMRA-*At*Pep1 in Col-0, *bkk1-1*, *serk1-8 bak1-4 bkk1-1*, and *bik1*. Five-day-old seedlings were treated with 100 nM of TAMRA-*At*Pep1 for 10 sec and washed. Root epidermal meristem cells imaged after 40 min chase. For *serk1-8 bak1-4 bkk1*, 10-day-old seedlings were used. Scale bar, 10 µm. (**B**) Quantification of TAMRA-*At*Pep1 internalization of images in (A). Graph represents the ratio between the plasma membrane signal intensity divided by the intracellular signal intensity (n = 42–51 cells). Error bars indicate S.D. *P* values (*t*-test), *<0.05 relative to Col-0 (**C**) Representative image of the phenotypes in 10-day-old seedlings of the triple heterozygous SERK mutant *serk1-8 bak1-4 bkk1* -+-/---. Scale bar 10 µm

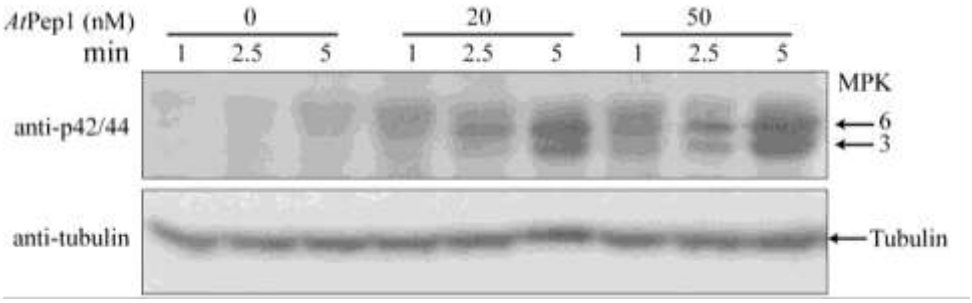

Supplemental Figure 2 – Early MAPK activation induced by *At*Pep1. MAPK activation was monitored in 6-day-old seedlings of Col-0 in the presence of 0, 20, or 50 nM of *At*Pep1 for 1, 2.5, and 5 min. MAPK phosphorylation was identified by immunoblotting with anti-phospho-p44/p42-MAPK antibody. The immunoblot with anti-tubulin shows protein loading. Individual MAPKs are identified by molecular mass and indicated by arrows

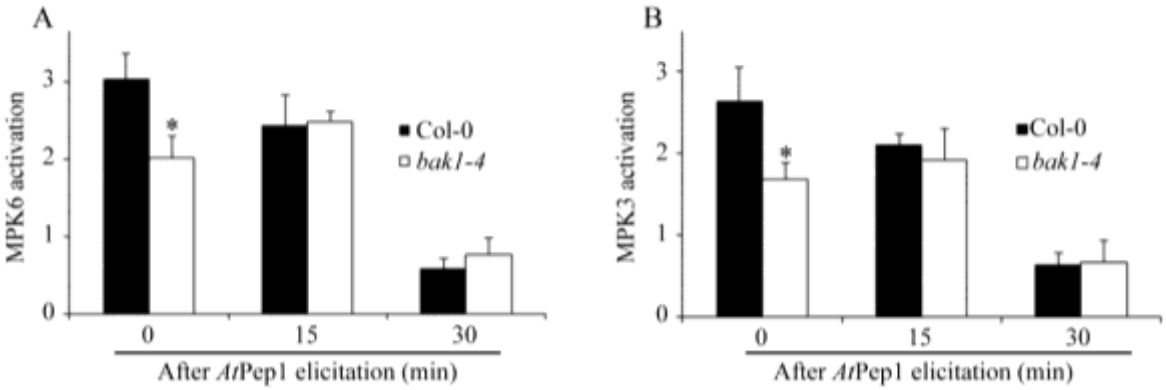

Supplemental Figure 3 – Early MAPK activation induced by *At*Pep1 is slightly reduced in *bak1-4*. Bar graphs shows relative MPK6 (A) and MPK3 (B) in 6-day-old seedlings of Col-0 and *bak1-4* after 0, 15, and 30 min of *At*Pep1 elicitation (20 nM, 5 min, followed by a wash and maintained in ½ liquid medium for the indicated time). MAPK phosphorylation was detected by immunoblotting with anti-phospho-p44/p42-MAPK antibody. Normalization was performed against loading (anti-tubulin) and untreated plants. Error bars indicate S.D. of three biological replicates. *P* values (*t*-test), *<0.05.

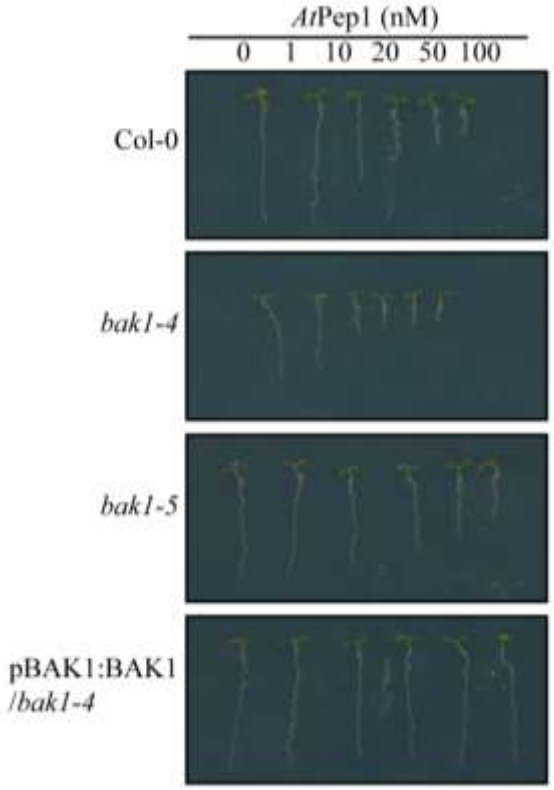

Supplemental Figure 4 – Phenotypes of Col-0, *bak1-4*, *bak1-5*, and *bak1-4*/proBAK1:BAK1 *Arabidopsis* seedling. Plants were grown on ½MS medium supplemented with 0, 1, 10, 20, 50 or 100 nM *At*Pep1.

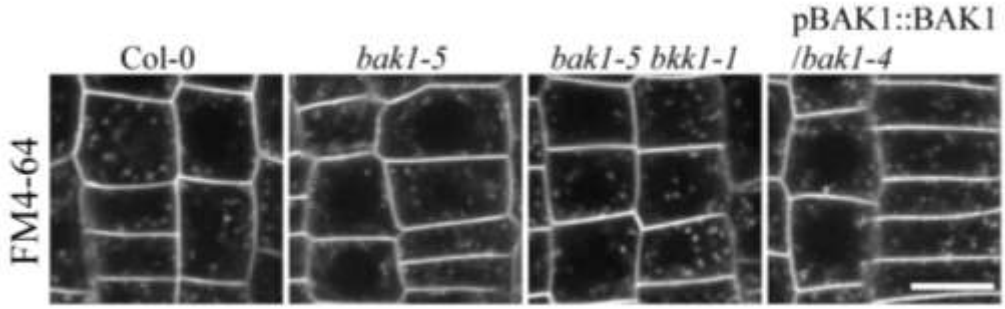

Supplemental Figure 5 - Uptake of the endocytic tracer dye FM4-64 after 30min in root meristem epidermal cells of Col-0, *bak1-5*, *bak1-5 bkk1-1*, and *bak1-4*/proBAK1:BAK1. Scale bar 10µm.

Supplemental Table 1 – Primer used for qPCR analysis

Gene	**Primer**	**Sequence 5' – 3'**
GAPDH	Forward	TTGGTGACAACAGGTCAAGCA
	Reverse	AAACTTGTCGCTCAATGCAA
BAK1	Forward	CTGGACAGCTCGTAATGCAA
	Reverse	GCTCACCAATTCCGTCAGAT
WRKY33	Forward	GAAACAAATGGTGGGAATGG
	Reverse	TGTCGTGTGATGCTCTCTCC
PDF1.2	Forward	AACCTTGAAGGAGCCAAACA
	Reverse	CACACGATTTAGCACCAAAGA

References

AAN DEN TOORN, M.; ALBRECHT, C.; DE VRIES, S. On the origin of SERKs: bioinformatics analysis of the somatic embryogenesis receptor kinases. **Molecular Plant**, Saint Paul, v.8, n. 5, p.762-782, 2015.

ALBRECHT, C.; BOUTROT, F.; SEGONZAC, C.; SCHWESSINGER, B.; GIMENEZ-IBANEZ, S.; CHINCHILLA, D.; RATHJEN, J. P.; DE VRIES, S. C.; ZIPFEL, C. Brassinosteroids inhibit pathogen-associated molecular pattern–triggered immune signaling independent of the receptor kinase BAK1. **Proceedings of the National Academy of Sciences,** Washington, v. 109, n. 1, p. 303-308, 2012.

BARTELS, S.; BOLLER, T. Quo vadis, Pep? Plant elicitor peptides at the crossroads of immunity, stress and development. **Journal of Experimental Botany**, Oxford, 2015. Disponível em: <http://jxb.oxfordjournals.org/content/early/2015/04/23/jxb.erv180.full>. Acesso em: 29 maio 2015.

BARTELS, S.; LORI, M.; MBENGUE, M.; VAN VERK, M.; KLAUSER, D.; HANDER, T.; BONI, R.; ROBATZEK, S.; BOLLER, T. The family of Peps and their precursors in Arabidopsis: differential expression and localization but similar induction of pattern-triggered immune responses. **Journal of Experimental Botany**, Oxford, v. 64, n. 17, p. 5309-5321, 2013.

CHINCHILLA, D.; BAUER, Z.; REGENASS, M.; BOLLER, T.; FELIX, G. The Arabidopsis receptor kinase FLS2 binds flg22 and determines the specificity of flagellin perception. **The Plant Cell**, Rockville, v. 18, n. 2, p. 465-476, 2006.

CHINCHILLA, D.; ZIPFEL, C.; ROBATZEK, S.; KEMMERLING, B.; NURNBERGER, T.; JONES, J.D.; FELIX, G.; BOLLER, T. A flagellin-induced complex of the receptor FLS2 and BAK1 initiates plant defence. **Nature**, London, v. 448, n. 7152, p. 497-500, 2007.

DELOM, F.; FESSART, D. Role of Phosphorylation in the Control of Clathrin-Mediated Internalization of GPCR **International Journal of Cell Biology,** New York, v. 2011, p. 246954, 2011.

GAO, M.; WANG, X.; WANG, D.; XU, F.; DING, X.; ZHANG, Z.; BI, D.; CHENG, Y.T.; CHEN, S.; LI, X.; ZHANG, Y. Regulation of cell death and innate immunity by two receptor-like kinases in Arabidopsis. **Cell Host & Microbe,** Cambridge, v. 6, n. 1, p. 34-44, 2009.

GOMEZ-GOMEZ, L.; BOLLER, T. FLS2: an LRR receptor-like kinase involved in the perception of the bacterial elicitor flagellin in Arabidopsis. **Molecular Cell**, Cambridge, v. 5, n. 6, p. 1003-1011, 2000.

GOU, X.; YIN, H.; HE, K.; DU, J.; YI, J.; XU, S.; LIN, H.; CLOUSE, S.D.; LI, J. Genetic evidence for an indispensable role of somatic embryogenesis receptor kinases in brassinosteroid signaling. **PLoS Genetics,** San Francisco, v. 8, n. 1, p. e1002452, 2012.

HALTER, T.; IMKAMPE, J.; BLAUM, B.S.; STEHLE, T.; KEMMERLING, B. BIR2 affects complex formation of BAK1 with ligand binding receptors in plant defense. **Plant Signaling & Behavior**, Georgetown, v. 9, n. 6, p 134-143, 2014.

HALTER, T.; IMKAMPE, J.; MAZZOTTA, S.; WIERZBA, M.; POSTEL, S.; BUCHERL, C.; KIEFER, C.; STAHL, M.; CHINCHILLA, D.; WANG, X.; NURNBERGER, T.; ZIPFEL, C.; CLOUSE, S.; BORST, J.W.; BOEREN, S.; DE VRIES, S.C.; TAX, F.; KEMMERLING, B. The leucine-rich repeat receptor kinase BIR2 is a negative regulator of BAK1 in plant immunity. **Current biology,** London, v. 24, n. 2, p. 134-143, 2014.

HE, K.; GOU, X.; YUAN, T.; LIN, H.; ASAMI, T.; YOSHIDA, S.; RUSSELL, S.D.; LI, J. BAK1 and BKK1 regulate brassinosteroid-dependent growth and brassinosteroid-independent cell-death pathways. **Current Biology,** London, v. 17, n. 13, p. 1109-1115, 2007.

HECHT, V.; VIELLE-CALZADA, J.P.; HARTOG, M.V.; SCHMIDT, E.D.; BOUTILIER, K.; GROSSNIKLAUS, U.; DE VRIES, S.C. The Arabidopsis somatic embryogenesis receptor kinase 1 gene is expressed in developing ovules and embryos and enhances embryogenic competence in culture **Plant Physiology,** Lancaster, v. 127, n. 3, p. 803-816, 2001.

HOU, S.; WANG, X.; CHEN, D.; YANG, X.; WANG, M.; TURRA, D.; DI PIETRO, A.; ZHANG, W. The secreted peptide PIP1 amplifies immunity through receptor-like kinase 7. **PLoS Pathogens,** San Francisco,v. 10, n. 9, p. e1004331, 2014.

HUFFAKER, A.; PEARCE, G.; RYAN, C.A. An endogenous peptide signal in Arabidopsis activates components of the innate immune response. **Proceedings of the National Academy of Sciences of the United States of America,** Washington, v. 103, n. 26, p. 10098-10103, 2006.

IRANI, N.G.; DI RUBBO, S.; MYLLE, E.; VAN DEN BEGIN, J.; SCHNEIDER-PIZON, J.; HNILIKOVA, J.; SISA, M.; BUYST, D.; VILARRASA-BLASI, J.; SZATMARI, A.M.; VAN DAMME, D.; MISHEV, K.; CODREANU, M.C.; KOHOUT, L.; STRNAD, M.; CANO-DELGADO, A.I.; FRIML, J.; MADDER, A.; RUSSINOVA, E. Fluorescent castasterone reveals BRI1 signaling from the plasma membrane. **Nature Chemical Biology,** London, v. 8, n. 6, p. 583-589, 2012.

KARLOVA, R.; BOEREN, S.; RUSSINOVA, E.; AKER, J.; VERVOORT, J.; DE VRIES, S. The Arabidopsis somatic embryogenesis receptor-like kinase1 protein complex includes brassinosteroid-insensitive1. **The Plant Cell**, Rockville, v. 18, n. 3, p. 626-638, 2006.

KROL, E.; MENTZEL, T.; CHINCHILLA, D.; BOLLER, T.; FELIX, G.; KEMMERLING, B.; POSTEL, S.; ARENTS, M.; JEWORUTZKI, E.; AL-RASHEID, K.A.; BECKER, D.; HEDRICH, R. Perception of the Arabidopsis danger signal peptide 1 involves the pattern recognition receptor AtPEPR1 and its close homologue AtPEPR2. **The Journal of biological chemistry,** Baltimore, v. 285, n. 18, p. 13471-13479, 2010.

LI, J.; WEN, J.; LEASE, K.A.; DOKE, J.T.; TAX, F.E.; WALKER, J.C. BAK1, an Arabidopsis LRR receptor-like protein kinase, interacts with BRI1 and modulates brassinosteroid signaling. **Cell**, Cambridge, v. 110, n. 2, p. 213-222, 2002.

LIU, Z.; WU, Y.; YANG, F.; ZHANG, Y.; CHEN, S.; XIE, Q.; TIAN, X.; ZHOU, J. M. BIK1 interacts with PEPRs to mediate ethylene-induced immunity. **Proceedings of the National Academy of Sciences of the United States of America,** Washington, v. 110, n. 15, p. 6205-6210, 2013.

LU, D.; WU, S.; GAO, X.; ZHANG, Y.; SHAN, L.; HE, P. A receptor-like cytoplasmic kinase, BIK1, associates with a flagellin receptor complex to initiate plant innate immunity. **Proceedings of the National Academy of Sciences of the United States of America,** Washington, v. 107, n. 1, p. 496-501, 2010.

MA, C.; GUO, J.; KANG, Y.; DOMAN, K.; BRYAN, A.C.; TAX, F.E.; YAMAGUCHI, Y.; QI, Z. Atpeptide receptor2 mediates the Atpeptide1-induced cytosolic Ca(2+) rise, which is required for the suppression of Glutamine Dumper gene expression in Arabidopsis roots. **Journal of Integrative Plant Biology,** Beijing, v. 56, n. 7, p. 684-694, 2014.

NTOUKAKIS, V.; SCHWESSINGER, B.; SEGONZAC, C.; ZIPFEL, C. Cautionary notes on the use of C-terminal BAK1 fusion proteins for functional studies. **The Plant Cell**, Rockville, v. 23, n. 11, p. 3871-3878, 2011.

PACIOREK, T.; SAUER, M.; BALLA, J.; WIŚNIEWSKA, J.; FRIML, J. Immunocytochemical technique for protein localization in sections of plant tissues. **Nature protocols,** London, v. 1, n. 1, p. 104-107, 2005.

POSTEL, S.; KUFNER, I.; BEUTER, C.; MAZZOTTA, S.; SCHWEDT, A.; BORLOTTI, A.; HALTER, T.; KEMMERLING, B.; NURNBERGER, T. The multifunctional leucine-rich repeat receptor kinase BAK1 is implicated in Arabidopsis development and immunity. **European Journal of Cell Biology,** Stuttgart, v. 89, n. 2/3, p. 169-174, 2010.

RANF, S.; ESCHEN-LIPPOLD, L.; PECHER, P.; LEE, J.; SCHEEL, D. Interplay between calcium signalling and early signalling elements during defence responses to microbe- or damage-associated molecular patterns. **The Plant Journal,** Oxford, v. 68, n. 1, p. 100-113, 2011.

ROUX, M.; SCHWESSINGER, B.; ALBRECHT, C.; CHINCHILLA, D.; JONES, A.; HOLTON, N.; MALINOVSKY, F.G.; TOR, M.; DE VRIES, S.; ZIPFEL, C. The Arabidopsis leucine-rich repeat receptor-like kinases BAK1/SERK3 and BKK1/SERK4 are required for innate immunity to hemibiotrophic and biotrophic pathogens. **The Plant Cell**, Rockville, v. 23, n. 6, p. 2440-2455, 2011.

SCHULZE, B.; MENTZEL, T.; JEHLE, A.K.; MUELLER, K.; BEELER, S.; BOLLER, T.; FELIX, G.; CHINCHILLA, D. Rapid heteromerization and phosphorylation of ligand-activated plant transmembrane receptors and their associated kinase BAK1. **The Journal of Biological Chemistry,** Baltimore, v. 285, n. 13, p. 9444-9451, 2010.

SCHWESSINGER, B.; BAHAR, O.; THOMAS, N.; HOLTON, N.; NEKRASOV, V.; RUAN, D.; CANLAS, P.E.; DAUDI, A.; PETZOLD, C.J.; SINGAN, V.R.; KUO, R.; CHOVATIA, M.; DAUM, C.; HEAZLEWOOD, J.L.; ZIPFEL, C.; RONALD, P.C. Transgenic expression of the dicotyledonous pattern recognition receptor EFR in rice leads to ligand-dependent activation of defense responses. **PLoS Genetics,** San Francisco, v. 11, n. 3, p. e1004809, 2015.

SCHWESSINGER, B.; ROUX, M.; KADOTA, Y.; NTOUKAKIS, V.; SKLENAR, J.; JONES, A.; ZIPFEL, C. Phosphorylation-dependent differential regulation of plant growth, cell death, and innate immunity by the regulatory receptor-like kinase BAK1. **PLoS Pathogens,** San Francisco, v. 7, n. 4, p. e1002046, 2011.

SLEPNEV, V.I.; OCHOA, G.C.; BUTLER, M.H.; GRABS, D.; DE CAMILLI, P. Role of phosphorylation in regulation of the assembly of endocytic coat complexes. **Science**, New York, v. 281, n. 5378, p. 821-824, 1998.

TANG, J.; HAN, Z.; SUN, Y.; ZHANG, H.; GONG, X.; CHAI, J. Structural basis for recognition of an endogenous peptide by the plant receptor kinase PEPR1. **Cell Research,** New york, v. 25, n. 1, p. 110-120, 2015.

WANG, Y.; LI, Z.; LIU, D.; XU, J.; WEI, X.; YAN, L.; YANG, C.; LOU, Z.; SHUI, W. Assessment of BAK1 activity in different plant receptor-like kinase complexes by quantitative profiling of phosphorylation patterns. **Journal of Proteomics**, Amsterdam, v. 108, p. 484-493, 2014.

YAMAGUCHI, Y.; HUFFAKER, A. Endogenous peptide elicitors in higher plants. **Current Opinion in Plant Biology,** London, v. 14, n. 4, p. 351-357, 2011.

YAMAGUCHI, Y.; HUFFAKER, A.; BRYAN, A.C.; TAX, F.E.; RYAN, C.A. PEPR2 is a second receptor for the Pep1 and Pep2 peptides and contributes to defense responses in Arabidopsis. **The Plant Cell**, Rockville, v. 22, n. 2, p. 508-522, 2010.

ZIPFEL, C. Plant pattern-recognition receptors. **Trends in Immunology,** London, v. 35, n. 7, p. 345-351, 2014.
ZIPFEL, C.; KUNZE, G.; CHINCHILLA, D.; CANIARD, A.; JONES, J.D.; BOLLER, T.; FELIX, G. Perception of the bacterial PAMP EF-Tu by the receptor EFR restricts Agrobacterium-mediated transformation. **Cell,** Cambridge, v. 125, n. 4, p. 749-760, 2006.

5 CONCLUSION AND FUTURE PERSPECTIVES

In the past years, a growing number of signaling peptides have been discovered that play an active role in cell-to-cell communication networks in plants and knowledge has been acquired about their responses and signaling components (ALBERT, 2013; GHORBANI et al., 2014). Nonetheless, the subcellular fate and dynamics of these molecules remain to be elucidated as well as their association with signaling responses. In this thesis, we characterized a fluorescent probe that allowed us to examine the subcellular dynamics of the plant endogenous elicitor peptide *At*Pep1 and its receptors *in vivo*, hence, providing new information to the understanding of endocytic trafficking and its interplay with signaling during plant immunity responses. This work also opens research avenues in the field and proposes novel technical approaches to carry out future investigations.

5.1 Fluorescently labeled ligands as a tool to study ligand-receptor pairs

Plant genomes are predicted to encode hundreds of plasma membrane-localized receptor kinases (RKs) that potentially could recognize ligands by their extracellular domains, thus triggering signaling events that lead to specific cell responses (GELDNER; ROBATZEK, 2008; SHIU et al., 2004). Ligands are self- or not self-produced molecules, they can have different biological structures, among which peptides, steroids and oligosaccharides are found (ALBERT, 2013; GELDNER; ROBATZEK, 2008; HOTHORN et al., 2011). Within the endogenous ligands, numerous genes (approximately 1000) are found in *Arabidopsis thaliana* that encode small proteins giving rise to secreted peptides that would bind RKs (LEASE; WALKER, 2006). Nonetheless, in spite of the large ligand-receptor pairings that are possible, only a few ligand-receptor combinations have been identified and experimentally demonstrated. Characterization of these regulatory pairs is essential for the advancement of our understanding of communication networks in plants, but this task is challenging because the genes encoding RKs and peptides are often redundant and their low expression is restricted to a few cells and/or particular developmental stages or stress conditions (BUTENKO et al., 2014).

In this thesis, we showed that the peptide *At*Pep1 can be fluorescently tagged without loss of its biological activity and that at low concentrations the labeled *At*Pep1complexed with its receptor underwent internalization. This observation was similar to that reported previously for the fluorescent brassinosteroid (BR) AFCS and its receptor BRASSINOSTEROID INSENSITIVE1 (BRI1) (IRANI et al., 2012), thus showing that ligands with different natures, such peptides and steroids, can be labeled with fluorescent dyes

and their subcellular dynamics can be assessed *in vivo*. Moreover, our results, showing that endocytosis of the *At*Pep1-induced PEPRs was triggered by ligands, together with previous reports on ligand-induced endocytosis of RKs such as FLAGELLIN-SENSITIVE2 (FLS2) and BRI1 (IRANI et al., 2012; ROBATZEK; CHINCHILLA; BOLLER, 2006), confirmed that this process is a hallmark of RKs. Thus, we propose the use of labeled ligands combined with the ectopic expression of receptor genes in suitable plant cells for matching ligand-pair candidates by assessing endocytosis as read-out of their interaction. This strategy would avoid the use of radiolabeled ligands to identify receptor pairs that is technically inconvenient because of the manipulation of the radioactive material, high costs and short half-life of the probes (BUTENKO et al., 2014; YAMAGUCHI; PEARCE; RYAN, 2006).

In addition, redundancy, specificity and low expression of the potential receptors can be overcome by ectopic expression of fluorescently tagged candidates in plant cell systems, employed as models for cell biology studies. These systems include the transient *Agrobacterium*-mediated gene expression system in leaves of *Nicotiana benthamina* (WYDRO; KOZUBEK; LEHMANN, 2006), and that explored in this thesis, namely expression of GFP-fused PEPRs in the root epidermal meristem cells in *Arabidopsis*, by means of transgenic lines of the *At*Pep1 receptors under the *RPS5A* promoter (WEIJERS et al., 2001). However, this approach should be consider as an initial indicator of ligand-receptor interaction, as molecules could be co-internalized without necessarily interacting, therefore the ligand-receptor interaction must be further supported through additional approaches.

5.2 Release of *At*Peps, the missing piece of the puzzle

In this thesis, we elucidated the internalization pathway of the peptide *At*Pep1, which is probably similar to the other members of the family, because they all trigger a comparable set of downstream signaling responses (BARTELS et al., 2013; YAMAGUCHI et al., 2010). However, the internalization of *At*Peps would happen after the release of active peptides from their precursor proteins (PROPEPs) into the extracellular space, which has not been shown yet.

We found that PROPEP1-GFP was attached to the tonoplast, in agreement with previous reports (BARTELS et al., 2013) and additionally; we observed that probably it is accumulated into the vacuole. Thus, it is possible that the vacuole is an organelle where PROPEP1 is stored before the active *At*Pep1 is released. Mechanism, localization and timing of release of active *At*Peps are largely unknown, but still of great interest in the field (BARTELS; BOLLER, 2015). In an attempt to clarify these issues, we analyzed the

subcellular localization of PROPEP1-GFP when treated with a cocktail composed by the MAMPs flg22 and *At*Pep1 that generates a biotic stress. As we did not observe any apparent changes, we hypothesized that the PROPEP1 would be delivered only when the cell integrity is compromised and, subsequently, that the protease action would cleave the active *At*Pep1, which, in turn, would bind the receptors located at the plasma membrane of neighboring cells, thus triggering defense responses. This assumption fits into the proposed damage model for activation of the *At*Peps-PEPRs (BARTELS; BOLLER, 2015). However this could be not the case for all PROPEPs, because PROPEP3-YFP accumulated in the cytosol (BARTELS et al., 2013). The accumulation of PROPEPs at two different subcellular compartments might hint at differences between release of the active *At*Peps and their contributions to the cellular immunity. Furthermore, because our transgenic plants expressing *35S:PROPEP1-GFP* did not up-regulate the A*t*Pep1-responsive genes, as seen for the lines expressing *35S:PROPEP1* (HUFFAKER; RYAN, 2007), we cannot disregard that the vacuolar localization and/or the non-secretion of PROPEP1-GFP upon biotic stresses are due to a disfunctionality of this chimeric protein.

Therefore, based on our data and published results, we propose that future experiments with the aim at solving the secretion mechanism of *At*Peps should consider the generation of transgenic plants expressing PROPEPs with a fluorescent tag located between the C-terminus of the active peptide-containing PROPEPs and the N-terminus with the precursor protein, thus allowing an eventual C-terminus cleavage given origin to possibly active GFP-*At*Peps. These plants should be exposed to different stresses, such as MAMPs and damage treatments, and subsequently the subcellular localization of the chimeric proteins should be assessed *in vivo*. Damage treatment could be carry out through laser ablation associated with confocal microscopy. This minimally invasive approach would allow mimicking more accurately the injury caused by invasive organisms.

Approaches that don not include the use of fused proteins can also be proposed, such as immunolocalization and cell fractionation. Immunolocalization would permit to identify the localization of PROPEPs or *At*Peps *in situ* at subcellular resolution avoiding the risk of inducing side effects by a fusion protein, such as misexpression, mistargeting and altered stability; however, its use depends on specific antibodies that would recognize the protein of interest (PACIOREK et al., 2005). Currently, it has not been reported any antibody that would recognize PROPEPs or *At*Peps, which limits the use of this technique to study their subcellular dynamics. Cell fractionation that allows the separation of organelles according to

their density, combined with mass spectrometry could also help to identify the subcellular localization of PROPEs and/or *At*Peps under different physiological conditions.

5.3 *At*Pep1/PEPR internalization reveals different endocytic pathways

In plants, endocytic trafficking requires sequential steps through the *trans*-Golgi network/early endosome (TGN/EE) that is the first place where endocytosed material is delivered. Moreover, the TGN/EE functions as a sorting station from where the cargo is further sorted back to the plasma membrane or into multivesicular bodies (MVBs)/late endosomes that fuse with the vacuole to release their intraluminal vesicles for degradation (VIOTTI et al., 2010).

Here, we found that the *At*Pep1-PEPR complexes are transported from the plasma membrane to the vacuole following a common endocytic trafficking route. However, distinct modes of receptor-mediated endocytosis (RME) might coexist in plant cells, because the spatio-temporal cellular dynamics of *At*Pep1-PEPRs showed unique features in comparison with the described subcellular dynamics of AFCS-BRI1 and partially overlapped with the FLS2 behavior upon flg22 treatment. These features can be listed as: (i) inactive PEPRs from the plasma membrane did not accumulate in large bodies in the presence of the fungal toxin brefeldin A (BFA) that inhibits protein secretion and vesicle recycling of endocytosed proteins to the plasma membrane (GELDNER et al., 2003), as seen for FLS2 and BRI1 that undergo constitutive endocytic recycling under steady-state conditions (BECK et al., 2012; GELDNER et al., 2007; IRANI et al., 2012); (ii) the temporal dynamics of the internalization of *At*Pep1-PEPR complexes differed from those of BRI1-AFCS that internalized more quickly (2 min after ligand application) (IRANI et al., 2012), but matched more those of the FLS2 receptor, in which endosomes were visualized in leaves 30 min after flg22 application (ROBATZEK; CHINCHILLA; BOLLER, 2006); (iii) the molecular probe of *At*Pep1 (TAMRA-*At*Pep1) presented low colocalization with the TGN/EE marker VHA-a1, as seen for flg22-activated FLS2 (CHOI et al., 2013), in contrast to the AFCS-BRI1 complex that highly colabeled with this TGN/EE marker (IRANI et al., 2012); and finally, (iv) the endocytic trafficking of *At*Pep1-PEPR complexes was not blocked by ConcA, which inhibits the V-ATPase activity in the TGN/EE, leading to an increase in the pH of this organelle and blocking the vacuolar transport of endocytic cargos, as observed for AFCS-BRI1 (DETTMER et al., 2006; IRANI et al., 2012; SHEN et al., 2013). For flg22-activated FLS2, trafficking was not largely impaired in the presence of ConcA and colocalization with endosomal

compartments occurred (BECK et al., 2012), suggesting that its transport is not blocked as for *At*Pep1-PEPR complexes.

The apparent existence of distinct RME pathways raises interesting questions about their regulation. As *At*Pep1 and the bacterial peptide flg22 are elicitor peptides that, albeit with a different origin, activate similar swift and transient plant immunity responses under biotic stresses (BARTELS; BOLLER, 2015), whereas AFCS is an analog of the ubiquitous plant hormone BR mainly associated to plant growth and development (IRANI et al., 2012), it is tempting to argue that RME is modulated by the nature of the ligand.

This ligand modulation could be mediated by pH changes, because an early hallmark of *At*Pep1 and flg22 activities is the induction of changes in the ion fluxes, including H^+ and Ca^{2+} influxes, leading to membrane depolarization and extracellular alkalinization (KROL et al., 2010; MITHÖFER; EBEL; FELLE, 2005; YAMAGUCHI; PEARCE; RYAN, 2006). Interestingly, the opposite effect is triggered by BR that induces hyperpolarization of the plasma membrane and slight medium acidification (ZHANG et al., 2005). Furthermore, regulation and pH homeostasis within intracellular compartments are well known to be essential for the viability of all eukaryotic cells, in which each endomembrane compartment presents particular luminal pH-dependent environments that assure their optimal operation and fulfillment of their specific functions (CASEY; GRINSTEIN; ORLOWSKI, 2010; SCHUMACHER, 2014; SHEN et al., 2013). In animals, the pH participation during the endomembrane trafficking is evidenced by its role that modulates luminal processes, such as proteolytic processing and receptor-ligand interaction. Moreover, pH has been shown to affect recruitment of the trafficking machinery components to the cytosolic membrane face and cargo sorting (HUANG; CHANG, 2011; MARANDA et al., 2001; MARSHANSKY; FUTAI, 2008).

Based on the results of this thesis and previous literature reports, we hypothesize that a refined model for RME exists that relies on a pH-dependent cargo sorting mechanism that operates at the plasma membrane, as illustrated by the subcellular dynamics of *At*Pep1-PEPRs and AFCS-BRI1 (Figure 1). Thus, we propose a scenario in which after the *At*Pep1 binding of PEPRs a rapid change is triggered in the ion fluxes, leading to membrane depolarization and extracellular alkalinization and dictating the cues for recruitment of the endocytic machinery. Moreover, the alkaline environment would maintain the interaction between *At*Pep1 and PEPRs that had been shown to depend on the pH (TANG et al., 2015). Later, between 15-20 min after the high alkalinization activity has been found (HUFFAKER; PEARCE; RYAN, 2006), the transport of *At*Pep1-PEPR complexes from the plasma membrane to the

intracellular compartments begins. Then, the *At*Pep1-PEPR complexes are transported via a VHA-a1-negative SYP42/SYP61/ARA7-positive TGN/EE population or subdomains that rapidly mature, first into ARA7/ARA6 compartments and then into ARA7/ARA6/VAMP727-positive compartments, which fuse with the vacuole where the *At*Pep1-PEPR complexes are released for final dissociation and degradation. Moreover, the compartments through which the *At*Pep1-PEPR complexes are transported might have an alkaline pH, thus ensuring that peptides and receptors reach the lytic vacuoles as a complex.

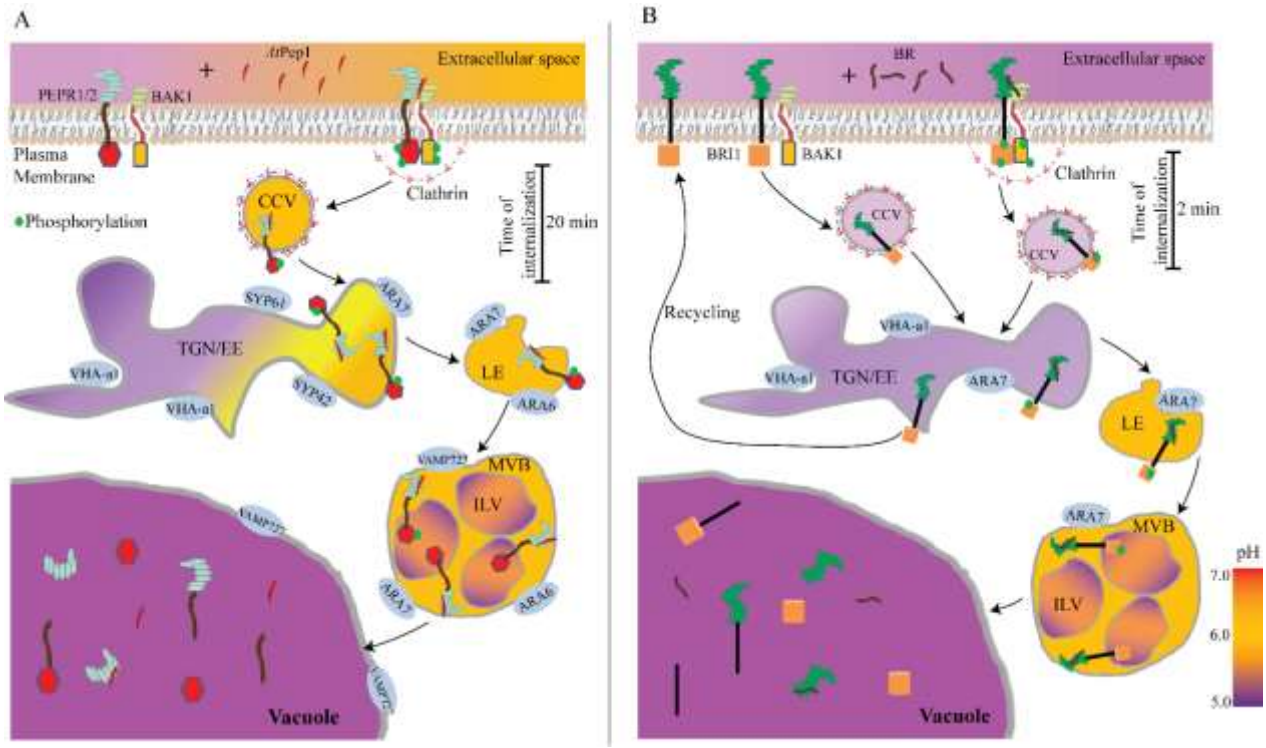

Figure 1 – Schematic overview of the endocytic pathways of PEPRs and BRI1. (A) After *At*Pep1 binding, PEPRs associates with BAK1, triggering phosphorylation of the kinase domains and extracellular alkalinization. After 20 min *At*Pep1-PEPRs undergoes endocytosis mediated by clathrin and are sorted in specific SYP42/SYP61/ARA7-positive subdomains of the *trans*-Golgi network/early endosomes (TGN/EE). Here, the complex rapidly maturate into ARA7/ARA6-positive late endosomes (LE) and is directed to the vacuole via ARA7/ARA6/VAMP727-positive multivesicular bodies (MVB). (**B**) Independent of ligand BRI1 undergoes constitutive endocytosis. In this case BRI1 is targeted to TGN/EE, from where it is recycled back to the plasma membrane. *Upon brassinosteroid (BR) binding, BRI1* form complex with BAK1, triggering phosphorylation events and slight extracellular acidification. Quickly, activated BIR1 undergoes endocytosis mediated by clathrin and is sorted to TGN/EE. Subsequently, BR-BRI1 mature to late endosomes and is targeted to the vacuole via MVB. Endocytosis of BR-BRI1 requires a functional TGN/EE localized V-ATPase VHA-a1, but not *At*Pep1-PEPRs. For simplicity only the PEPRs, BRI1 and BAK1 are shown in the schematic representation, without referring to other regulators of PEPRs and BRI1. CCV, clathrin coated vesicle; ILV, *intraluminal vesicles*

However, to verify our hypothetic model, we need to prove that the VHA-a1-negative TGN/EE population or subdomains indeed exist or appear under *At*Pep1 elicitation. To this end, it would be interesting to generate plant genotypes expressing TGN markers (VHA-a1 and SYP42 or SYP61) in combination with PEPRs and the endosomal marker ARA7 fused to fluorescent proteins with different spectrums, and to evaluate their localization upon *At*Pep1 stimulation over time. Another point that has to be assessed is the pH behavior in the different endocytic compartments during the ligand-induced internalization of PEPRs and BRI1, which would provide information to understand how different cargos influence the pH of subcellular compartments and the relationship with RME. An interesting strategy would be to fuse PEPRs and BRI1 to pH-fluorescent protein sensors, such as PEpHluorin and PrpHluorin, that permit *in vivo* measurements (SHEN et al., 2013) and to assess the pH of the different endomembrane compartments through which ligand-activated PEPRs and BRI1 are transported.

5.4 The *At*Pep1-PEPR system, a new suitable model to study clathrin-mediated endocytosis in plants and its implication in immunity

In this thesis, we provide solid proof that the endocytosis of *At*Pep1-PEPRs is mediated by clathrin proteins, supporting its role as the primary endocytic route in plants (BAISA; MAYERS; BEDNAREK, 2013). Previously, endocytosis of BRI1, a membrane-localized RK structurally similar to *At*Pep1 receptors had also been found to depend on clathrin (IRANI et al., 2012) indicating that clathrin-mediated endocytosis (CME) can be a conserved mechanism for RK internalization. We propose that at least two different ligand-induced endocytic pathways exist; as exemplified by the spatio-temporal dynamics of *At*Pep1-PEPRs and AFCS-BRI1, part of their endocytic machinery is probably pretty well conserved, including clathrin proteins, but some specificity-dictating components, which remain to be identified, might also occur. This specificity could be determined by adaptor proteins that recruit clathrin to perform the coat assembly of the specific cargos, because clathrin cannot bind directly to the membrane (LEE; HWANG, 2014; SCHMID; MCMAHON, 2007).

The role of adaptor proteins for cargo selection has been characterized extensively in animal and yeast cells (SCHMID; MCMAHON, 2007; TRAUB, 2009). Although plant CME is far away from having well-defined CME network as described in animals, in the past decade, significant progress has been made in understanding and identifying the CME components in plants. For instance, the role of the adaptor protein complex 2 (AP2) that represents the core complex during the cargo recognition/selection of the CME in animals has

also been reported to mediate CME in plants (DI RUBBO et al., 2013); more recently, the TPLATE adaptor complex (TPC) that consists of eight core subunits has been found to accumulate at the plasma membrane, preceding the recruitment of future components for formation of clathrin coat vesicles (GADEYNE et al., 2014). However, to get a deeper insight into the CME in plants, it is still necessary to identify the functional CME constituents as well as to elucidate how they participate in the endocytosis of cargos with different physiological roles and subcellular dynamics. A starting point could be the identification of the interactome of proteins that undergo CME, providing refined information about the missing CME components. To this end, PEPRs appear excellent candidates due to the *At*Pep1 inducibility, temporal dynamics and transient behavior of their endocytosis. Hence, it would be possible to sequentially assess the endocytic machinery associated with PEPRs through the different steps of CME. These endocytic features of PEPRs also turn these receptors into good candidates to study *in vivo* the recruitment dynamics of the clathrin assembly machinery at the plasma membrane by means of high-end microscopy techniques, such as total internal reaction fluorescence (TIRF)/variable angle epifluorescence microscope (VAEM) and Spinning Disc Microscopy, which allow the evaluation of the behavior of candidate proteins at the plasma membrane.

During this thesis, we also detected that CME impairment compromised the *At*Pep1 responses, thus providing evidence that pattern-triggered immunity (PTI) can be regulated by CME, a physiological role not reported so far. Although the defects in the *At*Pep1 responses could not be attributed to a specific inhibition of the endocytosis of *At*Pep1-PEPRs because the CME is affected in a general manner, these defects could also reflect impairment of the endosomal signaling that would not operate when endocytosis is blocked. Therefore, tools have to be developed that allow specific blocking of the *At*Pep1-PEPR endocytosis. Remarkably, we identified putative endocytic motifs at the cytoplasmic domain of the *At*Pep1 receptors (Figure 2) that are carried by proteins interacting with the AP2 complex and clathrin (GADEYNE et al., 2014; TRAUB, 2009). It would be worthwhile to generate specific mutations into these endocytic motifs and to evaluate whether through this approach the *At*Pep1-PEPR trafficking could be blocked specifically. This tool could be used to address issues about endosomal signaling in plants.

Figure 2 – Alignment of the cytoplasmic domain of *At*Pep1 receptors displaying putative protein endocytic motifs. [DE]XXXL[LI]and YXXØ function as cargo sorting signals; L[IVLMF]X[IVLMF][DE] is a clathrin binding motif. Endocytosis motifs were manually searched using the ScanProsite tool from the bioinformatics research portal expasy (http://prosite.expasy.org/scanprosite/)

5.5 BAK1 modulates endocytosis and signaling of the plant elicitor peptide *At*Pep1

Through the use of the hypoactive kinase *bak1-5*, we showed that endocytosis of *At*Pep1 is modulated by BAK1, which interacts with *At*Pep1 receptors in a ligand-dependent manner. As *bak1-5* presents altered phosphorylation patterns (SCHWESSINGER et al., 2011; WANG et al., 2014), it is possible to argue that phosphorylation events occurring after the PEPR1-BAK1 heterodimerization upon *At*Pep1 treatments dictate the bases for recruitment of the endocytic machinery. Moreover, we also confirmed that the *At*Pep1 signaling is largely impaired in *bak1-5*, thus raising the question whether there is interplay between endocytosis and signaling or whether they are processes regulated independently by phosphorylation. Examination of different phosphorylating *bak1* mutants would help to clarify this issue. Another mutant worthwhile to assess is *bak1-4*/proBAK1:BAK1* that expresses a BAK1-5 kinase inactive in the null *bak1-4* mutant and does not strongly inhibit immunity responses, as seen for *bak1-5* and *bak1-4*/proBAK1::BAK1-5 (SCHWESSINGER et al., 2011); therefore, if endocytosis and signaling would regulate each other, a lower impact in the *At*Pep1 internalization is expected in this genotype.

Interestingly, we also found that overexpression of BAK1 leads to a dominant-negative effect in *At*Pep1 endocytosis and signaling, suggesting that BAK1 could be required to attenuate and balance the system after *At*Pep1 elicitation; however, this effect is not well

understood and further experiments are needed. It would be relevant to generate transgenic plants with different levels of BAK1 expression and to examine whether there is a dose-response effect in the endocytosis and signaling, as expected if this effect indeed represents a biological process.

An open question that remains to be elucidated is whether BAK1 undergoes internalization together with the *At*Pep1-PEPR complexes. To address this question is a challenging task because the C-Terminal fusion proteins antagonize the BAK1 activity linked to immunity responses (NTOUKAKIS et al., 2011); hence, various versions of biologically active fluorescent BAK1 tags have to be engineered. A good strategy would be to introduce the fluorescent protein into the juxtamembrane domain of BAK1 without compromising the activity of the kinase domain localized at the C-terminus. As a specific antibody of BAK1 is available, another approach that could be explored to solve this question is the antibody-based immunological detection, thus avoiding the risks of side effects by the fusion of a protein to BAK1.

References

ALBERT, M. Peptides as triggers of plant defence. **Journal of Experimental Botany** , Oxford, v. 64, n. 17, p.5269-5279, 2013

BAISA, G.A.; MAYERS, J.R.; BEDNAREK, S.Y. Budding and braking news about clathrin-mediated endocytosis. **Current Opinion in Plant Biology,** London, v. 16, n. 6, p. 718-725, 2013.

BARTELS, S.; BOLLER, T. Quo vadis, Pep? Plant elicitor peptides at the crossroads of immunity, stress and development. **Journal of Experimental Botany**, Oxford, v. 66, n. 17, p. 5183-5193, 2015.

BARTELS, S.; LORI, M.; MBENGUE, M.; VAN VERK, M.; KLAUSER, D.; HANDER, T.; BONI, R.; ROBATZEK, S.; BOLLER, T. The family of Peps and their precursors in Arabidopsis: differential expression and localization but similar induction of pattern-triggered immune responses. **Journal of Experimental Botany**, Oxford, v. 64, n. 17, p. 5309-5321, 2013.

BECK, M.; ZHOU, J.; FAULKNER, C.; MACLEAN, D.; ROBATZEK, S. Spatio-temporal cellular dynamics of the Arabidopsis flagellin receptor reveal activation status-dependent endosomal sorting. **The Plant Cell**, Rockville, v. 24, n. 10, p. 4205-4219, 2012.

BUTENKO, M.A.; WILDHAGEN, M.; ALBERT, M.; JEHLE, A.; KALBACHER, H.; AALEN, R.B.; FELIX, G. Tools and strategies to match peptide-ligand receptor pairs. **The Plant Cell**, Rockville, v. 26, n. 5, p. 1838-1847, 2014.

CASEY, J.R.; GRINSTEIN, S.; ORLOWSKI, J. Sensors and regulators of intracellular pH. **Nature Reviews Molecular Cell biology,** London, v. 11, n. 1, p. 50-61, 2010.

CHOI, S.W.; TAMAKI, T.; EBINE, K.; UEMURA, T.; UEDA, T.; NAKANO, A. RABA members act in distinct steps of subcellular trafficking of the flagellin sensing2 receptor. **The Plant Cell**, Rockville, v. 25, n. 3, p. 1174-1187, 2013.

DETTMER, J.; HONG-HERMESDORF, A.; STIERHOF, Y.D.; SCHUMACHER, K. Vacuolar H+-ATPase activity is required for endocytic and secretory trafficking in Arabidopsis. **The Plant Cell**, Rockville, v. 18, n. 3, p. 715-730, 2006.

DI RUBBO, S.; IRANI, N.G.; KIM, S.Y.; XU, Z.Y.; GADEYNE, A.; DEJONGHE, W.; VANHOUTTE, I.; PERSIAU, G.; EECKHOUT, D.; SIMON, S.; SONG, K.; KLEINE-VEHN, J.; FRIML, J.; DE JAEGER, G.; VAN DAMME, D.; HWANG, I.; RUSSINOVA, E. The clathrin adaptor complex AP-2 mediates endocytosis of brassinosteroid insensitive1 in Arabidopsis. **The Plant Cell**,Rockville, v. 25, n. 8, p. 2986-2997, 2013.

GADEYNE, A.; SANCHEZ-RODRIGUEZ, C.; VANNESTE, S.; DI RUBBO, S.; ZAUBER, H.; VANNESTE, K.; VAN LEENE, J.; DE WINNE, N.; EECKHOUT, D.; PERSIAU, G.; VAN DE SLIJKE, E.; CANNOOT, B.; VERCRUYSSE, L.; MAYERS, J.R.; ADAMOWSKI, M.; KANIA, U.; EHRLICH, M.; SCHWEIGHOFER, A.; KETELAAR, T.; MAERE, S.; BEDNAREK, S.Y.; FRIML, J.; GEVAERT, K.; WITTERS, E.; RUSSINOVA, E.; PERSSON, S.; DE JAEGER, G.; VAN DAMME, D. The TPLATE adaptor complex drives clathrin-mediated endocytosis in plants. **Cell,** Cambridge, v. 156, n. 4, p. 691-704, 2014.

GELDNER, N.; ROBATZEK, S. Plant receptors go endosomal: a moving view on signal transduction. **Plant Physiology,** Washington, v. 147, n. 4, p. 1565-1574, 2008.

GELDNER, N.; HYMAN, D.L.; WANG, X.; SCHUMACHER, K.; CHORY, J. Endosomal signaling of plant steroid receptor kinase BRI1. **Genes & Development,** Cold Spring Harbor, v. 21, n. 13, p. 1598-1602, 2007.

GELDNER, N.; ANDERS, N.; WOLTERS, H.; KEICHER, J.; KORNBERGER, W.; MULLER, P.; DELBARRE, A.; UEDA, T.; NAKANO, A.; JÜRGENS, G. The Arabidopsis GNOM ARF-GEF mediates endosomal recycling, auxin transport, and auxin-dependent plant growth. **Cell,** Cambridge, v. 112, n. 2, p. 219-230, 2003.

GHORBANI, S.; FERNANDEZ SALINA, A.; HILSON, P.; BEECKMAN, T. Signaling peptides in plants. **Cell & Developmental Biology,** Oxford, v. 3, n. 2, p. 1-11, 2014.

HOTHORN, M.; BELKHADIR, Y.; DREUX, M.; DABI, T.; NOEL, J. P.; WILSON, I. A.; CHORY, J. Structural basis of steroid hormone perception by the receptor kinase BRI1. **Nature,** London**,** v. 474, n. 7352, p. 467-471, 2011.
HUANG, C.; CHANG, A. pH-dependent cargo sorting from the Golgi. **The Journal of biological chemistry,** Bethesda, v. 286, n. 12, p. 10058-10065, 2011.

HUFFAKER, A.; RYAN, C.A. Endogenous peptide defense signals in Arabidopsis differentially amplify signaling for the innate immune response. **Proceedings of the National Academy of Sciences of the United States of America,** Washington, v. 104, n. 25, p. 10732-10736, 2007.

HUFFAKER, A.; PEARCE, G.; RYAN, C.A. An endogenous peptide signal in Arabidopsis activates components of the innate immune response. **Proceedings of the National Academy of Sciences of the United States of America,** Washington, v. 103, n. 26, p. 10098-10103, 2006.

IRANI, N.G.; DI RUBBO, S.; MYLLE, E.; VAN DEN BEGIN, J.; SCHNEIDER-PIZON, J.; HNILIKOVA, J.; SISA, M.; BUYST, D.; VILARRASA-BLASI, J.; SZATMARI, A.M.; VAN DAMME, D.; MISHEV, K.; CODREANU, M.C.; KOHOUT, L.; STRNAD, M.; CANO-DELGADO, A.I.; FRIML, J.; MADDER, A.; RUSSINOVA, E. Fluorescent castasterone reveals BRI1 signaling from the plasma membrane. **Nature Chemical Biology,** London,v. 8, n. 6, p. 583-589, 2012.

KROL, E.; MENTZEL, T.; CHINCHILLA, D.; BOLLER, T.; FELIX, G.; KEMMERLING, B.; POSTEL, S.; ARENTS, M.; JEWORUTZKI, E.; AL-RASHEID, K.A.; BECKER, D.; HEDRICH, R. Perception of the Arabidopsis danger signal peptide 1 involves the pattern recognition receptor AtPEPR1 and its close homologue AtPEPR2. **The Journal of biological chemistry,** Baltimore, v. 285, n. 18, p. 13471-13479, 2010.

LEASE, K.A.; WALKER, J.C. The Arabidopsis unannotated secreted peptide database, a resource for plant peptidomics. **Plant Physiology,** Washington, v. 142, n. 3, p. 831-838, 2006.

LEE, M.H.; HWANG, I. Adaptor proteins in protein trafficking between endomembrane compartments in plants. **Journal of Plant Biology,** New York, v. 57, n. 5, p. 265-273, 2014.

MARANDA, B.; BROWN, D.; BOURGOIN, S.; CASANOVA, J.E.; VINAY, P.; AUSIELLO, D.A.; MARSHANSKY, V. Intra-endosomal pH-sensitive recruitment of the Arf-nucleotide exchange factor ARNO and Arf6 from cytoplasm to proximal tubule endosomes. **The Journal of Biological Chemistry,** Baltimore, v. 276, n. 21, p. 18540-18550, 2001.

MARSHANSKY, V.; FUTAI, M. The V-type H+-ATPase in vesicular trafficking: targeting, regulation and function. **Current Opinion in Cell Biology,** London, v. 20, n. 4, p. 415-426, 2008.

MITHÖFER, A.; EBEL, J.; FELLE, H.H. Cation fluxes cause plasma membrane depolarization involved in β-glucan elicitor-signaling in soybean roots. **Molecular Plant-Microbe Interactions,** Saint Paul, v. 18, n. 9, p. 983-990, 2005.

NTOUKAKIS, V.; SCHWESSINGER, B.; SEGONZAC, C.; ZIPFEL, C. Cautionary notes on the use of C-terminal BAK1 fusion proteins for functional studies. **The Plant Cell**, Rockville, v. 23, n. 11, p. 3871-3878, 2011.

ROBATZEK, S.; CHINCHILLA, D.; BOLLER, T. Ligand-induced endocytosis of the pattern recognition receptor FLS2 in Arabidopsis. **Genes & Development,** New York, v. 20, n. 5, p. 537-542, 2006.

SCHMID, E.M.; MCMAHON, H.T. Integrating molecular and network biology to decode endocytosis. **Nature,** London, v. 448, n. 7156, p. 883-888, 2007.

SCHUMACHER, K. pH in the plant endomembrane system-an import and export business. **Current Opinion in Plant Biology,** London, v. 22, p. 71-76, 2014.

SCHWESSINGER, B.; ROUX, M.; KADOTA, Y.; NTOUKAKIS, V.; SKLENAR, J.; JONES, A.; ZIPFEL, C. Phosphorylation-dependent differential regulation of plant growth, cell death, and innate immunity by the regulatory receptor-like kinase BAK1. **PLoS Genetics,** San Francisco, v. 7, n. 4, p. e1002046, 2011.

SHEN, J.; ZENG, Y.; ZHUANG, X.; SUN, L.; YAO, X.; PIMPL, P.; JIANG, L. Organelle pH in the Arabidopsis endomembrane system. **Molecular Plant**, Saint Paul, v. 6, n. 5, p. 1419-1437, 2013.

SHIU, S.H.; KARLOWSKI, W.M.; PAN, R.; TZENG, Y.H.; MAYER, K.F.; LI, W.H. Comparative analysis of the receptor-like kinase family in Arabidopsis and rice. **The Plant Cell**, Rockville, v. 16, n. 5, p. 1220-1234, 2004.

TANG, J.; HAN, Z.; SUN, Y.; ZHANG, H.; GONG, X.; CHAI, J. Structural basis for recognition of an endogenous peptide by the plant receptor kinase PEPR1. **Cell Research,** New York, v. 25, n. 1, p. 110-120, 2015.

TRAUB, L.M. Tickets to ride: selecting cargo for clathrin-regulated internalization. **Nature Reviews Molecular Cell Biology,** London, v. 10, n. 9, p. 583-596, 2009.

VIOTTI, C.; BUBECK, J.; STIERHOF, Y.D.; KREBS, M.; LANGHANS, M.; VAN DEN BERG, W.; VAN DONGEN, W.; RICHTER, S.; GELDNER, N.; TAKANO, J.; JURGENS, G.; DE VRIES, S.C.; ROBINSON, D.G.; SCHUMACHER, K. Endocytic and secretory traffic in *Arabidopsis merge* in the trans-Golgi network/early endosome, an independent and highly dynamic organelle. **The Plant Cell**, Rockville, v. 22, n. 4, p. 1344-1357, 2010.

WANG, Y.; LI, Z.; LIU, D.; XU, J.; WEI, X.; YAN, L.; YANG, C.; LOU, Z.; SHUI, W. Assessment of BAK1 activity in different plant receptor-like kinase complexes by quantitative profiling of phosphorylation patterns. **Journal of Proteomics,** Amsterdam, v. 108, p. 484-493, 2014.

WEIJERS, D.; FRANKE-VAN DIJK, M.; VENCKEN, R.J.; QUINT, A.; HOOYKAAS, P.; OFFRINGA, R. An Arabidopsis minute-like phenotype caused by a semi-dominant mutation in a ribosomal protein S5 gene. **Development**, New York, v. 128, n. 21, p. 4289-4299, 2001.

WYDRO, M.; KOZUBEK, E.; LEHMANN, P. Optimization of transient *Agrobacterium*-mediated gene expression system in leaves of Nicotiana benthamiana. **Acta Biochimica Polonica,** Warsaw, v. 53, n. 2, p. 289, 2006.

YAMAGUCHI, Y.; PEARCE, G.; RYAN, C.A. The cell surface leucine-rich repeat receptor for AtPep1, an endogenous peptide elicitor in Arabidopsis, is functional in transgenic tobacco cells **Proceedings of the National Academy of Sciences of the United States of America,** Washington, v. 103, n. 26, p. 10104-10109, 2006.

YAMAGUCHI, Y.; HUFFAKER, A.; BRYAN, A.C.; TAX, F.E.; RYAN, C.A. PEPR2 is a second receptor for the Pep1 and Pep2 peptides and contributes to defense responses in Arabidopsis. **The Plant Cell**, Rockville, v. 22, n. 2, p. 508-522, 2010.

Curriculum vitae

Professional profile

Professional experience in genetics, plant physiology, and molecular biology. Proficiency at analysis of gene expression analysis, plant genetic transformation (sugarcane and *Arabidopsis*), confocal microscopy, in-vitro tissue culture, data acquisition and processing. With ability to work with a great diversity of personalities and people from divergent backgrounds and skill sets.

Personal information

First name: Fausto Andrés

Last name: Ortiz – Morea

Date of birth: March, 14, 1985

Place of birth: Florencia – Caquetá (Colombia)

Nationality: Colombian

Email address: fandortiz@gmail.com

Education

2011 – Present

Joint PhD between University of São Paulo (Brazil) and Gent University (Belgium)

Doctorate in Science. Area Genetics and Plant Breeding - University of São Paulo

Doctorate in Biochemistry and Biotechnology – Gent University

Thesis: Subcellular dynamics of the endogenous elicitor peptide *At*Pep1 and its receptors in *Arabidopsis* - implications for the plant immunity

Promoter University of São Paulo: Prof. Dr. Daniel Scherer de Moura

Promoter Gent University: Prof. Dr. Eugenia Russinova

2008 -2011

Master degree in Science. Area Plant Physiology and Biochemistry

Thesis: Analysis of the role(s) of the miRNA156/SPL pathway on branching/tillering and molecular characterization of sugarcane lateral bud outgrowth

Promoter: Prof Dr. Fabio Tibaldi Silveira Nogueira

University of São Paulo - Brazil

2001 – 2006
Undergraduate course: Engineer Agroecologist
University of the Amazonia – Colombia

Language skills:
Spanish: Mother tongue
English: Proficient in written and spoken language
Portuguese: Proficient in written and spoken language

Publications:
Ortiz Morea F. A., Luo Y., Adamowski M., Friml J., De Moura, D., Russinova E. (2015) **Internalization and intracellular trafficking of the endogenous peptide *At*Pep1 and its receptors in *Arabidopsis*.** In preparation.

Ortiz Morea F. A., Luo Y., Dressano K., De Moura D., Russinova, E. (2015) **BAK1 modulates endocytosis and signaling of the plant elicitor peptide *At*Pep1.** In preparation

Dejonghe W., Kuenen S., Vasileva M., Mylle E., Keech O., Viotti C., **Ortiz-Morea F.A.**, Mishev K., Fendrych M., Delang S., Scholl S., Kourelis J., Kasprowicz J., Nguyen L., Drozdzecki A., Van Houtte I., Szatmári A.M., Majda M., Baisa G., Bednarek S., Testerink C., Robert S., Audenaert D., Van Damme D., Schumacher K, Friml I., Winne J., Verstreken P. & Russinova E. (2015) **Mitochondrial uncouplers inhibit clathrin-mediated endocytosis in plants through acidification of the cytosol.** Under revision in the Nature Communications.

Campos Pereira T., Santis A.C.., Ferreira e Silva G.F., **Ortiz-Morea, F. A.** Nogueira, F.T.S. (2015) **Action mechanisms of microRNAs. In: Campos Pereira T. Introduction to the world of microRNAs.** Language: Portuguese, ISBN 978-85-89265-21-8.

Morato Do Canto A., Ceciliato P., Ribeiro B., O**rtiz-Morea F.A.,** Franco Garcia A., Silva-Filho M.C., De Moura D. (2014) **Biological activity of nine recombinant *A*tRALF peptides: Implications for their perception and function in *Arabidopsis*.** Plant Physiology and Biochemistry, doi.org/10.1016/j.plaphy.

Ortiz-Morea F. A., Vicentini R., Silva G. F. F., Ssilva, E. M., Carrer H., Rrodrigues A.P., Nogueira F. T. S. (2013) **Global analysis of the sugarcane microtranscriptome reveals a unique composition of small RNAs associated with axillary bud outgrowth.** Journal of Experimental Botany, doi:10.1093/jxb/ert089.

Ortiz-Morea, F. A., Jesus F.A., Nogueira F.T.S. (2012) **Sugarcane Biotechnology. In: Almeida Cançado G., Londe Nogueira L. Agricultural Biotechnology**. Language: Portuguese, ISBN 978-85-99764-29-9

Zanca, A., Vicentini R., **Ortiz-Morea F.A.,** Luiz E.V., Da Silva M.J., Vincentz M., Nogueira F.T. (2010) **Identification and expression analysis of microRNAs and targets in the biofuel crop sugarcane.** BMC Plant Biology, doi:10.1186/1471-2229-10-260.

Meetings attended

2015

- 26th International Conference on Arabidopsis Research (ICAR), Oral Presentation
  Paris, France
- VIB seminar 2015, Oral presentation
  Blankenberge, Belgium

2014

- 17th European Network of Plant Endomembrane Research (ENPER) meeting, Oral Presentation
  Lecce, Italy

2010

- XII Brazilian congresso of Plant physyology, Poster Presentation
  Fortaleza, Brazil

Teaching experience

- October - December 2014: Supervision of Masters 1 thesis in Biochemistry and Biotechnology, Ghent University
- February 2011: Promoter of a bachelor thesis in Biology, University of Amazonia.

References

Prof. Dr. Daniel Scherer de Moura,
Assistant professor, Department of Biological Sciences, University of São Paulo - Brazil
E-mail: danielmoura@usp.br

Prof. Dr. Eugenia Russinova
Department of Plant Systems Biology, VIB, Ghent, Belgium
Department of Plant Biotechnology and Bioinformatics, Ghent University, Ghent, Belgium.
E-mail: jenny.russinova@psb.vib-ugent.be

Prof. Dr. Fabio Tibaldi Silveira Nogueira
Assistant professor, Department of Biological Sciences, University of São Paulo - Brazil
E-mail: ftsnogue@ibb.unesp.br